THE UNIVERSITY OF QUEENSLAND

AUSTRALIA

Dynamic Analysis of Dense Medium Circuits

Nerrida Julienne Catherine Scott

Master of Business Administration

Bachelor of Chemical Engineering

Bachelor of Business Administration

A thesis submitted for the degree of Doctor of Philosophy at

The University of Queensland in 2017

Sustainable Minerals Institute

Julius Kruttschnitt Mineral Research Centre

Abstract

Dense Medium Cyclone (DMC) geometry and DMC performance have been widely explored in the past. Some investigations have been made into the dynamic changes that take place over a DMC circuit while the plant is running, however this has been limited by the lack of on-line plant data. Understanding of the dynamics of the whole DMC circuit requires further enquiry. This includes, following changes in medium density, medium to coal ratio, %non-magnetics, velocities and pressures, classification and sizing of the magnetite, the effects of bleeds and wing tank dynamics.

Plant operators typically run coal preparation plants to a set of conditions stipulated based on mine yield/ash predictions, steady-state measurements and design parameters without a full knowledge of how dynamic changes affect the DMC circuit. Essentially, they operate the plant on a macro level, controlling tonnage, volume, and density cut point to align with variations in plant feed. Furthermore, technology has limited operators' ability to see the subtle changes that occur in the dense medium, for example, when the circuit is unstable. This project addresses those issues and should therefore be able to advance knowledge in the area of dynamic analysis of dense medium cyclone circuits.

Declaration by author

This thesis is composed of my original work, and contains no material previously published or written by another person except where due reference has been made in the text. I have clearly stated the contribution by others to jointly-authored works that I have included in my thesis.

I have clearly stated the contribution of others to my thesis as a whole, including statistical assistance, survey design, data analysis, significant technical procedures, professional editorial advice, and any other original research work used or reported in my thesis. The content of my thesis is the result of work I have carried out since the commencement of my research higher degree candidature and does not include a substantial part of work that has been submitted to qualify for the award of any other degree or diploma in any university or other tertiary institution. I have clearly stated which parts of my thesis, if any, have been submitted to qualify for another award.

I acknowledge that an electronic copy of my thesis must be lodged with the University Library and, subject to the policy and procedures of The University of Queensland, the thesis be made available for research and study in accordance with the Copyright Act 1968 unless a period of embargo has been approved by the Dean of the Graduate School.

I acknowledge that copyright of all material contained in my thesis resides with the copyright holder(s) of that material. Where appropriate I have obtained copyright permission from the copyright holder to reproduce material in this thesis.

Publications during candidature

Scott,N., Holtham,P., Firth,B., O'Brien,M., (2013) On-line Simulation & Dynamic Analysis of Dense Medium Cyclone Circuits., International Coal Preparation Congress, 2013, Istanbul, Turkey.

Firth,B., O'Brien,M., Holtham,P., Scott,N., Hu,S., Dixon,R., Burger,A., (2014) Dynamic Impacts of Plant Feed and Operating practices on a Dense Medium Cyclone (DMC) Circuit, 15th Australian Coal Preparation Conference Proceedings 14-18th Sept 2014, Gold Coast, Australia

Firth, B., Holtham,P., O'Brien, M., Hu,S., Dixon,R., Burger, A., Scott,N., Linkage of Dynamic Changes in DMC Circuits to Plant Conditions, ACARP Report C50152, Australian Coal Association Research Program, February 2013.

Scott,N., Wood,C., Holtham,P., O'Brien,M., Firth,B., (2015) Integration of Plant Residence Time Measurement Into a Dynamic Model of a Coal Dense Medium Circuit, Coal Prep 2015, April 27-29th2015, Lexington, Kentucky, USA.

O'Brien,M., Firth,B., Holtham,P., Hu,S., Scott,N., Burger,A., Optimisation and Control of Dense Medium Cyclone Circuits, International Coal Preparation Congress, July 2016, St Petersburg, Russia

Publications included in this thesis

No publications included

Contributions by others to the thesis

A collaborative body of work has been ongoing between the University of Queensland and CSIRO and a series of these ACARP sponsored projects preceded this project. The technical and plant data collected was predominantly obtained by CSIRO/UQ coordinated sampling campaigns in which I actively took part. Data was also collected from CSIRO and UQ developed instruments and the New Acland plant instrumentation. Results of this research have been shared amongst these organisations, however, some data remains the property of CSIRO and New Acland mine and due to confidentiality cannot be specifically detailed in this thesis.

I would like to acknowledge the assistance of CSIRO in providing laboratory resources, training and technical support, and also the assistance of New Acland Coal Handling and Preparation Plant for supporting access to their site for this research to take place. Their assistance in finding and providing plant production information has been invaluable. Collaborative efforts between CSIRO, UQ and New Acland are gratefully acknowledged, particularly the assistance of Dr Peter Holtham, Dr Bruce Firth and Mr Michael O'Brien and technical support from their team. Parallel research conducted by CSIRO in other ACARP projects has been beneficial to this PhD.

I would also like to acknowledge the technical support of Partition Enterprises and members of my fellow student cohort who assisted with RFID tracer testing and the collection of standard tracers at the New Acland mine. Partition Enterprises also assisted this PhD thesis by providing RFID tracer times collected from their instruments.

Statement of parts of the thesis submitted to qualify for the award of another degree

None

Acknowledgements

I would like to acknowledge the support of the following people and organisations:

My parents, Yvonne and Eric Scott – whom without their steadfast support through the ups and downs, I could not have embarked nor continued on this journey. My brothers, Roger and Stuart have also offered great moral support. Luke, my son, who was two years old when I started this journey and who kindly offered to fix my simulation model at age 4 by tickling my computer and purportedly doing magic has now reached the tender age of 7 years and has grown more than 30 centimetres in height since I started. His continual streams of questions, amusing and insightful conversations have inspired me to keep on learning and acquiring new knowledge, whatever my stage or circumstances in life.

Australian Coal Association Research Programme – Who generously funded the various CSIRO / JKMRC research projects that contributed to this PhD and who also funded my PhD Scholarship. ACARP continue to be wonderful supporters of coal processing research in Australia. I would also like to specifically acknowledge the amazing support of Roger Wischusen, Anne Mabardi, Peter Newling, Phil Enderby and Nicole Youngman. The ACARP Coal Preparation committee have also offered amazing support and valuable guidance along my journey, in particular Phil Enderby, Dion Lucke, Frank Mercuri, Kevin Rowe, Rebecca Fleming and Dr David Osborne.

Mr David Wiseman (LIMN), whom I first met during my work at Rio Tinto when using LIMN software, and who was a wealth of information on computer modelling and dynamic simulation. David offered wonderful guidance on the best approaches, as well as assisting in engaging external support from software supplier, Kenwalt Australia P/L. Kenwalt supported my project through the offering of SysCAD software for the model. Despite not using this software in the final model, the SysCAD software provided valuable insight and proved to be a good tool for modelling, particularly in the processing industries where it originated.

AusIMM – who provided a grant of $2000 to enable the hiring of a mini-bus to transport JKMRC students to the New Acland mine site, and who thereby allowed some students to see a coal mine and processing facility for their first time. It also gave me the opportunity to mentor students and teach them about coal processing while working with industry

experts such as Dr Chris Wood, Mr Michael O'Brien and the CSIRO team. The JKMRC students were instrumental in providing assistance with density tracer tests onsite.

Dr Chris Wood (Partition Enterprises) and Mr Ray Wood (Partition Enterprises) who provided tracers and RFID equipment for the tracer testwork. Chris and Ray have been extremely helpful and it has been an absolute pleasure to conduct this research work with them and also assist them with the testing of their innovative new technology.

The University of Queensland, who facilitated my PhD studies at their institution and who contributed to part of my travel expenses to assist me to attend the 2015 Coal Prep conference in Lexington, Kentucky.

Current and former JKMRC staff - Mr Graham Sheridan, Dr Gary Cavanough, Mr Jon Worth, Mrs Karen Holtham, and Professor Tim Napier-Munn who offered valuable support and technical advice, particularly in the early stages of the project. Mr John Wedmaier who designed and built the apparatus to support the JKMRC probes installed under the screens at New Acland.

My former work colleagues: Mr Darren Thompson, Mr James Pollack and Mr Harvey Crowden, who helped me to embark on the coal processing journey. Miss Rebecca Fleming, Mr Adam Higham and Mr Diego Dal Molin, with whom I continued the journey during my time at Rio Tinto and who have been a great support since.

My colleagues in the coal preparation industry of whom there are too many to name individually, have often provided useful pieces of information and insights that have helped me.

New Acland Mine and Coal Handling and Preparation Plant for supporting access to their site for this research to take place. New Acland CHPP production and maintenance teams, assisted in many ways. Much time was devoted, even during busy production runs, to providing context to control room operation and assistance with isolations and equipment support during trials. In particular I would like to thank Mr Robert Rashleigh, Mr Rick Balsamo, Mr Andy Scouller, Mr Paul Kruger, and Mr Kristof McDonald. Their assistance with plant access, Health, Safety & Environmental authorisation support, and in finding and providing plant production information has been invaluable.

Last but not least I would like to thank my PhD Supervisors and the research team at CSIRO. I have been extremely privileged to have worked with this team of people:

- My Principal Supervisor, Dr Peter Holtham, has been amazing. Peter has encouraged me to push through those many moments when the obstacles seemed insurmountable, and I admire his meticulous attention to detail. It has been both a pleasure and an honour to work with Peter, even when it involved complete rewriting of chapters! Peter's support with modelling has also been invaluable.
- My co-supervisor, Dr Bruce Firth, who has provided wonderful support throughout the project with his incredible depth of technical coal processing knowledge and experience. Bruce also facilitated laboratory and office access at CSIRO with the assistance of Mike O'Brien. With experience also come many anecdotes and stories shared from the past, which I thoroughly enjoyed listening to.
- Mr Mike O'Brien, who has been the CSIRO ACARP Project leader, as well as coordinating site trial work, has a great deal of knowledge in both coal processing and sample analysis. Mike has provided many aspects of technical support to this project and I am truly grateful for his generosity of both time and sharing of his knowledge. Mike was also instrumental in providing laboratory support from his team to this and the other CSIRO/UQ combined projects.
- The CSIRO Coal Preparation team, Dr Shenggen Hu, Mr Ian Hutchinson, Dr Philip Ofori, Dr Graham O'Brien, Mr Robert Dixon, Mr Andrew Taylor, Mr Clint McNally and Mr Adrian Berger all deserve a special mention for their ongoing support and assistance during the project.

Keywords

DMC, Dense Medium Cyclone, Coal, Processing, Simulation, dynamic modelling, separation, beneficiation, Coal Preparation, CHPP.

Australian and New Zealand Standard Research Classifications (ANZSRC)

ANZSRC code: 090407 Process Control and Simulation, 50%
ANZSRC code: 091404 Mineral Processing/Beneficiation, 40%
ANZSRC code: 090403 Chemical Engineering Design, 10%

Fields of Research (FoR) Classification

FoR code: 0914 Resources Engineering and Extractive Metallurgy, 50%
FoR code: 0904 Chemical Engineering, 50%

TABLE OF CONTENTS

Contents

List of Figures and Tables

List of Abbreviations and Nomenclature used in the thesis

Abbreviation	Definition
CSIRO	Commonwealth Scientific and Industrial Research Organization
DMC	Dense Medium Cyclone
DMB	Dense Medium Bath
UQ	The University of Queensland
Ep	Ecart Probable
JKMRC	Julius Kruttschnitt Mineral Research Centre
SMI	Sustainable Minerals Institute
ad	Air Dried moisture basis
ρ	Density
RD	Relative density
SG	Specific Gravity
ROM	Run of Mine
RFID	Radio Frequency Identification
RD50	Cut Point of the cyclone
EIS	Electrical Impedance Spectroscopy
D&R	Drain and Rinse Screen
CHPP	Coal Handling and Preparation Plant
LIMN	An abbreviation of the LIMN^{TM} trademark for LIMN the Flowsheet Processor software developed by David Wiseman
MATLAB	Matlab trademark software
SysCAD	SysCAD trademark software

Empirical formulae nomenclature are detailed with each equation.

1. Statement of Contributions to Knowledge

The subject matters that comprise original contributions to this field of knowledge are briefly outlined below:

- The development of a dynamic model of the New Acland dense medium cyclone circuit which, supported through experimental results and existing empirical models, predicted the behaviour of a dense medium circuit.
- The inclusion of dense medium non-magnetics concentration in the dynamic model, predicted using a breakage model.
- The use of novel instrumentation and measurement techniques to collect experimental data for the dynamic model, in particular:
    - The use of RFID density tracers to measure residence times of particles of various densities as they travel through the parts of a coal preparation plant and the dense medium circuit.
    - This technique led to the discovery that 13mm RFID tracer particles of differing densities flow through the medium circuit with variable residence times, however particles travelling through the coal sections of the circuit demonstrated little variation in residence time.
    - Residence times from the RFID tracer work were then used to predict delays in the model.
    - The parallel comparison of 32mm standard density tracers and 13mm RFID density tracers and the discovery that a cut point reversal existed with the above particle sizes on the 1300mm DMC. The 13mm tracers had a lower cut point than the 32mm tracers which is contrary to conventional expectations. The observations were also confirmed when a literature review of a thesis by Wood (1990) demonstrated similar effects. It was therefore determined that one of the original causes postulated by Wood was able to be ruled out as no float sink chemicals were present, therefore eliminating chemical absorption as a possible cause.

2. Literature Review

2.1 Introduction

The subject of this thesis is a dynamic analysis of dense medium circuits. The intention of the research was to utilise dynamic modelling and plant data to describe circuit behaviours in the dense medium circuit at New Acland coal mine. New Acland is a fairly typical example of a coal wash plant treating coarse coal via the DMC and fine coal using spirals and therefore this dynamic model is potentially applicable to other coal mines with a similar plant configuration.

In Australia, it is estimated that over 55% of Australian black coal is washed in dense medium cyclones Kempnich (2000). In a typical Coal Handling and Preparation Plant (CHPP) using dense medium cyclones, it is reasonable to assume that between, 40-70% of the coal fed to the plant would likely be processed by the DMC circuit. For a plant processing 10 million Run of Mine (ROM) tonnes per annum of coal, and 60% of feed entering the DMC circuit, six million tonnes would be processed by dense medium cyclones. At a coal price of $50/tonne, a 1% yield loss due to inefficient operation of this circuit would represent $3 million per year in lost sales. Figure 2.1 shows the potential lost value in a Dense Medium Cyclone circuit through poor operation for a 10 million ROM (Run of Mine) tonne per annum plant. The relative proportions of feed tonnes going to the DMC circuit per annum and the cost of lost coal sales are compared. This is a simplistic view and only considers lost sales due to misplaced tonnes to rejects. Consideration of real value lost should also include the cost of mining, processing and storage of the misplaced rejects.

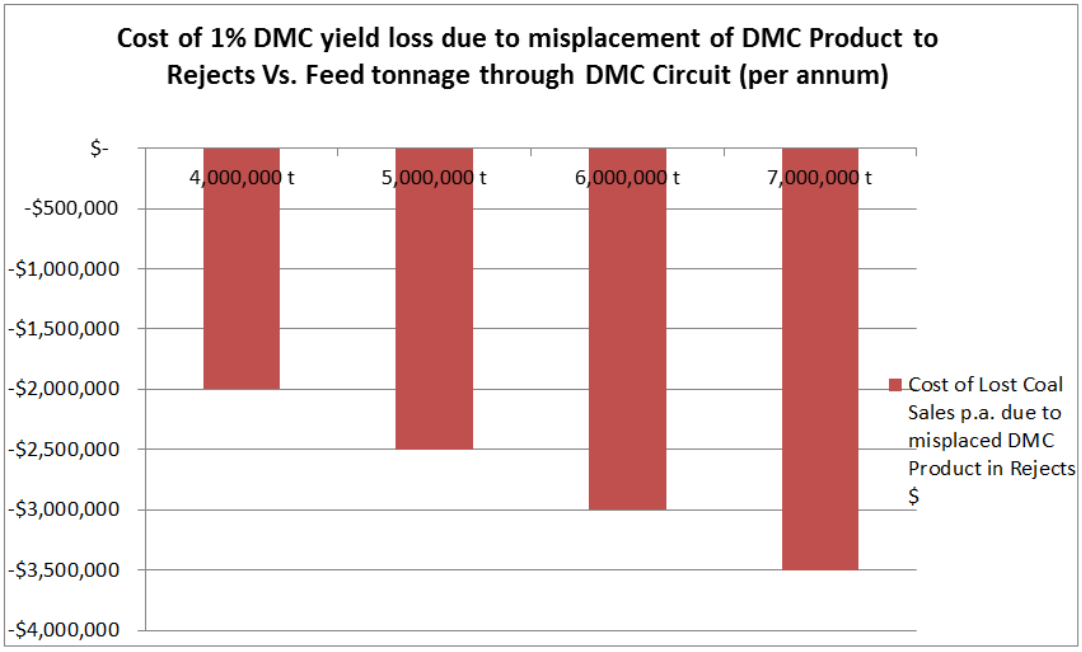

Figure 2.1 Cost of lost coal sales based on a coal sale price estimate of $50/t for a DMC circuit with poor operation causing a 1% yield loss.

Given that the dense medium circuit of a coal preparation plant is critical to the overall performance of the mining operation, a complete and comprehensive understanding of how the dense medium circuit can operate to optimum efficiency is essential. Dense Medium Cyclone (DMC) geometry and DMC performance have been extensively investigated and documented since 1942 when the first DMC patent was registered. Under steady-state conditions, the DMC is generally well predicted, but few have investigated the dynamic changes that take place in a DMC circuit while the plant is running. Research into the dynamic behaviour of dense medium circuits has been limited in the past by a lack of on-line plant data. Recent work has enabled additional data about changes in the circuit to be collected in real time. Medium density fluctuations, screen tonnage rates, medium to coal ratios, changes in the proportion of non-magnetics in the medium, DMC inlet velocities and pressures, classification and sizing of the magnetite, the effects of bleed changes can now be looked at in greater depth.

With a more comprehensive knowledge of the behaviour of a dense medium circuit, plant operators will be able to respond more swiftly to plant changes, thereby minimising yield losses. In a typical coal preparation plant, operator set points are stipulated based on mine yield/ash predictions, steady-state measurements and design parameters. The plant is controlled on a macro level, with tonnage, volume, and density set-point determined to align with variations in plant feed. Existing standard CHPP control technology does not

allow operators to see the subtle changes that occur in the dense medium, for example, when the circuit is unstable. The measurement of non-magnetics in the medium has shown some interesting relationships to DMC circuit stability, highlighting the need for a thorough understanding of the medium changes that occur while the plant is in operation. Better measurement, coupled with empirically derived models developed in past research over the last 40 years, have enabled more accurate predictions to be used in a dynamic model. It is important to note that the intention of this research was not to rework existing empirical models, nor was it to develop new empirical models for DMC operation. Rather, the purpose was to bring together the most useful and industry tested empirical models for each unit operation and to establish a dynamic model for accurate plant prediction using plant data for verification.

2.2 Separation Techniques

There have been numerous techniques employed over time to separate coal from its surrounding mineral matter. Early coal sorting was done by hand and the use of water jigs were employed. The modern Baum or ROM jig is still in use in some applications due to its ability to remove stone effectively. Jig applications in Australia are becoming less frequent due to the increase in size ranges treatable by DMC and also due to the relatively high amount of near gravity material in Australian coals. Near gravity material is defined as the material that lies within 0.02 relative density of the cut point, and the cut point refers to the density fraction of coal in which approximately 50% of the coal will go to product and 50% to reject. This near gravity material can significantly affect the efficiency of the separation equipment. When compared with water based processes, regardless of jig or water washing cyclone type, the dense medium processes have been found to be superior in separating the coal when there is a high presence of near gravity material. The use of jigs are still considered practical in situations where a stone separation is made to the feed, thereby releasing downstream capacity for additional processing loads, however the prominence of jigs in the Australian coal industry is dwindling.

Historically the early dense medium processes in the coal industry used dense medium baths as they allowed high throughput. As dense medium cyclones have become larger in diameter, the need for separate top-size and mid-size processing has diminished. Baths are also limited because Australian coals do not universally liberate well at a bath top size of 100 millimetres. In many cases Australian coals liberate at or below 50 millimetre top

size. This is not the case for other coals such as those in North America where a higher degree of liberation is possible at sizes over 100 millimetres. Ultimately it is the capital cost, operational costs, coal characteristics and footprint that will determine the decision as to which option to use. Nowadays, a DMC can process 100 millimetre top-sized particles and can also process well below 10 millimetre top size efficiently, therefore eliminating the need for an additional process to handle the mid-sized coals. There are still cases where a bath is suitable and can upgrade a plant's capacity at relatively low cost, however DMCs have generally surpassed baths in Australia due to their versatility for a wide range of coal types and size ranges. Furthermore, the use of centrifugal forces in a DMC increases the sharpness of separation when compared to a bath for high near gravity situations. By far the most dominant coarse coal processing equipment option utilised in Australia is the dense medium cyclone as will be discussed later.

2.3 The Development of the Dense Medium Process

The principle of dense medium separation is based on fine grains in suspension in water that behaves like a heavy fluid. In the presence of this heavy fluid called the "medium", material of lower density floats, and the material of higher density sinks. (Osborne, 1988) Coal dense mediums are typically comprised of a suspension of magnetite, water, fine coal and clays. The coal product floats as it is at a lower relative density compared to the medium. Heavier rock and clay materials sink relative to the medium density. The existence of significant amounts of near gravity material in a processing plant can lead to misplacement of coal and rejects during the separation. While today, magnetite is widely used as the main component of the medium for coal separation, this was not always the case. Other fluids were previously trialled for early dense mediums.

In 1858, Henry Bessemer pioneered the first dense medium separator using metal chloride salts in a cone shaped vessel. (Wood,1990, Davis,1987). One of the first separators to be trialled in coal washing was the Chance cone in 1917, which used a slurry of sand and water as the medium. (Scott, 1988) When in 1939, Dutch State Mines used a loess suspension as a separating medium and utilised a hydrocyclone as a thickener for the loess suspension, it was discovered that the overflow pipe occasionally blocked with floating coal. Essentially the hydrocyclone was acting as a dense medium washer using the loess suspension as the dense medium. (Davis, 1987) This led to the development of the modern dense medium cyclone by Dutch State Mines.

The first dense medium baths that were developed used clay or loess as a medium (Williamson and Davis, 2002). The disadvantage of utilising clay or loess, was similar to the other organic liquids and metal salts previously tried. The difficulty and high cost of medium regeneration prevented widespread adoption (Davis, 1987). Magnetite and ferrosilicon were preferred due to their higher densities and strong magnetic recovery advantages. It was not until 1922 that the first use of magnetite medium for coal cleaning occurred on an experimental basis, and not until 1938 that magnetite was used commercially as a medium. (Napier-Munn et al., 2013) It is here where a divergence occurred between use of clays such as Loess and the use of magnetite and ferrosilicon. The focus for Dutch State Mines in developing the dense medium was to find an easily recoverable medium. Once magnetite and ferrosilicon came into widespread use, clays were viewed as contamination and the emphasis was heavily placed on their removal using magnetic separators. Recent research in to the role of non-magnetics in the medium suggested that this insistence on contamination removal may have also had some detrimental effects. This will be discussed later in Section 2.8.

The use of magnetite marked a key difference between dense medium applications in the coal industry when compared with iron ore and diamonds. As the relative density and composition of the dense medium required for coal was lower than for heavier minerals, magnetite was able to be used in place of ferrosilicon. Coal dense medium processes typically operate in the relative density range of 1.30 to 1.80. (Osborne 1988) Magnetite is used as the dense medium and it has a density in the range of 4.2-5.1. The floats material in the case for iron ore and diamonds is the reject as the density of the ore product is higher than its surrounding in-situ mineral matter whereas the floats material for coal is the product. For heavier minerals, ferrosilicon is used instead of magnetite when a higher density range of operation is required, and sometimes a combination of the two are used.

Large diameter DMCs have permitted the use of coarser grades of media than in the past. A reduction in the rate of loss of finer magnetite has been a major benefit, however, the use of coarser grades is contingent on the DMC maintaining medium stability. At the lower densities targeted for coal, the viscosity of the dense medium is rarely an issue in Australia, though medium stability is significant. Other coal types, such as those in North America may exhibit more frequent viscosity problems. While most coal plants are

designed to continually clean non-magnetics from the circuit, too little non-magnetic material can also be detrimental to the stability of a circuit.

The early research in to the use of loess as a medium was abandoned due to the difficulty of medium recovery, however, natural clay bands in the coal seam could be considered as a potential medium stability enhancer in a dense medium cyclone or bath circuit in the future. Recent research by Firth et al. (2011) has revealed that the presence of clays and other fine non-magnetic material in the medium can be instrumental in determining its stability. This is particularly the case when operating at a density target below 1.4RD (Relative Density). This is currently an area of ongoing research. In the drive to maintain high levels of production, and to rid coarse coal circuits of clay contamination, an opportunity to acknowledge the benefits of the natural medium created by clays and fine materials in the suspension of a cyclone may have been missed. This will be discussed further in Section 2.8.

The effect of medium stability on the control of the dense medium cyclone circuit has been an interesting subject of recent research. The New Acland coal mine in the Clarence Moreton basin of South Queensland has provided some interesting data with numerous instruments installed in the dense medium circuit. Coupled with regular sampling audits, the CSIRO in conjunction with The University of Queensland have been collating data on how a circuit responds to various changes, including the changing levels of non-magnetic material in the medium. The outcome of this work will enable greater knowledge of circuit behaviour and better control system design for faster response to stability issues in the circuit.

The following sections will discuss the evolution of the dense medium cyclone, the role of the medium and aspects of control of the dense medium cyclone circuit.

2.4 The Dense Medium Cyclone

In 1942, the first Dense Medium Cyclone was patented by Driessen, Krijgsman and Leeman. Although the first design patent did not include a vortex finder, this feature was added to the patent a few years later. (Wood, 1990) Dutch State Mines realised the transferability of their invention to other minerals such as iron ore and diamonds, and in 1955 dense medium cyclones were first used in diamond processing (Napier-Munn, Bosman and Holtham 2013). By 1960, there were twenty-three dense medium cyclones in operation worldwide. (Wood, 1990) The modern DMC varies only slightly from the original 1960s designs by Stamicarbon. Some higher capacity designs have evolved, but many manufacturers still adhere closely to the original DSM specifications (de Korte and Engelbrecht 2007) The original handbook, entitled "The Heavy Medium Cyclone Washery for Minerals and Coal" (Stamicarbon 1969) detailed key design parameters for the dense medium circuit and is still referred to today. More recent additions have also been made to the handbook, with the most recent being in 1994 (Cresswell, 2005). By 1980 approximately 370 DMC plants had been built and 270 of these were in the coal industry. In Australia, by 1990, over 100 million tonnes of coal were processed by DMC (Wood, 1990) and today, the majority of wet processing coal plants in Australia use DMCs as a key component.

Materials of construction such as alumina tile linings and 'Ni-hard' cast bodies have improved dense medium cyclone component wear rates. Changed cyclone inlet designs such as tangential, involute and scrolled evolute have advanced the flow patterns in the DMC. Application of computational fluid dynamics has been used to improve flow patterns and consequently wear rates for the redesigned inlets. In recent years, with the increased use of DMCs in high volume commodities such as coal and iron ore, higher capacity and larger diameter cyclones have emerged. Currently in the coal industry in Australia, the largest DMCs in operation are 1500mm in diameter.

Although dense medium cyclones have existed since the 1940s, there have been only minor adjustments to their design. Entry designs such as evolute entry have enabled more consistent wear profiles when compared with the more traditional tangential entry designs. The barrel and lower cone lengths have been varied from traditional DSM designs in some cases to increase residence time in the cyclone, and higher capacity units

have also been developed. Essentially though, the structure and fundamental design of the dense medium cyclone remains the same as it did 70 years ago.

Advances in dense medium processing have been more pronounced in the circuit design area rather than in the DMC itself. The introduction of gravel pumps and variable speed drives have improved the stability of operation, (*Crowden, et al.,2013).* Nucleonic gauges and better tuning of process control loops have enhanced the control aspects of dense medium processing. There have also been improvements to the magnetic separator designs, (*Cresswell 2005).* Co-current separators have been replaced by counter-current, and the strength of magnets has increased, thereby reducing the need for auxiliary magnetic separators to do a second stage recovery. There are now new designs using radial magnets and self-levelling magnetic separators. All of these advances have enhanced the recovery of magnetite from the circuit while at the same time, efficiently removing non-magnetics from the medium. Screening technology has also advanced with the development of multi-slope screens (sometimes called “banana screens”) and static “flume” screens. Screens are now larger with higher capacities, and screen panels have also gone through various design improvements. Density tracers have also enabled better monitoring of circuit performance without the need to wait several weeks for a result to be returned from the laboratory, (*Cresswell, 2005).*

Despite worldwide improvements in dry sorting technology, dense medium cyclones remain an efficient means of separating coal. Dry sorting technologies such as optical, laser and X-Ray transmission sorting are unlikely to be widely adopted in Australia due to their low capability for processing the high levels of near-gravity material normally present in Australian coals. The presence of sticky clays that require desliming is also a limiting factor. (*Cresswell, 2005)*. It is likely that dry sorting technologies may be used as a pre-treatment step at the front-end of a process to remove stone from the plant feed thereby boosting overall CHPP capacity, however dense medium processes will remain integral in future plant development.

The use of dense medium baths is less prevalent in Australia than overseas. In Australia, approximately 11% of black coal (versus 20% overseas) is processed via dense medium baths. (Kempnich, 2000) The presence of significant quantities of near-gravity coal and the tendency of Australian coals to liberate at smaller top-sizes than in the USA, may be the primary driver for this trend. As larger DMCs can now process at top-sizes of 100mm,

the need for dense medium baths has become less common in Australian new plant designs, and plant upgrades often result in a switch to large DMCs.

Increases in cyclone diameter in recent years has prompted additional research into cyclone efficiency. Original Dutch State Mines design parameters did not cater for larger DMC sizes. The increased diameters have enabled treatment of coarser particles, therefore generating higher throughput per unit. Larger DMCs have also in some cases, eliminated efficiency drawbacks of running a biased Y-piece distributor adjoining two DMCs in parallel. The introduction of gravel pumps that can handle larger top-size particles has also played an enabling role in the evolution of larger DMCs. Clarkson and Holtham (1998) noted that inefficiencies created by poor distribution of the slurry between parallel modules can be equally as important as the intrinsic unit process efficiency. There can also be efficiency losses associated with twin DMC pairs that are not geometrically identical due to uneven wear, or different internal profiles. Where one DMC does not operate at the same RD_{50} as its twin, misplaced coal will result. The author recalls one such situation where a maintenance team thought that money could be saved by replacing the single DMCs when individually worn instead of the entire DMC pair, with drastic efficiency consequences. In plants where DMC maintenance is not tightly controlled with metallurgical supervision, it is often preferable to replace twin DMCs with a single, larger sized DMC, thereby eliminating the temptation to not replace the pair with identical twins, and also eliminating the Y-piece bias effects. The benefits of better (lower) Eps for smaller diameter DMCs are quickly negated if twin units operate at different cut-points. Larger DMCs also allow easier entry for inspection and repair (Davidson, 2000).

Table 2.1: Typical cyclone dimension design trends compared with Dutch State Mines (DSM) original recommendations (De Korte and Engelbrecht, 2007)

Parameter	**DSM Recommendations**	**Current Manufacturing Trends**
Cyclone Diameter		**Up to 1500mm**
Inlet Size	**0.2 x cyclone diameter**	**0.2, 0.25 or 0.3 x cyclone diameter**
Vortex Finder Diameter	**0.43 x cyclone diameter**	**0.43 or 0.50 x cyclone diameter**
Barrel Length	**0.5 x cyclone diameter**	**0.5 to 2.5 x cyclone diameter**
Spigot Diameter	**0.3 x cyclone diameter**	**0.3 to 0.4 x cyclone diameter**

Table 2.2: DMC Sizes. As dense medium cyclones increase in diameter, both capacity and top size increase, thereby providing opportunities for capacity expansion with fewer equipment items. Below dimensions are for Multotec cyclones. (de Korte and Engelbrecht 2007)

	Standard-capacity Cyclones		High-capacity Cyclones	
Cyclone diameter	Maximum particle size	Coal Feed	Maximum particle size	Coal Feed
mm	mm	t/h	mm	t/h
510	34	54	51	99
610	41	81	61	145
660	44	97	66	175
710	47	114	71	207
800	53	149	80	270
900	60	196	94	355
1000	67	249	100	454
1150	77	351	115	638
1300	87	468	130	854
1450	97	608	145	1108

As cyclone diameter increases, centrifugal acceleration decreases, (Mengelers, 1982). However, for coarser particles, the efficiency of a large diameter cyclone is equal or better

than that of a dense medium bath due to the presence of centrifugal acceleration which creates increased g-forces inside the cyclone. The three product DMCs in use in coal wash plants in China and South Africa are designed to utilise the ease of separation of a large proportion of the feed in the inlet and first part of the DMC body to separate off a first product, and diverting the middlings stream into a second cyclone-shaped chamber. This early separation of coal in the inlet and entry to the DMC body is also observable in the typical wear patterns of a DMC where considerable wear is present in the first revolution after entry. Wear then reduces until the rejects reach the spigot where wear again increases. The early removal of easily separated material allows more time for the near-gravity material to separate without the increased particle interactions.

For finer sized particles, a breakaway size is thought to exist. Engelbrecht and Bosman (1994) identified a potential drop in efficiency of minus 4mm particles in large cyclone separators and a shift in cut density as cyclone diameter is increased (de Korte and Engelbrecht 2007). Below the breakaway size, it is thought that efficiency deteriorates and a shift in cut density will also occur (Crowden et al. 2013). Figure 2.2 demonstrates the concept of breakaway size. De Korte and Engelbrecht (2007) noted that although a breakaway size may exist, the perceived drop off in efficiency obtained in dense medium cyclones is still much better than the efficiency of a water-based process such as a spiral or teeter-bed separator (TBS).

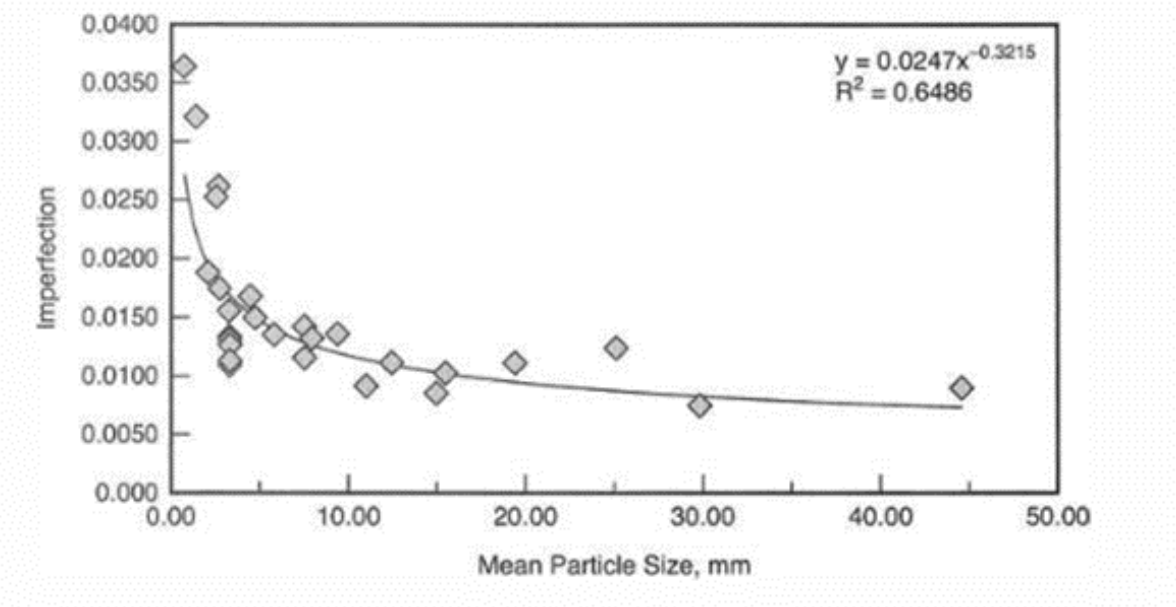

Figure 2.2: Particle size versus imperfection for South African cyclones (mostly 610mm) suggesting that a breakaway size may exist. (de Korte and Engelbrecht 2007))

Anecdotally, there is considerable conjecture among Australian coal preparation experts, as to whether the breakaway size issue really exists, or whether its appearance results from sampling difficulties in plants. Finer coals can adhere to surfaces and not wash off at the desliming screen, thereby being carried over into the coarse fraction. Sizing of screen apertures can vary the bottom size of the coarse coal fraction, and misplaced coarse material, particularly if flat in shape, can slip through screen apertures. The sample treatment and analysis need to take into account the screen aperture size and possible material misplacement of this size fraction. In addition to the potential for errors in sampling around the screen cut point, Clarkson et al. (2002) found that over a series of studies of larger DMC operations that processed particles larger than 1.0mm, no significant degradation in performance (in terms of Ep) was found. Clarkson et al. also found that there was no discernible difference in the +4mm and -4mm by 1mm size fractions in terms of Ep performance. They suggested that other changes to plant conditions and designs, such as operating at high medium to coal ratios to mitigate the effects of high near gravity material could influence cyclone efficiency.

The presence of near gravity material can greatly influence the efficiency of separation of a cyclone as shown in Figure 2.3 below.

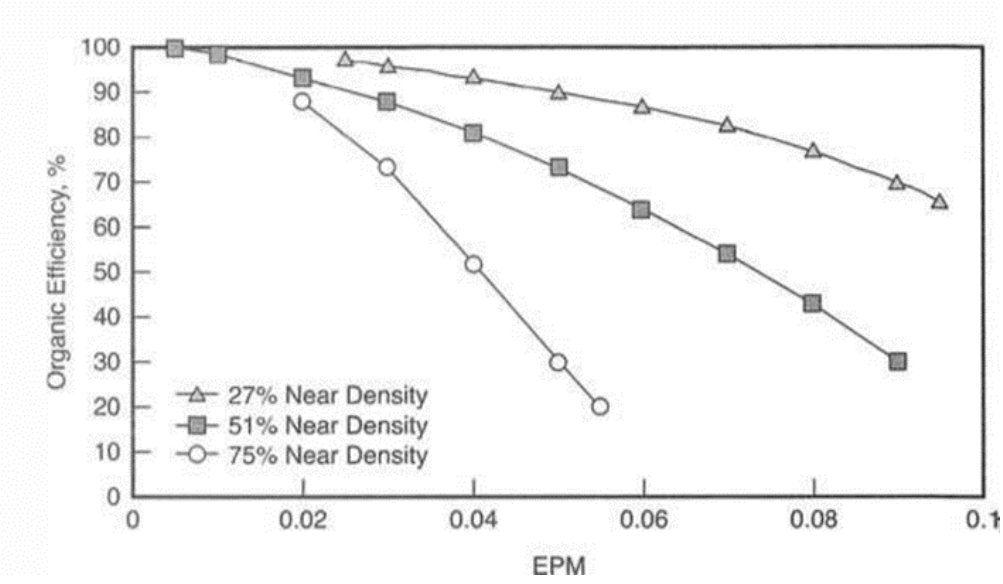

Figure 2.3: Organic efficiency versus Ep for various percentages of near gravity material. (de Korte and Engelbrecht, 2007)

Clearly with higher proportions of near gravity material, determining the correct cut-point (RD_{50}) for the cyclone is critical to achieving the target yield and organic efficiency for a particular coal.

As knowledge of dense medium cyclones and their efficiency parameters have evolved, so have research and development of empirical models to describe DMC behaviour under plant conditions. The following section outlines the most recent research into empirical model development and also highlights some of the models that have been widely relied upon in the coal industry for some time.

2.5 Empirical Models

Much of the previous work relating to dense medium cyclone modelling has been achieved with steady state models based on empirical derivations. Wood et al. (1989), looked at various aspects of dense medium cyclone operation from an empirical perspective. Past experimental data and literature were utilized to develop a series of sub-models consisting of empirically derived relationships between a number of measured parameters. (Figure 2.4) The eight sub-models in the Wood model considered medium behaviour as an important parameter in predicting partitioning performance. The models also considered unstable operation and factors influencing surging. 5mm tracers were used under “no load” conditions to determine the partitioning performance without the presence of coal feed or contamination in a pilot plant at the JKMRC (Wood, et al. 1989). The JKMRC Wood Model has been widely used by coal industry practitioners as a predictor of DMC performance. Under standard plant conditions, without surging or unusual events, and with DSM Handbook design parameters for the cyclone, this model provides reasonable predictions. As newer cyclone designs deviate from DSM standard designs, and diameters increase beyond the limits provided by the experimental data used to derive the Wood model, empirical model parameters may need to be modified.

Sub Model No.	Description	Symbol	Value	Units
	FEED CHARACTERISTICS			
	The Task			
	circuit Feed rate (adb)		800	t/h
	product ash required		7.0	%
	M:C in feed (minimum)		3.75	-
	Washability Data - preliminary estimate			
	feed coal density		1.45	RDU
	RD for target ash		1.36	RDU
	yield at target ash		62.0	%
	floats density at target ash		1.30	RDU
	Estimates of Flows of Feed Coal, Floats and Sinks			
	Mass Flows			
	floats		496	tph
	sinks		304	tph
	Volume Flows			
	feed coal		552	m³/h
	floats		382	m³/h
	sinks		170	m³/h
	feed slurry for target M:C		2621	m³/h
	DMC SELECTION (DSM design) ∴ D_o = 0.43 D_c and Di equiv is 0.20 D_c			
	cyclone diameter	D_c	1.000	m
	vortex finder diameter	D_o	0.430	m
	spigot diameter	D_u	0.320	m
	inlet head (cyclone diameters)	Head	9.0	Dc
	inlet head (m of slurry)		9.0	m
SM1	feed slurry flow	Q_f	704	m³/h
	cyclones Required		3.73	(1)
	Decision Point			
	(1) *Round the number up to an integer commensurate with preferred plant layout, or enter an alternative Dc.*			
	number of cyclones to be used		4	
	For a single cyclone			
SM1	feed coal solids	Q_{fs}	138	m³/h
	floats coal solids	Q_{os}	95	m³/h
	sinks solids	Q_{us}	43	m³/h

Figure 2.4a

Sub Model No.	Description	Symbol	Value	Units
	MEDIUM FLOWS per cyclone, if operating with medium alone			
SM2.1	medium split to u/f	Q_{uz}/Q_{fz}	0.101	-
SM2.2	underflow rate	Q_{uz}	71	m³/h
SM2.3	overflow rate	Q_{oz}	632	m³/h
	MEDIUM FLOWS per cyclone, if operating with medium plus coal			
SM2.4	underflow rate (increases with sinks loading)	Q_{um}	86	m³/h
SM2.5	overflow rate	Q_{om}	537	m³/h
	feed rate (also increases, improving M:C in feed)		623	m³/h
SM2.6	medium split to u/f Qum/(Qum+Qom)		0.138	m³/h
	Check Point - medium-to-coal ratios			
	feed recommended to be	4	4.5	
	overflow recommended to be	3	5.6	
	underflow recommended to be >	2	2.0	
	MAGNETITE SIZE and MEDIUM DENSITIES			
	Magnetite size intercept	P_{rr}	31.0	microns
	Medium Densities in RD units			
	feed (prelim estimate)	ρ_{fm}	1.21	
SM3	underflow	ρ_{um}	1.642	
Sm4	overflow	ρ_{om}	1.143	
	differential (u/f - o/f)		0.249	(3)
	CUTPOINTS, RETENTION and VALUES OF E_p (75-25) in RD units			
SM5	Cutpoint for +4mm particles	ρ_{50A}	1.298	(2)
SM6	Retention Upper Limit (treat as indicator only)	R_{max}	1.389	
	Retention Range (treat as indicator only)		0.091	(4)

Check Point

(2) *Is the cutpoint where we want it? If not, adjust ρ_{fm} to bring cutpoint within 0.002 RDU of target.*
(3) *If differential > 0.4 RDU there may be retention which can progress to surging and loss of yield.*
(4) *If retention range > 0.15 RDU and topsize >20mm there is danger of surging with loss of yield. Take steps to reduce it.*

Figure 2.4b

Predicted Partition Curves *sub-models 7 and 8, using Whiten partition curves*

Original - as in thesis

	+4mm	-4+2mm	-2+1mm	-1+0.5mm
ρ_{50}	1.298	1.321	1.352	1.414
$E_{p(75-25)}$	0.004	0.013	0.026	0.052

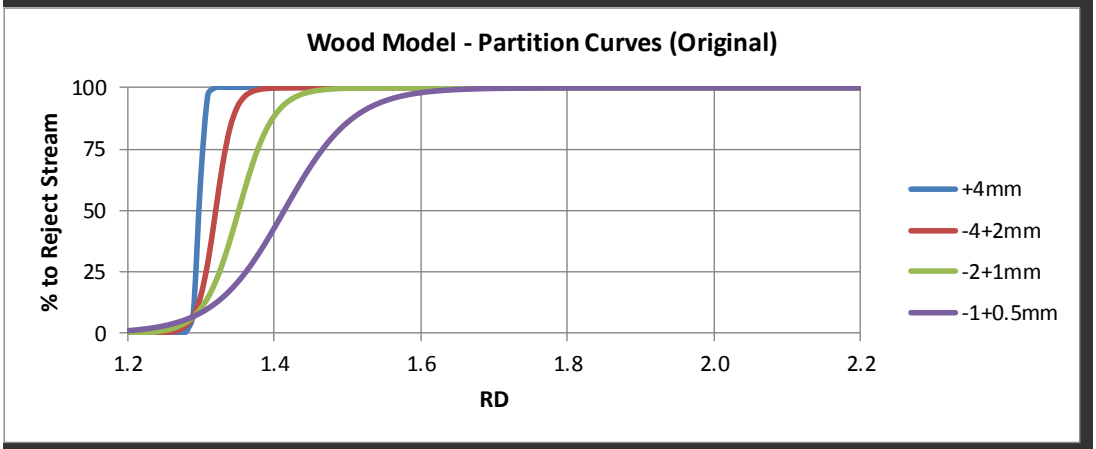

Modified - incorporating Pivot phenomenon, which has not been fully assessed against coal data

	+4mm	-4+2mm	-2+1mm	-1+0.5mm
ρ_{50}	1.298	1.314	1.336	1.379
$E_{p(75-25)}$	0.004	0.013	0.026	0.052

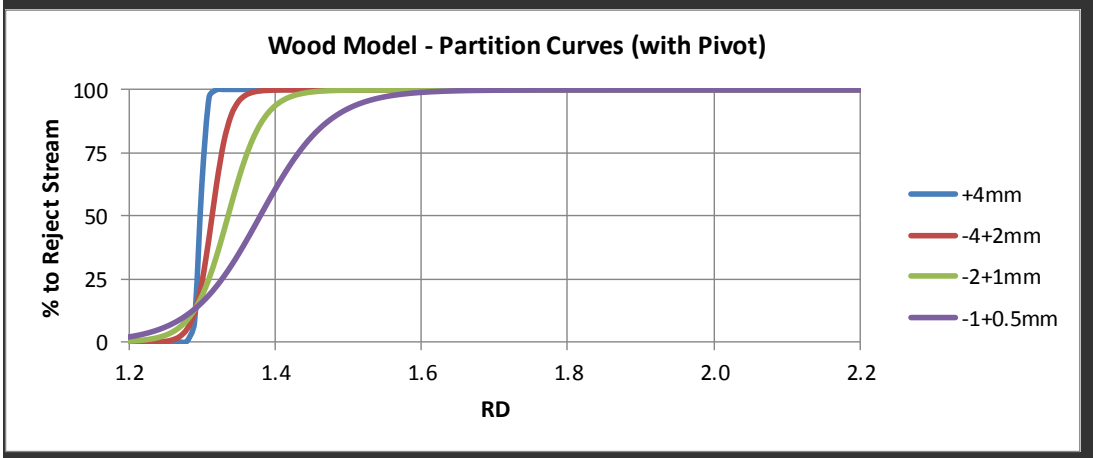

True E_p levels may be smaller than can be adequately resolved by float/sink techniques or even by tracers. They may or may not be as small as indicated here.

Figure 2.4c

Figure 2.4 (a, b and c): The JKMRC Wood model calculation spreadsheet with input parameters and calculated results. (Crowden et al., 2013) The model predicts the cut point, medium splits between underflow and overflow, flow rates, and a partition curve.

The Wood model was developed specifically for coal washing DMCs with diameters up to 710mm (Wood, 1990; Clarkson and Wood, 1991). The first equation in the Wood model

(Scott et al., 2013) uses cyclone dimensions and inlet pressure to predict the total volumetric flow of medium and raw coal combined entering the DMC:

$$Q_f = 2.87 \times 10^{-5} D_c^{2.30} Head^{0.46} \left(\frac{D_u}{D_o} \right)^{0.17} \quad 1$$

where D_c, D_u, D_o are the cyclone, spigot and vortex finder diameters respectively in mm, and $Head$ is the inlet pressure in 'diameters'. Q_f is in the units m^3hr^{-1}

Once the volumetric flowrate of the feed is known, the second equation calculates the fractional flow split of slurry (reject plus medium) to the spigot where Q_u/Q_f. This assumes that there are low loadings of reject and Q_u is the volumetric flowrate to underflow for coarse rejects and medium combined in m^3hr^{-1}:

$$\frac{Q_u}{Q_f} = 9.29 D_c^{-0.31} Head^{-0.46} \left(\frac{D_u}{D_o} \right)^{4.16} \quad 2$$

This flow split is then used to predict the underflow medium density ρ_u in Equation 3:

$$\rho_u = \rho_f + 7.28 \times 10^{-3} \left[\rho_f \left(\frac{Q_u}{Q_f} \right)^{[0.194(\rho f - 2.07)]} - \rho_f \right] \times \rho^{1.34} Head^{0.562} D_c^{-0.145} \left(1 - \frac{0.5}{M:C} \right)$$

3where ρ_f is the feed medium density, p is the medium grind size in microns (the Rosin-Rammler intercept), and $M:C$ is the volumetric feed medium to coal ratio. (Scott et al., 2013)

With the medium split and underflow medium density now predicted, Equation 4 calculates overflow density. The factor 1.52 in equation 4 below compensates for error in the flow split equation due to cyclone head and sinks loading:

$$\rho_o = \rho_f - 1.52\left[\rho_f - \frac{\rho_f - \left(\frac{Q_u}{Q_f}\right)\rho_u}{1-\frac{Q_u}{Q_f}}\right] \qquad 4$$

The corrected cut point ρ_{50c} for coarse particles (plus 4mm) is calculated using the feed, overflow and underflow medium densities:

$$\rho_{50c} = \rho_f + 0.125 + 0.154\rho_u - 0.215\rho_o \qquad 5$$

If there is particle retention in the coarse fraction, then this is can be used to approximate the minimum density of retention, Rmin. (Wood, 1990)

The sixth sub-model estimates the relative density range for retention of particles in the cyclone. This relationship serves as a guide for cyclones with a feed topsize (d_{max}) of 0.04 to 0.05 times the cyclone diameter. Rmin is the minimum density of retention. (Wood, 1990)

$$\mathrm{R_{max}} - \mathrm{R_{min}} = 0.59 - 0.3\rho_f + 8\frac{d}{D_c} - 3\left(\frac{D_u}{D_c}\right) + 0.02 * Head - \left(\frac{0.2}{M:C}\right) + 0.01P \qquad 6$$

Equation 7 predicts the separation density (cut point, ρ_{50d}) and equation 8 the Ecart Probable (Ep_d) for particles of any size:

$$\rho_{50d} = \rho_{50c} + 0.0674\left(\frac{1}{d} - \frac{1}{10}\right) \qquad 7$$

$$Ep_d = 0.0333\frac{\rho_{50c}}{d} \qquad 8$$

where d is the particle size (square mesh) in millimetres, and the factor 1/10 in equation 6 implies that the mean size of coarse particles is 10 mm.

Equation 8 generally predicts extremely low Eps for coarse particles, and is often 'corrected' by a factor to give values more in-line with those obtained experimentally (Wood, 1990).

Once the ρ_{50} and Ep are determined, the modified Whiten equation (equation 9) is used to generate a partition curve. The form of the equation means that a symmetrical S-shaped curve is produced, with the high and low density tails constrained to give partition numbers of 100 and 0 respectively. If DMC operating conditions are such that tails exist, eg coal lost to reject, this model will not reflect actual DMC performance. (Scott et al, 2013)

$$PN = \frac{100}{1 + e^{1.0986\left(\frac{\rho_{50} - \rho}{Ep}\right)}} \qquad 9$$

Figure 2.5 below demonstrates the process flow for the use of the Wood model.

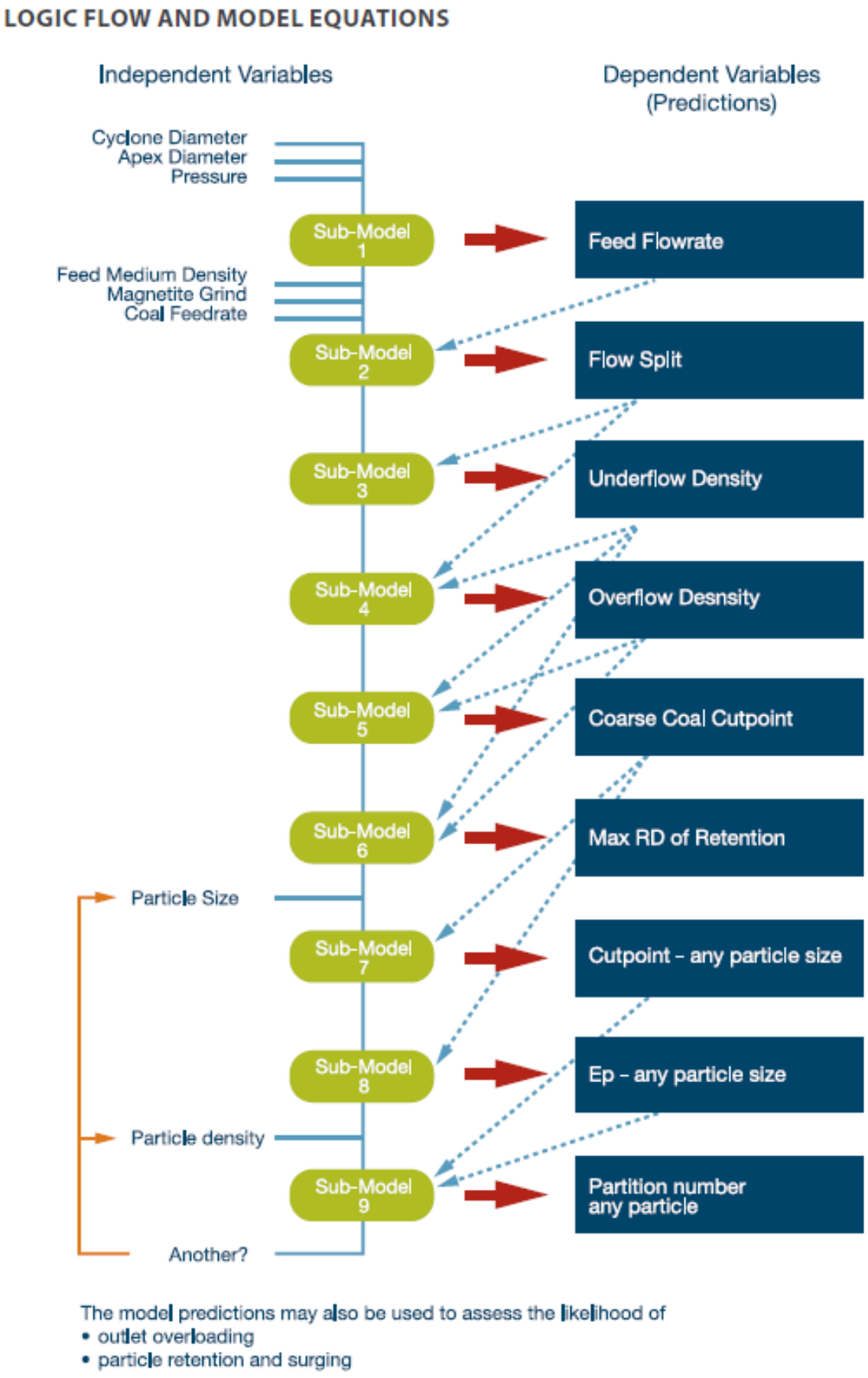

Figure 2.5 Flow of model equations in the Wood Model. (Crowden et al. 2013, p145)

The JKMRC/Wood model (Wood et al. 1989) has proven to be a suitable predictor of DMC behaviour under standard conditions, and is often used in practice due to its simplicity. The model developed by Dunglison (1999) at the JKMRC also provides a good prediction based on verification from experimental data, however, it is significantly more complex than the Wood Model and was not widely published, thereby leading to its reduced use. It does however, have broader application to iron ore, diamonds and larger dense medium cyclones.

Dunglison (1999) extended the existing JKMRC models and developed a robust quantitative mathematical DMC model which incorporated past work by Wood (1990), and expanded it to include larger diameter cyclones greater than one metre. The Dunglison Model also increased the applicability of the existing model by applying it to heavier density applications such as diamonds. The model predicted the characteristic partition curves, flow rates, medium splits and product densities. The Dunglison model utilised elements of the Concha and Christiansen (1986) model and the pulp split model developed by Schubert and Neese (1973). Its complexity is considerably higher than that of the Wood model, though it is still readily implemented in an Excel spreadsheet or similar software. Medium viscosity used in the Concha and Christiansen model, is considerably more important in applications such as diamonds and iron ore where ferro-silicon medium is used at higher densities, however for coal, viscosity is not normally an issue. Scott et al. (2013) ran a side-by-side online comparison of the Wood and Dunglison models using one hour of coal plant data and observed that the differences between the two models were relatively minor. Ep comparisons were similar with the mean cut point over one hour differing by 0.001 relative density point between the two models. While the Dunglison model consistently predicted slightly lower overflow densities and slightly higher overflow medium densities when compared with the Wood model, the cut point differences between the Wood and Dunglison models were negligibly small. Experimental results from sampling taken on the same day revealed that the predicted yield results aligned well with the measured yields with a difference of 0.9%. Although this difference would be of considerable significance over time, the other DMC predictions suggested that the comparison was satisfactory. (Scott et al. 2013) In the case of the plant under study as part of this PhD thesis, the benefit of online instrumentation measuring underflow and overflow density over time has meant that this difference, however slight, in underflow and overflow density model predictions can be ignored. In addition, the low focus on viscosity negates the need for a more complex model. The author therefore recommends using the

Wood model, with its reduced complexity and direct applicability to coal applications, along with online instrumentation measuring overflow and underflow density as part of the dynamic model.

Prediction of separation density (RD_{50}) and Efficiency (E_p) have also been investigated by Hu and Firth (2010). They utilised measured medium densities of the feed, overflow and underflow streams to predict RD_{50} and E_p without the need for float sink analysis. A modified suspension-partition model was used to derive the following three equations to describe medium density and RD_{50} for a conventional DMC.

$$\rho_m = \rho_f + (\rho_u - \rho_0)\left(1 - \left(\frac{2y}{H_t}\right)\right) \quad 9$$

$$H_M = 0.37H_t \quad 10$$

$$RD_{50c} = \rho_f + 0.26(\rho_u - \rho_o) \quad 11$$

Where H_m is the middle point of the effective separation region for the medium;
H_t is the DMC radius;
ρ_m is the density of the medium which is a linear function of the radial distance from the wall, y;
ρ_f is the medium density of the feed;
ρ_o is the medium density of the overflow;
ρ_u is the medium density of the underflow;
and RD_{50c} is the separation cut point.

The Partition number, P_N is given by Equation 12:

$$P_N = \left(\frac{H_S \alpha_{c,S}}{H_t \alpha_{c,H}}\right) \quad 12$$

Where $\alpha_{c,S}$ and $\alpha_{c,H}$ are the mean values of α_c (the volume fraction of particles) in the ranges of H_S and $H_{t'}$ respectively and where H_S and $H_{t'}$ are parameters in the suspension-partition model. ($H_{t'}$ is the radius of the DMC and H_s is the particle separation boundary).

They found that these models generally fitted the partition curves for the plant data used, with close agreement with the tracer test results. It was determined that the results showed a sufficiently close indication for use in on-line monitoring. A comparison of accuracy of the Hu and Firth (2010) model and the Wood model has not been made here, however it appears that either model would work for the purpose of the dynamic model for typical Australian coals provided that the DMC is of conventional design. If the DMC were to deviate from DSM design geometry conventions, it would be necessary to modify the equations.

Desliming Screen Models

Various other models are useful in determining a dynamic model of a coal dense medium circuit. Desliming screen designs follow various rules of thumb outlined in the DSM Handbook and as specified by McKay (1984), and drainage capacities for multi-slope screens were experimentally determined in ACARP report C7048 (Crowden et al. 2013). Table 2.3 represents the best estimates of drainage rates for multi-slope de-sliming screens based on this research.

Table 2.3: Recommended drainage capacities for multislope screens

From Crowden et al. (2013, p52) Nine modules from six plants were studied as part of ACARP study C7048 and screen apertures from 0.5mm to 1.4mm wedge wire were considered.

Aperture mm (wedge wire)	Drainage $m^3/h/m^2$
0.5	20
1.0	65
1.4	80

Screen loadings are generally determined using the DSM Handbook formula as follows:

$$C = 19 \times \sqrt[3]{(d_a \times \rho_{pr})^2} \qquad 13$$

Where C is t/h per m width, d_a is average grain size in mm, and ρ_{pr} is the RD of an average particle

When comparing desliming screens with drain and rinse screens, the factor of 19 is changed to 12 for drain and rinse screens. (Crowden et al. 2013, *p52*)

The above formula is applicable for multislope or low head screens, though a mechanical tonnage limit of 80 t/h/m typically applies for low head screens. Multislope screens are generally higher velocity and thinner bed depth, so water flow and fines transport is less restricted when compared with a low head screen. The formula was derived from multislope screen experimental data.

Commonly used in steady state software, is the Whiten and White Equation (Napier-Munn,et al. 2005, p298)

$$E(x) = e^{\left[-N f_0 \left(1-\frac{x}{h}\right)^k\right]} \qquad 14$$

Where E(x) is the fraction of particles in the feed of size x which enter the coarse product, h is the screen aperture, f_0 is the fraction of open area, N is the efficiency parameter which is analogous to the number of trials, and k is a minor parameter used for precise fitting purposes. (generally k≈2)

Equation 14 was not designed for the multi-slope screen and would generally apply, however, the DSM screen model would be more typical to the types of screens used in a coal operation.

Drain and rinse screen models

Recent work by Firth & O'Brien (in Crowden et al. 2013) in ACARP Project (O'Brien et al. 2010) determined new empirical relationships for drain and rinse screens. Prior to this, designers relied upon rules of thumb detailed in the DSM Handbook (1968) of 30-40m^3/h depending on topsize for the volume of rinse water required for a low head screen. Another rule of thumb was to use one cubic meter per hour of rinse water for each t/h of solids. Since multislope screens have significantly greater drainage capacity compared with low head screens, the specific drain rate is dependent on open area and aperture. Firth and O'Brien in 2010, (Crowden et al 2013) derived the following measure of actual screening efficiency (Equation 15)

$$Pa = Rf + (1 - Rf) \times (\frac{x}{Ap})^N$$ 15

Where Pa is the partition number for actual screening efficiency, *Rf* is the proportion of water originally in the feed that reports to the oversize flow stream, and Ap is the screen aperture for N attempts of a particle passing through the screen. x represents particle size

Specific Drain Rate was determined from a study in 2000 by Meyers et al. where a strong relationship between solids drain rate and volume drain was found. The key relationship identified was that the main factor influencing transport through the particle bed was hydraulic, and not stratification. From this, the specific drain rate formula (O'Brien et al. 2002) was derived in equation 16.

$$SDR = \frac{C1 \times Q^{0.5} \times Ap^{0.5} \times OA^{0.5}}{e^{C2.ThiC}}$$ 16

Where SDR is the specific drain rate ($m^3/h/m^2$), C1 and C2 are constants, Q is the volumetric flow rate of the medium or water and underflow solids per m^2 of screen, Ap is the screen aperture width (mm), OA is the Open Area fraction, and ThiC is the volume fraction of coarse coal in the feed. (Crowden et al. 2013)

From the specific drain rate equation, the relative medium drain rate (RMDR) is determined by dividing the equation by the volumetric flow rate of the medium or water and underflow solids per square metre of screen. Firth and O'Brien 2010 showed that Rf for the drain section could be described by another relationship which gives an estimate of the final drain section moisture level given that the drain rate is reasonable.

$$Rf = \frac{1 - 0.98 \times Ap^{0.56}}{Q^{0.2}}$$ 17

As a rule of thumb, it is generally assumed that the rinse section final moisture level is around 20% by mass of the oversize stream. (Crowden et al. 2013)

Magnetic Separator Models

Numerous models have been developed to describe the dilute circuit of a dense medium plant. Often a figure of 99.8% recovery of magnetite is quoted for modern magnetic separators. This is usually based on the level of magnetite loss in the tailings stream.

Another method of measurement plants use is to reconcile deliveries of magnetite against plant tonnage rates to estimate losses. This provides an average rate of loss over time but will not give instantaneous results and is therefore not particularly useful for troubleshooting causes unless they occur continuously over the period studied. The advantage of the reconciliation method is that it includes losses through adhesion, maintenance of rinsing sprays and housekeeping which in the author's experience, often comprise the most significant losses. The model developed by Rayner (1999) was experimentally determined under laboratory conditions and gives a good indication of what a magnetic separator is capable of achieving when operating well, excluding factors such as adhesion and housekeeping.

Rayner and Napier-Munn (2003) determined the following relationship for estimating potential magnetite loss, (L):

$$L = \left(1 + \frac{2.7M}{N^{-0.7}}\right) Q_{sf}^{-0.13} \times f^{0.12} \qquad 18$$

Where:
Q_{sf} is the feed flow rate ($m^3/h/m$) and f is the % by mass of solids in the feed

The amount of water reporting to the concentrate (over-dense) stream of the magnetic separator is assumed to be constant at 25% when calculating the water flow rate of magnetic separator concentrate Q_{scw}

$$Q_{scw} = 0.25 \times Q_{sfw} \qquad 19$$

Where Q_{sfw} is the water flow rate in the magnetic separator feed ($m^3/h/m$)

The third equation used in the magnetic separator model utilised the work of *Hart et al. (2007)* to calculate the level of entrainment of non-magnetic particles in the separator.

$$Ent\% = 4.5 \times NM^{-0.23} \times M^{0.96} \qquad 20$$

Where M is the tonnes of magnetics per 100 tonnes of slurry and NM is the tonnes of non-magnetics per 100 tonnes of slurry.

The equations described in this section assisted in determining balances around the unit operations in the dynamic model. They were used in conjunction with the material balance and washability data to determine the performance of the circuit. The critical distinction between this and prior work was that the breakdown of components into non-magnetics, magnetics, coal and water has not been fully explored previously. The influence of the level of non-magnetics on the circuit over time with various perturbations has not previously been dynamically modelled, and the availability of new instruments enabled better circuit measurement.

2.6 Practical Application of DMC Models

Practical realities of coal processing plants introduce additional variation due to imperfect maintenance practices, lack of comprehensive information, variations in operator practices, varying levels of medium contamination, seam and working section variation, regularity of feed-off events (stoppages), continuous variation in feed quality and the degree of high near gravity material present. In this environment it is difficult to develop empirical models that hold over a range of operating conditions.

Under plant conditions, dynamics can play a significant part in the final efficiency outcomes. Yields and recovery are often affected by dilution, weightometer error, varying size distributions and circuit loadings. The influence of medium contamination on coarse coal DMC circuit efficiencies and throughput has been partially explored by O'Brien et al. (2013), and Firth et al. (2013) and research is ongoing. Differing manual operator input decisions made at the time of production can also influence yields, often without the cause of the yield change being visible to the operator from the control panel. Ongoing monitoring of plant conditions using on-line or real-time data provides an opportunity to present the realities of plant dynamics and overlay the prediction of theoretical DMC models to use as a guide to where plants may be deviating from ideal operation.

Where plants operate under relatively standard, stable conditions, the Wood Model provides a simplistic yet reasonably accurate guide to the efficiency of a plant. Coupled with density tracer tests, plant metallurgists can obtain a virtually instantaneous indicator of their plant efficiency on any particular day. Dynamic measurements of DMC underflow and overflow medium densities provide a useful comparison and a guide to the stability of

the circuit. More difficult is the measurement of medium to coal ratios. In general, CHPP instrumentation such as feed weightometers are not sufficient to provide an accurate measure if consideration is given to the constant variation in raw coal sizing, and the coarse versus fines circuit split at the desliming screen. However, CSIRO equipment is available and can be retrofitted onto a screen to analyse screen motion and measure mass flow across the screens. Provided that it has been calibrated, this gives a more accurate measure of screen yields and therefore coal flowrates. The medium flowrates can be estimated based on pump curves and using the density gauge also as a guide.

Analysis of online results showing differential and offset pose an interesting challenge. Often it is assumed that plant conditions are relatively stable once a plant has been operating on a particular seam for some time. In practice, the concentration of non-magnetic material in the circulating medium can raise or lower depending on bleed rates and momentary feed-off events. The offset, which is commonly assumed to be constant when making calculations around a DMC circuit, can change, and the relative density can vary considerably from the cut point despite the nucleonic gauge indicating that no change has occurred. Recent research by Firth et al. (2014) has indicated that the prediction of differential by measurement of overflow and underflow densities is linked with stability of the circuit. Where the level of non-magnetics in the medium drops to a relatively low level, the traditional plant indicator of nucleonic density lacks the ability to show this instability. In their work, Firth et al. (2014) observed that the underflow density behaved differently to the overflow density over time leading to an observed higher differential and consequent circuit instability. Figure 2.6 below showed a typical Australian coal DMC circuit operating in a low density range of 1.32-1.42. It can be observed from this figure that following an increase in the density set point by the plant operator, the circuit became unstable and the underflow density RhoU rose while the nucleonic density gauge (RhoFN) remained steady. Figure 2.7 demonstrates the same example with the differential and offset moving when the underflow density rises.

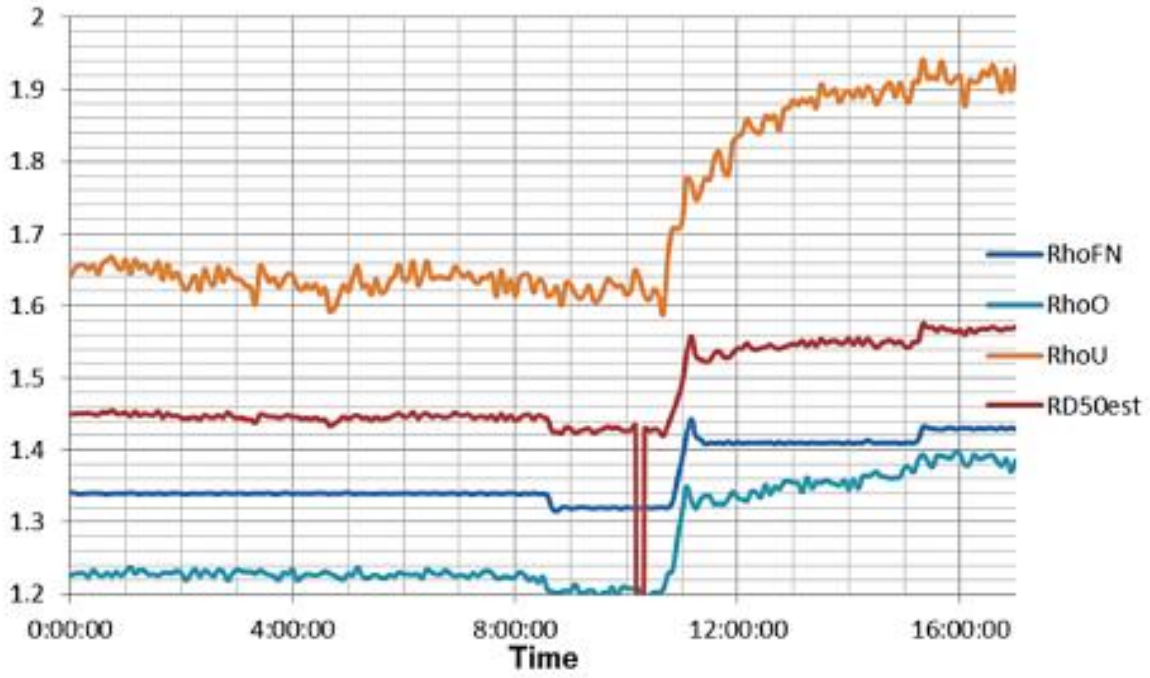

Figure 2.6: (after Firth et al. 2014, p150) Observation of underflow density RhoU, Overflow density RhoO, Feed medium density RhoFN and the calculated cut point estimate RD50est following a density change from 1.32 to 1.4.

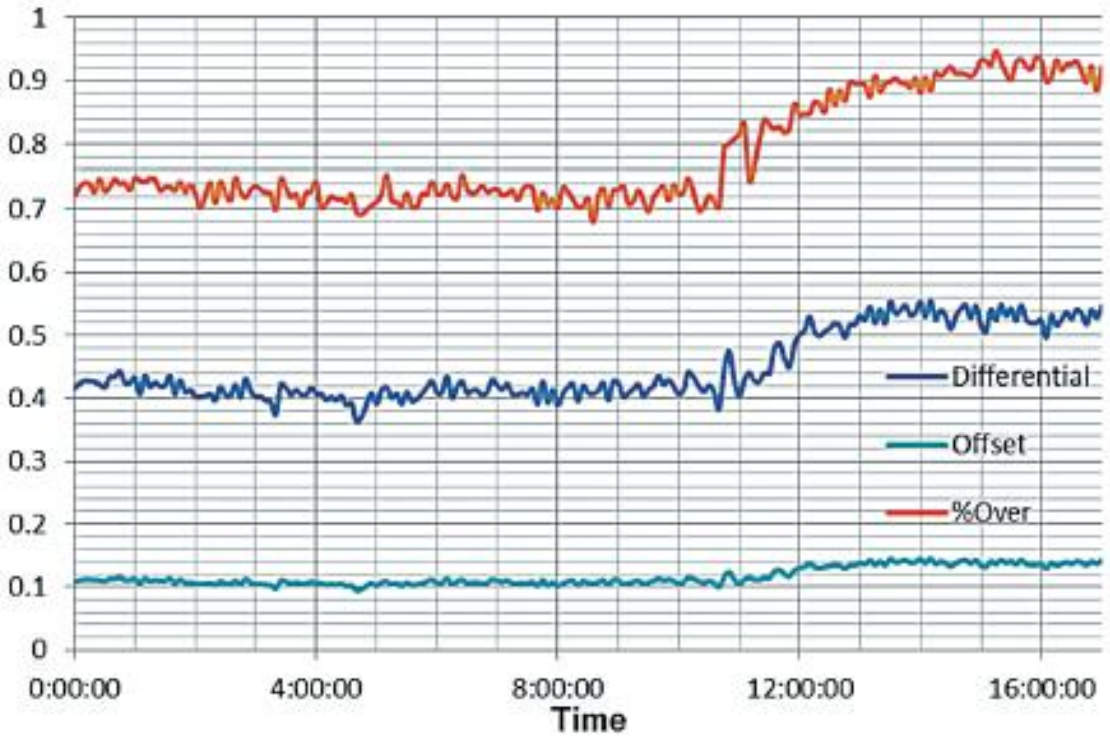

Figure 2.7: (after Firth et al. 2014, p151) Differential measured for the situation described in the previous figure. Offset can also be seen to move by 0.04 RD upwards.

An explanation for the circuit instability observed is proposed below.

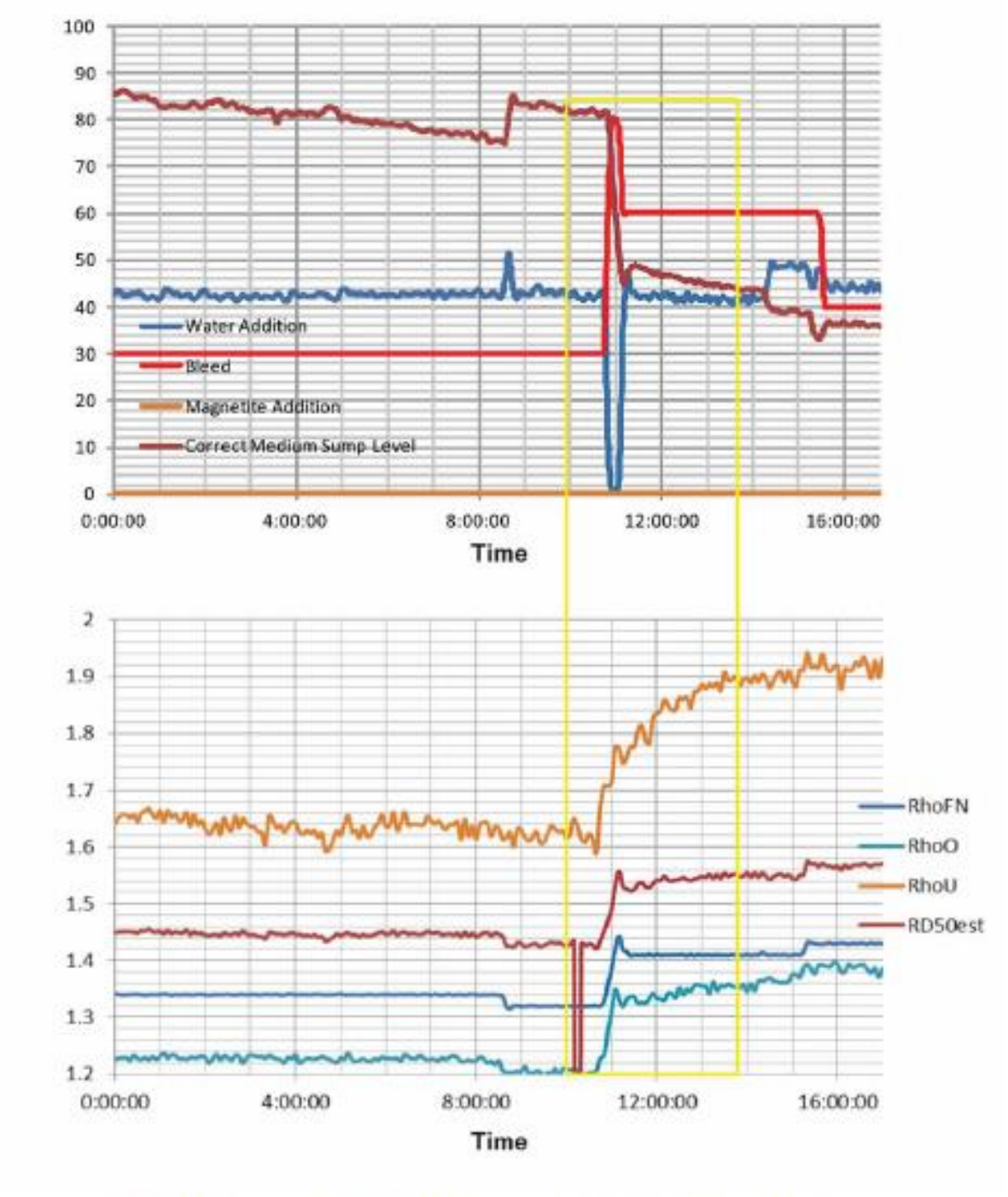

Figure 2.8: after Firth et al. (2014) Increase in feed medium density in a low relative density range.

Corresponding underflow density becomes unstable when a rapid density change upwards is coupled with an increased bleed of medium to the dilute circuit. The correct medium sump level is controlled by the operator via a bleed valve to transfer correct medium to the dilute circuit. Water additions to the correct medium sump are automatically controlled via a feedback loop to the nucleonic density gauge (RhoFN).

A density change upwards occurred at approximately 11:00hrs. (Figure 2.8) This corresponded with an increase in the level of bleed to the dilute circuit to reduce the sump

volume. The bleeding to the dilute would have caused a change to the level of non-magnetics in the circuit and as the circuit was operated at a relatively low density (1.32-1.4), the underflow density began to rise markedly in comparison with the overflow density. The cut point estimate (RD50est) which was calculated, was also seen to rise slightly as the underflow density increased. This was despite the nucleonic gauge density (RhoFN) remaining steady during this time. The calculated differential rose to 0.55 which is outside the range for stable operation and indicated the potential for retention and surging in the DMC.

Figure 2.9 on the following page is an example of a coal DMC circuit where the feed medium density was decreased at 14:00 hours, by 0.04RD. The underflow medium density increased due to an overflowing correct medium sump level. The overflowing sump acted as a bleed to the dilute circuit, thereby losing non-magnetics. The increase in underflow density changed the differential to 0.4. While the nucleonic gauge (RhoFN) was steady at 1.34RD, the estimated cut point (RD50est) moved upwards from 1.40RD to 1.44RD. This situation could have significant yield implications for a coal washery.

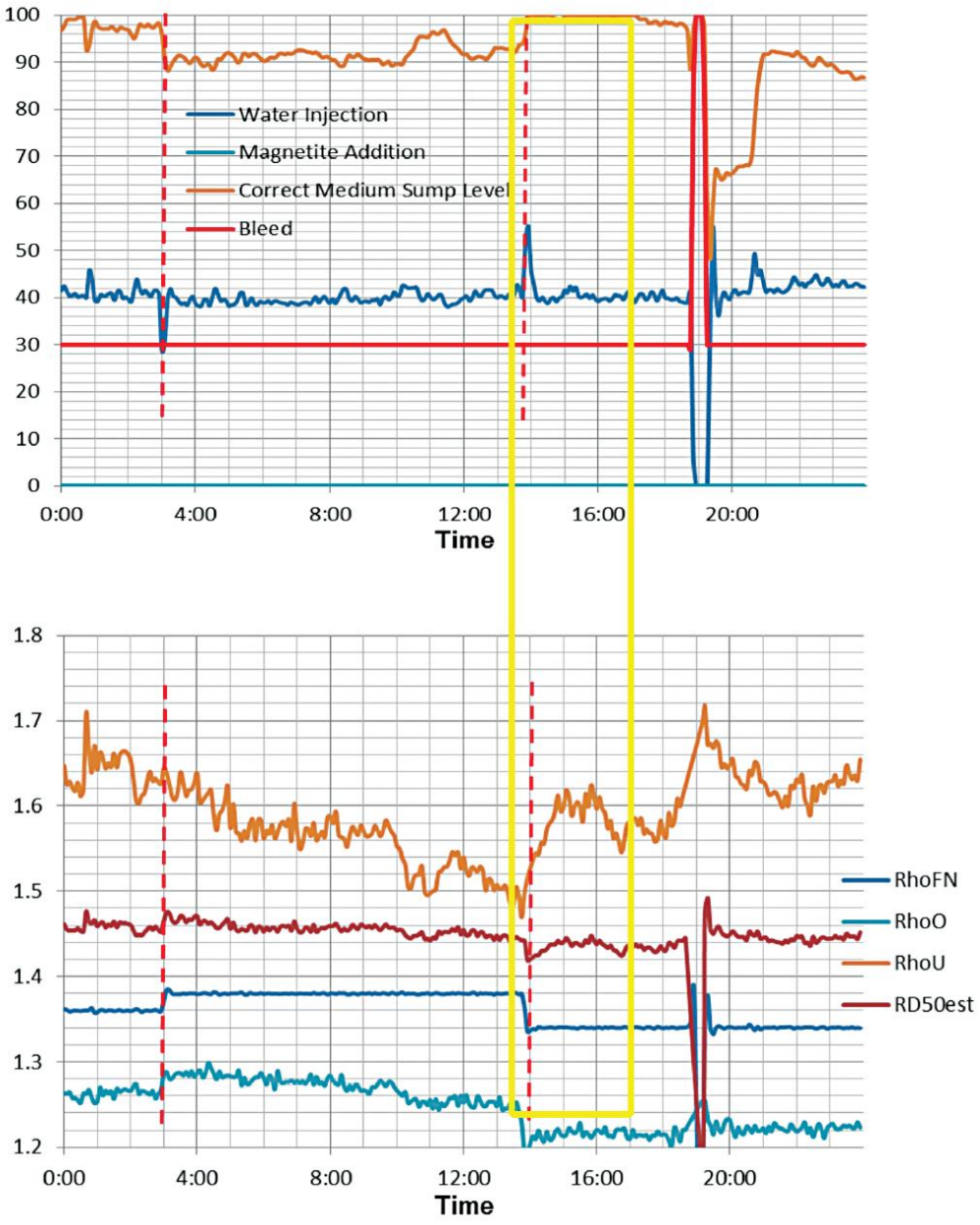

Figure 2.9: after Firth et al. (2014,p159) The effect on DMC circuit with a feed medium density decreased at 14:00hrs from 1.38RD to 1.34RD.

Estimated separation density remained unchanged and not 0.04RD below due to an increase in underflow density and consequently differential.

2.7 Density Tracers

One of the most effective tools developed to assist plant process engineers to assess their circuit efficiency on any given day is the density tracer. These simple, typically cube shaped, plastic resin particles cover a range of densities and allow a partition curve to be

generated, thereby giving a relatively instantaneous indication of dense medium circuit health. The use of density tracers as an alternative to traditional float sink analysis (ISO Standard 7936:1992 Hard coal – Determination and presentation of float and sink characteristics) provides a cost effective and fast turnaround solution of determination of cyclone efficiency. Davis (1987), used specially prepared 5 millimetre density tracers in a 200mm gravity fed cyclone to monitor a magnetite medium and medium viscosity under pilot plant conditions to assess DMC efficiency at two different densities and two spigot sizes. He measured the viscosity continuously using an on-line viscometer and used varying amounts of montmorillonite clay addition. This research did not investigate relative densities below 1.4, and only high swelling clays were considered. More will be discussed regarding viscosity effects in Section 2.8 - The Medium.

Recent advances by the Council for Science and Industrial Research (CSIR) in South Africa and collaborative work by Wood (2012), and Virginia Tech and also a separate study have developed the use of transponder technology for online monitoring of density separation efficiency (Wood et al. 2014). Radio frequency Identification (RFID) density tracers were developed to measure DMC efficiency with fewer people required to administer the test (Honaker, et al. 2007). RFID tracer technology was utilized as part of the research discussed here and is outlined under the Experimental Work section of this thesis. The purpose of RFID Tracer use for this research was to determine residence times in and transfer times between vessels within the plant. Tracers are a consumable item and are relatively low in cost when compared with float-sink alternatives. Residence times of coarse particles in vessels have been previously achieved using the smart rock technology developed by the CSIRO in a previous ACARP Project. The requirement to recover 100% of the smart rocks however, is considered too difficult to practically achieve in the plant. Smart rocks are by comparison, more expensive to replace than the radio frequency tracer technology. The company Metso has also developed an RFID tracer product which can trace coal particles from the mine to the port. These blast and crusher resistant tracers are comprised of only one density (approximately 1.3), however they serve a useful purpose in tracking mining batches through the processing plant to the port.

2.8 The Medium

Medium Composition

The medium is a slurry mixture of magnetite, water, fine coal and clays. Ideally a medium should be stable but of relatively low viscosity (Rayner, 1999). At high densities, viscosity can be a problem, however at low densities, some level of stabilisation of the medium prevents coarser solids from settling out from the dense medium. In the case of low stability of a dense medium, and particularly where high near gravity coal also exists, there is a tendency for retention to occur in the cyclone and the magnetite to classify in the dense medium cyclone. If a high differential exists between overflow and underflow densities of the medium, then surging can occur. (Crowden et al. 2011)

Medium stability and the efficiency of clay removal at New Acland CHPP has been the subject of further investigation by Firth et al. (2011), O'Brien et al. (2008) and O'Brien et al, (2013). Firth et al. (2011) found that the major factors influencing the settling behaviour of the medium were the volume fraction of non-magnetic material and the mean size of the magnetic particles.

Further definition of the medium has been developed with respect to size distribution. It was found that the constituents of the medium are as follows (Firth et al, 2011):

- clay with a nominal size of about 0.010mm
- magnetite with a nominal size of 0.040mm
- fine coal with a nominal size of 0.080mm, and
- small coal with a nominal size of 0.450mm.

Firth et al. (2011) also determined that for the sites studied, medium stability became more significant for plants operating at relative densities below 1.4. They concluded that small coal was not considered to be part of the medium while fine coal was. It was considered that material below 200 microns could be considered to be part of the medium while particles greater than 200 microns were not. (Firth et al. 2011) Material that is part of the medium is significant in terms of influencing medium stability, while material that is not part of the medium will affect overall medium density but not greatly influence medium stability.

Medium viscosity and stability

For many dense medium plants, removal of contamination (non-magnetics) in the medium is critical because the clays can accumulate in the circuits. This is a known problem with dense medium circuit performance and is important in diamonds, iron ore, and other high density dense medium applications. The primary reasoning behind removal of non-magnetic contamination in dense medium circuits is related to viscosity. Iron ore, diamonds and other high density applications of dense medium circuits suffer from excessive viscosity related to the presence of clays and other contamination in the medium. (Napier-Munn and Scott, 1990) Figure 2.10 demonstrates the difference in apparent viscosity at higher densities when comparing fresh medium with contaminated medium.

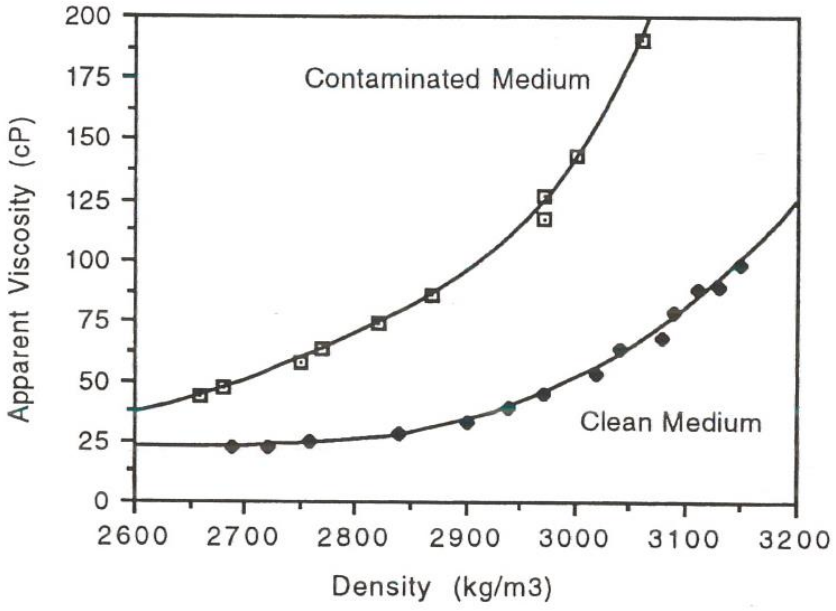

Viscosity-density relationship for fresh and contaminated medium (after Napier-Munn and Scott, 1990)

Figure 2.10: The difference in apparent viscosity when medium is contaminated versus fresh medium for a diamond operation. (Rayner 1999)

The densities used in the graph were for much higher densities than for those used in coal. It not clear from this data whether the relationship still holds for coal densities, however a flattening of the apparent viscosity line at lower densities is visible on this graph.

The inclusion of a demagnetising coil in these cases was found to be beneficial in reducing viscosity, however, in Australian coal plants, the presence of demagnetising coils to remove magnetic flocculation is extremely rare. Napier-Munn and Scott also listed medium density, solids density, particle size distribution, particle shape and fine contamination as other factors influencing medium viscosity. Viscosity is also sensitive to

temperature and may be a more significant issue in cooler climates. It is interesting to note that in Figure 2.10, the curves both approach each other as density drops. This would tend to suggest that at typical coal densities between 1.2 and 1.8, the influence of contamination on viscosity would be minimal.

Davis and Napier-Munn (1987), conducted twelve experiments using specially prepared 5 millimetre density tracers in a 200mm gravity fed cyclone to monitor online medium viscosity at relative densities of 1.40 and 1.55 and at two different spigot sizes. They measured the viscosity continuously using an on-line viscometer and used varying amounts of montmorillonite clay addition. This research did not investigate relative densities below 1.4, and only high swelling montmorillonite clays were considered. The offset, measured as the separating density or cut point minus the feed density, was found to approach zero as the viscosity increased. They also noted that at low viscosities (ie. zero contamination by montmorillonite clays), the offset was essentially independent of viscosity. As viscosity increased, the Ep, or measure of the separation inefficiency, was found to also increase, thereby indicating that the process became less efficient at higher viscosities.

In practice on a mine site, finding a pure montmorillonite swelling clay in situ with the coal seam is unlikely. More commonly, there will be elements of a number of different types of clays, exhibiting varying influences on the viscosity of the medium, hence the work of Davis and Napier Munn consisted of an extreme case of contamination at levels not commonly seen in Australian coal preparation plants. This limits the application of Davis and Napier-Munn's work to higher density applications. O'Brien and Firth (2008) conducted further experiments using kaolinite as the clay at lower densities and noted different results. They showed that medium viscosities for a number of Australian coal preparation plants were only slightly higher than that of water.

Wood (1990) proposed that in coal operations, it could be inferred that viscosity increases due to medium contamination would rarely be high enough to severely hinder partitioning. Wood (1990) also mentioned that the Walloon Coal measures may need special attention due to their clay-induced viscosities. The presence of sodium montmorillonite and calcium montmorillonite clays can cause major processing difficulties. (Crisafulli, et al. 1985). While New Acland Mine treats coal from the Walloon Coal Measures, instances of viscosity problems with the medium in this circuit are not common. Anecdotally operators

have indicated that at high density set-points, above 1.6RD, they sometimes experience blockages in the plant rejects system, however this may not necessarily be due to the proportion of non-magnetics in the medium. The plant has been designed to efficiently strip out non-magnetic contamination material from the dense medium circuit to avoid a recirculating clay load within the plant. It appears that the recommendations made by Crisafulli et al. 1985, of direct feeding, adding water at the feeder breaker to move clays beyond the 'sticky' region, and minimising raw coal storage, have been followed in this plant design. Through the work of O'Brien et al. (2013) on New Acland medium samples, it has been demonstrated that the plant non-magnetics levels are generally low. This could mean that the magnetic separators are over-compensating by removing too much of the stabilising contamination in the medium. Davis and Napier-Munn (1987) did note that in coal washing in which the volume solids concentration of feed medium was relatively low, typically 7-18%, classification of the medium in the cyclone played a predominant role in determining the product medium density whereas for diamonds and other higher density operations, sedimentation was the major factor.

Viscosity is an interesting point of contrast between the work of these researchers. The narrow range of tests applied, the different clays selected, and comparison with real plant situations provide some insight into why these differences exist. It appears that there are instances where viscosity can play a part in coal washing, however, instances are not widely acknowledged and certainly not widely measured in plant operations. Extreme cases occasionally present to a plant, however, often processing difficulties are attributed to other causes such as blocked chutes, or sticky clays without consideration of the minute by minute differences in efficiency that could potentially be caused by viscosity effects. For the purposes of modelling the coal plant at New Acland, the Wood model is the most appropriate choice, however the Dunglison model could be applied in future dynamic models for coal and other minerals if more online viscosity information were to become available.

Medium rheology, stability and viscosity have been extensively explored by Davis and Napier Munn (1987) and also by He and Laskowski (1993). The former identified a reduction in efficiency with increasing clay contamination due to medium rheology. He and Laskowski highlighted the influence of stability, separation cut-point and differential and investigated the effects of different particle sizes on medium properties. The density differential between the cyclone underflow and overflow is thought to characterise medium

stability. He and Laskowski (1993) tested a number of grades of magnetite and found that for the same medium density, the density differential was higher for coarser grades of magnetite. In coal applications, typical DSM guidelines are for finer magnetite to be used in lower density applications and coarser grades in higher density applications.

In day to day operations, the importance of the medium is often overlooked. Plants are given tools to manage density, pressures and levels, however, the medium composition is not a visible measure and can therefore be easily ignored. Despite the importance of relative proportions of non-magnetics in the medium, online measurement has not been available to plant operators and metallurgists in the past. Plant operators have relied upon other metrics such as density and DMC pressure to give indications of how the circuit is performing without visual indication of the density differential. When the density differential exceeds 0.4, DMC surging is more likely to occur (Crowden et al, 2013) Evidence of surging in the presence of very low percent non-magnetics has not been measured except on reject weightometers which are notoriously high in error (commonly $\pm$2%) and may not be able to distinguish a surging event against the background of plant noise. In some cases, DMC surges can be observed visually on the primary reject drain and rinse screens. Apart from visual inspections, surging DMCs are difficult to detect unless they drastically affect the product quality readings. Product and reject weightometers can be affected by surging centrifuges which may mask or confuse the issue. Similarly, variations in feed from one haul truck to the next can generate fluctuations on weightometers that resemble surging. With new instrumentation at the New Acland plant, surges have been detectable by use of accelerometers on the product and reject drain and rinse screens as well as by observation of the density differential between drain and rinse screen under-pans for product and reject screens.

Medium Recovery and stability

Recovery of medium in a coal DMC circuit can be critical to plant profitability. Large losses of magnetite are costly and considerable efforts are employed by plant metallurgists to stem losses of magnetite through the various possible sources. Masinja (1992) identified sources of medium losses in dense medium plants, and in particular, developed an empirical model for adhesion losses – where medium adheres to the coal or ore on the screens. Considerable losses of magnetite were also noted by Masinja (1992) in coal plants where a high rate of stoppages occurred. Given that an appropriately sized, well

designed and maintained modern magnetic separator is over 99.8% efficient, (Norrgran, 2010) the recovery of magnetite is less important in relation to the focus of this study. In the author's experience, for a magnetic separator that is properly installed and maintained, much of the magnetite losses can be attributed to housekeeping, floor sump overflows, and poor operation of drain and rinse screen sprays.

Rayner (1999) developed an empirical model for magnetic separators, however, non-magnetic contamination was included as a percentage of feed solids. He recommended further work that considered the influence of different size distributions of non-magnetics. Rayner noted that it was the finest solids which most greatly influenced the rheology of the medium. Dunglison (1999) also noted that the concentration of solids influences the rheology of the medium. Likely sources of the fine solids are from recirculating loads, coal breakage and de-slimed coal and mineral matter present in the feed that carry over into the coarse circuit.

Stabilising the medium

In addition to finer magnetite, the clays and fine coal present in the medium are also stability enhancers. Too much medium contamination by non-magnetics can occur in iron ore and diamonds processing leading to high viscosity in the medium. This has generated a widespread fear of viscosity causing damaging ramifications for processing in coal applications. Whereas in iron ore and diamonds DMC operations removal of contamination is done to reduce viscosity, in Australian coals, viscosity is significantly less important. There are, of course, exceptions, and in the case of bentonite clay types, the high swelling characteristics can induce viscosity effects at very low concentrations. In some coal plants on certain seams, this can be a reason to bleed more medium to the dilute circuit. It is, however, possible to go too far. Circuits can lose stability by bleeding excessive amounts of non-magnetics from the system via the dilute circuit and plants then compensate for this by adding finer magnetite. This results in higher operating costs.

It is commonplace in Australian coal plants to select a finer grade of magnetite to combat instability problems in a circuit. The difficulty of using finer magnetite is that the highest losses of magnetite often occur in the finer size ranges. This was confirmed by Davis and Lyman (1983) who showed that magnetite losses in separator tailings were finer than in the feed when new magnetite was used in the circuit, and when very dilute feeds were

presented to the magnetic separator. Consequently, a plant may invest in finer magnetite only to have it rapidly lost due to overflowing sumps, surface adhesion on rinse screens, inadequate coal rinsing, poor housekeeping, or surging volumes in the magnetic separator**.**

Medium samples are thought to vary in size distribution according to fresh feed additions of magnetite, however, analysis of some magnetite samples from New Acland coal preparation plant by O'Brien and Taylor (2013) revealed that the sizing of the magnetite in the correct medium remained largely the same regardless of new magnetite additions. This is shown in Figures 2.11, 2.12 and 2.13 below.

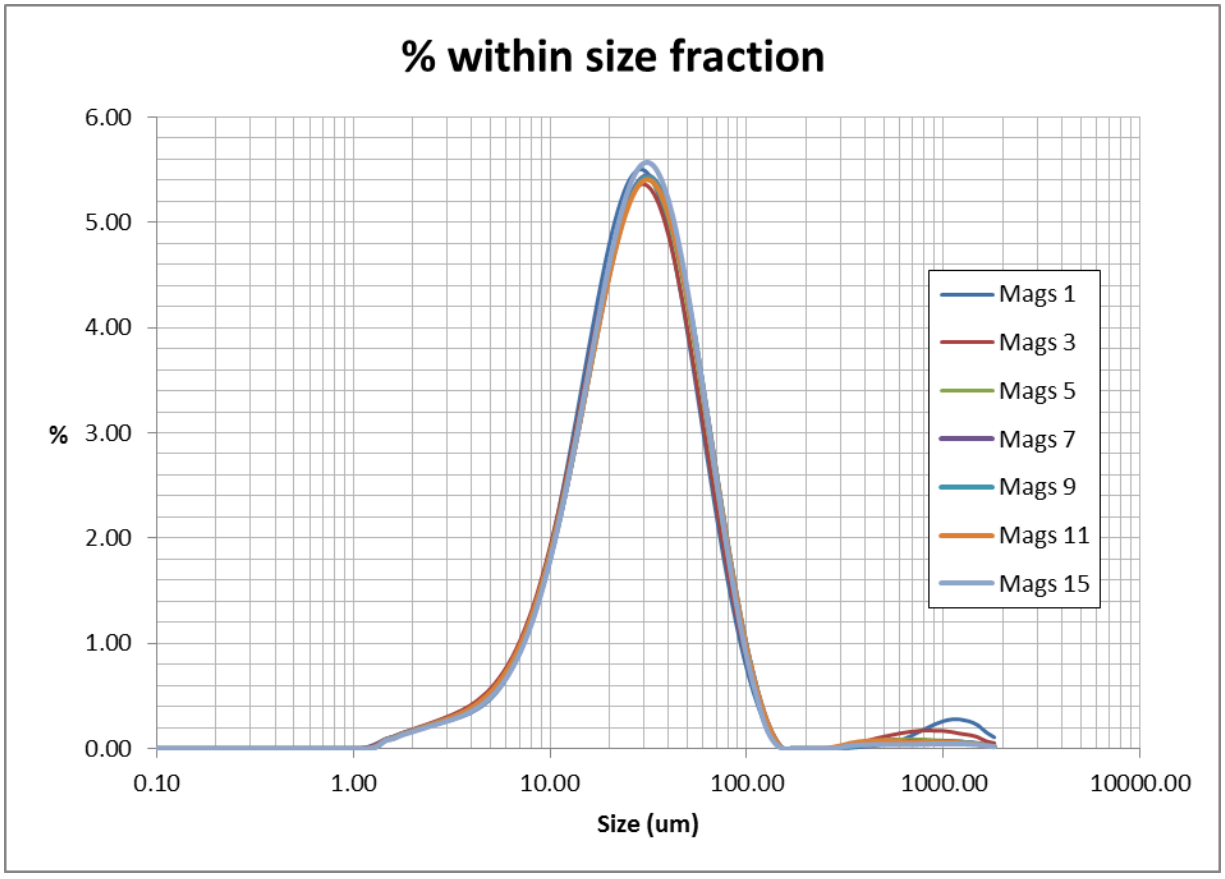

Figure 2.11: Correct medium magnetite samples from New Acland analysed using a Malvern laser particle sizer. Size distribution fractions for the various samples

Individual samples show very high correlation. (O'Brien and Taylor, 2013).

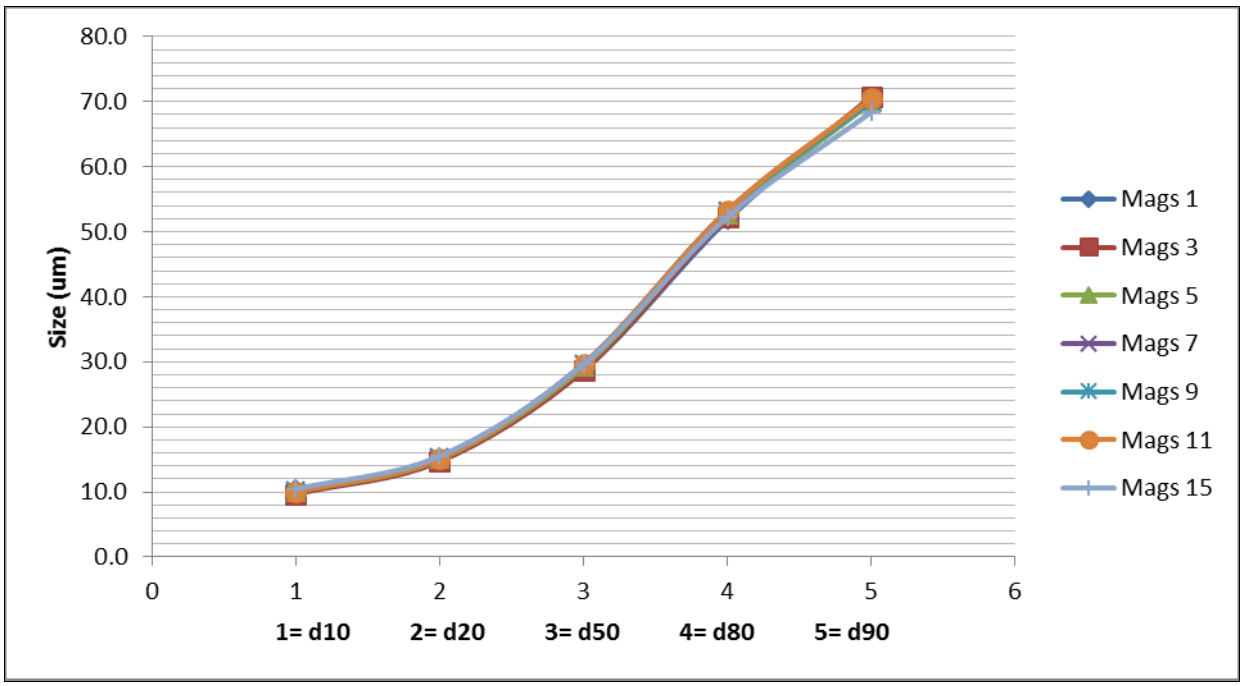

Figure 2.12: Correct medium magnetite samples from New Acland analysed using a Malvern laser particle sizer. Particle size vs. d10 to d90

Individual samples show very high correlation. (O'Brien and Taylor, 2013)

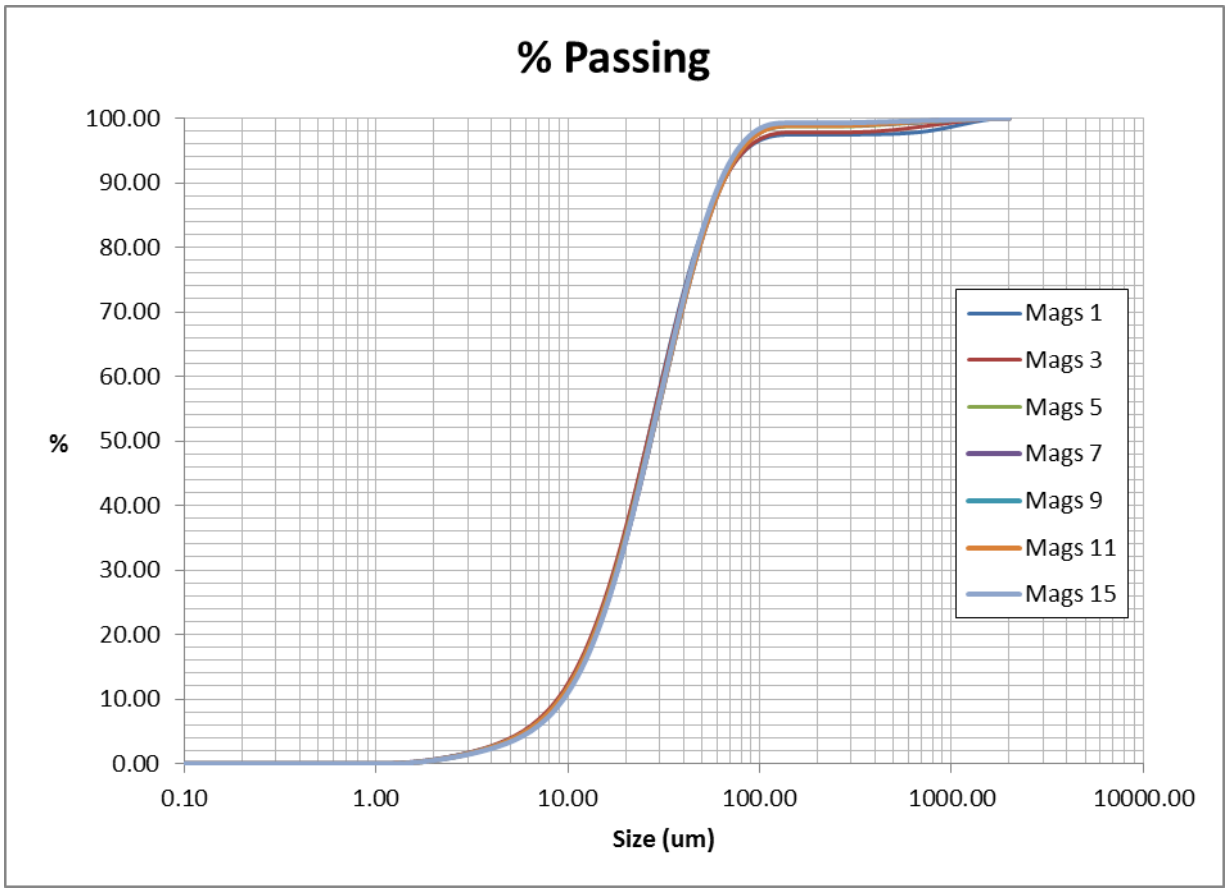

Figure 2.13: Correct medium magnetite samples from New Acland analysed using a Malvern laser particle sizer. (O'Brien and Taylor, 2013) Size partition curve

A possible reason suggested for the lack of variation in magnetite sizing was that there could have been an immediate loss of non-magnetics and finer magnetite particles within the first revolution through the magnetic separators and therefore, the finer magnetite additions may not be generating the expected stability in the circuit. (O'Brien,et al. 2013)

It is proposed that while expensive finer magnetite has the effect of stabilising a medium, the same effect may be available from the free clays which are so efficiently removed from the system by the magnetic separators. Plants could potentially utilise natural clays inherent in the raw coal feed to enhance DMC circuit operation to create a similar effect to the traditional use of Loess as a medium. In this case, however, recovery of the clays would not be an issue because the feed would continually refresh non-magnetic material into the circuit. Maintaining and controlling the level of non-magnetics in a circuit when targeting low density cut points may generate the same stability benefits at significantly lower cost. Achieving this in practice however, may be more difficult. Non-magnetics are currently not measured on an on-line basis although work in this area is progressing. Level control in a DMC circuit is also affected by sump volumes and capacity at a variety of differing densities. The correct medium bleed to the dilute is often used by plant operators to control volume in the correct medium sump. Practical application therefore, may require a shift in design to enable greater volumes to be handled in sumps and possibly the reintroduction of an additional over-dense sump into the circuit. This could be tested using a dynamic model.

The Role of Non-magnetic Material in the Medium

Recent work by O'Brien et al (2013) studied the levels of non-magnetics in the coal medium at New Acland plant. While this particular plant is able to operate relatively well with below 20% non-magnetics in the dense medium circuit, stability begins to become apparent when low density regions (below 1.4 RD) are targeted and low levels of non-magnetics are present in the system. At densities below 1.4, it is recommended by O'Brien et al (2013), that the level of non-magnetics be at approximately 20%w/w or greater. This has the effect of reducing the differential between the overflow medium and underflow medium densities. It has been identified that the density differential should be kept in the range of 0.2 to 0.5 (Collins et al. 1983), though above 0.4, instability can occur. This parameter agrees with recent plant experience at New Acland where circuit instability was noted at a density differential of above 0.4.

Figure 2.14 demonstrates the danger zones where stability of a DMC may be affected by low concentration of non-magnetics and magnetite sizing.

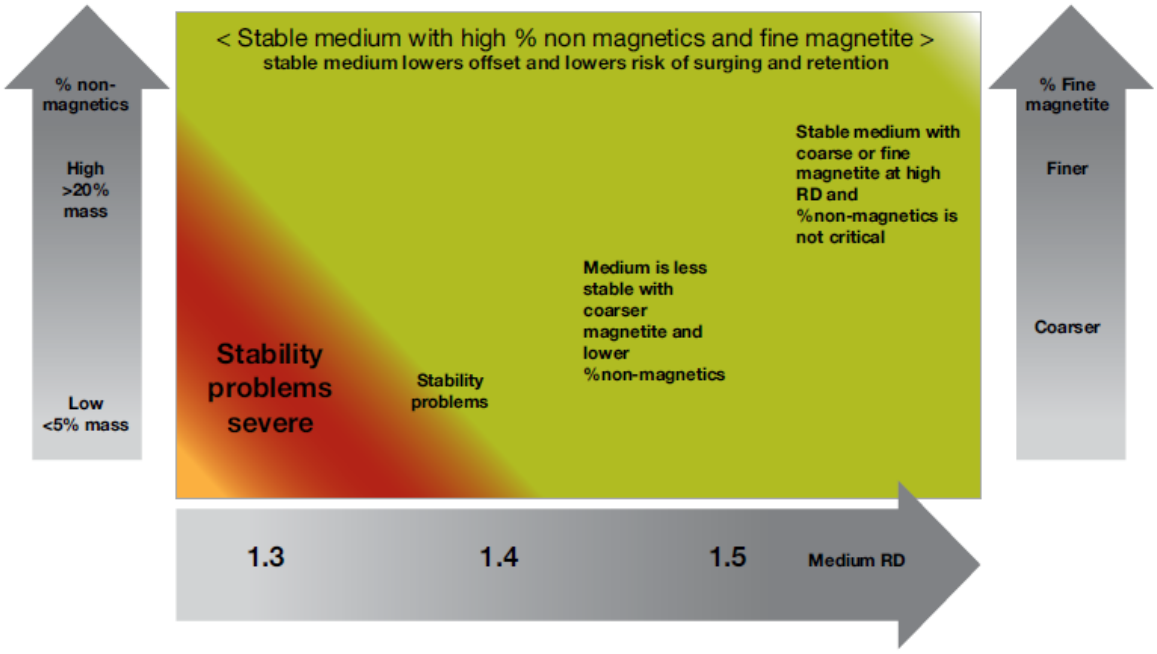

Figure 2.14: Crowden et al. (2013, p3), Stability at low densities compared with magnetite grade and non-magnetics concentration.

In situations where instability occurs in a coarse coal dense medium cyclone, the addition of fine clays and fine coal or finer magnetite in the size range 0 to 150 microns has the effect of improving medium stability. Typical ranges recommend a % non-magnetics by weight of approximately 20% (Crowden et al, 2013), although in the specific case of our test site, New Acland, typical non-magnetics concentrations are closer to 15%. This is potentially a cause of instability when operating at low densities.

It is postulated that as an alternative to using finer magnetite, some degree of clay contamination could be utilised to enhance stability. What remains is determining a means of controlling the level of contamination so that it does not exceed an efficient operating threshold. Instruments for measuring the amount of contamination are still in their infancy. The magnetic susceptibility meter developed by Cavanough et al. (2008) at the JKMRC and the EIS instrument developed CSIRO are showing great promise, but a true measure may not be available for some time. This does not mean that an alternative cannot be used in the meantime. Measurement of under-pan densities on the drain side of the product and reject screens give an indication of the density differential (the difference

between the underflow and overflow density). The differential can be used as a proxy for stability in the dynamic model.

2.9 Dense Medium Circuits

Over recent years, dense medium plant complexity has been reduced by the introduction of fewer, large diameter DMCs replacing pairs (or even quads) of parallel smaller diameter DMCs. Traditional dense medium circuits utilised two-stage magnetic separators, thickening of the magnetite using cyclones and densifiers, and included over-dense sumps. (Leach and Meyers, 2010) This was the traditional Dutch State Mines (Stamicarbon) design (Figure 2.15). Improvements in magnetic separator design and consequently, recovery efficiency have reduced the need for a secondary magnetic separator stage, and the use of a magnetite thickener and over dense sump are now becoming less common.

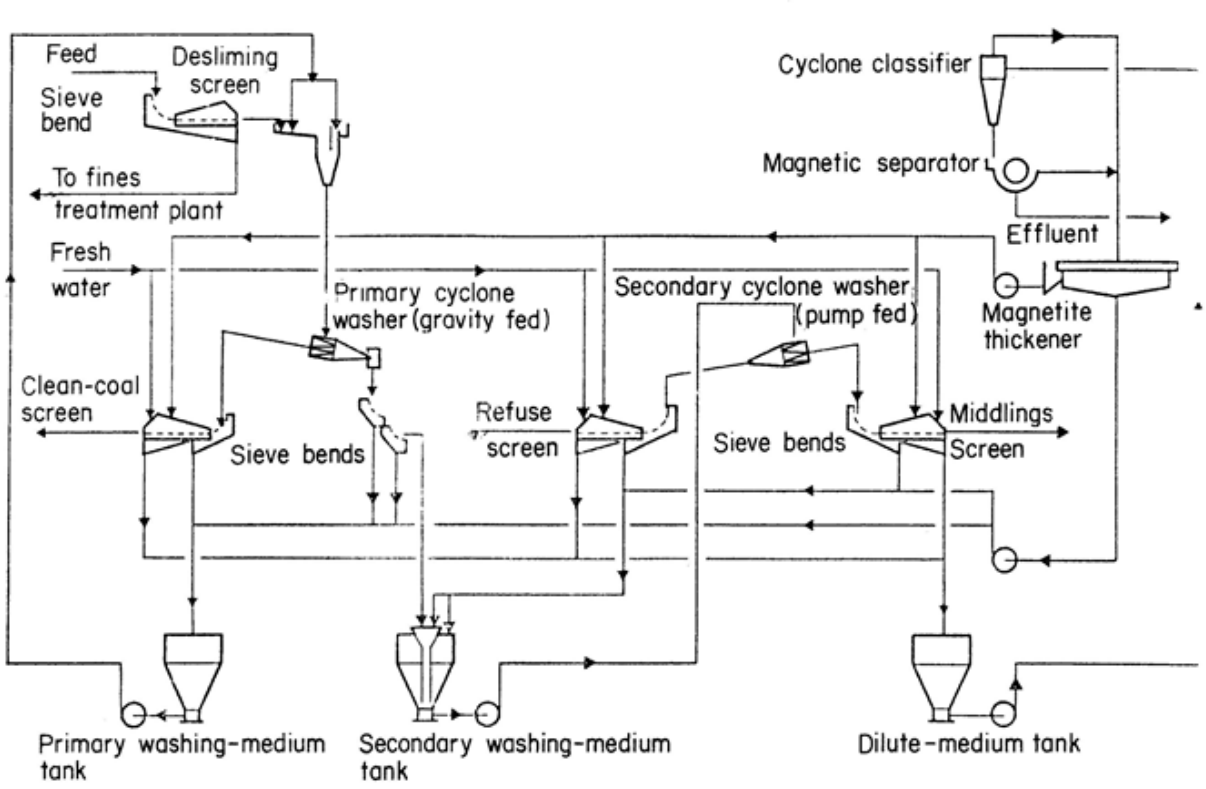

Figure 2.15: Traditional Stamicarbon Dense Medium Cyclone Circuit design for coal. (Osborne, 1988, p266)

Modern control loops are often set up as a rising density system where water addition is made via a control valve at the exit of the correct medium sump and controlled by a feedback loop from the nucleonic density gauge in the same line (Figure 2.16). The advantage of this design is the fast response time for density adjustments. The opportunity to directly add magnetite into the correct medium sump from the magnetic separators reduces the need for an over dense sump, and hence results in a smaller plant footprint. (Leach and Meyers, 2010)

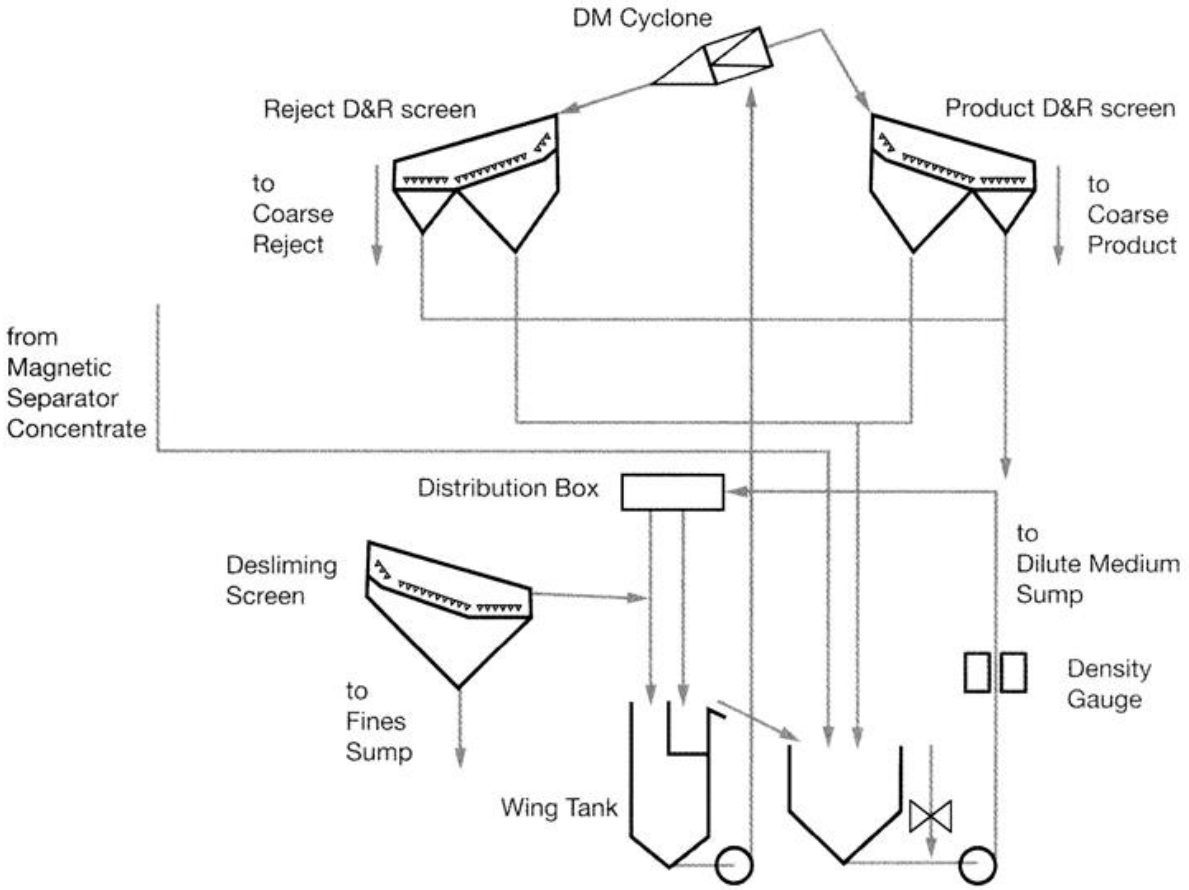

Figure 2.16: Typical modern rising density system design for coal (Crowden, et al. 2013)

The system used at New Acland CHPP is a rising density system (Figure 2.17). No over-dense sump or magnetite thickening circuit exists. Fresh magnetite is pumped directly into the correct medium sump, and return magnetite, recovered from the magnetic separators, also flows directly into the correct medium sump. Density adjustment occurs at the exit of the correct medium sump via a clarified water control valve linked by a feedback loop to

the nucleonic density gauge further down the correct medium line. Coal is mixed with correct medium at the oversize launder of the desliming screen and enters the DMC wing tank. It is then pumped directly into the dense medium cyclone. The dilute sump takes feed from the bleed valve on the correct medium line and also from the rinse side of the drain and rinse screens and includes centrifuge effluent and floor sump effluent. The dilute sump is pumped to the magnetic separator and concentrated magnetite returns directly back to the correct medium sump.

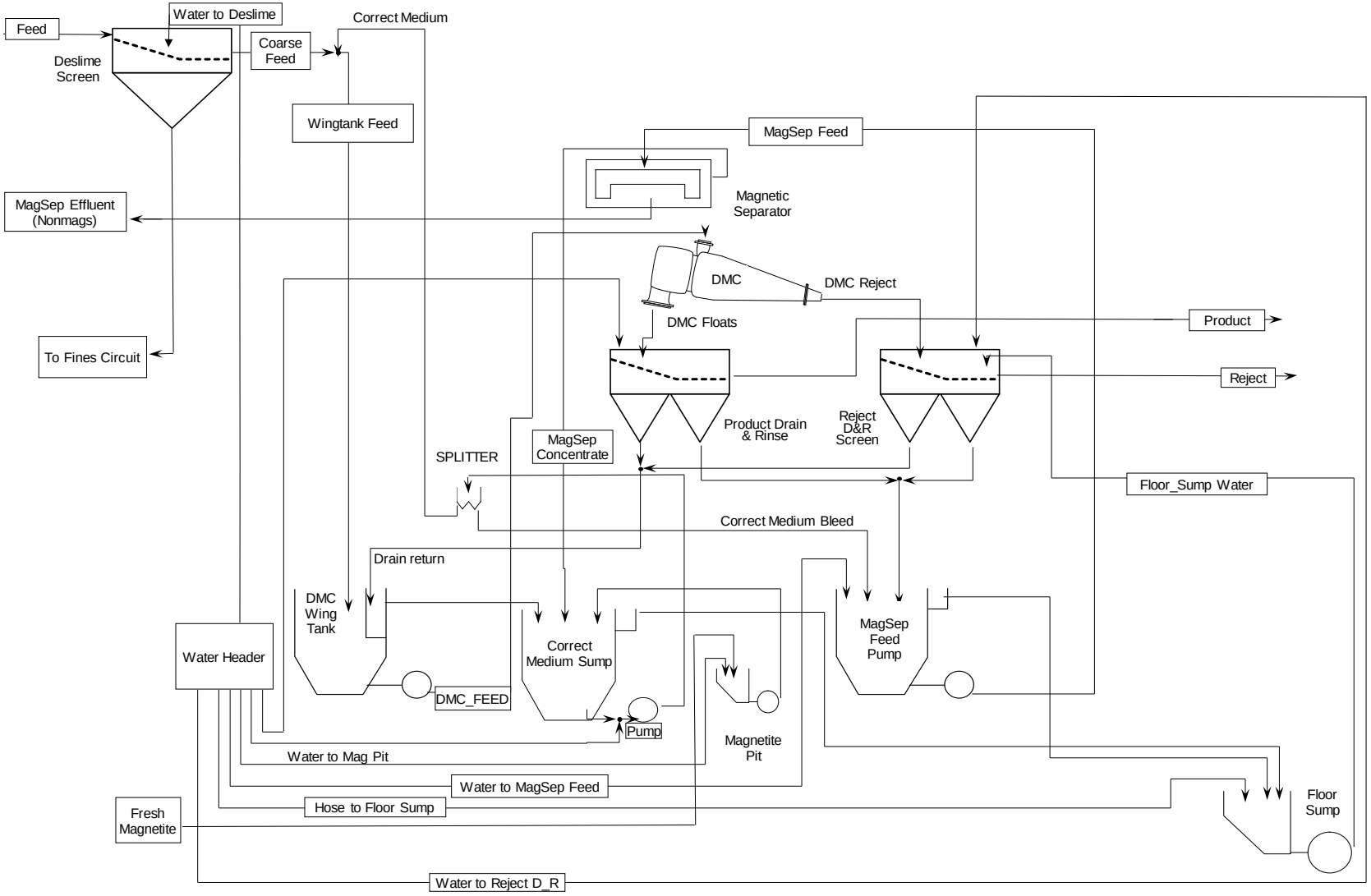

Figure 2.17 The New Acland Plant 2 DMC circuit is shown pictorially below: The single stage magnetic separator is fed directly from the dilute sump and return concentrated magnetite is directly added to the correct medium sump.

Coal plant design is often influenced by the need to handle clays. The use of selective thin-seam coal mining practices can alleviate some clay contamination in the feed, however, in the case of Walloon coal measures, at New Acland and in the Clarence-Moreton Basin coal region, it is not uncommon for the non-coal material to be layered within the coal bands, therefore making total removal almost impossible. (Crisafulli, et al. 1985) "The major problem… is the distinct degradable shale bands interbedded within the coal as thin litholitic markers usually no more than 150mm thick. These degradable bands are composed mainly of montmorillonite with minor amounts of kaolinite and quartz." (Crisafulli, et al. 1985) Because these clay types tend to rapidly degrade upon atmospheric exposure after mining, every effort is made to process the coal rapidly at New Acland mine to avoid breakdown into highly dispersed binding clays. The New Acland coal plant is designed with water introduced at the ROM to avoid stickiness in the feeder-breaker, and no raw coal stockpiles exist.

The New Acland CHPP has two single-stage plants, the first is a Jig, DMC and spirals circuit, and the second, known as Plant 2, is a DMC and spirals circuit. The JKMRC and CSIRO instruments that have been set up to monitor the dense medium circuit have been installed in Plant 2. Raw coal feed to Plant 2 is transferred by conveyor from the feeder breaker into a secondary and tertiary sizing station at the rate of 550 tph. The coal passing through the sizer drops directly into a sump and is pumped with water addition (from clarified water and magnetic separator effluent) to the desliming screen. This design is uncommon. Generally, the coal would be conveyed dry until it enters the plant directly above the desliming screen. As sticky clays are prominent in this coal basin, handling issues in the materials handling system can be reduced by adding water to the system at an earlier point. Anecdotally, operators at the plant have described finding large clay balls on the desliming screen. The 1.4mm aperture desliming screen separates the coarse coal into the DMC circuit, and the fine coal passes to the spirals circuit. The beneficiated coarse coal product is then dewatered via a basket centrifuge and conveyed to trucks which transfer the coal to the rail system. Coarse rejects is combined with Plant 1 rejects and returned to the mine via a rejects bin.

2.10 Circuit Instrumentation and Control

Density Control

Gaining a more comprehensive understanding about optimal operation of dense medium cyclone circuits is critical to maximising profitability of coal mines, particularly in light of falling coal prices. A collaborative effort between CSIRO and the JKMRC on ACARP Project C17037 - *Joint Evaluation of Monitoring Instrumentation for Dense Medium Cyclones* led to the successful commissioning of new instruments in the New Acland coal preparation plant. These instruments comprised accelerometers, Electrical Impedance Spectrometers (EIS) and magnetic susceptibility probes, and provide real-time, on-line measurements. This range of data is the first of its kind to become available in the Australian Coal Industry and has the potential to become the new benchmark for future coal plants worldwide. The accumulation of long-range data is also an industry first and provides the opportunity to look at coal plant dynamics over a long period of time rather than relying only on spot-audits for verification.

The most common form of medium density measurement in modern CHPP is the nucleonic density gauge. A significant drawback with this instrument is the presence of a hazardous radioactive source which presents a risk to personnel. Nucleonic gauges are generally reliable and require little maintenance (Cavanough 2008). Concern over the risks of a radioactive hazard have prompted alternatives to the Nucleonic gauge to be investigated. Cavanough et al. (2008) developed a medium density measurement device that used magnetic susceptibility to determine density of the medium in the drain and rinse screen underpans. This type of apparatus has been in place at New Acland Coal mine for the past three years and has proven to be a very robust piece of equipment. Another instrument installed at the site was developed by Sheridan (2011), and was capable of measuring the density of a slurry circulating in a DMC unit at the overflow and underflow points. This Through-Tile Density Meter instrument, measured the combined medium and coal density in the DMC overflow with the presence of an air core. This device used the Hall Effect, capitalising on the presence of magnetic material in the slurry.

Other non-nucleonic devices available include the differential pressure technique which utilises a measure of differential pressure on a tester leg. (Cavanough 2008). Zhang (2010) developed a Heavy Medium Suspension Density-Viscosity detection device which

essentially used differential pressure and was non-nucleonic. Firth et al, (2010) developed Electrical Impedance Spectrometers (EIS) which provided measurements of the medium density and composition. These instruments have been in place at New Acland in various locations in the Dense Medium Circuit and have provided useful online data about the circuit behaviour. In addition to the density measurement devices at New Acland, other additional instrumentation was installed. Screen motion analysers based on accelerometer technology were used for measuring screen health as well as mass flows over screens, and a Cross-Correlation Flowmeter was installed in the DMC feed line from the wing tank. (Firth 2010) By combining these instruments with the existing standard CHPP nucleonic gauge and a SCADA control system, the information enabled more in-depth measurement of circuit behaviour than had been previously accomplished in the past.

There have been some drawbacks to monitoring coal dense medium circuits using existing standard plant instrumentation. Traditionally, plants used density measurement and controlled sump volumes and DMC pressure to obtain a satisfactory operating circuit. Pumps were either single speed or variable speed drives, with current trends gravitating towards variable speed drives to maintain DMC pressures. This introduced another dynamic variable to the system. Mineral Matter (commonly referred to as Ash) measurements were manually fed back to the control room and adjustments to density set point on the DMC circuit were made to change the ash result. The time taken for samples to be analysed caused a lag to occur before a plant correction was made. During the time period that a sample was being analysed, the plant may have processed a number of thousands of tonnes of coal. In many plants where ash was critical, sampling was conducted on an hourly or two hourly basis, but some plants only sampled on a 12 hourly basis. In this period, the amount of coal processed could have been as high as 10000 tonnes between ash adjustments. Some plants were less concerned with controlling ash and were able to blend to achieve a satisfactory product, however others required the density to be tightly controlled. Attempts to address this problem were mostly focused around installation of on-line ash gauges, however, these have been met with limited success in the coal industry, and in most successful cases, on-line ash gauges have been installed in single seam operations with minimal variation. The author has not yet encountered a coal processing plant that has been able to exclusively rely on an online ash gauge for the purposes of plant density control.

Outside of the limited instrumentation provided in most plants, little is known about how a circuit changes with variations in feed, and in particular, how the medium varies in a dynamic sense. Recent work by Addison (2010) has enabled a better understanding. Addison installed additional nucleonic density gauges around a circuit to monitor feed, overflow and underflow density and to look at the relationship between measuring density with coal present in the stream and without coal present in the stream. Typical circuits in the USA have a draft tube arrangement where medium and coal are present where the nucleonic gauge sits and this has been found to give different measurements when compared to wing tank arrangements such as those present in many Australian coal plants. With a wing tank arrangement, the medium is measured separately to the medium and coal slurry.

Addison (2010) looked at responses to changes in plant feed, and in particular, to low yielding versus high yielding coals at Tom's Creek mine in Virginia, USA. Critically, Addison identified that when high amounts of reject material were present in the coal medium mix, the nucleonic density measurement for a coal and medium slurry was significantly different from a nucleonic density measurement for a medium-only slurry. It was proposed that the presence of a large amount of reject material in the medium had an influence on the density reading as the nucleonic gauge interpreted the presence of large amounts of high density rock as over-dense medium. Addison recommended that future plant designs include a means of measuring the 'true' density of the medium without coal present as is typically done with Wing tank design plants. Addison also recommended the recombination of return medium streams from drain and rinse screen under-pans (product and reject) and using this stream to analyse medium density.

The use of nucleonic gauges as in Addison's work led him to conclude that gauges should be installed on the medium return lines, however current installations of JKMRC and CSIRO instruments at New Acland have advantages over nucleonic technology as they do not require changes to head-room due to their compact nature, and they are non-radioactive. Addison did not consider the role that non-magnetics may play in the stabilization of the medium circuit.

Phillips (2010) performed a steady-state desktop analysis using a spreadsheet to compare advantages and disadvantages of heavy media circuit control. He looked in particular at bleed and sump volume fluctuations. He mentioned the importance of focusing on density

rather than correct medium sump level and he noted that the sump level should be allowed to fluctuate so that density can be better controlled. Phillips looked at both a rising and falling density systems for comparison. The rising density system is commonly in use in modern plants as it allows faster response time to density fluctuation by means of an automatic water valve at the inlet to the correct medium pump. This is the same system that is in place at New Acland. Phillips profiled the effects of upsets on the dense medium circuit, such as feed changes, adjustments of the bleed, higher water addition with the feed, and the difference between the addition of density control water with and without the bleed operating. He found that the operation of the bleed could assist with reducing the requirement of density control water. His analysis of changes in feed size distribution found that a finer feed could lead to subsequent short-term overloading of the magnetic separator with a subsequent loss of magnetite. Phillips did mention the effect of non-magnetics on influencing density, stating that when the plant feed is off, the rapid drop in density could be partially attributed to a loss in non-magnetics by bleeding to the magnetic separator. His consideration of the effect of non-magnetics however, was fleeting and was focused on high media viscosity and poor separation, not on medium stability. His study was essentially a steady state balance and apart from a few test conditions, it did not examine dynamic changes with time.

Plants are typically designed with minimal capital expenditure and minimal footprint in mind. This drives sumps to be designed for minimum volume capacity. The outcome is that during extremes of plant operation, there is little room for error. Tight constraints on sump capacities exacerbate the influence of volume on plant control. In the operator's drive to limit spillage and avoid the plant feed cutting off due to insufficient sump volume, levels in sumps are typically maintained within a specified range. The bleed valve to the dilute sump is often used for the purpose of adjusting correct medium sump level. By operating the bleed valve in this manner, the volume in the sump will change, however, the level of non-magnetics can also drop without the operator's knowledge. There exists a trade-off between operating for stable volume and for optimum density. The key lever in plant performance is of course, density, and as Phillips (2010) states in his study, positioning the bleed system manually and letting the sump level float provides a tighter density control than if the focus were to be on controlling the bleed for sump level.

When a density change is required, volume control becomes critical. For instance, if the density is lowered, additional water will automatically be introduced into the system,

thereby increasing the level in the correct medium tank. If there is insufficient room in the correct medium sump, the operator will likely increase the bleed to reduce level. Firth et al. (2014) explored the effects of non-magnetics levels during plant operation from start-up conditions. When the bleed is opened, the operator is generally unaware that the open bleed can leave insufficient non-magnetic material in the correct medium, because the control system does not show them that the level of non-magnetics is dropping. Although the density of the medium may respond relatively quickly, within say, ten minutes, the non-magnetics concentration can take some time to recover. Figure 2.18 demonstrates the time taken for a coal circuit to recover from a plant shutdown with non-magnetics levels experimentally determined.

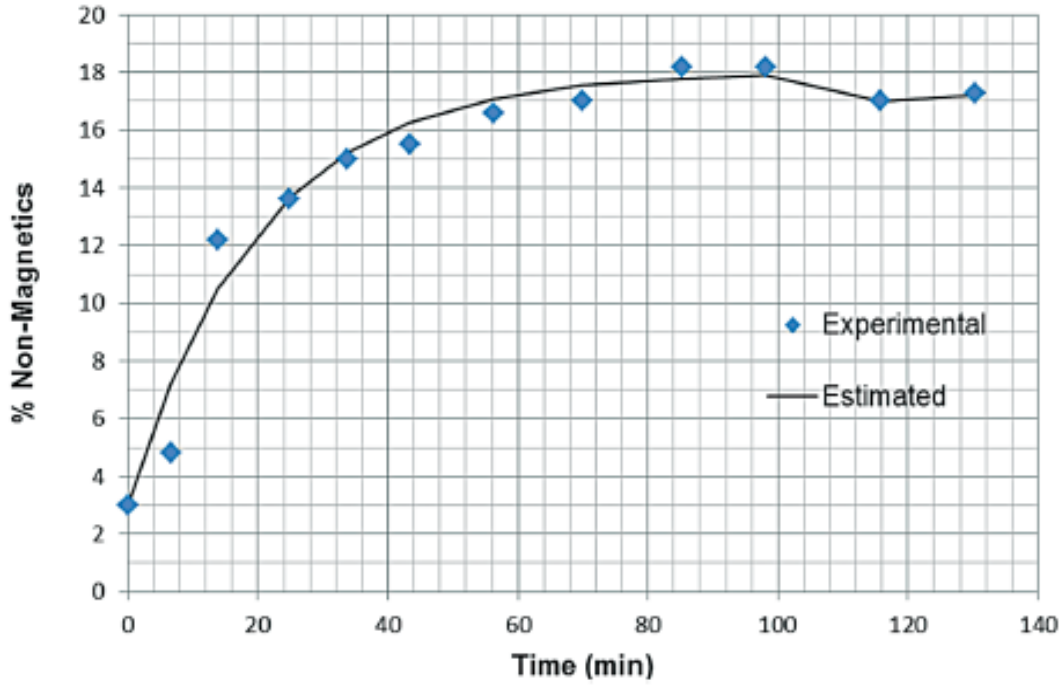

Figure 2.18: Comparison of % non-magnetic material in the correct medium after a plant start up over time. (Firth et al. 2014)

In this particular case, it took more than sixty minutes before the non-magnetics level stabilised. In some cases, if the correct medium bleed to the dilute circuit is left at a high rate, the system may not recover and non-magnetics could reach a level where the system becomes unstable and the DMC surges.

2.11 Modelling and Simulation

In recent times the constant challenge to improve business profitability has driven an increased demand for dynamic modelling expertise. The availability of online instrumentation and connection into plant control systems have enabled more inputs to be analysed and interpreted. Models developed in the past, while still relevant today, were constructed with less available information and in older programming languages such as Fortran. The process layouts of the plants studied at that time were also somewhat different from the more modern designs. The improved capability of current modelling software has broadened the potential for more in-depth analysis in dynamic computer models. Plant designers have historically used steady state modelling for design and construction purposes, however insights from online instrumentation could be extremely valuable, particularly in terms of designing for changing circumstances in a coal plant such as a seam change. While steady state models assume many constants, in practice, many of these parameters shift in real time. The ability to see the magnitudes of the shifts and the downstream effects can be better observed using dynamic modelling. The following section will review existing models and modelling methods in common use and review the reasons why a dynamic model is required in this project.

In 1982, Lyman et al. developed a dynamic model of a DMC circuit at Westcliff Collieries. The research included interfacing of plant control system instruments with a computer to log plant data. The model divided the dense medium circuit into individual units of operation and performed calculations around each unit. A number of important assumptions were made in this model. It was found by experiment that sumps behaved as variable volume plug flow devices. The DMC was found to have virtually no residence time and was therefore modelled as a pipe. The drain and rinse screens were assumed to have perfect recovery of magnetite on the rinse section with a second assumption that the coarse screened material moisture content at the desliming screen was the same as the moisture content at the drain and rinse screens. The volume of medium carried on the coal from draining to rinsing was calculated as a function of coal surface area and rinse water rates were held constant. The magnetic separator model used was determined based on earlier work by Davis (1981). His model used an experimentally determined percentage recovery based on the mass flow to the magnetic separator. Stream splitters

were assumed to have no delay and were designed as a pre-determined proportional split of the incoming stream.

This early work was critical to control system design, particularly with respect to modelling locations for water addition points into the correct medium for improved density control. The research of Lyman et al (1982) was further developed to form part of Askew's (1983) Fortran model. While Askew was also involved in Lyman et al.'s earlier work, he modelled an additional site, Buchanan Borehole Colliery in his later research. These circuits were not identical to the New Acland design, and in some cases were two-stage operations with a primary and secondary product. Askew's research into water locations for density control led to the simulated change to the design of water addition to the dense medium circuit at Buchanan Borehole Colliery being successfully implemented in the plant, with resulting improvements in density response time.

Both of the dynamic models used by Lyman et al. and Askew were structured using discrete volume elements of data expressed in an array format, with each volume parcel containing specific properties. At each time step, a volume parcel was moved into the pipe or unit of operation, and another parcel of equal volume removed. Multiple components in each stream were dealt with by creating dummy pipes in parallel. Throughout the time steps, each volume parcel retained its properties and the time taken for the parcel to reach the exit of that particular unit of operation was determined based on the variation in flowrate into the unit. All elements were considered to be full with the exception of the first and last elements (inlet and outlet) which had a combined volume equal to one full element. The properties in each volume exiting the unit were calculated from previous volume parcels. This volume parcel concept has been adopted for the development of the new dynamic model.

The key deficiency in Askew and Lyman's research was that the modelling of components did not consider the behaviour of non-magnetic components in the medium, but rather, simply modelled magnetite and water. The unit operations modelled used simplified models that required tuning to plant data, and it was acknowledged that further improvements could be made to the unit operation models in future research. Since this research was completed in the 1980's, considerable advances in empirical models have occurred, leading to better prediction of plant behaviour and new opportunities for dynamic modelling.

Following on from Askew's work, Wiseman et al. (1987) developed, and tested a dynamic model of a coal preparation plant and verified the data using plant audits and an on-line ash gauge. The model comprised menu driven operation to select unit operation models from a library. In addition to DMCs, other types of coarse coal processing equipment were also modelled. The dynamic model also extended beyond the coarse coal circuit to include other aspects of CHPP operation such as size classification, fine coal and feed washability. It was noted that computer memory was a limitation of the research, and this drove innovative solutions to handling of washability data for streams using arrays and mathematical models. Unit operation empirical models available for this research were still limited and have been considerably improved since this time.

The body of research by Wiseman et al. (1987) is still useful as a general model and formed the basis for JKSimMet and JKSimCoal steady state models. The work of Wiseman also led to the development of LIMN steady state software. It is now very common for CHPP designers and coal producers to use LIMN as their standard software package. The advantage of LIMN for coal use is its user-friendly structure in a familiar Microsoft Excel software program. More simulation software such as JKSimMet and JKSimFloat exist for metalliferous applications, but the need for this level of complexity in coal has not yet been identified. Many other steady-state modelling software options exist and are applicable to the coal industry. The use of LIMN has prevailed over the past twenty years due to its ease of use and coal-specific design. LIMN however, does not have a dynamic modelling component. Dynamic models of coal plants have been fewer in number, and their use has been relatively limited. There is, a general growing interest in dynamic modelling in the coal industry at the moment. Its potential to model from mine to port with multiple complex variants allows great flexibility and insight into a coal operation.

The interest in dynamic modelling has led to further research by Meyer (2010). Meyer dynamically modelled and verified a coal preparation plant at Leeuwpan Colliery in South Africa using Matlab Simulink. His approach was from a process control perspective and he did not appear to have the benefit of a coal preparation background, and therefore was reliant on the plant metallurgist for practical input. Meyer and Craig (2011) then developed a steady state partition curve from the dynamic model. The use of a dynamic model to create a steady state model also seemed somewhat superfluous from a coal processing

viewpoint given that many steady state models already existed and provided good predictions.

Meyer derived equations for the dynamic model from first principles and used verification from spot audits, however, it is surprising that Meyer did not fully utilise historical empirical models such as (Wood et al, 1989 and Wood, 1990) that were experimentally determined for relatively small DMCs based on significantly more coal data than that used by Meyer (2010). The fine coal DMC circuit studied at Leeuwpan had significant complexity, and some areas of the model were simplified. For instance, in Meyer (2010) the medium components were not considered in the model, and the dynamic model simulated underflow and overflow densities based on the work of He and Laskowski (1993) rather than measuring actual values in the Leeuwpan Colliery. The work of He and Laskowski was conducted in a laboratory environment and therefore may not have provided a close fit to data from the South African coal wash plant itself.

Meyer and Craig (2014) then extended the model to encompass the coarse coal DMC circuit and to create a steady state model. The testwork completed for the coarse coal circuit simulation looked at only two plant validation cases; one where the plant feed was varied but the medium density was held constant, and the other where the medium density was varied and the tonnage held constant. Meyer noted that the degree of influence from the two verification audits was far greater for the medium density variation than from the tonnage variation. It has however been widely acknowledged in the coal industry for some time that a medium-based model (Wood et al. 1989) is appropriate for a dense medium cyclone circuit as the medium has a strong influence on DMC behaviour. This has been further supported by more recent work by Firth et al. (2014).

A number of factors were assumed by Meyer to be constant due to lack of information, for example, the coarse material feed rate to a module was calculated as the difference between the primary screen feed and the oversize feed, feed rates to the circuit were weighted based on weightometer readings from the total plant feed which incorporated significant noise. Meyer also assumed that the volumetric flowrates of the feed, between underflow and overflow were constant before and after a step was introduced to the medium density or feed rate. He used product yield and product quality data from the Leeuwpan Coal plant to determine whether or not there was an opportunity to improve or optimize the process control system. Product yield data however, was hampered by

weightometer inaccuracy and the lack of measurement points within the actual DMC circuit. The feed rate of coal to the DMC mixing box was not measured and therefore estimations had to be made based on screen splits using expected particle size distribution rather than from in-plant sampling. Similarly, the density of the mix was not measured and DMC inlet pressure was used for indication, however other factors such as sump level changes, surges or uneven feed of coal from de-sliming screens and pump cavitation could have influenced the values. Medium density was measured but medium behaviour was not modelled.

A simulated output of overflow and underflow densities was modelled, but Meyer (2010) proposed that the increase in differential was due to the feed being reduced, ie. a change in medium to coal ratio. Meyer did not delve further into this and quite likely would not have realised that the increase in differential could have been related to the loss of non-magnetics from the system via the bleed line if tonnage dropped but bleed levels remained constant. The change in differential also seemed to track the water and magnetite model where the water valve closed while density was increased which logically would have resulted in a gradual increase in magnetite concentrate returning from the magnetic separator into the correct medium without a corresponding increase in non-magnetics as plant feed rate dropped. Meyer's work from 2010 was verified with only one audit, and the latter work in 2014 with an additional two audits, only one of which used a change in medium density. This verification may therefore not hold across all plant situations.

While components of the feed were considered by Meyer according to the principle of conservation of mass, these were limited to ash, sulphur, moisture, medium and fixed carbon components without detailing medium constituents such as non-magnetics. It was found that the model did closely approximate the results found in the spot verification audits, most data points of which were taken from the control system. Meyer's recent work highlights the lack of adequate information and measurement systems available in dense medium circuits and in coal preparation plants in general. He recommended further work on a longer-term basis to do additional verification of his model.

In the above research efforts, a lack of adequate online information hampered research efforts. Verification was by snapshot audits due to a lack of long range data. The models did not attempt to model non-magnetic components in the medium. Accurate measurement of changes to the dense medium proved difficult due to the absence of

sufficient instrumentation. By comparison, the New Acland instruments adopted for this project allowed the modelling work to be advanced as the in-stream monitoring of drain and rinse screen underflows, the correct medium, screen mass flow rates and DMC feed flow rates could be incorporated with traditional plant instrumentation to obtain a far more comprehensive understanding of what happens over time. Previous modelling efforts also focused on smaller diameter DMCs whereas the New Acland DMCs, being a larger 1300mm diameter, yielded considerably more large DMC data for modelling.

The use of a dynamic model for coal preparation has not become commonplace, largely due to the high level of complexity and cost required to set up the models. For engineering design purposes, steady state modelling has provided sufficient approximations to achieve a satisfactory design. The advantage of dynamic simulation however, is the ability to achieve optimisation of control circuits and to make incremental adjustments for the plant to perform at optimum levels for a higher proportion of the time. The incremental losses from poor instantaneous performance can compound into significant yield losses over time. Capturing these incremental gains can greatly enhance profitability.

Non-coal examples of dynamic modelling include alumina and petrochemicals. SysCAD was used at the Yarwun Alumina Refinery in Gladstone for both plant design and operations, the latter use including the training of control room operators on a simulator. This has proven to be a very useful mimic of the real plant operation. Pilot tests can be run using dynamic models without the high cost of plant trials or without potentially dangerous consequences of a plant incident occurring. The Yarwun example has given the author confidence that the dynamic model's potential as a training tool and for testing control system changes will be extremely valuable. Similar examples exist in petrochemicals for operator training systems and dynamic models for advanced process control.

2.12 Literature Review Findings

Although dynamic models have been built in the past for Coal Handling and Preparation Plants, most notably Lyman et al. (1982), Askew (1983), Wiseman et al. (1987) and Meyer (2010), modelling of changes in the coal medium and non-magnetics have not been sufficiently studied. Development of dynamic models has been limited in the past by a lack of available plant data, computer memory and processing capability. Currently available technology allows far greater processing power and software capability. Novel instruments installed at the New Acland CHPP allow information to be collected that was previously unavailable. New experimental procedures using RFID density tracer technology provide additional plant data such as residence times for individual particles. Empirical models for DMC circuits such as those detailed in Crowden et al. (2013) have been significantly improved since early modelling work was done and a wider range of plant information is now able to be collected. Recent studies of changes in DMC medium composition within and between plants (O'Brien, et al. 2013) have shown that the level of non-magnetics influences medium stability when targeting a low density cut-point and therefore has an influence on plant behaviour. This new knowledge of non-magnetics will also be integrated into a dynamic model.

The outcome of this research will be a dynamic model of the New Acland dense medium circuit which, supported through experimental results and existing empirical models, better explains the behaviour of a dense medium circuit. The model will utilise existing empirical relationships that are accepted by industry as providing reasonable predictions of plant behaviour. Non-magnetics concentration in the medium will be predicted using a breakage model and results will then be verified against past plant event data collected during the experimental work stage.

This research differs from past research efforts in that novel instrumentation and techniques have been used to collect experimental data, and the inclusion of medium components to predict the proportion of non-magnetics in the medium has not previously been attempted. Changes that result from fluctuations in magnetite additions, density adjustments and the bleed valve which diverts non-magnetics to the magnetic separators

can also be incorporated into the dynamic model. The dynamic model can then be used to guide operators to better understand DMC circuit behaviour.

A dynamic model will provide coal producers with critical drivers for optimal dynamic DMC circuit performance and operator training. Plant observations and physical measurements will be used alongside on-line data to verify the model. Samples of the medium, analysed for %non-magnetics will be incorporated into the dynamic model. Benefits derived from this project include potential improvement of plant profitability through better utilisation and optimal operation of dense medium circuits and improved understanding of dense medium circuit fluctuations.

Experimental Work

3.1 Process Description

Numerous site visits to the New Acland coal handling and preparation plant (CHPP) were conducted over the course of the research. Some visits were for the purpose of plant observation and discussion with plant personnel. This provided valuable insight into the circuit operation and limitations. Other visits were on designated test dates with sampling and subsequent analysis. The author would like to acknowledge the work of the control room operators who obligingly operated the plant to test the various case conditions. The New Acland plant consisted of two separate modules. The focus of the PhD was on Plant 2 dense medium circuit. A schematic of the plant 2 dense medium circuit is shown in Figure 3.1.

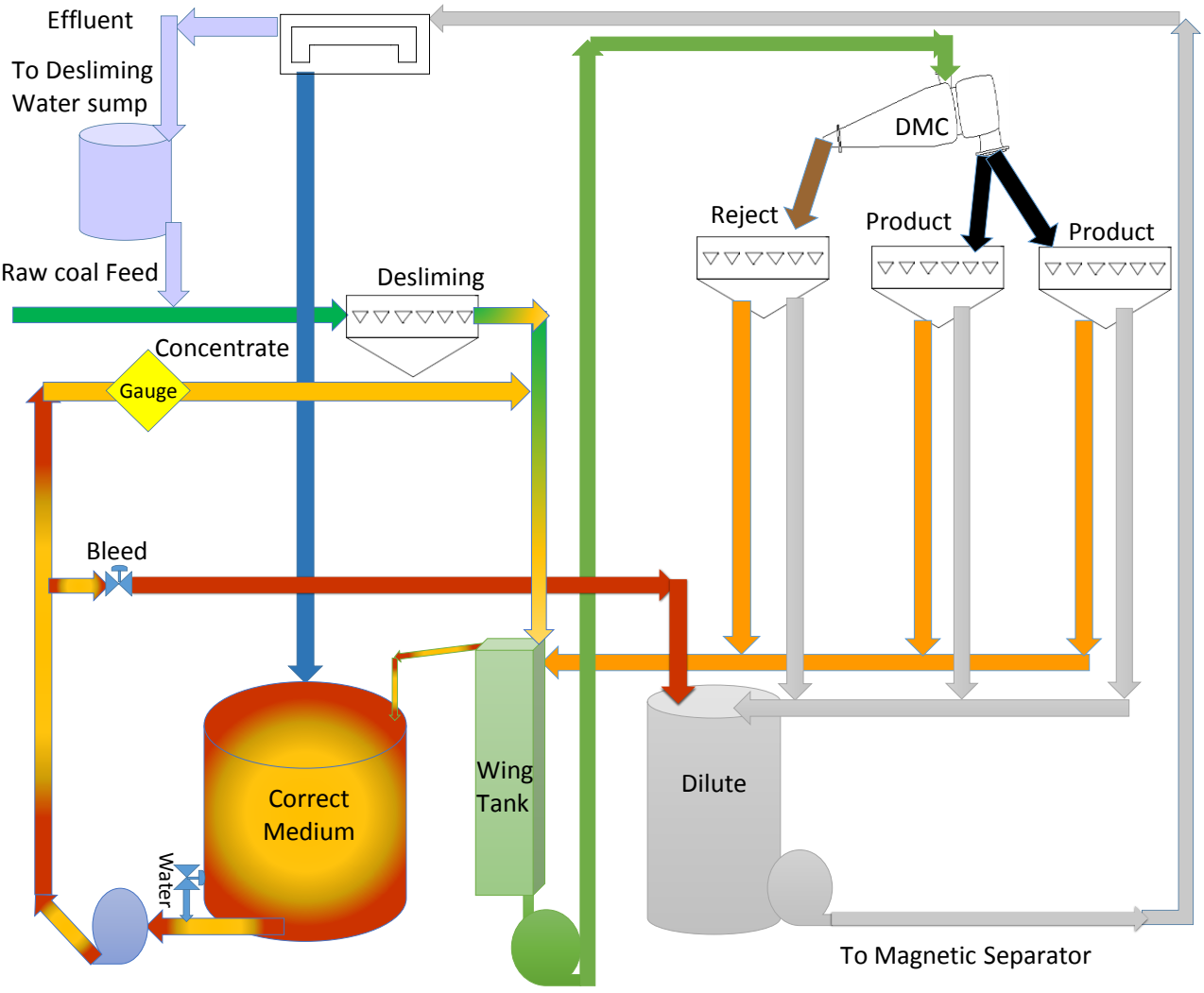

Figure 3.1 The New Acland Dense Medium Circuit plant 2.

Plant 2, which processes approximately 550 tph of raw coal, is comprised of a single-stage DMC circuit treating the deslimed coarse material which is minus 50mm by 1.4mm w/w (wedge wire) material. The minus 1.4mm w/w material reports to the spirals circuit. The plant does not have a flotation circuit and thus, the minus 150 micron material reports directly to the thickener. The deslimed coarse raw coal is mixed with medium after the desliming screen and enters the coal side of the wing tank. The wing tank is split into two parts, the coal side which pumps to the DMC, and the seal leg side which overflows back to the correct medium sump. The two sides of the tank are separated by an orifice plate and normal operation is for medium to flow downwards through the orifice plate from the seal side into the coal side. The drained medium returns to the wing tank via the seal side, and a portion of this overflows into the correct medium sump. The wing tank coal side pumps to the DMC and the overflow reports to the product drain and rinse screen. The underflow of the DMC reports to the reject drain and rinse screen.

The coarse coal product is then centrifuged and sent to the stockpile. The coarse rejects are transported to the rejects bin and are then transferred back to the mining pit waste area. The underflow from the drain and rinse screens is split with the drain sides combining and returning to the seal leg of the wing tank, while the rinse underpans are combined and sent to the dilute sump which then pumps to the magnetic separator. The effluent of the magnetic separator returns to the desliming water sump at the start of the process. The concentrated magnetite from the magnetic separator is returned to the correct medium sump. Within the dense medium circuit, a rising density system exists. The outlet of the correct medium sump has a water addition valve which is controlled in a feedback loop to the nucleonic gauge which is situated further down the correct medium line. When the medium density is too high, the water addition valve opens to dilute the medium density. When density is too low, the water addition valve shuts.

A bleed line exists in the correct medium line between the automatic water addition valve and the nucleonic gauge (Figure 3.2). The butterfly valve on the bleed is controlled manually by the control room operator. The bleed line runs directly to the dilute sump. Controlling the bleed valve enables the operator to control volume in the correct medium sump, but also enables non-magnetic material to be removed from the medium in the magnetic separator, thereby concentrating the medium density. The bleed line is a nominal 100mm diameter pipe which rises approximately 500mm directly above the

correct medium pipe which is 330mm diameter and oriented in a horizontal plane. There are three elbows in the line from the pump to the bleed take-off therefore segregation due to bends is possible. As the bleed take off is on the top of the correct medium pipe approximately 1500mm from the preceding elbow, particles could also segregate in the horizontal pipe allowing lighter density floating particles to flow up into the bleed line. The installation of the nucleonic gauge on a horizontal plane is also not ideal.

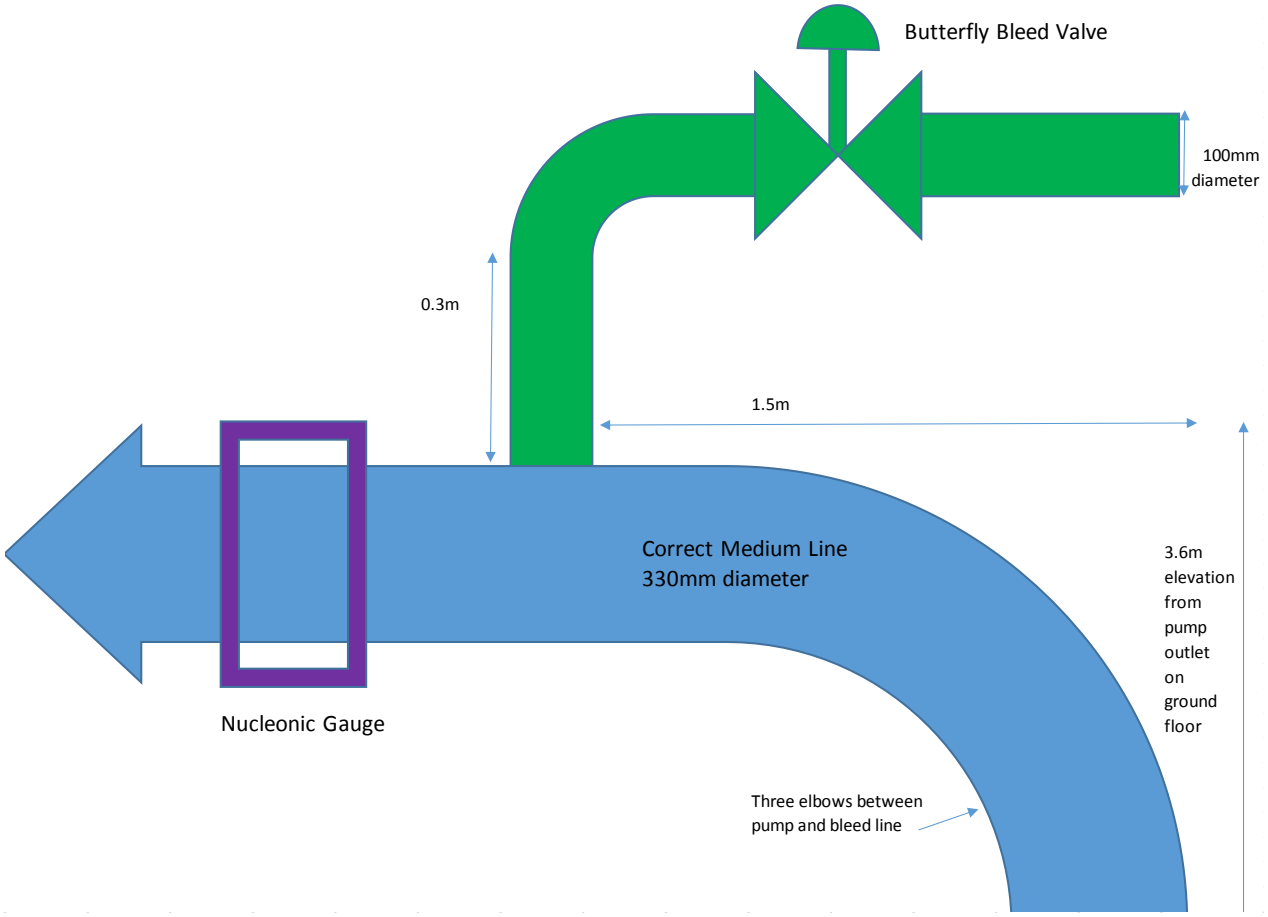

Figure 3.2: An elevation view of the piping layout for the bleed split to the dilute sump in the correct medium line.

Prior research by O'Brien et.al. (2013) has demonstrated that the level of non-magnetics in the medium is important and therefore, the function of the bleed valve is integral to successful DMC circuit operation. The program of experimental work outlined below has incorporated monitoring of the bleed valve in order to assist with developing a dynamic plant simulator.

3.2 Outline of Experimental Research

The literature review has identified a number of areas in which further research is warranted. It was established that there is a need to better understand the behaviour of non-magnetics during various plant events. Depending on seam variation and mining method, the plant feed can vary widely, triggering a wide range of plant operating set points. For instance, a plant feed change could lead to a change in density target from 1.30RD to 1.60RD, or a step down by a similar amount. This plant feed variation, coupled with technical marketing product ash requirements, can necessitate multiple density set point changes per day. The broad range of plant feeds at New Acland mine means that changing the density set point is a regular occurrence. The corresponding plant responses to large and small changes, as well as incremental changes, has not been widely documented. Quantifying the cumulative yield impacts of density changes is expected to lead to generation of ideas for better circuit control and management and a consequential reduction in yield losses. In terms of non-magnetics, it is only through the collaborative work with CSIRO that plant responses are now being measured. Measurement of the changes in non-magnetics aligned with plant events will also assist in better plant control, and will provide vital data for the dynamic model.

A number of tests were devised to assess plant behaviour under changing plant conditions. The difference between a single step change and an incremental change in density, and the difference between an increase and a decrease in density need to be assessed based on the plant response. Similarly, the effect of an unstable environment, with overflowing sumps, and the plant operating at its density extremes would yield useful information about how the plant copes and how long it takes to return to stable operation. Finally, the observations made of the New Acland plant during the course of this research and the related body of collaborative work has suggested that the operation of the bleed is often done for volume control, not for metallurgical control and that the effect of the bleed operation on non-magnetics concentration in the medium needs to be further quantified.

Reviews of prior research did not reveal the time taken for coal particles to travel through the coal washery, nor how long some particles may linger in the dense medium circuit. A

test therefore needed to be devised to determine residence time for the model. Using recently developed technology radio frequency identification (RFID) density tracer technology, a new application was found. If the RFID density tracers, each with individual identifier tags, were timed as they travelled through the circuit, it would be possible to achieve residence times for each individual particle. This information could then feed into the dynamic model as a delay or time-lag measurement. The presence of two different sized tracer particles, 13mm RFID tracers and 32mm standard tracers also offered an opportunity to investigate the relative differences between particle size, cut-point and efficiency by developing partition curves.

A number of test cases were established for data collection at New Acland site. These cases were determined from specific events observed in previous instrument data collection. A summary of the test cases is given below:

Case A: Good density change.

This test intended to ascertain how the plant would respond in a stable situation where a controlled density change occurred with minimal instability. This test also considered a controlled bleed volume to ensure that the non-magnetics remained relatively constant. A plant with well controlled levels in sumps and no feed interruptions was also required for this test. The test then aimed to follow what happened to the density and the concentration of non-magnetics when plant was initially in a stable condition and a controlled change occurred.

Test: Following a stable transition of density in the dense medium circuit, collect correct medium samples at 10 min intervals for an hour and then for 20min intervals for 2 hrs thereafter. Analyse for the proportion (dry weight %) non-magnetics, density, and particle size.

Case B: Unstable Volume.

When plants are operating at a low density set point, a situation can arise where volumes are unstable. The amount of water in the system is too high and the sumps overflow. The cause of this, is the inability of the circuit to rid itself of excessive magnetite in the system.

If there is a high level in the correct medium sump due to a change from high density to low density, the water valve on the correct medium sump compensates for the concentrated magnetite being added back into the correct sump from the dilute circuit. This can lead to an overflow situation, however the overflows return magnetite to the dilute which recycles back into the correct sump via the magnetic separator, thereby leading to further water addition. It can take some time for the plant to regain stable sump levels after this type of density change, particularly if the previous density set point was high. This test aimed to look at the plant response to such a change in terms of the level of non-magnetics and the time for the density to reach set point. The test also looked at the effect of changing bleed levels during this type of situation.

Test: High level in the correct medium sump and a high level in the dilute sump before density drop. Open Bleed to 100%. Collect correct medium samples at 10 min intervals for an hour and then for 20min intervals for 2 hrs thereafter. Analyse for the proportion (dry weight %) non-magnetics, density, and particle size.

Case C: Stepwise density change:

While normally a density change would be done in one single step, eg. 1.3 to 1.4, or from 1.4 to 1.6, it was noticed that some operators prefer to step the density up in increments. The effect of stepping up in increments compared with a standard single step was tested using this case.

Test: Measure the time for the circuit to recover from a density change (Rise / Fall) after a large step change in density. Do the same for a change in small increments. Collect correct medium samples at 10 min intervals for an hour and then for 20min intervals for 2 hrs thereafter. Analyse for the proportion (dry weight %) non-magnetics, density, and particle size.

Case D: The low density stability test:

The intention of this test was to investigate the behaviour of the circuit in a low density situation where there was an unstable level of non-magnetics in the medium. Testing of the case required certain conditions to be present in the plant. The plant would need to be operating below a density of 1.40RD, and there needed to be a relatively low level of non-

magnetics in the system. In essence, a high differential, and potential surging situation. The test was then intended to add back non-magnetics into the system and measure the effect.

Test: Running on a low density set point, open bleed fully. Collect correct medium samples at 10 min intervals for an hour and then add non-magnetics to the system by adding thickener underflow. Measure Collect correct medium samples at 10 min intervals for an hour and then for 20 minute intervals for approximately 2 hours thereafter. Analyse for the proportion (dry weight %) non-magnetics, density, and particle size.

In practice, the aims of this particular test were only partially achieved due to plant conditions not being ideal at the time. While a low density target was achieved, the plant had significant quantities of non-magnetics present in the medium and was therefore not running at a high differential at the time.

Case E: Desliming sprays response test:

The intended aim of this case was to assess the plant response when an increased amount of clay slimes entered the dense medium circuit due to reducing the spray water on the desliming screen. Reducing sprays on the desliming screen had the effect of diverting some slimes adhering to the coarse coal over into the dense medium circuit. The effect of the change on the proportion of non-magnetics in the medium was then monitored.

Test: Running on a low density set point, open bleed fully, hose in magnetite, Collect correct medium samples at 10 min intervals for an hour and then add non-magnetics to the system by turning off desliming sprays. Collect correct medium samples at 10 min intervals for an hour and then for 20min intervals for 2 hours thereafter. Analyse for the proportion (dry weight %) non-magnetics, density, and particle size.

Case F: Tracer testing and determination of residence times in the DMC circuit

Partitioning Test: Insert a range of densities of 13mm and 32mm tracer sizes into the DMC circuit and compare partition performance.

This case was intended to measure both partitioning performance and the time taken for coarse coal particles to travel through the dense medium circuit. The full range of standard

tracer densities were inserted concurrently with the RFID tracers at the desliming screen. These were collected at the drain and rinse screens either via the antenna detection or by manual collection in the case of the standard tracers.

Residence Time Test: Insert a selection of 13mm RFID tracers at various densities into the dense medium circuit to analyse times for coarse particles to travel through the various sections of the DMC and dilute circuits.

As the RFID tracers contained a variety of densities, it was possible to measure the effect of density on residence time, both in the coal and medium circuits. Tracers of three different densities; one high, one low, and one density close to the medium density were inserted. The RFID tracers were inserted in a number of locations throughout the dilute and correct medium circuits and were detected using the antennas on the drain and rinse screens. This gave information about the relative times taken for particles to travel through the different routes in the DMC and dilute circuits.

3.3 Experimental Results

The outcomes of the various cases studied are detailed below:

Case A: Good density change.

Test: A stable transition of density in the dense medium circuit

On 14th June 2013 and 24th October 2013, correct medium density was monitored. The 24th October 2013 also coincided with a tracer test run. On the 14th June event, the level of non-magnetics was monitored and the figure 3.3 below demonstrates the results.

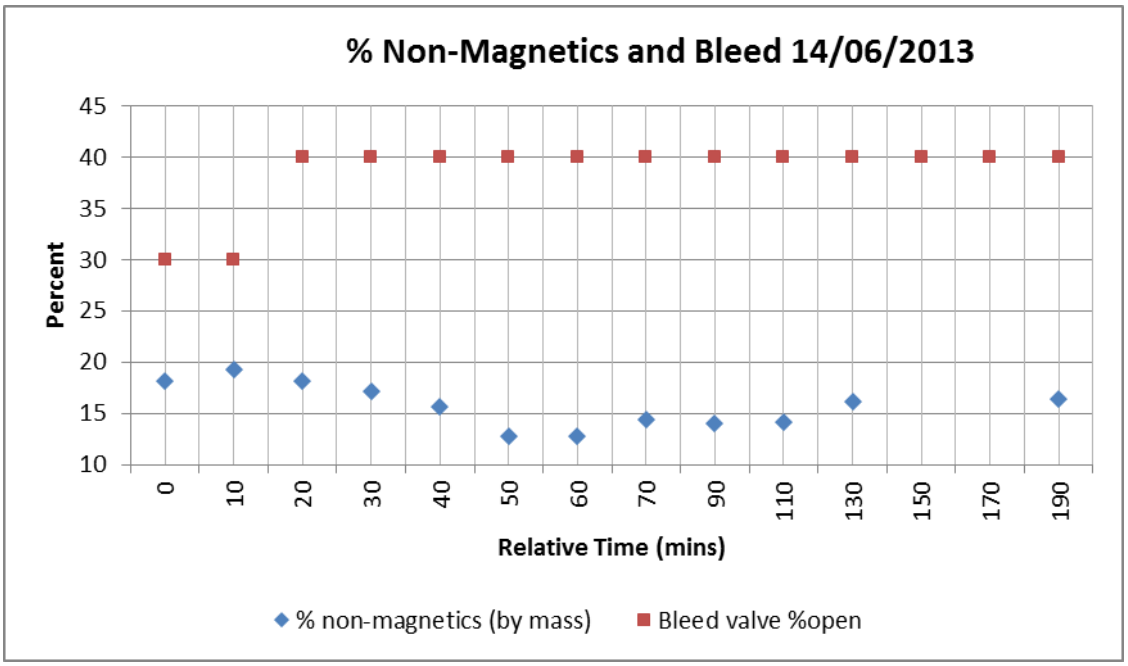

Figure 3.3: %Non-Magnetics measured on the day of the good density change trial

The following dot-points give a chronology of events:

- At t=0mins, which was 10 mins prior to the density change, a sample was taken of the medium
- At t=6 mins, the density was raised from 1.367 to 1.410 on the control panel
- At t=14 mins, The bleed valve which bleeds correct medium to the dilute was fully opened for one minute and then closed at 40% (previously it was 30%)
- At t=31 mins density was decreased from 1.410 to 1.398
- Between 40mins and 42mins the plant feed dropped off and then recovered

In Figure 3.3, the level of non-magnetics decreased as the bleed level was increased. The increase in density target would have also required additional magnetite which would have had low levels of non-magnetics associated in the fresh magnetite feed. This suggests that the choice of 40% open was too high and led to a loss of non-magnetics over time. The loss of non-magnetics was then exacerbated by the feed off event at the 40 minute mark. The differential of the cyclone remained steady however, and was well within the normal operating range (approximately 0.2). Despite the plant operation of the density change being done carefully, the reduction in non-magnetics was still quite pronounced with an increase in bleed valve opening. This indicated that the magnetic separators have the ability to rapidly change the amount of non-magnetics present in the medium, and also that feed off events can be severely detrimental to % non-magnetics. While this is a stable operation case, if the density target had been around 1.3, then the system potentially could have had a wider differential. This case also highlights that it can take a considerable period of time for non-magnetics to build up again in the system. In this particular case, the non-magnetics had still not reached its original level after sixty minutes.

Case B: Unstable Volume.

Test: A high level in the correct medium sump and a high level in the dilute sump before a density drop. Open the bleed valve to 100%.

On the 26th March 2014 the plant was found to be operating at 1.35 density and the density set point was lowered to 1.30 at 87 minutes. A chronology of events is given in Table 3.1. The plant had run on the previous day and night on a density set point of 1.6, so considerable amounts of magnetite and non-magnetics were thought to still be in the system at the time of sampling. The level of non-magnetics in the medium at the start of the trial was found to be 14.7%. During the trial period, DMC feed pressure remained relatively steady apart from a slight adjustment following the density change. (Figure 3.4) Plant feed rate was variable due to normal weightometer variability, however the average feed rate remained the same until approximately 200 minutes after which it increased by about twenty tonnes per hour. This was a considerable length of time after the density change occurred.

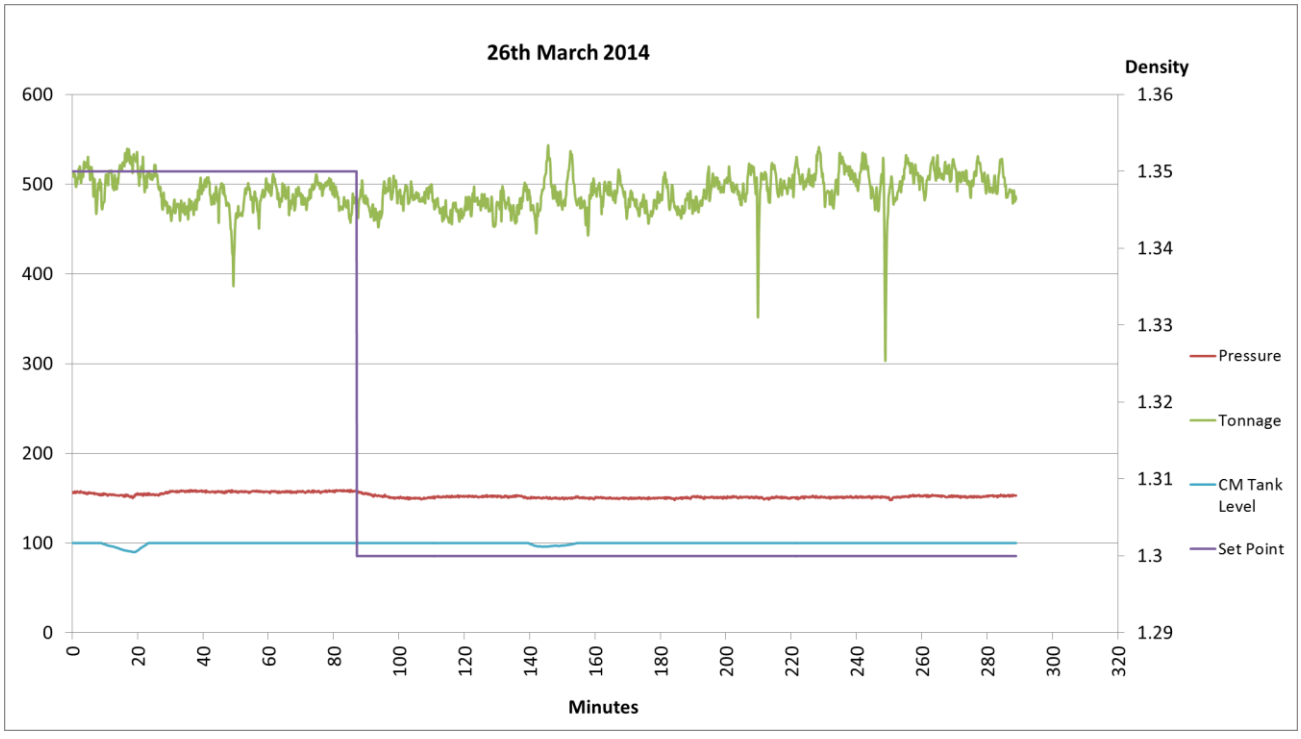

Figure 3.4: 26th March 2014 Plant conditions

Plant feed tonnage was relatively continuous during the trial at 500tph and increased by approximately 20tph from approximately 200 minutes. A density change downwards was observed at 96 minutes from 1.35 to 1.30. The correct medium sump was at maximum level.

Samples were taken of the correct medium from 10:30am in intervals of ten to twenty minutes. During this time, the bleed was opened to 100% on two occasions, one at each density set point. In both cases, the level in the correct medium sump dropped corresponding to the opening of the bleed. The level in the correct medium sump gradually recovered to 100% full at which point the dilute sump also returned to an overflowing state. In the time that the bleed was fully open, the level of non-magnetics dropped from 14.7% to 11.8% when operating on a density of 1.35, and in the second case at a density of 1.30, the level of non-magnetics dropped from 12.1% to 11.4%. It is thought that this second drop was less in magnitude because the system had not had sufficient time to recover from the previous density change and from the earlier opening of the bleed prior to the density change. This confirms expectations that the fully open bleed would be expected to remove non-magnetics from the correct medium under normal operation.

When the density was lowered to 1.30, (Figure 3.5) it was clear that the plant had difficulty maintaining control at such a low density. This was partly due to the fact that the night before, the plant had built up excess magnetite in the sumps from operating at a density of 1.6. Excess magnetite was visible in the floor sump area and suggested that the system could not effectively rid itself of the excess magnetite while the sumps continued to overflow. This was because the correct medium sump overflowed to the floor sump, the floor sump pumped back into the dilute sump which then overflowed back to the floor sump. In addition, the concentrated magnetite continued to return to the correct medium sump via the magnetic separators which were fed from the dilute sump pump. As the system was already struggling to achieve a sufficiently low density, the continual flow of concentrated magnetite meant that more water was continually being added to the system to compensate for the increasing density. This further exacerbated the existing water balance problem. In this particular low density case, the sump control issues suggested that it would have been useful to have a splitter box so that excess concentrated magnetite could be returned back to the magnetite pit or to an over-dense system rather than into the correct medium sump which generated more water addition to sumps that were already full in order to control the density.

The non-magnetics was also somewhat unstable. Although there was a noticeable drop in non-magnetics once the bleed was fully opened at 138 minutes, this drop in non-

magnetics did not sustain once the correct sump and dilute sumps began to both overflow. The level of non-magnetics then began to once again gradually build up in the system. A visual observation during sampling indicated that the medium did not rapidly settle out of solution when placed in a clear measuring cylinder suggesting that the medium was still quite stable despite the low density set point.

The results of this test case were analysed and it was found that the level of non-magnetics dropped for both density set points when the bleed fully opened but once the dilute and correct sumps began overflowing at the lower density, the level of non-magnetics began to recover slightly. Once the bleed valve was returned to the normal operating level of 20%, non-magnetics increased in the system by almost 2% to a level of just under 13.7% (Figure 3.5). This was some time after the density change had occurred and it is possible that the plant was beginning to return to a steady state. No surging of the DMC was noticeable at any time during the plant trial. The overflowing nature of the sumps during the trial at low density meant that the magnetite in the floor sump was continually recycling back through the system, leading to difficulties achieving density and volume control in the plant.

Table 3.1: Chronology for 26th March 2013

Relative time	**Timeline for 26/03/2014**
0 mins	Plant operating at a density of 1.35. Bleed at normal level of 30% open. Non-magnetics was 14.71% before any changes were made.
5 mins	Bleed was opened to 100% on request (not normal operating procedure)
10 mins	Correct medium sump ceased overflowing to the floor sump (flows to dilute)
20 mins	Bleed was closed fully (note butterfly valve still leaks when fully closed). Dilute sump was overflowed briefly (<5mins). Correct medium sump level dropped to 90%
25 mins	Correct medium sump resumed overflowing to floor sump (flows to dilute)
37 mins	Density set point dropped to 1.30, bleed remained closed.
79 mins	Bleed opened to 100% on request (not normal operating procedure)
81 mins	Correct medium sump ceased overflowing until 12:56pm when it again overflowed.
102 mins	Bleed valve was cycled by operator. Correct medium sump continued to overflow despite bleed valve being fully open. Valve was checked for blockage but no complete blockage was found. Partial blockage suspected.
131 mins	Bleed valve returned to 20% open by operator. (normal operation)
140 mins	Plant tonnage increased slightly by approximately 10 tonnes per hour.

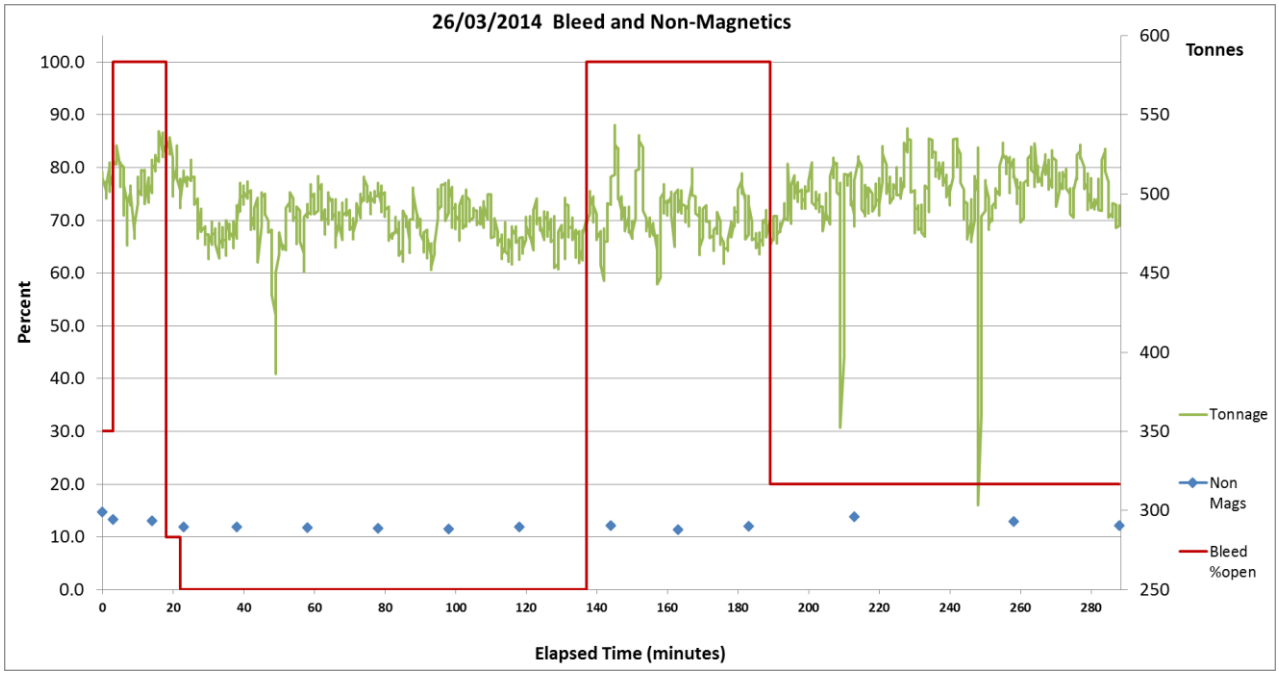

Figure 3.5: 26th March 2014 Plant conditions and Non-magnetics analysis.

26th March 2014 trial with density change from 1.35 to 1.30 and opening of the bleed to 100% in both density cases. Correct medium sump was at maximum level and overflowing during the trial.

Case C: Stepwise density change:

Completed 25/03/2014 from a density set point change from 1.427 to 1.500 and then to 1.600. Test: Measure the time for the circuit to recover from a density change (Rise / Fall) after a large step change in density.

On the 25th March 2013 the plant made a density change from 1.427 up to 1.600. (Figure 3.6) On this particular day, there was also a feed off event for approximately one hour while running at a target density set-point of 1.600. Sampling was continued during the feed off event to ascertain the system response. It was noted that during the feed off event, there was still a considerable amount of water that overflowed into the wing tank from the desliming screen. When the plant was restored to normal operation, the operator was requested to open the bleed valve to 100%. Non-magnetics was measured before, during and after the changes.

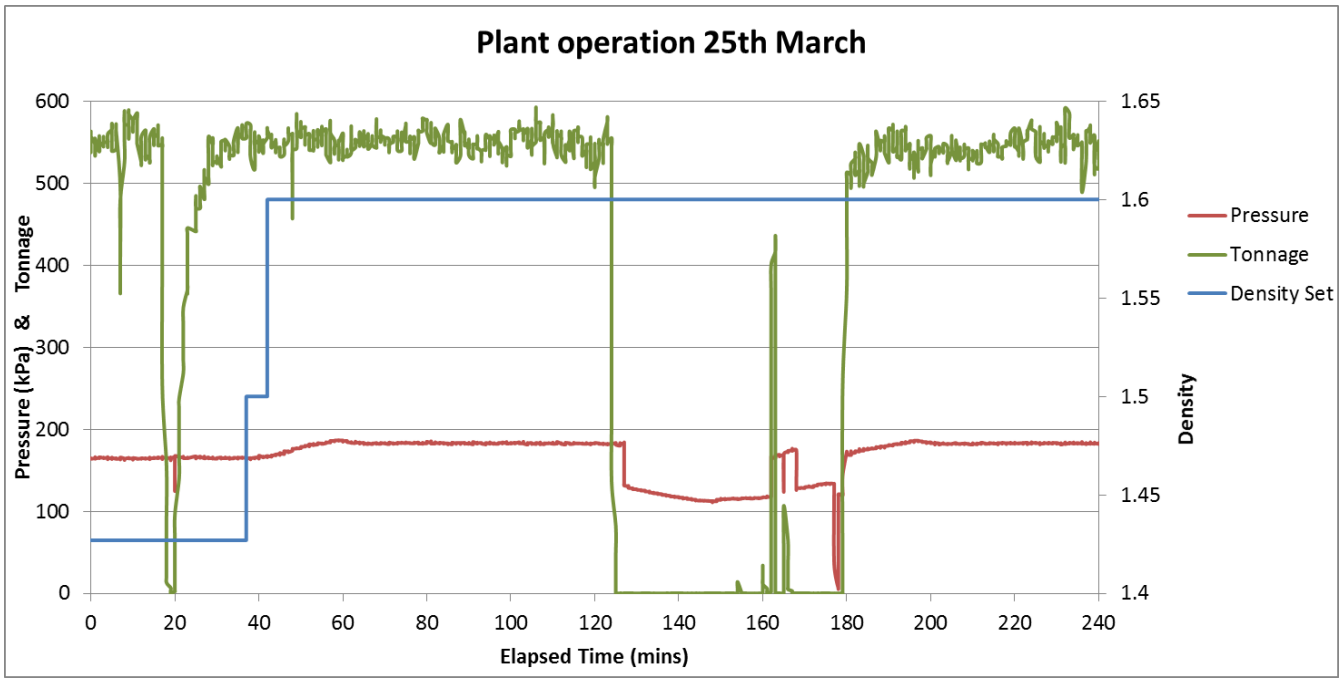

Figure 3.6: The density set point was raised from 1.427 up to 1.6. This caused a high requirement for magnetite in the system.

At a target density of 1.600, it was expected that the levels of non-magnetics in the dense medium circuit would be relatively high, and at the commencement of the experiment, and at the 1.427 density set point, the non-magnetics concentration was 20%. However, it is

known from past experiments that non-magnetics can be depleted when a feed off event occurs, particularly if the dilute circuit continues to remove non-magnetics from the system while no fresh coal feed is entering the circuit. A chronology of events is given in Table 3.2. In figure 3.7 the drop in non-magnetics concentration can clearly be seen to correspond with the two feed off events observed.

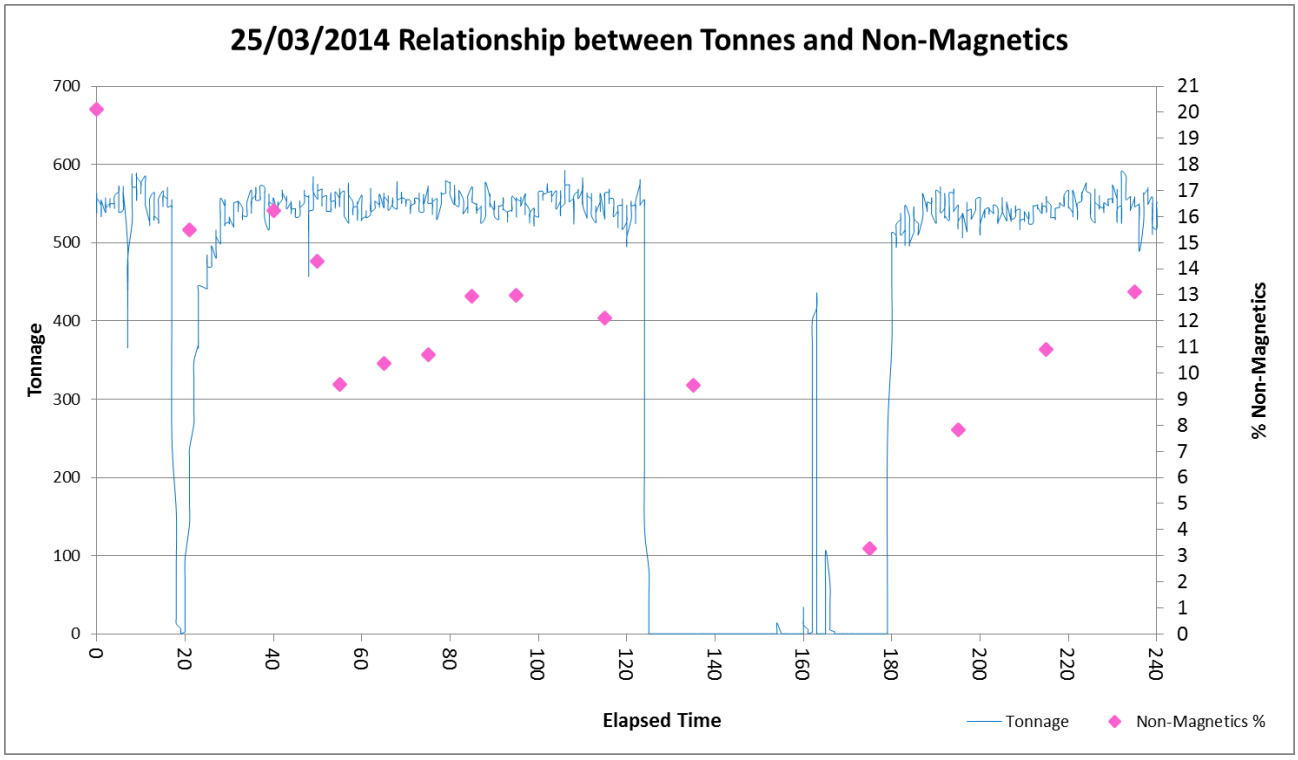

Figure 3.7: 25th March 2014. Plant feed tonnage and non-magnetics.

Density change and a feed off (coal off) event occurred. The density change from 1.427 to 1.600 occurs at 37 mins. Feed off events are clearly visible when the blue line dropped to zero.

Some indications of volumetric flows were also gained on this day because the desliming screen sprays were closed for two minutes and then reopened with a resulting change in flowrates to the dilute circuit. The level of the dilute sump clearly changed rapidly during this period. Within two minutes, the dilute sump volume filled from 40% to 100%. The reason for the fast filling of the dilute sump related to the clarified water line design. The water to the desliming screen branched off the same clarified water main as the rinse water to the drain and rinse screens. As the valve to the desliming screen was closed, water normally intended for the desliming screen instead diverted to the rinse screens which drain directly to the dilute sump. This result indicated that the water balance is extremely sensitive in this plant design. The desliming system response experiment is discussed later in Case E.

Table 3.2: Chronology for 25th March 2014

Elapsed Time	Event
0 mins	Pre density change. Correct medium sump (CMS) at 96%, **Density at 1.427, Plant feed rate 560tph, pressure 164kPa, bleed 30% open, non-magnetics 20.1%, actual density was 1.427.**
15 mins	New coal type in ROM. approx. 15 mins till change filters through. Actual density was 1.431
17 mins	**Feed off.** CMS dropped from 96% to 82% during feed off event. Bleed remained at 30% open. Actual density was 1.428
25 mins	**Feed on again. Bleed closed**, CMS 82%, non-magnetics 15.5%, actual density was 1.435
37 mins	**Density changed up to 1.500 from 1.427, Bleed opened 100%,** CMS at 94%, non-magnetics16.2%, actual density was 1.425
42 mins	**Density changed up from 1.500 to 1.600** actual density was 1.4701. Bleed 100% open, CMS 77%, Dilute overflowing by 10:39am.
47 mins	**Bleed changed to 20%,** Density set point 1.600, CMS 55%, Pressure 172kPa, non-magnetics was 14.3%, actual density was 1.536
58 mins	**Bleed changed to 10%**, CMS 42%, Pressure 185 kPa, Actual density was 1.633, non-magnetics was 9.6%
67 mins	**Bleed changed to 15% open,** CMS 46%, tonnage approx. 550tph, DMC pressure 182kPa, actual density was 1.596, non-magnetics was 10.39%
77-79 mins	Desliming sprays manually turned off for 2 mins then turned on again. Dilute sump rose from 40% to 100%(overflowing) during this 2 minute period. Non-magnetics was 10.7% before the change and 12.9% after the change, Actual density was 1.602
124 mins	**Feed off due to conveyor tracking problem**. CMS 43%, DMC pressure was 184kPa, non-magnetics was 12.1% just prior to the plant feed going off. Actual density was 1.599
127 mins	**Bleed fully closed**. Pressure dropped to 131 kPa, CMS at 34%, feed still off, Actual density was 1.600
132 mins	**Bleed opened to 50%** to control volume, CMS at 100% overflowing, feed still off, non-magnetics at 12:10pm was 9.52%, actual density was 1.407
137 mins	**Bleed changed to 10% open**, CM sump stopped overflowing, Operator also backed off desliming spray volumes to reduce overflow of water into the coarse launder feeding the wing tank. Feed still off, actual density was 1.386
144 mins	**Bleed changed to 50% open.** Feed still off, actual density was 1.407
151 mins	**Bleed dropped to 10%,** CMS at 58%. Feed still off.
153 mins	**Bleed opened to 50%,** CMS at 48%, actual density was 1.486
154 mins	**Bleed closed to 10% again.** CMS 41%, actual density was 1.504
155 mins	**Bleed closed completely (0%),** CMS 36%, actual density was 1.529
156 mins	**Bleed opened to 50%,** CMS 36%, actual density was 1.561
161 mins	**Bleed closed completely (0%),** CMS 26%. feed still off. non-magnetics measured at 12:50pm was 3.3%, actual density was 1.618
165 mins	CM sump level had reached 22.3% with the bleed closed and then proceeded to climb with the bleed still closed until 12:55pm. Possibly the operator may have opened the desliming sprays again leading to water entering the wing tank. There was a corresponding drop in density from 1.60 to 1.44 which indicates that water entered the system while the bleed valve was closed. The CMS level must be above 30% to start the plant. feed still off, Actual density was 1.628, but non-magnetics was very low (3.3% at 12:50pm)
168 mins	**Feed ON at 501 tph and building to 550tph target, Bleed opened to 20%,** CMS at 42%, DMC pressure at 170kpa, density target was 1.600 but actual density was 1.438
169 mins	**Bleed dropped to 10%,** CMS 42%, density target remained at 1.600 but actual density was 1.505, feed tonnes 523 tph, pressure 170kPa,
179 mins	**Target density of 1.6 reached,** bleed at 10%, Pressure 181kpa, tonnage 550tph, CMS 36%, actual density 1.595 This was a total of 11 mins run at an average of 18% yield loss due to slow time to reach density. (approximately 17 tonnes of product lost to rejects),
180 mins	**Bleed dropped to 5%,** (CMS level too low, operator had to preserve volume in the Correct sump to keep the plant running), feed tonnage 560tph, DMC pressure 181kPa, actual density 1.605, non-magnetics at 1:10pm was measured at 7.8%
198 mins	hose in floor sump for 5 mins (approx. 200 l/min), actual density was 1.598, non-magnetics measured at 1:30pm was 10.9% and at 1:50pm was 13.1%
233 mins (3h:53m)	Bleed remained at 5%, CMS 39.5%, density 1.600, trial period ended. Non-magnetics at 2:00pm was measured as 15.9%, and actual density was at set point of 1.600.

The density response is detailed in Figure 3.8 below. The time taken for the density to reach set point after the density change was 11 minutes. The yield loss of product averaged 6.7% over this time which equated to approximately 6.8 tonnes of misplaced coal.

The time taken for the density to stabilise after the second feed off event was also 11 minutes. It is estimated that during the period following the reintroduction of feed, the yield loss of product averaged 17% which equated to approximately 18 tonnes of misplaced coal.

While in isolation these losses may not seem significant, the frequency of these type of losses can be high, leading to an accumulation of yield losses over time. The speed of the density recovery could be enhanced by enabling faster addition and removal of magnetite from the system when a density change is needed. Operators are constrained by volume in the current situation and therefore cannot easily speed up the density response, particularly in the event of an unplanned situation such as the feed going off.

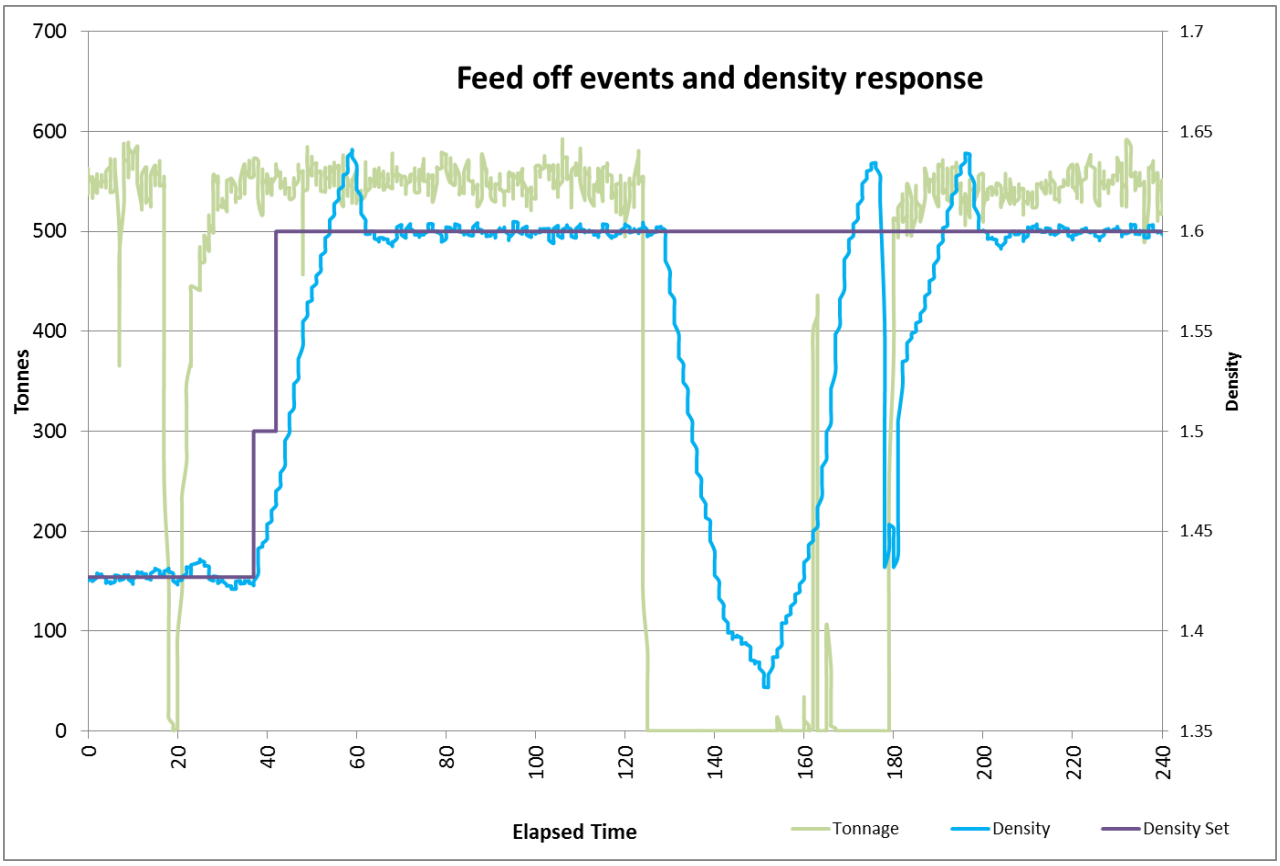

Figure 3.8: Density response to feed off events and to the density change.

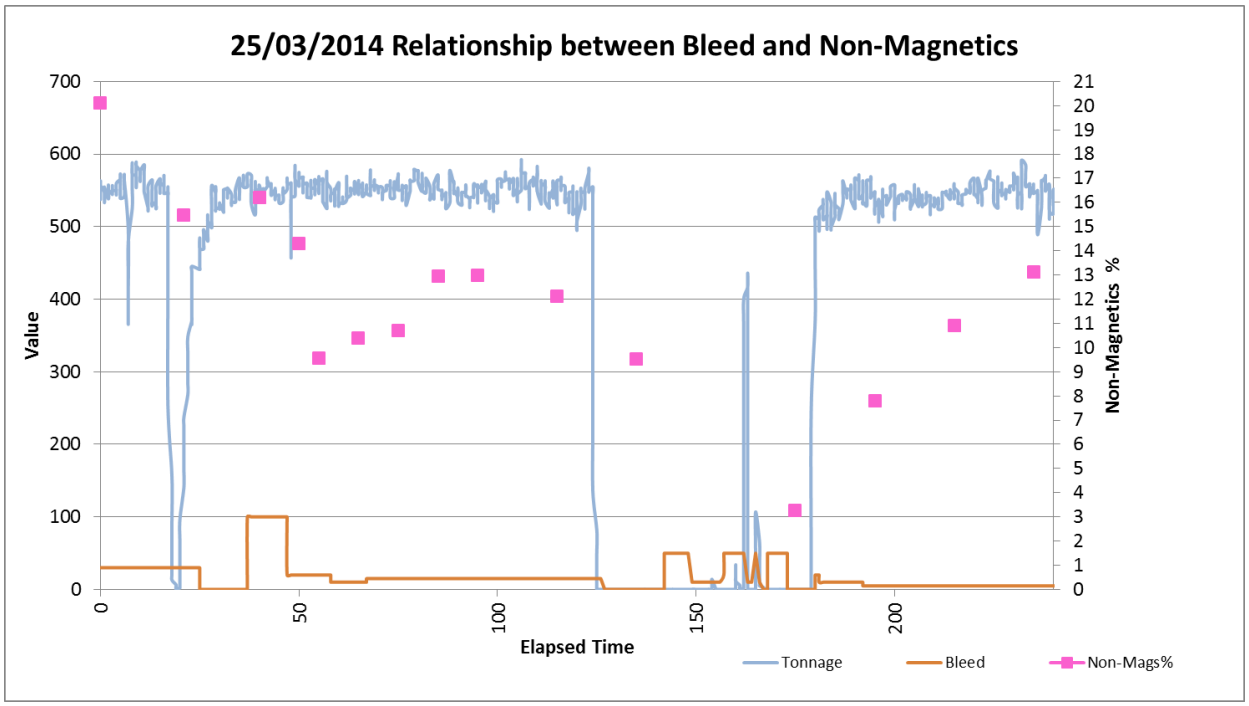

Figure 3.9: Relationship between bleed and feed off events with non-magnetics

Figure 3.9 demonstrates the effect of a drop in feed on non-magnetics in the medium. When the feed was off, non-magnetics experienced a gradual decline as the magnetic separator continued to clean the medium while the feed was off. When the bleed was opened to 100% a very clear drop in non-magnetics was observed. At lower bleed rates, the amount of non-magnetics declined more slowly.

Case D: The low density stability test:

Test: Running on a low density set point, open bleed fully, hose in magnetite, Collect correct medium samples at 10 min intervals for an hour and then add non-magnetics.

On 26/03/2014 the plant was operated at 1.30RD however, on observation, the medium visually appeared to be stable. It is thought that this was due to the previous night shift operating the plant at a target density of 1.6 and the higher levels of residual non-magnetics in the system. In general the plant volumes were unstable on this day and it was determined that it was not an ideal day to run this test. Observation of the desliming spray test and the bleed operation and the effects on non-magnetics levels in the other case tests (eg. 25/3/2014) demonstrated that non-magnetics can be quickly lost from a system, but also quickly regained if the desliming sprays are turned off for a short period. On this day, it can be seen that the level of non-magnetics in the circulating medium responded well in the first test at 1.35RD, but after the density change at the 85 minute mark, from 1.35RD to 1.30RD, the sump levels reached overflow (Figure 3.10a and 3.10b). Essentially, there was too much magnetite in the system and the plant did not have a means of removing the excess. The non-magnetics did not respond as significantly on the second occasion that the bleed was open, and in fact, went up after a short drop. It was noted that the correct medium sump was overflowing to the dilute via the floor sump part way through the second 100% bleed open test, which effectively meant that the bleed was occurring via the overflow on the correct sump. In this situation, operation of the bleed valve was ineffectual. As sump levels were already out of control in the plant circuits it is not surprising that the level of non-magnetics in circulation didn't respond clearly to an opening of the bleed in the second test. Under a more controlled sump level, it is expected that the outcome would have been different and that a more pronounced drop in non-magnetics would have been evident. It is important to note that this situation was a fairly extreme density change and the reasons for the plant sumps overflowing primarily related to the design limitations of a plant without an overdense storage system.

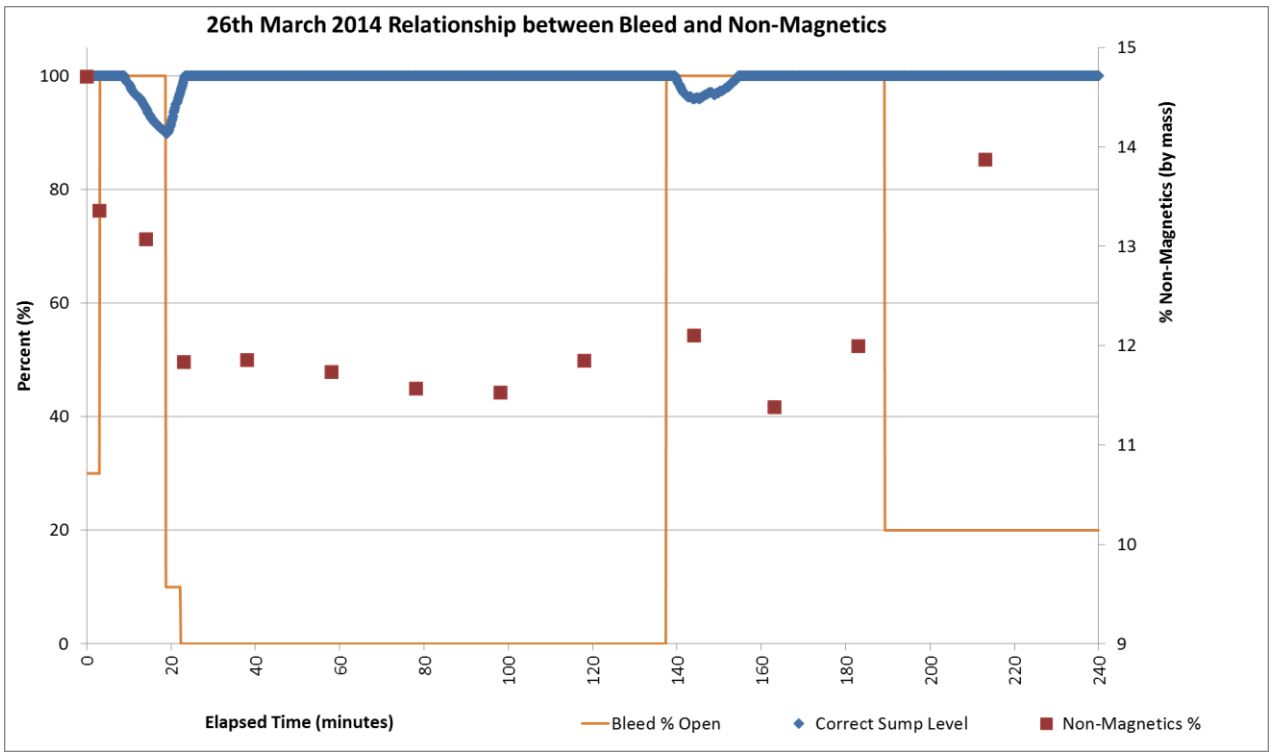

Figure 3.10a: Relationship between bleed and non-magnetics. When bleed was fully opened on two separate occasions on the same day, the level of non-magnetics dropped. The correct medium sump was full during the majority of the test work, however the drop in level can be seen when the bleed was initially opened fully. Figure 3.10b below shows the density and density set point during the same period.

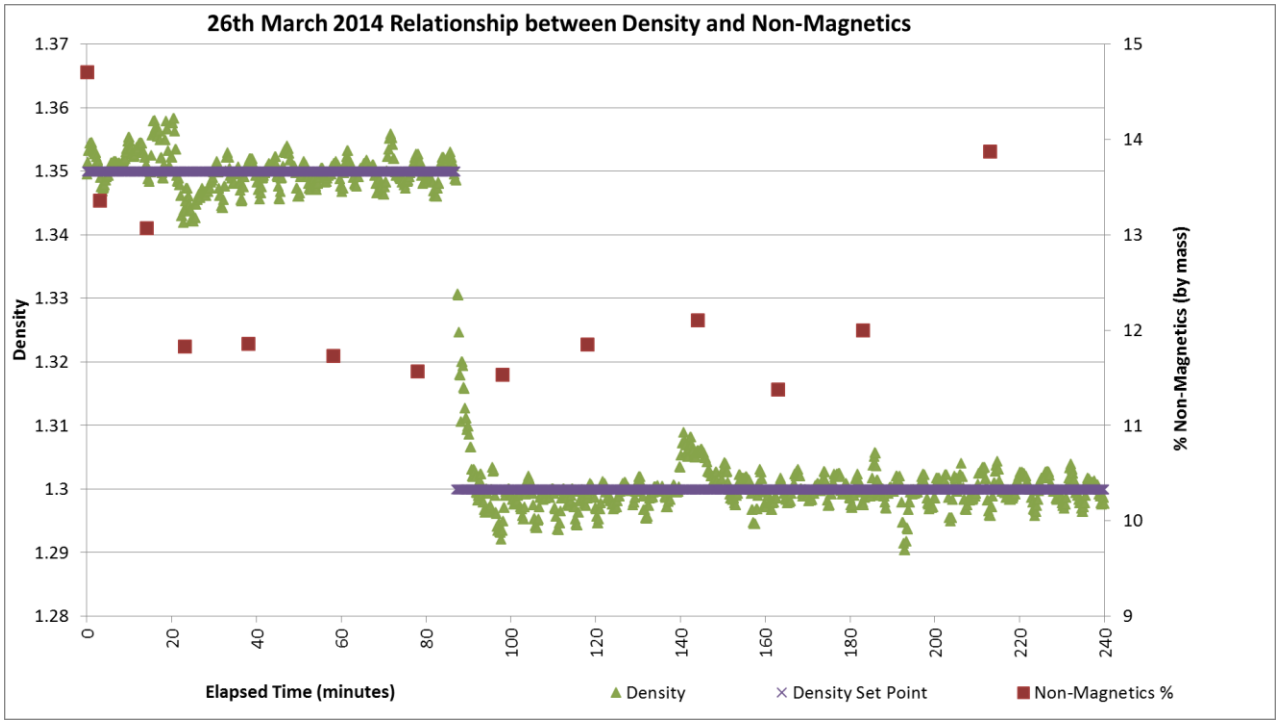

Figure 3.10b: Relationship between density and %non-magnetics on the test day. The setpoint was dropped from 1.35 to 1.3 and non-magnetics remained relatively steady during the density change. This particular day was one where there had been a very high density setpoint of 1.6 overnight and the plant showed evidence of excess magnetite in the system.

Case E: Low density stability desliming sprays response test:

Test: Running on a low density set point, open bleed fully, hose in magnetite, Collect correct medium samples at 10 min intervals for an hour and then add non-magnetics to the system by turning off the desliming sprays.

On 25th March, 2014 the desliming sprays were turned off, however the density setpoint was high because of production requirements to operate at a higher density. Nevertheless, a decision was made to proceed. During this period, there was no water spraying on the desliming screen which meant that less of the fine material would pass through the screen to the fines circuit. A proportion of the fine material, including non-magnetics, instead overflowed the desliming screen into the coarse launder and then into the wing tank. The desliming spray response test at New Acland revealed that the build up of non-magnetics was rapid, however, the corresponding build-up of water in the dilute circuit due to the spray water diverting across to the drain and rinse screens meant that it was not feasible to continue. An increase in non-magnetics of 2.2% was observed after the sprays had been turned off for two minutes (Figure 3.11). This increase was thought to be due to the increase in fines entering the dense medium circuit. The desliming spray water entered the dilute via the drain & rinse screen sprays and the dilute sump rose from 40% full to 100% full and overflowing within 2 minutes.

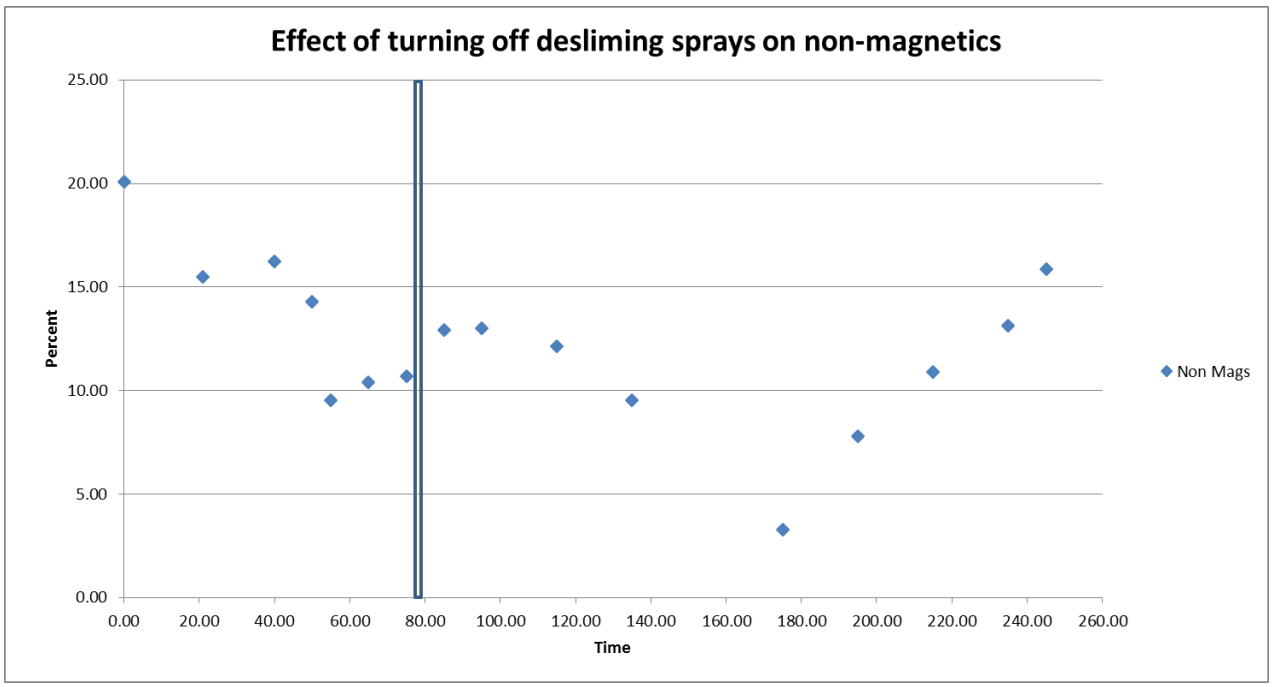

Figure 3.11: Desliming spray test period is marked by the vertical line. An increase in non-magnetics of 2.2% was observed after the change.

Test of using de-sliming sprays to control non-magnetics was abandoned after 2 minutes due to the rapid water balance response for this particular plant. (Figure 3.11) Despite the rapid response at New Acland, it is possible that some of the older plant designs may have a slower water balance response. The author recalls seeing de-sliming screens running without sprays on at other CHPP plants in the past. The results of this test suggest that non-magnetic material from the de-sliming screen will rapidly improve non-magnetics content in the medium, however, an alternative means of adding non-magnetics, such as recycling a portion of thickener underflow or magnetic separator effluent may impact less on the water balance.

Case F: Partition Testing and Determination of Residence Times for coarse particles in various sections of a DMC circuit:

Test: This case comprised two tests, both using cubic density tracers. A partition test which compared standard 32mm tracers with 13mm RFID tracers was done. A residence time test using a selection of radio frequency identification (RFID) *tracers at various densities to analyse times for coarse particles to travel through the various sections of the DMC circuit was also completed on two separate test dates.*

The Partition Tests

Figure 3.12 below demonstrates the normal route for a coarse coal particle travelling through the DMC circuit.

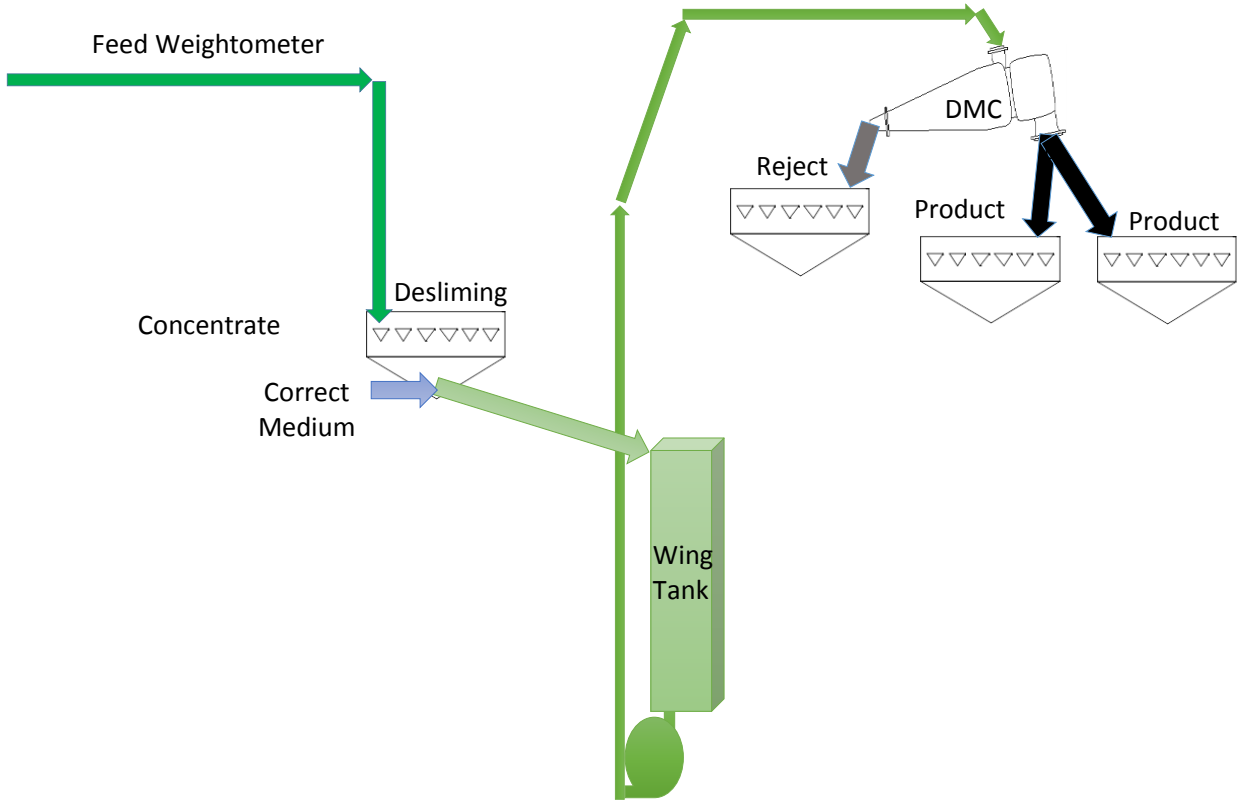

Figure 3.12: Normal route for coal particles.

Tracers are dispensed at the desliming screen and flow into the coarse launder. The tracer particles then enter the wing tank with the coal and are pumped to the DMC which then outflows onto the three drain and rinse screens where they are detected, or in the case of standard tracers, are manually collected.

For the two test days, tracers were dispensed at the de-sliming screen and detected at the product and reject drain and rinse screens using a fixed antenna on the coarse launder of each screen. As each RFID tracer had a unique identifier number, the travel time of each individual particle as it travelled through the circuit could be measured. As tracer particles also had a unique density, the partition curve could be determined for this route. Standard density tracers were manually collected from the screens whereas the antennae on the drain and rinse screens detected the RFID tracers. On both of the chosen test days, the plant showed good stability with a differential calculated to be 0.21 on the first day, and 0.20 on the second test day. A differential below 0.4 would suggest that surging or retention in the DMC was highly unlikely to occur. This was confirmed when it was observed during the test that no retained particles were retrieved at the end of the test.

Figures 3.13 and 3.14 below show the percent (dry w/w) non-magnetics in the medium on the test days. This was measured by comparing the relative masses of dried magnetics and non-magnetics (expressed as a percentage) after running through a Davis Tube. This indicates that the level of non-magnetics was at a sufficient level to avoid retention and did not vary widely during the test.

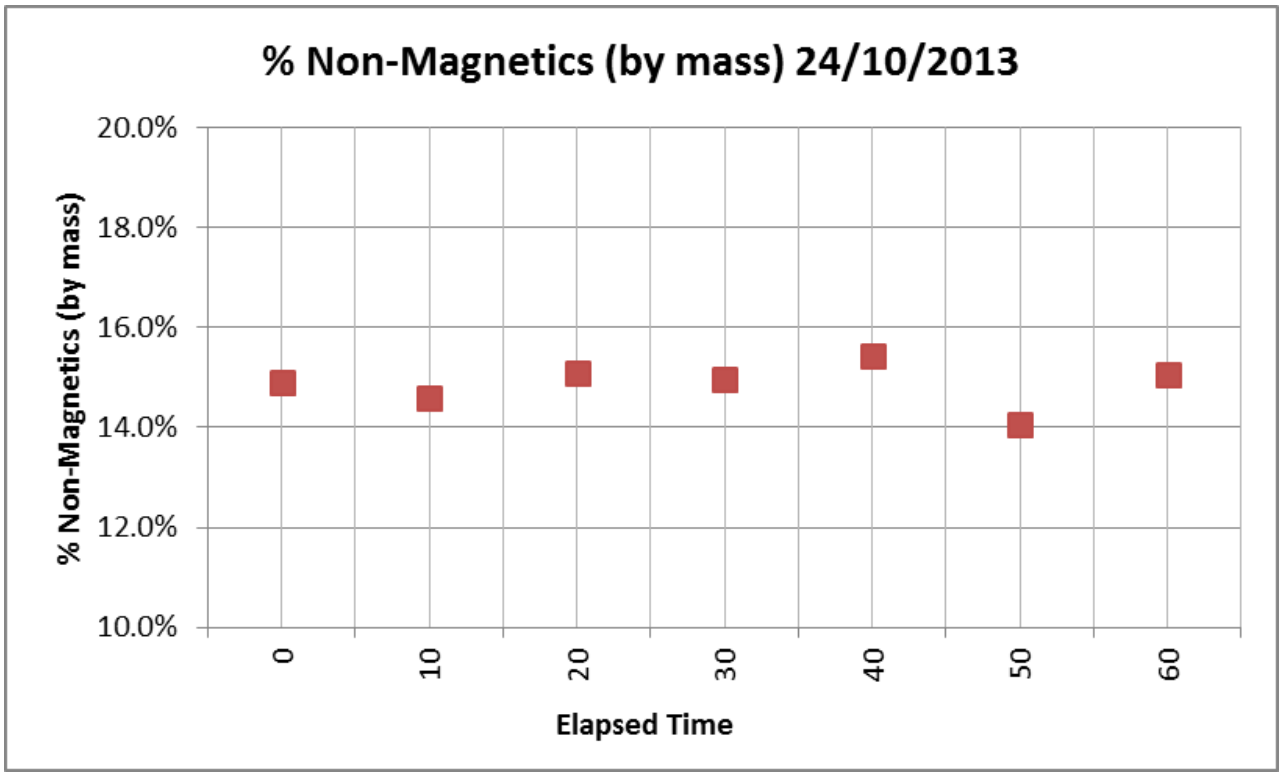

Figure 3.13: % Non-magnetics (by weight) in the correct medium samples taken during the first day of tracer testing (Test 1) 24/10/2013 (Scott et.al. 2015)

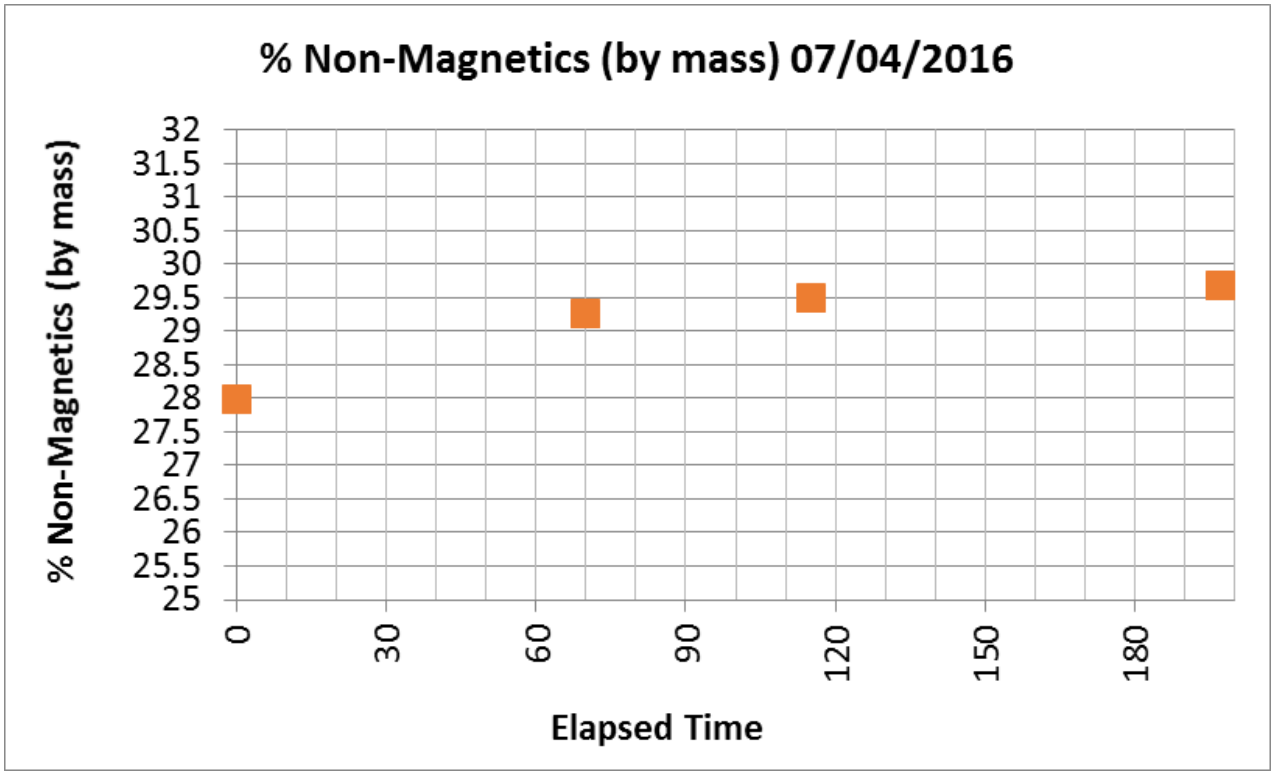

Figure 3.14: %Non-magnetics (by weight) in the correct medium samples taken during the second day of testing at New Acland. (Test 2) 7th April 2016 (O'Brien 2016).

Non-magnetics levels were higher on this day, possibly due to a high rejects loading but the differential was only slightly lower than for the first test day.

Yields between the two test days were quite different. The first test had a yield of 45% whereas the second test had a yield of 30%. The low second test yield created a high degree of difficulty with recovering standard tracers from the reject screen due to a high bed depth of over 100mm. The RFID tracers by comparison, were recoverable in higher numbers during the second test as the antennae were able to detect tracers in spite of the high bed depth. Partition curves were produced for the route from the desliming screen to the drain and rinse screens. A discussion of the first test was also given in Scott et.al. (2015). Both types of tracers were dispensed side by side onto the de-sliming screen and tracers were collected on the two product drain and rinse screens and on the reject drain and rinse screen. In the collection launders at the end of the drain and rinse screen, Partition Enterprises placed RFID antennas to count individually labelled 13mm RFID Tracers. The expectation from this partition test comparison of different sized tracers was that results from both tests would be relatively similar for the given sets of plant conditions, with the 13mm cut point being higher than the 32mm cutpoint. Tables 3.3 and 3.4 show the recoveries for the standard tracers.

Table 3.3: Standard 32mm Tracer Results Test 1

Number of Tracers	Tracer Density	Collected on Product Screen	Collected on Reject Screen	Missed	Recovered	Proportion to Product	Proportion to Reject
30	1.41	29	0	1	29	100	0
30	1.43	28	0	2	28	100.0	0.0
30	1.45	28	0	2	28	100.0	0.0
30	1.47	28	0	2	28	100.0	0.0
30	1.49	28	0	2	28	100.0	0.0
30	1.5	30	0	0	30	100.0	0.0
30	1.51	29	0	1	29	100.0	0.0
30	1.52	30	0	0	30	100.0	0.0
30	1.53	28	0	2	28	100.0	0.0
30	1.54	28	0	2	28	100.0	0.0
30	1.55	30	0	0	30	100.0	0.0
30	1.56	22	4	4	26	84.6	15.4
30	1.57	16	13	1	29	55.2	44.8
30	1.58	4	22	4	26	15.4	84.6
30	1.59	0	30	0	30	0.0	100.0
30	1.6	0	29	1	29	0.0	100.0
30	1.62	0	27	3	27	0.0	100.0
30	1.64	0	24	6	24	0.0	100.0
30	1.66	0	30	0	30	0.0	100.0
30	1.68	0	27	3	27	0.0	100.0
30	1.77	0	24	6	24	0.0	100.0

Table 3.4: Standard 32mm Tracer Results Test 2

Number of 32mm Tracers	Tracer Density	Collected on Product Screen	Collected on Reject Screen	Missed	Recovered	Proportion to Product	Proportion to Reject
30	1.32	30	0	0	30	100.0	0.0
30	1.35	30	0	0	30	100.0	0.0
30	1.40	28	0	2	28	100.0	0.0
30	1.41	29	1	0	30	96.7	3.3
30	1.42	25	4	1	29	86.2	13.8
30	1.43	21	7	2	28	75.0	25.0
30	1.44	17	11	2	28	60.7	39.3
30	1.45	5	23	2	28	17.9	82.1
30	1.46	0	27	3	27	0.0	100.0
30	1.47	0	26	4	26	0.0	100.0
30	1.48	0	20	10	20	0.0	100.0
30	1.49	0	22	8	22	0.0	100.0
30	1.50	0	25	5	25	0.0	100.0
30	1.55	0	25	5	25	0.0	100.0
30	1.59	0	25	5	25	0.0	100.0

The 13mm RFID tracers had recoveries that were relatively low in Test 1. Approximately 60% of tracers were recovered or detected. Interference due to the close proximity of the screens influenced this result. Care was taken during set up of the second test to avoid interference and hence recoveries were considerably improved in spite of the higher bed depth. The problem of interference was remedied in the second test run and recovery time was also lengthened to allow for slower travelling tracers to be recovered. Consequently, the second test run had significantly better recovery rates for the 13mm tracers. (Table 3.5 and 3.6)

Table 3.5: Results of 13mm RFID Tracer test 1

Number of Tracers	Tracer Density	Collected on Product Screen	Collected on Reject Screen	Missed	Recovered	Proportion to Product	Proportion to Reject
30	1.32	17	0	13	17	100	0
30	1.48	22	0	8	22	100.0	0.0
30	1.49	23	0	7	23	100.0	0.0
30	1.5	17	1	12	18	94.4	5.6
30	1.51	22	0	8	22	100.0	0.0
30	1.52	19	2	9	21	90.5	9.5
30	1.53	18	3	9	21	85.7	14.3
30	1.54	11	9	10	20	55.0	45.0
30	1.55	7	12	11	19	36.8	63.2
30	1.56	3	17	10	20	15.0	85.0
30	1.57	5	14	11	19	26.3	73.7
30	1.58	0	20	10	20	0.0	100.0
30	1.59	2	19	9	21	9.5	90.5
30	2	0	18	12	18	0.0	100.0

Table 3.6: Results of 13mm RFID Tracer test 2

Number of Tracers	Tracer Density	Collected on Product Screen	Collected on Reject Screen	Missed	Recovered	Proportion to Product	Proportion to Reject
30	1.3	28	1	1	29	96.6	3.4
30	1.32	28	2	0	30	93.3	6.7
30	1.35	27	3	0	30	90.0	10.0
30	1.38	24	6	0	30	80.0	20.0
30	1.40	23	7	0	30	76.7	23.3
30	1.41	18	11	1	29	62.1	37.9
30	1.42	12	17	1	29	41.4	58.6
30	1.43	5	24	1	29	17.2	82.8
30	1.44	3	25	2	28	10.7	89.3
30	1.45	0	29	1	29	0.0	100.0
30	1.46	0	30	0	30	0.0	100.0
30	1.47	0	28	2	28	0.0	100.0
30	1.48	1	27	2	28	3.6	96.4
30	1.49	0	30	0	30	0.0	100.0
30	1.50	0	30	0	30	0.0	100.0
30	1.59	0	30	0	30	0.0	100.0

Results of the standard 32mm tracer tests indicated that the cut point of the cyclone was operating higher than for the 13mm RFID tracers. This was an unexpected result. Figure 3.15 is a graph of both partition curves showing the discrepancy in results. A comparison of cut point is given in table (Table 3.7)

Table 3.7: Comparison of cut point and Ep for the 13mm and 32mm tracers in both tests.

Test 1	RD50	Ep
13mm	1.55	0.013
32mm	1.57	0.007

Test 2	RD50	Ep
13mm	1.419	0.021
32mm	1.44	0.007

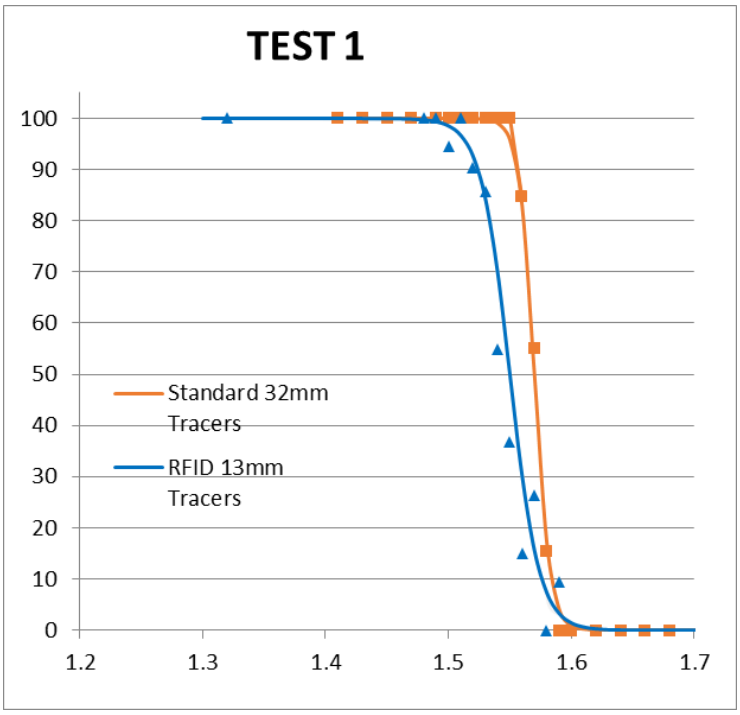

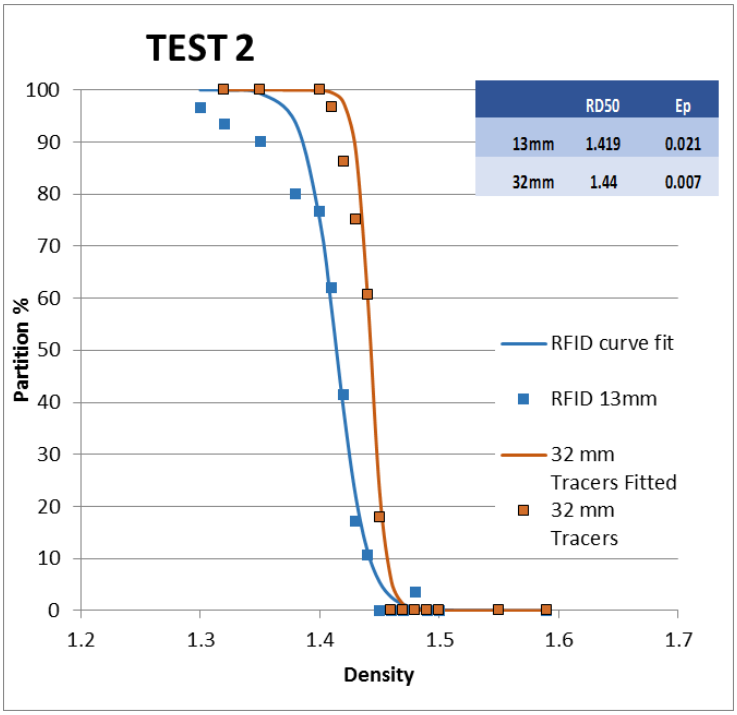

Figure 3.15: A comparison of the tracer tests for 13mm and 32mm tracers on the two test days.

A cut point difference was noted on both occasions with the 13mm tracers demonstrating a lower cut point than the 32mm tracers.

The low detection rate of the 13mm RFID tracers in Test 1 and the relatively low recoveries for the standard 32mm tracers were not ideal, but were sufficient for reliable determinations of cutpoint and Ep values. Results of the standard 32mm tracer test 1 indicated that the cut point of the cyclone was operating close to 1.57 when measured using the 32mm tracers and around 1.55 with the 13mm RFID tracers. The estimated Ep was 0.007 for the 32mm versus 0.013 for the 13mm tracers. The partition curve for the RFID tracer Test 2 suggested that the Ep of 0.021 was unusually high and that the cut point was 1.419. This could have been due to the fact that the DMC body was well worn and yields were low. The partition curve for the Standard 32mm tracers suggested that the Ep of 0.007 was similar to the previous testwork. The cut point for the Standard 32mm tracers was calculated to be 1.44. This again demonstrated that there was a cut point difference between the 13mm RFID tracers and the 32mm standard tracers. The difference in cut point would normally be expected to be higher for the smaller particles than the larger particles, however in this case, the cut point for the smaller particles was lower. This confirms that the same effect was visible in both tests.

Discussion of Partition Testing:

Possible reasons for the cut point reversal have been proposed by others, most notably Wood (1990). He observed a number of cases which did not exhibit the usual progressive increase of cutpoint with decreasing particle size. In these cases, the lowest cutpoint was for an intermediate size fraction such as -8mm by +4mm. In those instances, cutpoints for coarser coal or for 32mm tracers were slightly higher. Wood (in Crowden et.al. 2014) conjectured reasons for this relating to porosity of coal and absorption of float sink chemicals, however in the case of density tracers, no chemicals are required. Another reason suggested by Wood was that there could be more resistance to large particles flowing into the vortex finder where annular depth of slurry may be only 20mm and that this could pose more of a challenge than the ease of exit via the apex of the cyclone.

Tracers used in previous research by I.A. Scott, (1988) were found to be differently shaped to the tracers used in standard density tracer testing in coal plants. The tracers used by Scott were flat, shale-like particles, rough shaped and appeared to have been put through a crusher. The majority of particles were wide but flat in shape, which could have led to

differences in their behaviour in a DMC. This may suggest that particle shape could have had a role to play in determining the cut points of the particles, however drawing firm conclusions would require further work.

Prediction of residence times in a coal preparation plant.

The new design of RFID density tracers enabled a novel method to be used to determine particle residence times in various parts of the DMC circuit. The method involved timing RFID tracers passing through the circuit both during partition testing and also when inserting into other parts of the circuit. The RFID density tracers were inserted in the following locations (Figure 3.16):

- plant feed weightometer
- crusher feed at the end of the feed conveyor
- de-sliming water sump which feeds the de-sliming wing tank under the crusher
- de-sliming screen coarse launder (used for the partition testing)
- DMC outlets
- drain and rinse screen under-pans
- magnetic separator concentrate
- wing tank overflow

Other routes chosen for the RFID tracers were not used for producing partition curves due to the relatively lower number of densities and tracers used. The number of insertion points were changed slightly for the second day of testing in order to gain more information about the medium circuit. The insertion points at the DMC overflow and underflow were removed from the second test and additional tracers were instead added at the crusher feed, the desliming water sump and the wing tank overflow. A summary of the residence times through various parts of the circuits are given in table 3.8

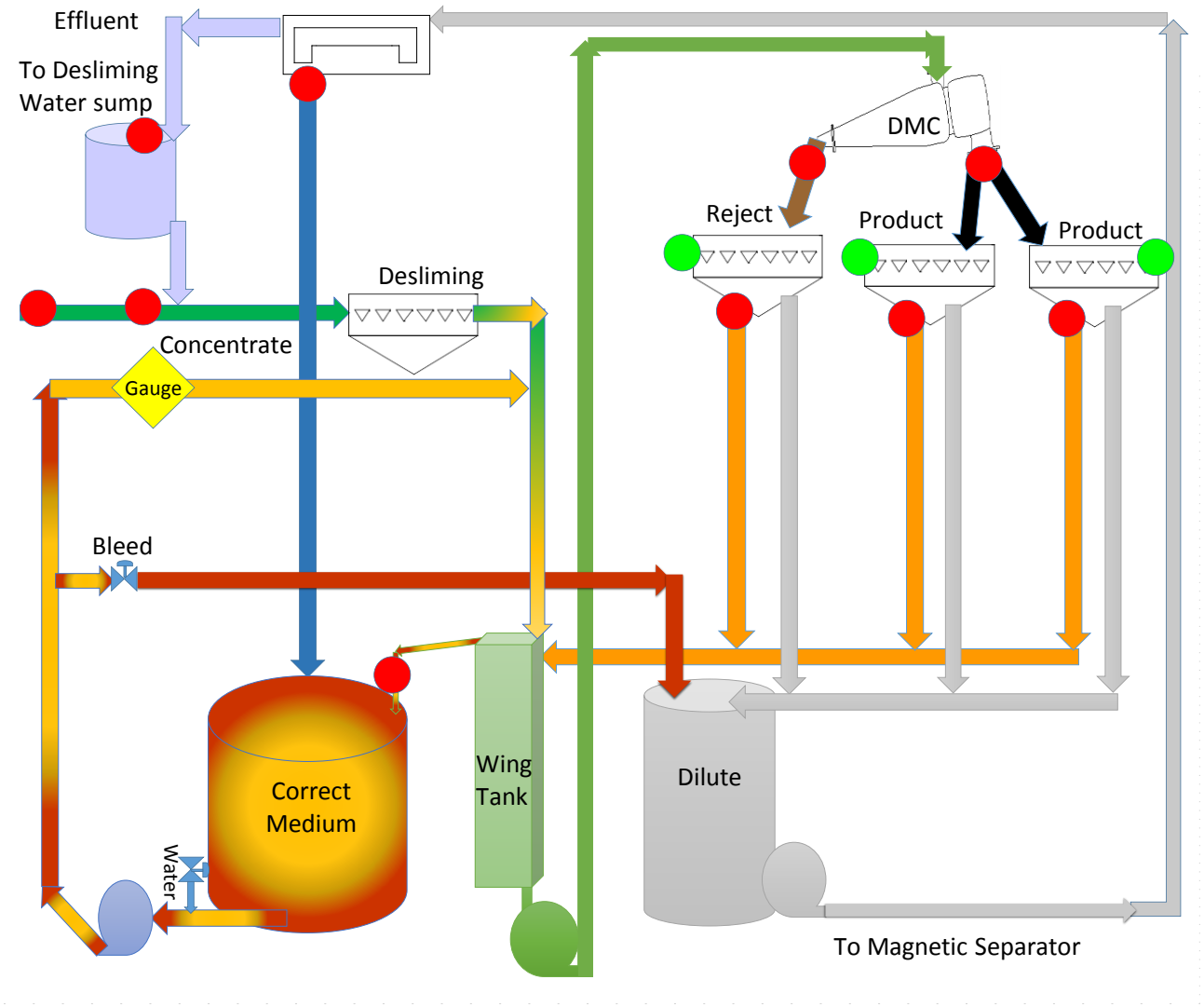

Figure 3.16: The DMC circuit and the associated feed and collection points for the tracers in the Residence time tests.

Red dots denote tracer insertion points and green dots denote RFID tracer detection antenna locations

Table 3.8: A summary of the residence times through various parts of the circuits.
(Times are in mm:ss format)

Test	Residence time From	Residence time to	Average	Min	Max
A	Desliming Screen	Drain & Rinse Screen	01:01	00:36	02:11
B	DMC Overflow / Underflow	Drain & Rinse Screen	00:20	00:15	00:26
C&D	Drain Underpan	Drain & Rinse Screen	02:36	00:43	29:06
E	Feed Weigher	Drain & Rinse Screen	02:25	02:00	03:27
F	Mag Separator Concentrate	Drain & Rinse Screen	09:50	01:10	39:36
G	Deslime Water Sump	Drain & Rinse Screen	08:37	02:09	35:51
H	Crusher Feed	Drain & Rinse Screen	01:55	01:36	02:25
I	Wing Tank Overflow (to CM)	Drain & Rinse Screen	06:53	01:23	31:48

The summary of residence times was used to estimate delays in the various parts of the circuit in the dynamic model. As can be seen in table 3.8, particles that were inserted into one piece of equipment did not necessarily take the same time to travel through the system. The broad range of times for each test suggested that the data was multi-modal and that some particles took different routes or settled out during transit. A discussion on standard deviation is detailed in Appendix 5. The test ran for 40 minutes in total after which any remaining particles that had not yet passed the antennae were considered lost. Recovery rates were high, however it is believed that some particles could still have been in transit at the 40 minute cut-off time. Further discussion of the routes taken is outlined below, however for the purposes of dynamic modelling, the above table was sufficient for use in the model to input delays. Table 3.9 is the model delay table. Consideration has been made to the multiple routes possible within the DMC circuit and to some extent the delays can be adjusted within a range. In many cases, the shortest particle residence time was taken to ensure that the particle had not taken multiple routes of the system before being detected.

Table 3.9: Delays used in the Dynamic Model (seconds)

Delay	Description	Delay time (s)
Bleedsplit_delta	Dead time from correct sump to bleed valve	15
Deslime_delta	Dead time from bleed valve to deslime	7
Wing_delta	Dead time from deslime to wing tank	6
DMC_delta	Dead time from feed to DMC	15
Drain_delta	Dead time from combined drain to wing tank	12
Rinse_delta	Dead time from combined rinse to wing tank	12
from_Dil_delta	Dead time from dilute sump to mag seps	28
MSCon_delta	Dead time from mag sep cons to correct sump	12
Bleed_delta	Dead time from bleed valve to dilute sump	6

Tracer Routes

The following is a description of the possible routes that a tracer particle may take from each entry point to its ultimate destination at the drain and rinse screen coarse launder.

Despite the normal route for coal particles being via the wing tank to the DMC, there are circumstances where the coal does not follow this route, an example of this is rafting coal. Inside the wing tank, the separation between the coal side and the seal leg side is via an orifice plate. When rafting occurs in the wing tank, coal travels up through the orifice plate into the seal leg of the wing tank, and then overflows instead of flowing down into the DMC pump. Rafting occurs when there is an insufficient downward flow in the wing tank to prevent low density coal particles from floating. If the orifice flow is reversed, then rafting can occur up into the seal leg. As there is no oversize protection on the correct medium sump, the coal particles are able to travel back to the desliming screen coarse launder or travel into the dilute sump via the bleed valve on the correct medium line. The bleed valve is a butterfly valve and although it may appear to be fully closed, operators have noted that occasionally rafted coal particles can get stuck in the valve causing the valve to pass when closed. The impact of coal particles in the dilute sump is that the magnetic separator may see particles of larger size. A 20mm square mesh oversize protection exists on the

magnetic separator underpan, however particles travelling through the magnetic separator underpan could still be of reasonable size to pass through the 20mm mesh. During the RFID tracer tests, the bleed valve was closed during addition to the correct medium lines, however, the time that some particles took to pass through the system was significantly longer than expected. It is therefore quite possible that some of the 13mm RFID tracer particles could have passed through the magnetic separator underpan, either due to a bleed valve that didn't fully close despite reading 0% open on the control room screen, or alternatively, due to the bleed being opened too early after the test. In general the bleed was closed for approximately five minutes. Based on the previous test work, this seemed to be a reasonable number to use. It was discovered in the second RFID tracer test, however, that some particles can take considerably longer to exit the circuit. Figure 3.17 below shows possible alternate routes for coarse coal particles due to rafting.

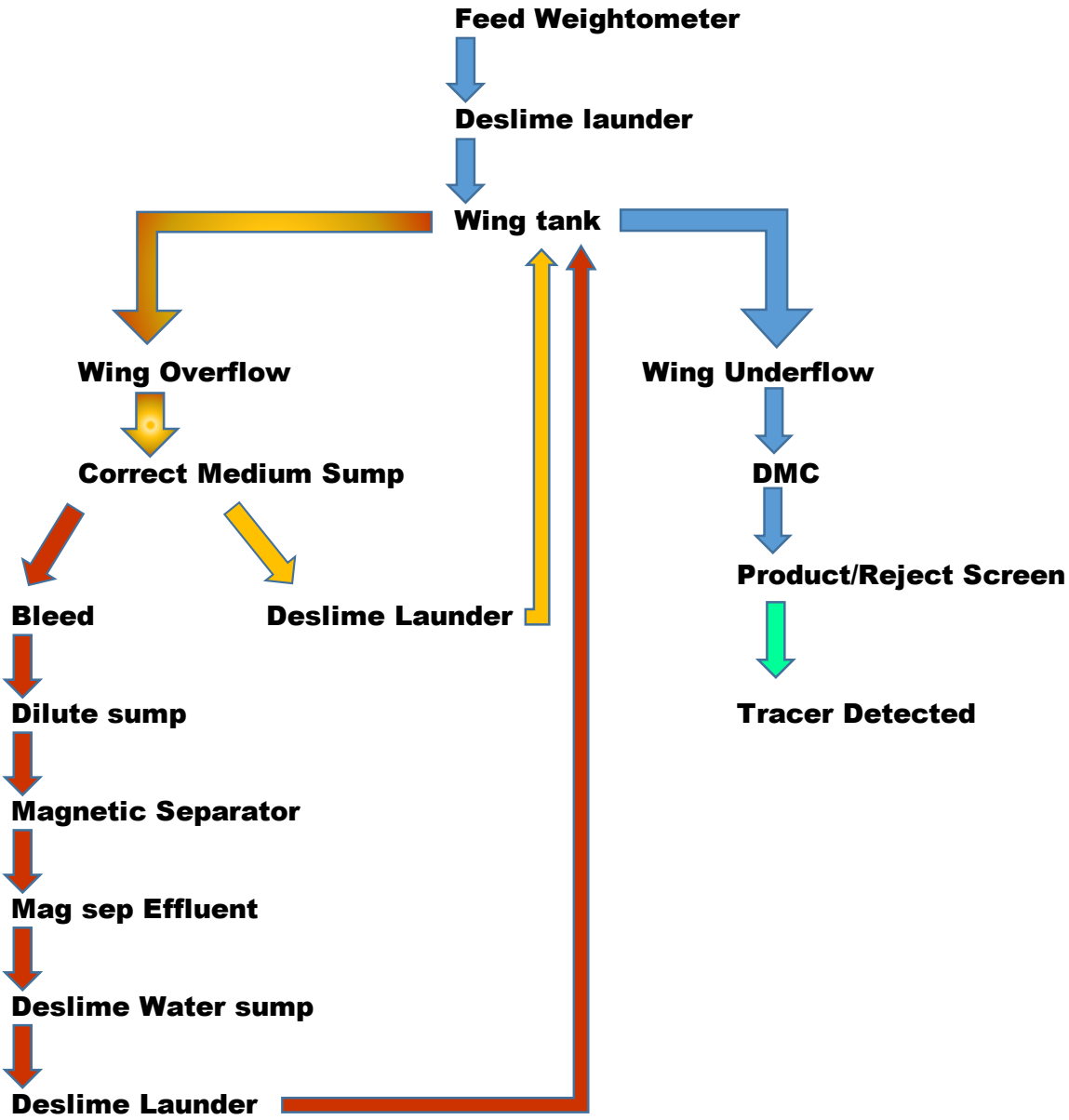

Figure 3.17: The pathways for a rafting coal particle. (Yellow / red paths)

The wing tank overflow carries medium and rafting coal particles. Oversize protection on the magnetic separator is 20mm square mesh so it is theoretically possible that a non-magnetic 13mm RFID tracer particle could slide through the under-pan of the magnetic separator and flow with the magnetic separator effluent stream back to the desliming water sump at the start of the circuit.

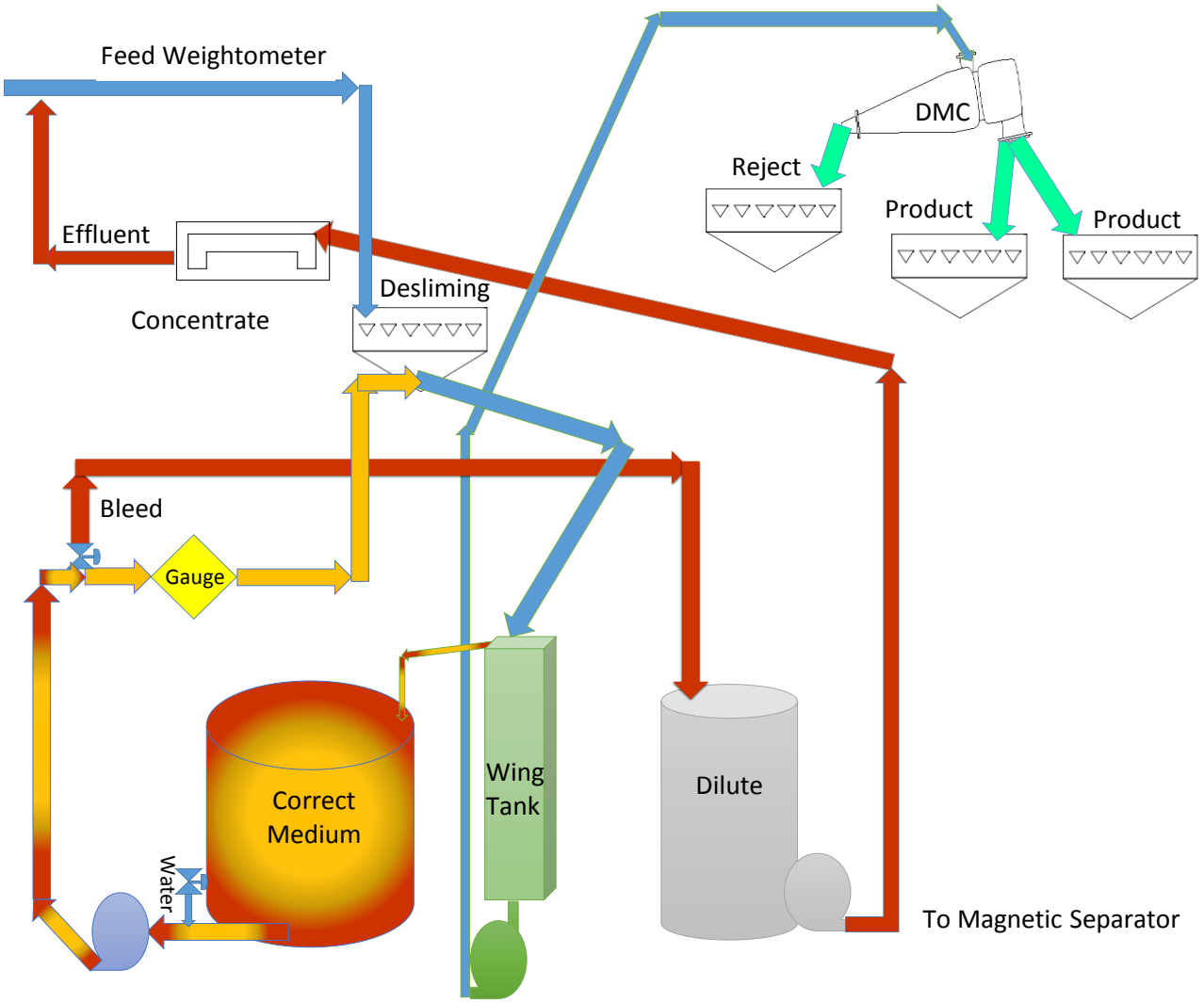

Figure 3.18: A pictorial view of the pathways for coal particles including rafting coal.

The pathway in which the medium travels through the DMC circuit is slightly different to that of the normal coal particles. Figure 3.19 shows the possible pathways for the medium to travel through the DMC circuit. The pathway of the medium also includes the dilute circuit as a bleed from the correct medium line and the rinsed medium ensures that there is a build-up of water in the system which needs to be removed via the magnetic separators. The magnetic separators also strip non-magnetic material out of the system via the dilute circuit.

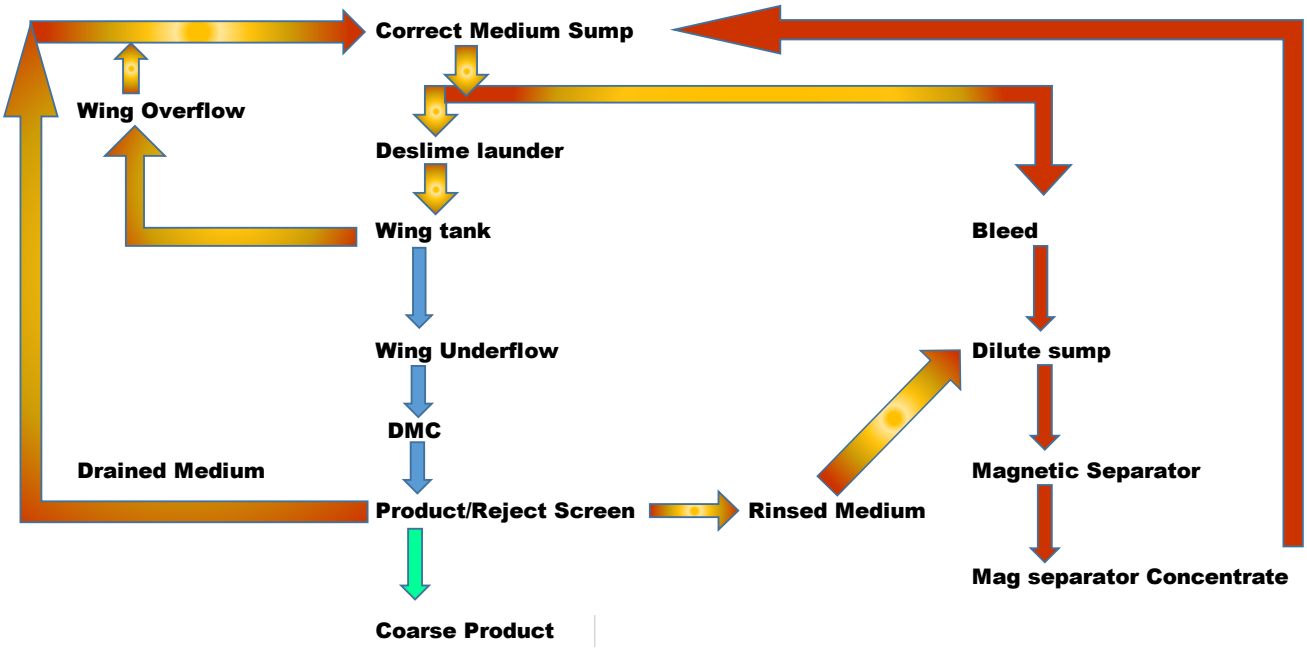

Figure 3.19: Possible routes for the medium.

The medium that follows the coal pathway will travel to the desliming screen coarse launder from the correct medium sump. It then passes through the wing tank and enters the DMC feed pump. Once through the DMC, the medium splits onto product and reject drain and rinse screens and a proportion of the medium will drain through, remaining medium will either wash through to the rinse underpan or carry over into the coarse launder with the product. The return drain medium enters the wing tank seal leg where either it passes through the orifice plate in the wing tank and follows the coal pathway, or it overflows into the correct sump. From the correct sump, medium is either diverted to the bleed line across to the dilute sump or is pumped to the desliming screen coarse launder. The return rinse medium flows to the dilute sump and is processed via the magnetic separator which returns concentrate directly into the correct medium sump.

For the residence time tracer test work, each RFID tracer had a unique identification label. Times were able to be tracked for each individual tracer and then compiled into a summarised data set. Below is a detailed analysis of individual circuits within the plant. In some cases only small quantities of RFID tracers were detected. The data was however sufficient to give an indication of times taken for coarse particles to travel through the circuit. Of particular interest also is the data which varies widely between individual particles which indicates that some particles may have travelled a different path to others. The multi-modal nature of the distributions suggested that there was little value in measuring standard deviations as it was difficult to determine exactly which route the particle took. What was clear, was that there was not one data set, but multiple sets of data for a specific insertion point. The travel time depended on the amount of time the particles settled out in the system, or the number of times that the particles circulated in the medium before joining the coal stream at the wing tank.

Desliming Screen to Drain and Rinse Screens

Test A was the route followed for the conventional tracer testwork and was done concurrently with the standard tracers. Tracers were dropped into the circuit at the desliming screen and travelled into the DMC wing tank. They were then pumped through the DMC and detected on the product and reject drain and rinse screens. Table 3.10

Table 3.10: Tracer times from de-sliming screen to drain and rinse screen oversize for both days of the testwork

Test	Residence time From	Residence time to	Average	Min	Max
A	Desliming Screen	Drain & Rinse Product 1	00:57	00:37	01:41
	Desliming Screen	Drain & Rinse Product 2	01:00	00:36	01:56
	Desliming Screen	Drain & Rinse Rejects	01:02	00:43	02:11
	Desliming Screen	Drain & Rinse Overall	01:01	00:36	02:11

When data from test A was compared by density, the following graph (Fig 3.20) was generated. Attempts to identify a trend in the data indicated that there was very low linear correlation of the density of the particles against the time taken to pass through the circuit. It is important to note however, that this data was collected only for particles travelling

between the desliming screen and the drain and rinse screens with virtually no opportunity for hold-up in the system apart from the possibility of rafting in the wing tank. It is thought that rafting was unlikely to have occurred on the two test days as the density target was not significantly high. Process operators have commented that rafting usually occurs when targeting a high density of over 1.60RD.

The correlation between density and travel time was low for this short route, which suggests that density does not have a strong influence on travel time for the coal through the DMC circuit. Relative travel times of particles in the medium recovery circuit are discussed later.

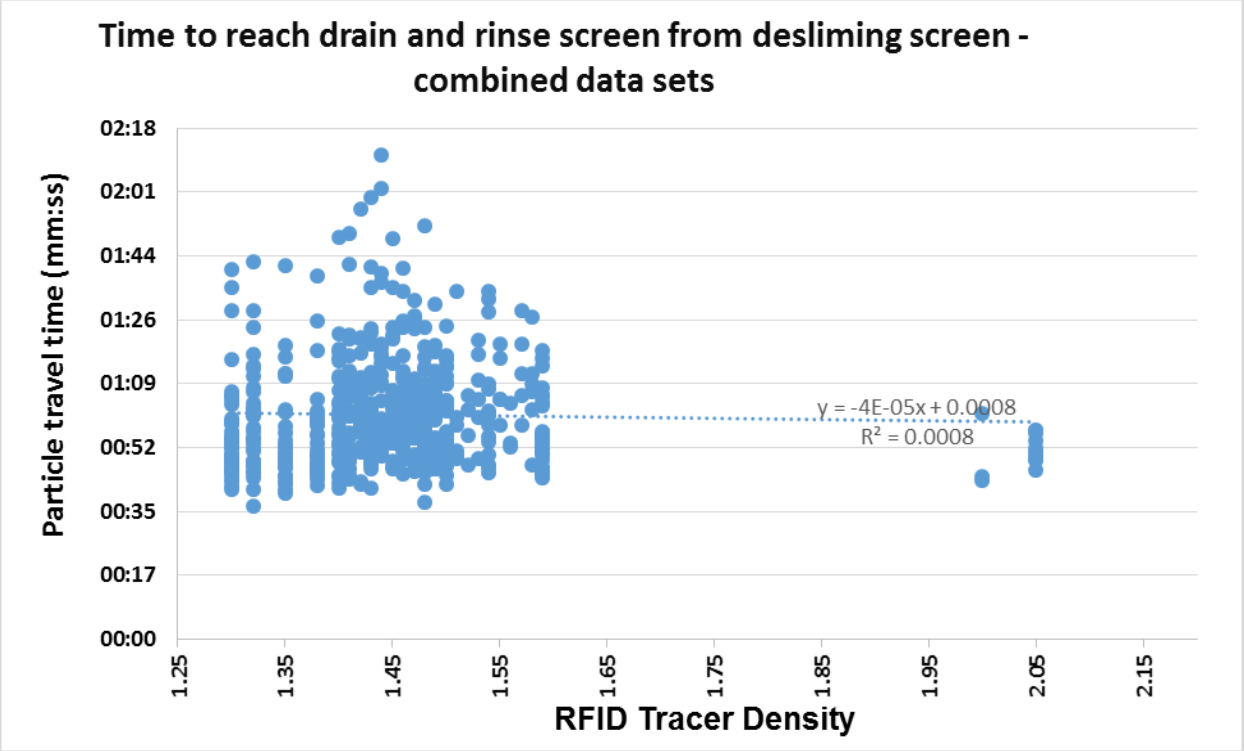

Figure 3.20: Relative transit times for different density particles to travel from the desliming screen to the drain and rinse screen coarse launders. This data is combined from both of the test days.

From the above table and figure 3.20, it can reasonably be concluded that when there is a single, short route to be taken through the circuit with a low chance of segregation of particles in vessels, there is not a density effect on residence time.

DMC overflow and underflow to the Drain and Rinse Screens

This test involved dispensing tracers at the outlets of the DMC and collecting them on the drain and rinse screens. Tracers travelled only a small distance, but this test gave an indication of how long it took for a coal particle to travel down the screen. (Table 3.11)

Table 3.11: Tracer times from DMC outlets to the drain and rinse screen oversize

Test	Residence time From	Residence time to	Average	Min	Max
B	DMC Overflow/Underflow	Drain & Rinse Screen	00:20	00:15	00:26

Drain underpans to the Drain and Rinse Screens

This test involved dispensing tracers into the correct medium (drain) side of the drain and rinse underpans and collecting them on the drain and rinse screen oversize. Particles travelled through the seal leg side of the wing tank and then either joined the DMC feed or overflowed into the correct medium sump. The results of this test showed a broad scatter indicating that some tracer particles took a different route through the circuit. (Table 3.12).

Table 3.12: Tracer times for travel from drain and rinse underpan (drain side) to the drain and rinse screen oversize.

Test	Residence time From	Residence time to	Average	Min	Max
C&D	Drain underpan	Drain and Rinse Screen	02:36	00:43	29:06

Closer inspection of the results indicated that density did not necessarily determine the residence time of the tracer particles. In one case, two particles of identical density of 1.34 took vastly different times to reach the end point. (Figure 3.21) This suggests that DMC retention was not to blame for the slower particle arrival. A possible reason was that the slower tracer could have overflowed from the wing tank seal leg into the correct medium sump and then returned to the de-sliming screen before being pumped back to the DMC via the wing tank. However, a more plausible explanation in this particular case is that there was observed silting of magnetite occurring in the drain and rinse screen under-pan, and that dispensing tracers into the side edge of the under-pan may have resulted in a slower transit due to the silt build up. In hindsight, the better location for dispensing the tracers would have been to find the exit point for the drain, however the difficulty of access to the under-pan made this particular test difficult under any circumstances. There is

insufficient data to draw a concrete conclusion that density does not have an effect for this particular part of the test, it does, however, give an indication of possible pathways that a particle may take.

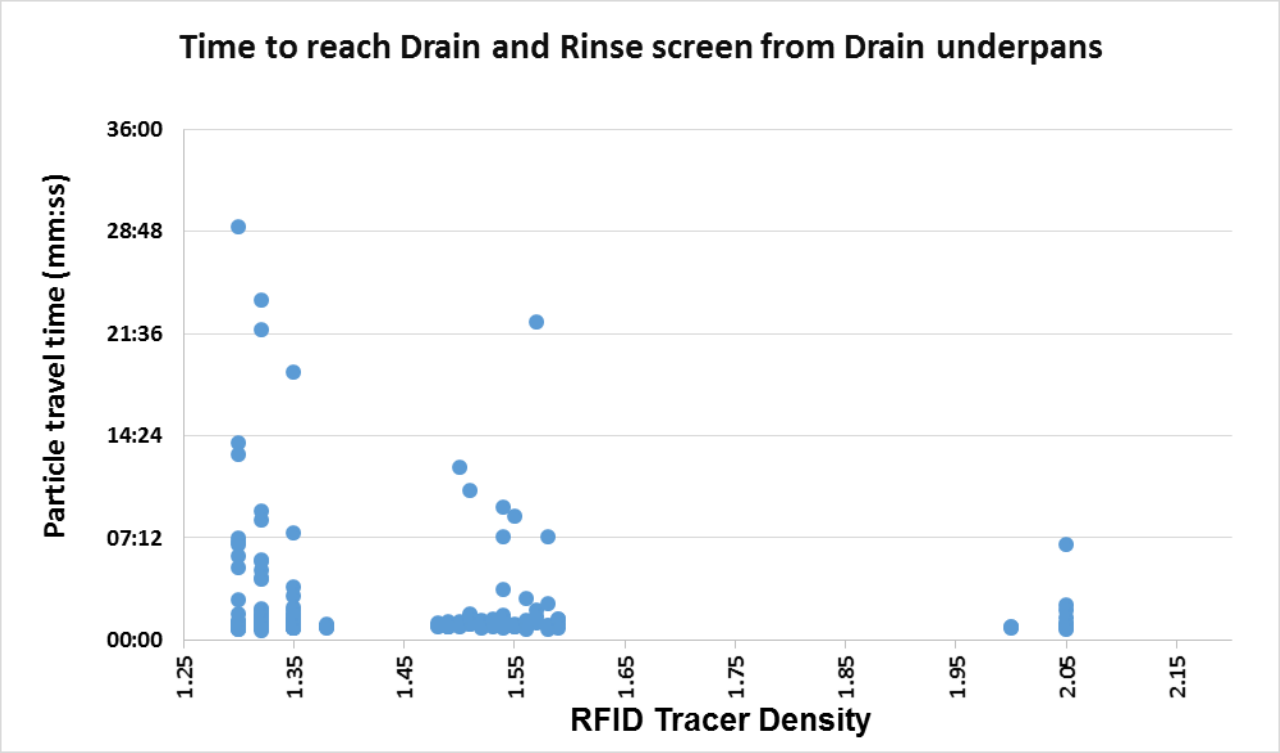

Figure 3.21: Individual RFID Tracer results for travel to the various drain and rinse screens from the drain side underpans

In the case of the particles of higher densities (around 2.00), the times to reach the drain and rinse screen were considerably more consistent, suggesting that the pathway of the heavier particles was less interrupted. This test was, however, deemed unreliable due to the silting in the underpan.

Feed belt weightometer to drain and rinse screens

This test involved inserting tracers at the feed belt weightometer and collecting them on the drain and rinse screens. The tracers travelled the full length of the plant, passing through the secondary and tertiary crushers into a feed sump and then onto the desliming screen. The tracers then entered the DMC circuit travelling with the coal, and were collected on the drain and rinse screens as per the other tests. This test gave an

indication of the time taken for a change to be registered on the weightometer and the time taken for the plant to respond. (Table 3.13)

Table 3.13: Timings from the feed belt weightometer to the drain and rinse screens

Test	Residence time From	Residence time to	Average	Min	Max
E	Feed Weigher	Drain and Rinse Screen	02:25	02:00	03:27

The average time for tracer particles to reach the drain and rinse screens from the weightometer was 2 minutes, 25 seconds. This indicated that despite particles travelling through a minimum of three sumps and a sizing station during their journey, they were still relatively consistent in the time taken to reach the end of the screens. It also suggests that coal particles do not have a long residence time in the plant. (Figure 3.22)

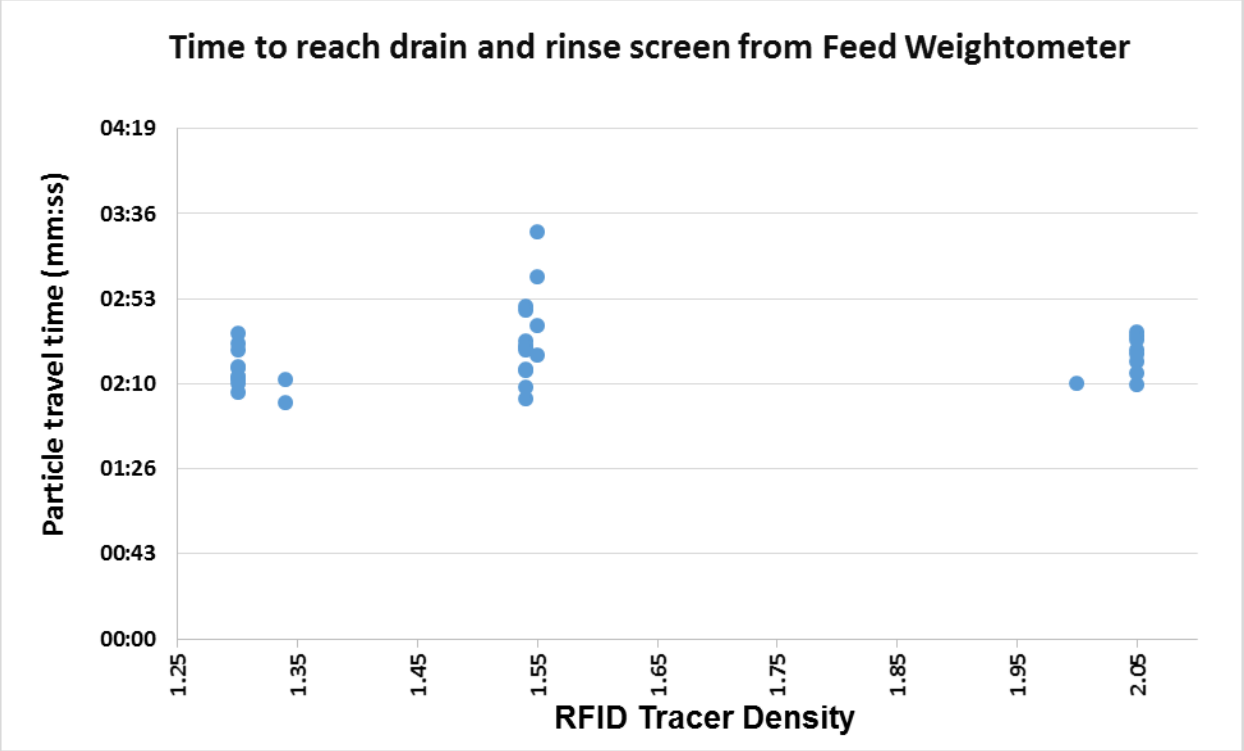

Figure 3.22: Tracer particle times from the feed belt weightometer to the drain and rinse screens via the DMC circuit.

Magnetic Separator concentrate to the Drain and Rinse Screens

This test involved inserting the tracers at the magnetic separator concentrate product side and detecting the tracers at the drain and rinse screens. The shortest time for a tracer to flow from the magnetic separator to the drain and rinse screens was 70 seconds. This suggests that the particle travelled directly into the correct medium pump and flowed to the wing tank without any detours. This data point gives a useful measure of delay time for this section of the circuit. (Table 3.14) Figure 3.23 shows that some particles took considerably longer to exit the circuit, with some taking up to 39 minutes to circulate. It is possible that the 39 minute particle could have taken several trips around the circuit or it could have settled out somewhere before being dislodged. From the data it is not possible to know which of these possibilities occurred.

Table 3.14 Residence times for particles leaving the magnetic separator and travelling to the drain and rinse screens.

Test	Residence time From	Residence time to	Average	Min	Max
F	Magnetic Separator	Drain and Rinse Screen	09:50	01:10	39:36

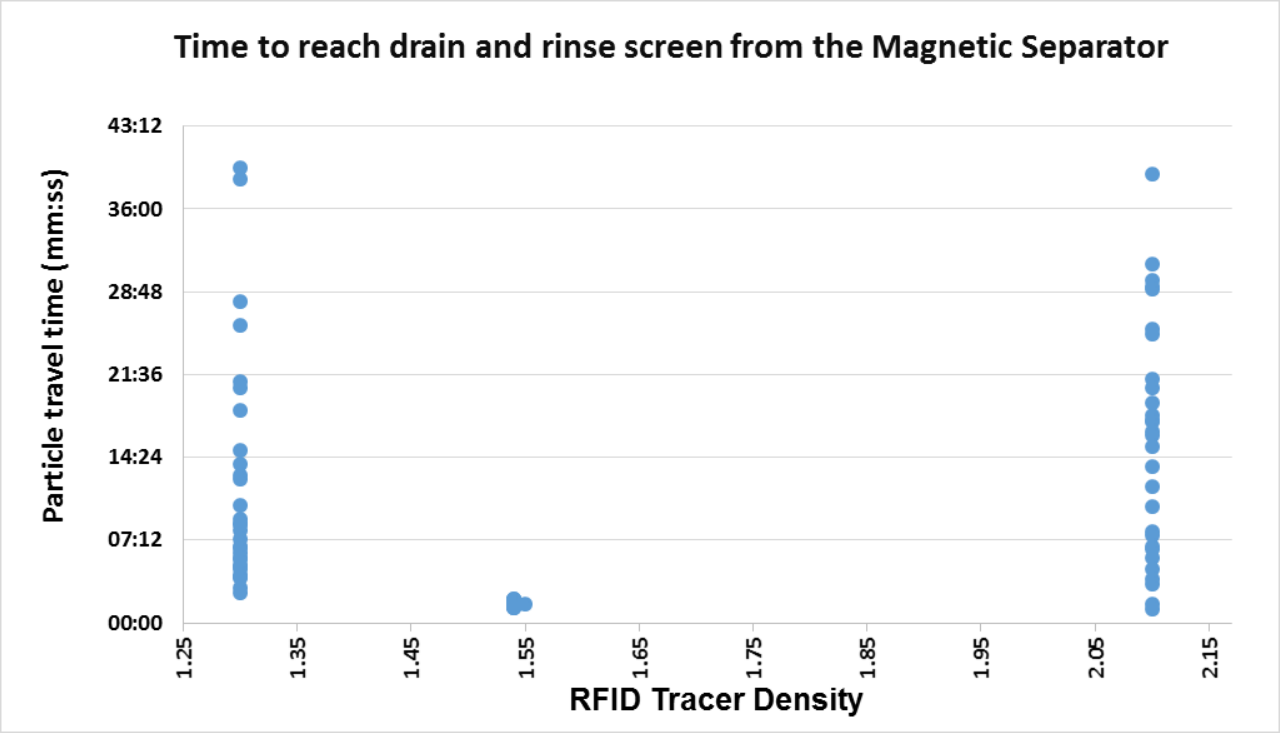

Figure 3.23: Particle tracer time vs. Tracer density for particles travelling to the Drain and Rinse Screens from the concentrate launder of the magnetic separator

Desliming Water Make-up Sump to the Drain and Rinse Screens

This test involved inserting the tracers at the desliming water make-up sump which exists under the secondary sizing station. Water from this sump is pumped into the desliming wing tank (desliming screen feed sump) and mixes with the sized raw coal before being pumped to the desliming screen. This sump is significant as effluent from the magnetic separator is pumped to this location and coarser particles will re-enter the DMC circuit via the desliming screen. Results of this test indicated that the average particle took over 8 minutes to transfer through the DMC circuit from this location, and some took up to 35 minutes. (Table 3.15) The long lead time is a possible reason why some tracers were not recovered after 40 mins. If particles travelled across to the dilute sump via the bleed, they would likely have travelled in the magnetic separator effluent stream back to the de-sliming water sump, thereby greatly extending their time in the circuit. In the de-sliming water sump, where the slurry is mostly diluted to water, the densest particles took the longest amount of time to travel through the system (Figure 3.24). This makes sense given that a particle with a density around 2.00 would normally sink in water. It is possible that the denser particles could have settled quickly to the bottom of the de-sliming sump before eventually being stirred up by mixing action.

Table 3.15 Residence times for particles leaving the Desliming water make-up sump and travelling to the drain and rinse screens.

Test	Residence time From	Residence time to	Average	Min	Max
G	Deslime Water Sump	Drain and Rinse Screen	08:37	02:09	35:51

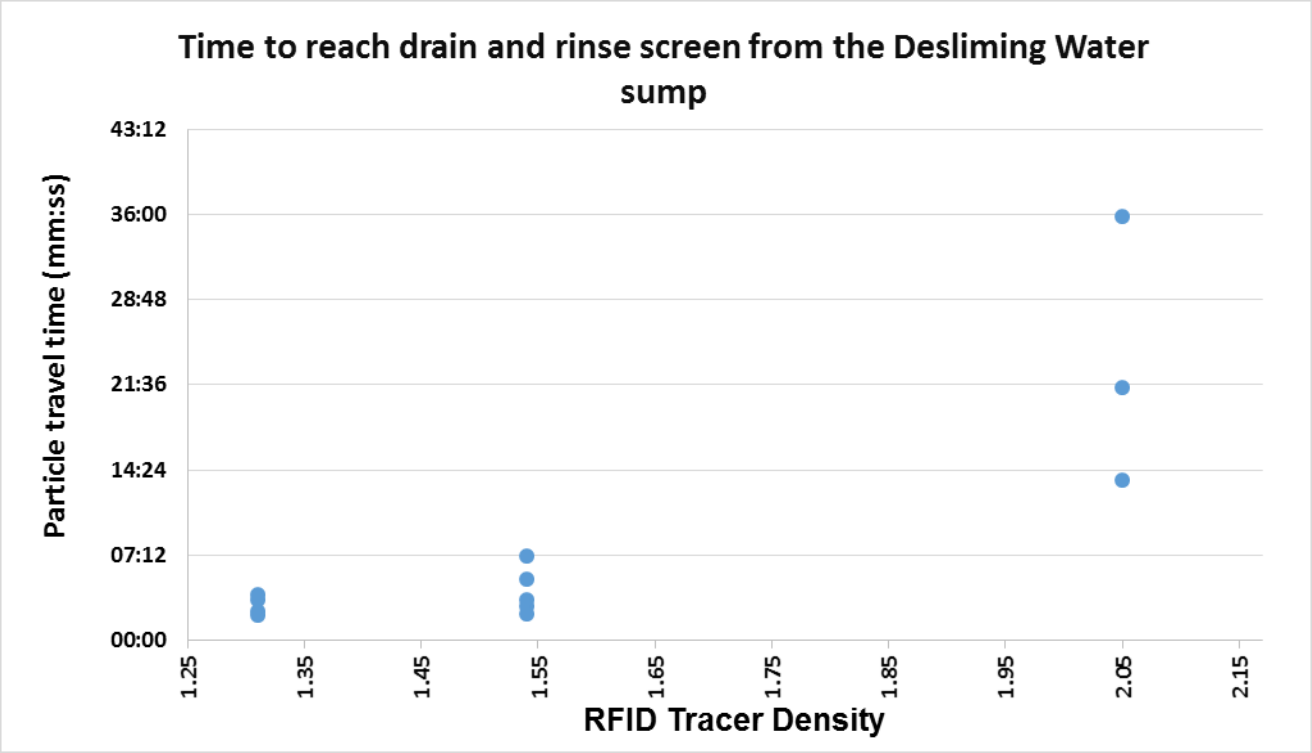

Figure 3.24 Particle residence time vs. Tracer density for particles travelling to the Drain and Rinse Screens from the Desliming Water Make-up Sump.

Crusher feed to the Drain and Rinse Screens

This test involved inserting the tracers at the feed to the secondary sizing station before the plant. The coal from this point enters the de-sliming wing tank and is pumped to the de-sliming screen where it follows the coal through the DMC circuit. Times for particles to travel through this circuit were consistently under two and a half minutes, suggesting that no particles took alternate routes through the plant. (Table 3.16 and Figure 3.25)

Table 3.16: Tracer times for travel from the feed to the secondary crusher/sizer to the drain and rinse screen oversize.

Test	Residence time From	Residence time to	Average	Min	Max
H	Crusher Feed	Drain and Rinse Screen	01:55	01:36	02:25

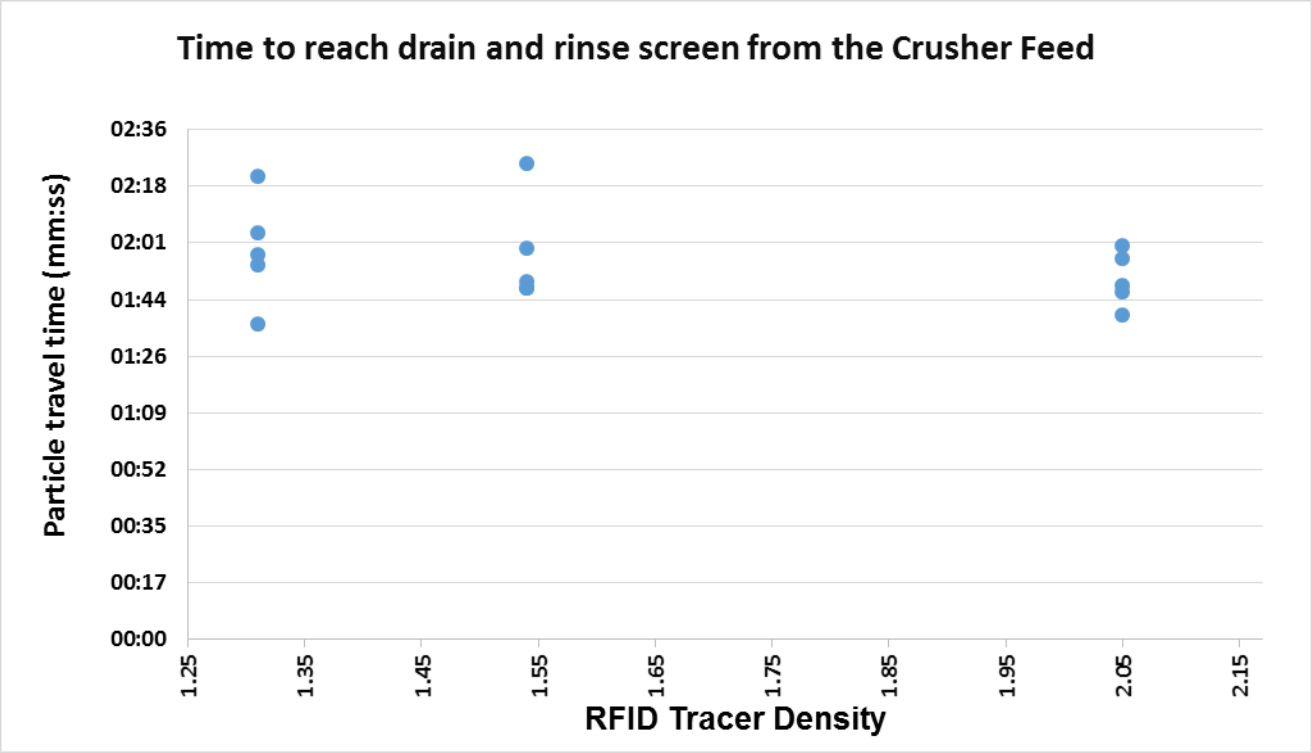

Figure 3.25: Particle residence time vs. Tracer density for particles travelling from the crusher feed to the drain and rinse screens.

Wing Tank Overflow to the Drain and Rinse Screens

This test involved inserting the tracers at the overflow exit of the wing tank where it travels into the correct medium sump. This was intended to give an indication of time in the correct medium sump. Times varied widely and from this, it can be concluded that the medium circuit residence times can be considerably longer than the coarse coal travel path. Particles taking 1 minute 23 seconds to exit the circuit are assumed to have entered the correct medium pump very shortly after being dropped into the overflow, and then were pumped directly to the DMC wing tank. (Table 3.17) Particles which took a longer period of time could have settled out in the correct medium sump, or have been pumped via the bleed across to the dilute circuit before eventually re-entering the circuit with the raw coal at the de-sliming screen. (Figure 3.26) Interestingly, particles of all densities took the short route, but only the heaviest and lightest density particles took the longer periods of time to exit the circuit.

Table 3.17: Tracer times for travel from the feed to the overflow side of the wing tank to the drain and rinse screen oversize.

Test	Residence time From	Residence time to	Average	Min	Max
I	Wing Tank Overflow	Drain and Rinse Screen	06:53	01:23	31:48

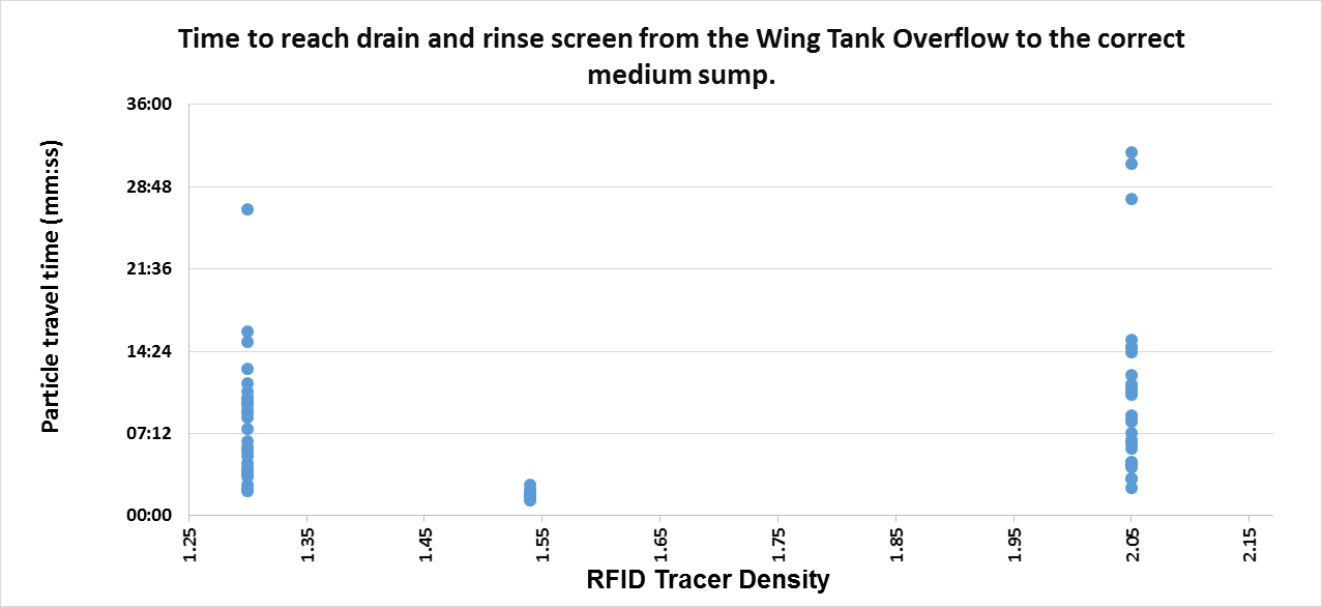

Figure 3.26: Particle residence time vs. Tracer density for particles travelling from the Wing Tank Overflow to the drain and rinse screens.

Discussion of residence time results

- It is reasonable to conclude from the data that rafting and DMC retention did not occur on the test dates because the tracer particle times for travel between the de-sliming screen and the drain and rinse screens were consistently within an expected range.
- While there were a substantial number of particles that took a relatively short period of time to travel through the medium part of the circuit, there were also particles that took considerably longer which suggests that multiple routes were taken.
- From the data overall, it seems that very low density or very high density particles have a greater tendency to take an alternate route of longer duration through the plant, or recirculate while particles with densities close to that of the medium have a tendency to remain part of the medium and follow the coal flows without settling or

floating. An explanation of medium flow observations from the above residence time tests is proposed in Reason 1 and 2 below.

- **Reason 1: Lighter particles floating into the bleed stream**
    - The design of the bleed line which branches off from the main correct medium line may be a cause of segregation of the medium. The main correct medium line is horizontal just after a right angled bend and then the bleed line runs vertically upwards from the top of the correct medium line. There is an opportunity for particles to begin to settle in the horizontal plane before reaching the bleed line. Particles of lighter density could have an increased tendency to migrate up into the bleed line whereas heavier particles would be more inclined to flow along the bottom of the horizontal pipe.

- **Reason 2: Silting in the Correct Medium sump and in underpans.**
    - The explanation of why heavier particles might take longer to arrive at their destination is thought to be due to build-up of heavier particles, or “silting” of material in the correct medium sump and in the underpans of the drain and rinse screens. As the correct medium sump operates at a higher density than the medium measured at the nucleonic gauge, and has no mechanical agitation, it is proposed that the multiple streams of higher density magnetite entering the sump create flow interruptions in the sump leading to a silting up of material in the sump.

3.4 Experimental work Conclusions

The experimental work conducted as part of this PhD Thesis is a sub-component of an ongoing body of research by CSIRO and the University of Queensland (JKMRC). Analysis of non-magnetics concentration and other sampling and data collection was done in parallel with this test work. Plant observations and regular interactions with CHPP personnel have provided unique insights into the operation of the DMC circuit under varying conditions. The comparisons of density tracers of two different particle sizes has provided an interesting comparison of cut point. In the partition tests, the expectation of smaller particles being of higher cut point did not occur. The density tracers were then used in a new experiment to determine residence times of individual particles in the DMC circuit. This data has enabled realistic delays to be determined for use in the dynamic model. The experimental work completed has highlighted that there are still further areas to investigate in relation to particle and medium behaviour in a DMC circuit. The findings of the experimental work are summarised below:

Summary of Experimental Work Findings

Case A: Good density change

- After a density increase during stable operation, the level of non-magnetics was found to reduce with an increase in correct medium bled to the dilute circuit.
- A feed off event which occurred during the trial demonstrated a rapid loss of non-magnetics from the medium, suggesting that the amount of non-magnetics in the coarse coal circuit is strongly affected by the feed.
- Despite a low differential (stable medium) and a carefully orchestrated good density change, the medium took over an hour to recover back to the level of non-magnetics before the density change.

Case B: Unstable Volume

- When operating at a high level in the correct medium sump, and at a low density set point, the plant demonstrated difficulty in maintaining a sufficiently low density due to excess magnetite. This suggested that an alternative means of removing

concentrated magnetite such as an over-dense or magnetite pit return line was needed as an alternative to returning magnetite to the correct medium sump.

- When the correct medium sump and the dilute sump were in an overflow situation, the level of non-magnetics also became difficult to control. An initial drop in non-magnetics was noticed upon opening of the bleed to 100%, and a slight recovery of non-magnetics was noted when the bleed was closed down to 20%.
- In a situation of unstable volume, it is difficult for the plant operator to achieve stable density operation. Volume control becomes a predominant issue at the expense of non-magnetics and density control.

Case C: Stepwise density change

- A step-wise density change resulted in a slower density response when compared with a single change in density.
- The level of non-magnetics dropped markedly when the feed was left off for an extended period of time. Density also dropped.
- The level of non-magnetics dropped when the bleed was opened, and began rising when the bleed was closed.
- After start up, the level of non-magnetics took over 60 minutes to return to prior levels despite operating on a high relative density.
- Time taken to reach density was slower when the amount of non-magnetics was low and the plant feed had been off for a considerable time. Yield losses were estimated at 17% over 11 minutes.

Case D: Low density stability

- Non-magnetics levels did not respond as well when sumps were in an overflow situation, however a drop in non-magnetics was noticeable when the bleed was opened.
- Stability at low density was impacted by volume control due to excess magnetite.
- Due to the fact that the plant had run at very high density just prior to the low density change, the medium was very stable on the test date and no surging events occurred.

Case E: Desliming sprays response test

- Closing the desliming sprays had the effect of rapidly increasing the level of non-magnetics in the medium.

- The rate of build-up of non-magnetics was 2% over 2 minutes.
- The use of desliming sprays to control non-magnetics was not feasible for this particular plant design due to the sensitivity of the water balance, however the concept may work for other designs.
- Ultimately another means of adding non-magnetics to the medium such as thickener underflow may need to be investigated.

Case F: Tracer Testing

- The prediction of cut point for different sized tracer particles showed an unusual cut point reversal between the 13mm RFID and 32mm standard tracers. This was observed on three separate occasions and it was concluded that the effect was real. The observations were also confirmed when a literature review of a thesis by Wood (1990) demonstrated similar effects. It was also determined that the original cause postulated by Wood was incorrect as no float sink chemicals were present in the case of the tracer tests at New Acland, therefore eliminating chemical absorption as a possible cause. Other possible reasons could relate to DMC geometry or particle shape, but more testwork would be needed to determine other causes.
- RFID residence time testing of coal particles travelling through the dense medium yielded valuable information on time delays within the circuit and assisted with model development.
- Times measured for tracers to travel through the DMC circuit were surprisingly short, with the times from the desliming screen through the DMC to the drain and rinse screens ranging from thirty-six seconds to just over two minutes. There was no significant difference based on the density of the coal particle for this pathway and rafting and DMC retention were not evident.
- The time for a coal particle to travel from the weightometer to the drain and rinse screens ranged between two minutes and three and a half minutes. This highlighted the rapid response of the circuit to changes in feed.
- A density effect was noticed for particles travelling in the medium streams. The time taken for particles to travel through the medium differed for denser tracers when compared with low-density particles and with particles of near gravity. This was concluded to be the result of settling out of some of the heavier particles from the

medium, and floating of some of the low density particles up into the bleed stream. Particles that were close to the cut point had a strong tendency to flow as part of the medium and not segregate out, resulting in shorter time travel.

4. Development of the New Acland DMC Circuit Dynamic Model

4.1 Introduction

For many years, steady state models have been used in process plant design. These simplified models have sufficed for developing capacity constraints for a coal handling and preparation plant. Designers then relied upon bore core data, commissioning measurements and process control instrumentation to ensure that the built processing plant operated within the design parameters established in the steady state models. The disadvantage of a steady state model is that cases may arise where efficiency is lost because of upsets in the plant that are undetectable unless tracked over time. For example, a drop in wing tank level may lead to surging of the dense medium cyclone or pumping inefficiencies that cause a short term loss of product into the rejects stream. In a steady state model this case would be difficult to incorporate, however in a dynamic model, time delays, and sump level effects are all included. Similarly, for components in a stream that change due to continual changes in feed quality or particle distribution, it is not easy to model as a steady state case other than with a basic mass balance. Dynamic modelling is also particularly useful for analysing plant start-up or shut-down events where delays may exist in the time it takes for material to reach each unit operation.

In the front end engineering design stage, a number of feeds or blended feeds are passed through a steady state model to establish the extremities of the plant capacity requirements and to predict yields. A plant that fluctuates from 15% fine coal in the feed to 40% fine coal in the feed would have a significant impact on the fines circuit in terms of capacity, and this can be modelled by putting both cases through a steady state model. This allows a snapshot in time to be analysed against other cases. Steady state systems are applicable when a simplified system is required or when little change occurs over time. A dynamic model, by comparison, is time-based, and has the capability to consider the incremental effects on the circuits when the plant is running. A dynamic model can identify opportunities for the control system to react faster and to alleviate plant upsets due to a

change in feed condition. The disadvantage of a dynamic model is that complexity can be high and this often drives the choice of a simpler steady state model.

The development of the dynamic model for the New Acland site followed a number of stages. LIMN™ and Microsoft Excel were initially used to create a steady state model of the dense medium circuit. LIMN is widely used in the coal industry as well as in other dense medium processes such as iron ore but is not capable of dynamic modelling at this time, so the choice of dynamic modelling software was made on the basis of functionality and compatibility with Microsoft Excel. Two options were considered in the software selection process for a dynamic model. SysCAD™, a process flowsheet and modelling software developed by Kenwalt, and MATLAB™, a mathematical programming software developed by Mathworks. Early attempts to model in SysCAD indicated that considerable customisation and work-arounds would be required, and although this software was well supported, a decision was made to use Matlab which could be completely tailored for the purpose.

Matlab is a mathematical programming language that utilises matrices and vectors to shorten code length. Its power is derived from the ability to manipulate large arrays of data in a few short lines of code. The program can combine functions, algorithms and matrices, solve complex equations and simplify other code languages using matrices and vectors. Matlab can also plot functions, create graphical user interfaces and interface with programs written in other languages code including C, C++, Java, Fortran and Python. The powerful toolboxes contained in Matlab-Simulink can be utilised for chemical engineering applications such as process control and automation. The capability of Matlab to take input tags from site equipment and upload data from excel spreadsheets is also extremely useful. While Matlab is not an intuitive programming language, it was decided that the functionality and potential to build in additional options into Matlab without the need to go through a program development step through third party support was an advantage.

4.2 Model Construction

The construction of the dynamic model began with a process of identification of the empirical models to be used with each unit operation. During the process of model

development, regular visits were made to New Acland Plant to confirm specific piping and design requirements for the model. Residence time information was also collected while onsite for later use in dynamic modelling. The specific test work carried out using density tracers is detailed in the Experimental Work chapter of this thesis. Calculations for residence times from plant measurements were inputted as time delays in the dynamic model. Where insufficient information existed, logical assumptions were made.

The inputs to the dynamic model consisted of four individual components: coal, water, magnetite and non-magnetics. This was done so that each component could be traced through each section of the circuit. The overall masses and volumes were also tallied at each stage of the model so that each unit operation balanced. The basis used throughout the model was volumetric flowrate, in cubic metres per second, with conversions to mass flow rate as necessary to suit specific empirical models. The most current and widely used DMC models were found in Crowden et.al. (2013). A Microsoft Excel mass balance of the DMC circuit enabled basic flows to be tested and verified against plant data.

In general terms, a material balance comprises the following equation:

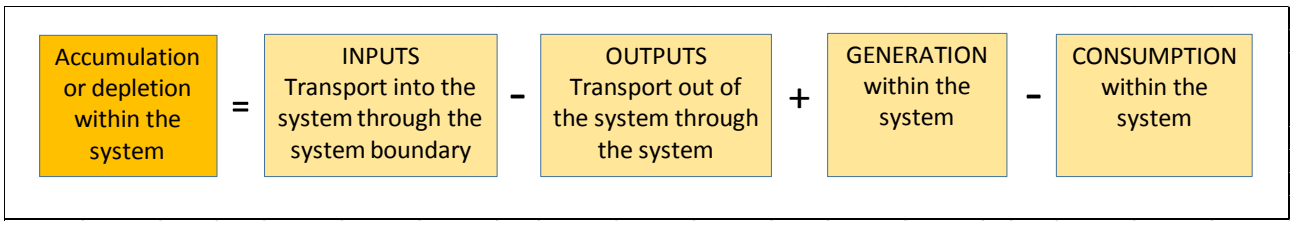

Fig 4.1: Material balance (Himmelblau 1989 eq.6.1,p628)

In the coal preparation case, the material balance could initially be assumed in terms of gross tonnes or volume, and that no generation or consumption occurs. Although some breakage of larger particles does occur in the coal preparation plant circuits, this may initially be discounted for simplification. The equation was then simplified to:

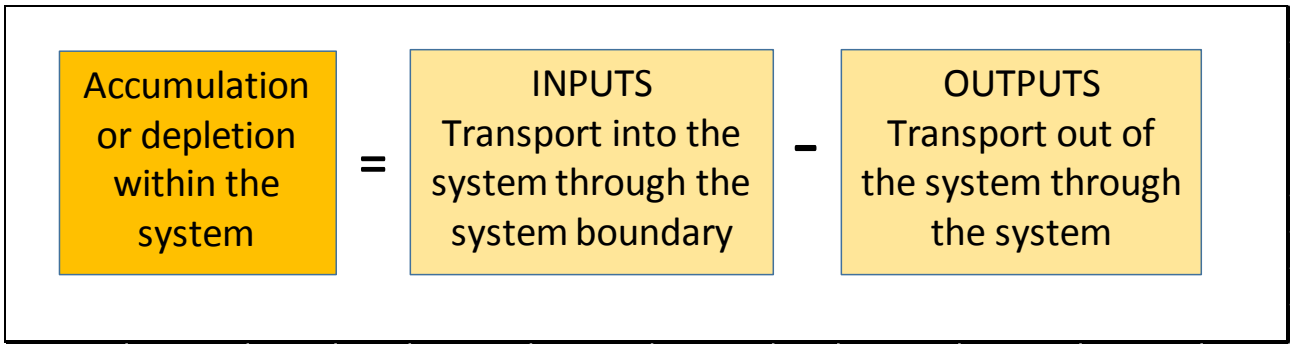

Figure 4.2: Material balance excluding generation and consumption

The balance could then be increased in detail to include individual stream components, namely magnetics, non-magnetics, coal and water. In practice, some breakdown of clays and particle size degradation due to breakage does occur in the circuits. This breakage has the effect of influencing the build-up of non-magnetics in the dense medium circuit. On an individual component balance level, this could be taken into account if wet tumbled coal data results and dry tumbled results were compared. As an alternative, a slimes factor could be applied, where breakage is assumed as a percentage of the total based on practical estimation from typical plant data. For this model, the 'slimes factor' method was used. In addition to the slimes factor, a slimes fraction was added to account for the proportion of non-magnetic slimes in the raw coal.

The Matlab dynamic simulation model was developed with a number of functions as separate files feeding into the main script in Matlab. Figure 4.3 shows the design of the Matlab simulation. The script also included global variables and these variables were used by both the supporting functions and by commands in the main script. Due to their multiple uses, they have been represented as a separate ring in figure 4.3, however, in practice, they are integrated into the script and function files and are not a separate file in themselves.

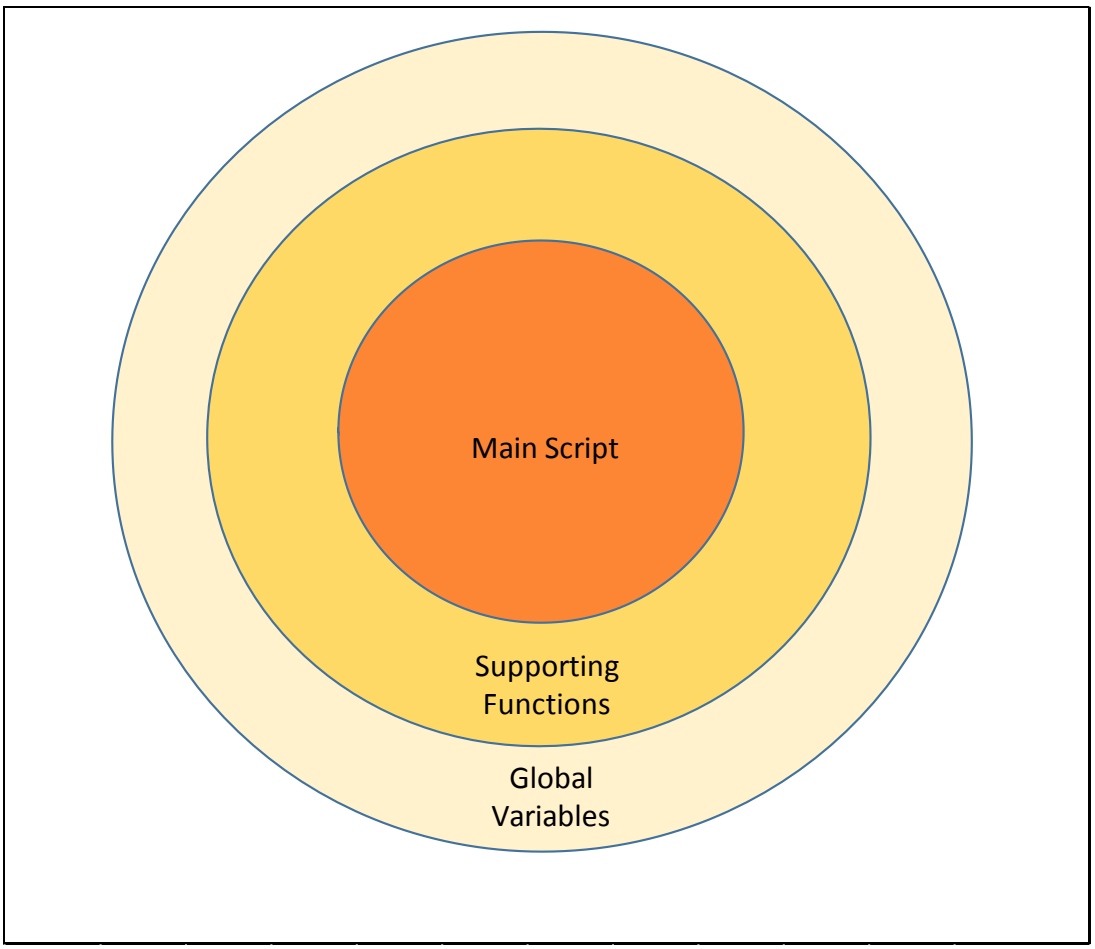

Figure 4.3: Matlab design used a main script with supporting functions in separate files which were called from the script.

Global variables can be used by either the supporting functions or by commands in the main script.

Within the main script of the model, initial variables were set to establish a basis for future calculations. The model comprised an inputs section, an iterative loop and an outputs section (Figure 4.4).

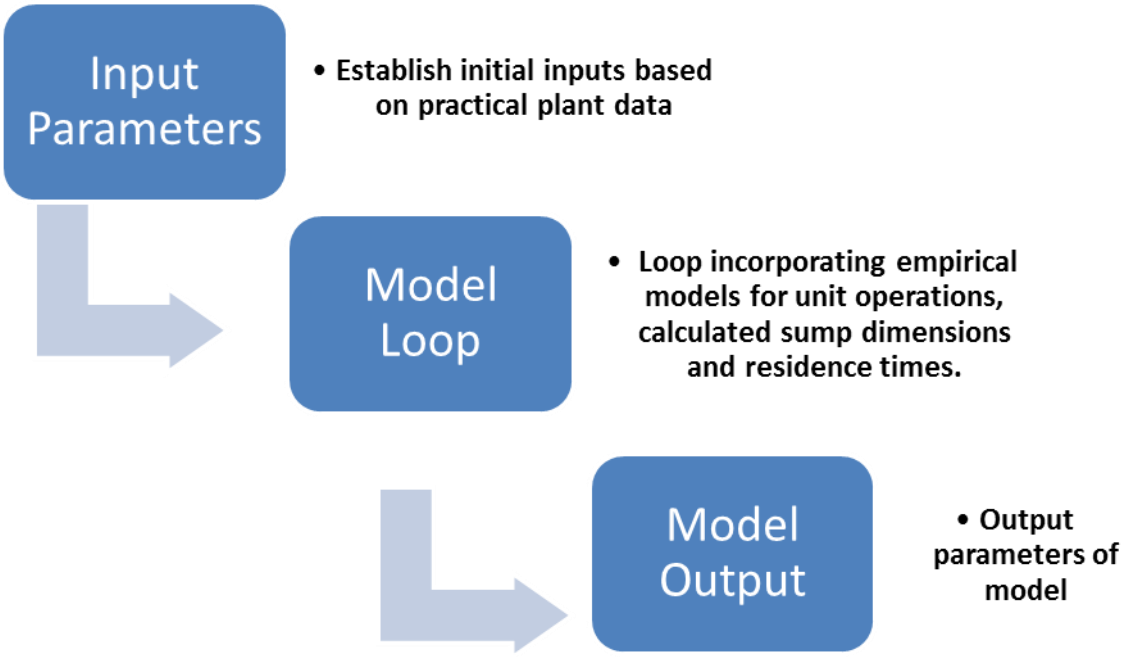

Figure 4.4: The dynamic model process flow

Empirical formulae for the unit operations were placed inside the loop. The loop essentially consisted of an operator selected run-time length of which each iteration step represented one second of plant time. The iterations stepped through for the length of the run-time, each time recalculating the material balance inside each unit operation. This design was based on the work of Askew (1983). Delays in the plant were represented as a table of values from 1 to n where the new value replaced the first value in the table and consequently displaced the n^{th} value where the nth value is the total time of the delay. (Figure 4.5)

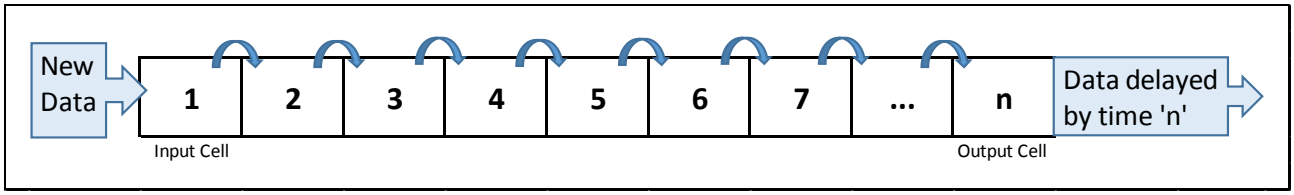

Figure 4.5: A visual representation of how the delays work in the model.

For example, for a delay of 15 seconds, the data will have to shift 15 spaces across (15 seconds). The delays in the plant were determined using RFID tracers and this is described in the Experimental Work section. The output of the model took the format of storage files used for plotting of trends of the data to view and ensure that the behaviour of the components and unit operations were typical of real plant situations. Figure 4.6 shows

the empirical relationships used in the model for each unit operation within the DMC circuit.

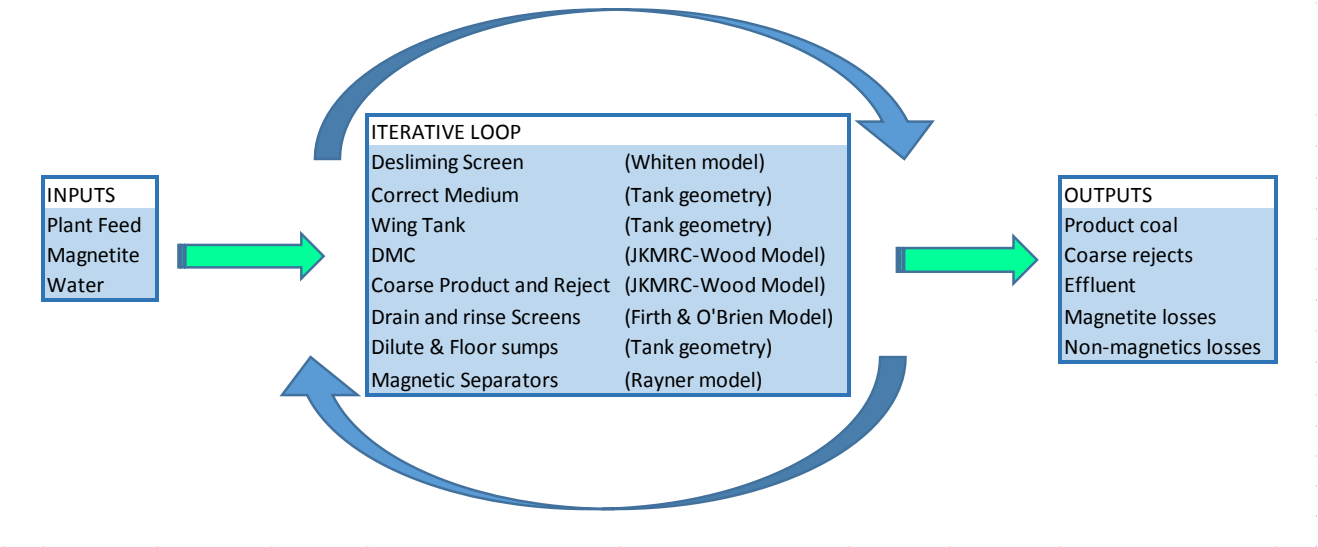

Figure 4.6: Model Architecture. The overall structure of the dynamic model is described in the above diagram.

The model outputs from each unit operation were checked using a "black box" method. In this method, all items within each unit operation were considered to be inside a box, and only input and output streams from that box were balanced. This was done for each unit to verify that the model would balance. These individually tested unit operations were then combined into the simulation model.

Once the overall mass balance and volume balances were established for each unit operation in the DMC circuit, each stream was split into individual components of coal, water, magnetite and non-magnetics. The non-magnetics was defined as fine clays and small coal material that formed part of the medium and this was experimentally measured using a Davis tube on samples of medium, and then weighing the dried samples of magnetics and non-magnetics and obtaining a dry mass% split. Representation of components was achieved using the format of a multicomponent vector [coal, water, magnetite, non-magnetics, total-stream]. This multicomponent vector format was very useful because it improved the ease of transfer of components through the unit operations without the need to create dummy streams or to write separate equations for each individual component, and it therefore considerably shortened the number of lines of code.

For the dynamic material balance, the time for material to reach one part of a circuit will differ from another part of the circuit, and therefore, system delays need to be built into the model. System delays were calculated as functions in Matlab™. The residence times for particles travelling through the circuit were measured using RFID tracers and were used as inputs for the delay functions. The delays and their descriptions are detailed in table 4.1.

Table 4.1: A full list of the delays for the dense medium circuit are below:

Delay	Description	Delay time (s)
Bleedsplit_delta	Dead time from correct sump to bleed valve	15
Deslime_delta	Dead time from bleed valve to deslime	7
Wing_delta	Dead time from deslime to wing tank	6
DMC_delta	Dead time from feed to DMC	15
Drain_delta	Dead time from combined drain to wing tank	12
Rinse_delta	Dead time from combined rinse to wing tank	12
from_Dil_delta	Dead time from dilute sump to mag seps	28
MSCon_delta	Dead time from mag sep cons to correct sump	12
Bleed_delta	Dead time from bleed valve to dilute sump	6

These delays formed part of the initial set up of the model before the first iteration. Initial volumes in the sumps and initial process parameters were also scripted prior to the iteration loop. These included setting density controls, wing tank, correct medium and dilute sump levels, setting initial stream compositions, feed tonnage, drain and rinse screen conditions, raw coal size distribution, washability data and desliming screen partition to the coarse stream. The length of the simulation was given by the variable sim_time, expressed in seconds. This variable was able to be changed to reflect longer or shorter run times. The number of iterations was then simply set as i=1 to ‘sim_time’.

The size distribution used for the dynamic model testing was entered into the model script as size_consist= [37, 18, 10, 6, 3, 1.4, .7, .46; 23.4, 43.1, 18.0, 8.6, 3.3 2.0, 0.8, 0.8];
This is represented in Table 4.2.

Table 4.2: Size Distribution

Size (mm)	37	18	10	6	3	1.4	0.7	0.46
Mass (g)	23.4	43.1	18.0	8.6	3.3	2.0	0.8	0.8

Washability data used for the model was uploaded as a separate .csv file. The washability data used for the dynamic model testing is shown in Table 4.3 below. This washability data can easily be replaced by renaming a new file in the same format:

Table 4.3: Washability data

Density	Mass	Ash
1.28	17.10	9.5
1.33	10.57	16.7
1.38	9.79	23.8
1.43	8.25	29.5
1.48	7.72	34.6
1.51	1.38	38.8
1.54	0.94	38.7
1.56	0.19	39.5
1.59	0.64	40.3
1.61	1.36	41.4
1.64	4.26	44.1
1.66	3.82	48.0
1.69	2.94	51.1
1.75	4.52	56.1
1.85	3.73	62.3
1.95	8.83	67.7
2.10	13.95	76.8

This size and washability data was based on a typical thermal coal from New Acland. Future work could include a graphical user interface which allows the user to upload various different formats for size and washability data.

4.3 Detailed Process Description for Individual Unit Operations

The following schematic diagram may be useful when reading the process descriptions. (Figure 4.7)

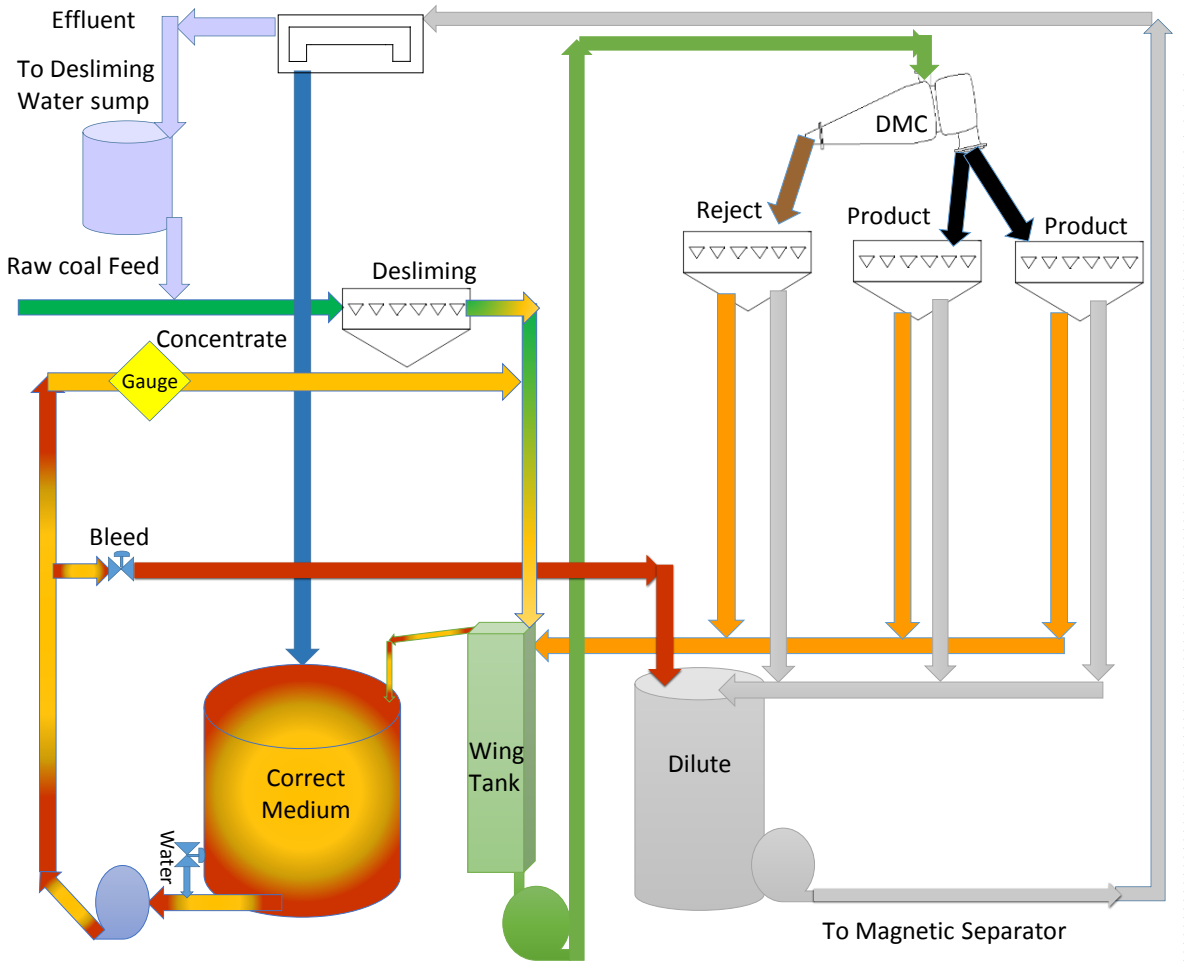

Figure 4.7: Plant schematic

Raw Coal Feed

Raw coal feed to the plant was determined by simulating the weightometer fluctuations using a random feed deviation. It was known that feed variation on this particular plant was significant due to the size of material passing over the weightometer. A deviation of 10 tonnes per hour was considered to be well within the operating range and a 20 tph deviation was possible. The feed deviation was also able to be set to zero to mimic a plant without feed noise. This enabled easier testing of model parameters.

feed = mean_feed + feed_dev * randn(1)

where mean_feed is the nominal tonnage per hour

feed_dev is the deviation in tonnage per hour

randn(1) is a random number generator between zero and one.

The feed calculation was then converted to a volumetric flowrate (m^3/s) using the mean coal density. The slimes component of the feed was calculated by multiplying the coal volume in cubic metres per second by the proportion of slimes in the raw coal (slimes_frac). Once the total volume was calculated by adding the volume of screen water to the feed, the raw coal vector was then compiled:

raw_coal = [vol_coal_ps vol_screen_water 0 vol_slimes total_vol]

where: - The component vector format is [coal, water, magnetite, non-magnetics, total] and the raw coal stream has a zero magnetite component.

The Desliming Screen

For the purpose of this dynamic simulation model, the boundary of the process is drawn at the desliming screen coarse launder after the fines fraction and the majority of water has been removed. Raw coal pumps to the desliming screen from the desliming wing tank which takes the sized coarse coal and slurries it with clarified water and return water from the magnetic separators. The slurry is fed to the desliming screen with additional clarified water sprayed onto the screen deck. Apertures on the desliming screen deck are nominally set at 1.4mm and the value of the aperture variable d50c can be changed to test different screen panels. Undersize coal drops in to the desliming screen underpan and is transported to the fine coal circuit via the desliming cyclone feed sump. The majority of the water on the desliming screen passes through the apertures and enters the fines circuit. A small proportion adheres to the coarse coal and enters the DMC circuit. The raw coal size distribution is split on a dry basis according to the Whiten partition equation in the dynamic model. The volume of wash water was initially determined based on the process flow diagram for the plant.

At the desliming screen launder, correct medium is added. This stream comprises magnetite, non-magnetics and water, with the coarse fraction of the coal from the desliming screen and remaining screen water combining before entering the DMC wing tank. The fraction of medium from the correct medium sump that returns to the desliming screen launder is determined by a bleed fraction. The simulation has been built with a density set point change to observe the effect on the system. The bleed fraction is also set using transport delay functions to account for the differing residence times for transport

within the system. The proportion of medium to the desliming screen is calculated by splitting the stream using the bleed fraction (a pre-set variable) and subtracting the bleed stream (Bleed) from the main correct medium stream (to_Bleedvalve). If there is no flow, the streams are automatically set to zero using a logical 'if' statement.

Density Measurement and Control

In the line feeding correct medium to the coarse launder of the desliming screen (to_Deslime), a nucleonic gauge measures the stream density. (Figure 4.7) Measurement of the medium density via this gauge works in a feedback loop to control the clarified water control valve at the inlet to the correct medium pump. As the density moves above the set point, the water valve opens to dilute the medium down to a lower density. If density falls below the set point, the water valve will remain closed until the density builds up again in the system. This rise in density normally occurs through the continual return of magnetic material from the magnetic separators and also through periodic manual fresh magnetite additions. In the Matlab™ programme, the medium density measurement is simulated by setting an initial value for the density (RD_old) and then calculating a new stream density based on the volumes and component densities expressed as a vector.

In the CHPP control room, the operator dials in a set-point in the SCADA computer system. The operator would typically change density set point in the event of an adverse laboratory result for ash outside of specification, or if there was a change in feed or product type. In a simulation, the density set point can be constrained to operate between 1.20RD and 1.80RD in line with normal plant practical limits. Due to washability characteristics of Australian coals, few plants exceed 1.70RD and it is rarely achievable to target a density below 1.25RD. Of course if this were to change in future, the constraint could be altered to suit.

To calculate the new value of the nucleonic gauge, a density is calculated around the base of the correct medium sump outlet using the mass and volume. In order to achieve this balance, other streams must be calculated first so that the composition and volumes of the stream leaving the correct medium sump is known. Let's assume for a moment that this has been calculated and that the density of the stream leaving the correct sump is now known. The adjustment of water additions at the control valve at the base of the correct

medium sump is controlled using a base amount of water with the error changing based on the difference between the nucleonic gauge reading and the density set-point. If the error is greater than zero, then this means that the real measured density is higher than the set-point and therefore the water valve will open. In practical terms, if the measured medium density is lower than the set-point, then the water valve would automatically close, so a logical statement is required to ensure that if the error was less than zero, then the water valve would remain closed. Water control to the correct medium is then determined by setting up a proportional integral controller. This has been represented by the function "Pi2" in the model. This calculates a process variable (PV) as follows:

PV = Kp * Error + Ki * Int

Where Kp is the proportional gain, Ki is the integral gain and Int is the integral sum

The value for controller gain makes adjustments for a lag in the readings for density and would only be adjusted during commissioning or calibration of the unit. It will not be changed by the control room operator. The PV value is then used in the main script for the water control algorithm;

control_water = auto_water_base + auto_water .* PV

where auto_water_base is a base quantity of water and auto_water is the additional amount to allow for controlling density.

This control_water variable is then limited to set to zero if the density is already at set point. The value of the stream from the correct medium sump is then adjusted to account for the water addition:

from_CM= from_CM + control_water

where from_CM is the volumetric flow from the correct medium sump

Figure 4.8 is a typical example of a density control system response.

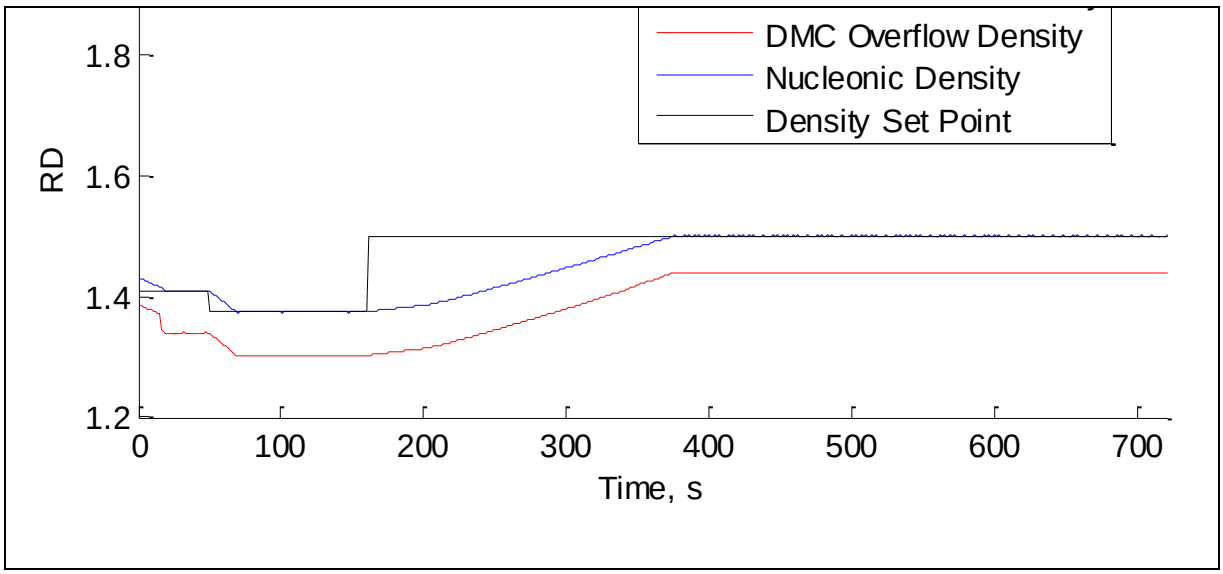

Figure 4.8: Figure showing a typical density control for a dynamic model. The nucleonic density (blue line) is tracking the set-point (black line).

In this figure, the Nucleonic density gauge, (blue line) is seen to track the density set point (black line). As the nucleonic gauge senses the density difference as the set point is dropped, the automatic water valve opens leading to a dilution of the medium and a consequent lowering of the density. As the nucleonic gauge senses the density difference as the set point is raised, the automatic water valve closes, allowing the concentration of magnetics to gradually increase by the addition of higher density concentrated magnetite from the magnetic separators.

Modelling and simulation of the wing tank

A wing tank is a tank designed to consistently feed medium and coal to the DMC pump at the desired head to supply sufficient velocity for a sharp separation in the cyclone. The wing-side (or coal-side) of the wing tank was called this because in older designs, it was shaped like a wing or tailrace running into the side of the tank. Nowadays, the wing portion of the tank is typically superseded by a cylindrical pipe open to atmosphere at the desliming screen end. Wing tanks are designed to continuously overflow so that head to the pump is kept at a constant level when coal is being delivered to the DMC. When no coal is present, the wing tank will typically operate just below the overflow. Figure 4.9 and 4.10 below demonstrates the coal off and coal on situations for a wing tank.

Wing tank Example below (Crowden et.al. 2013):

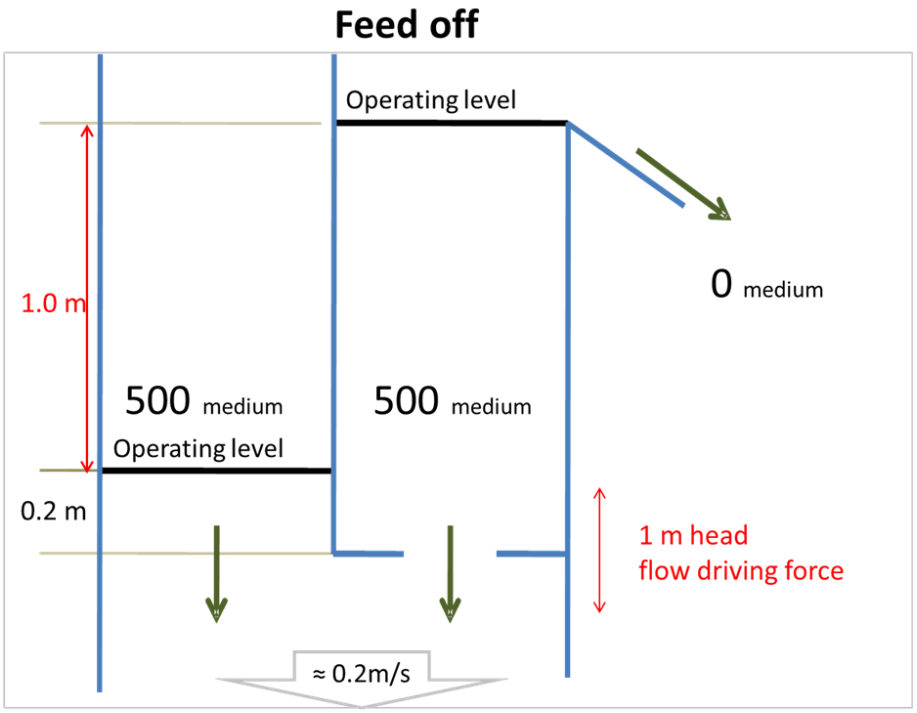

Figure 4.9: Schematic of wing tank cross-section for coal feed off (1,000 m³/h medium) Crowden et.al.(2013)

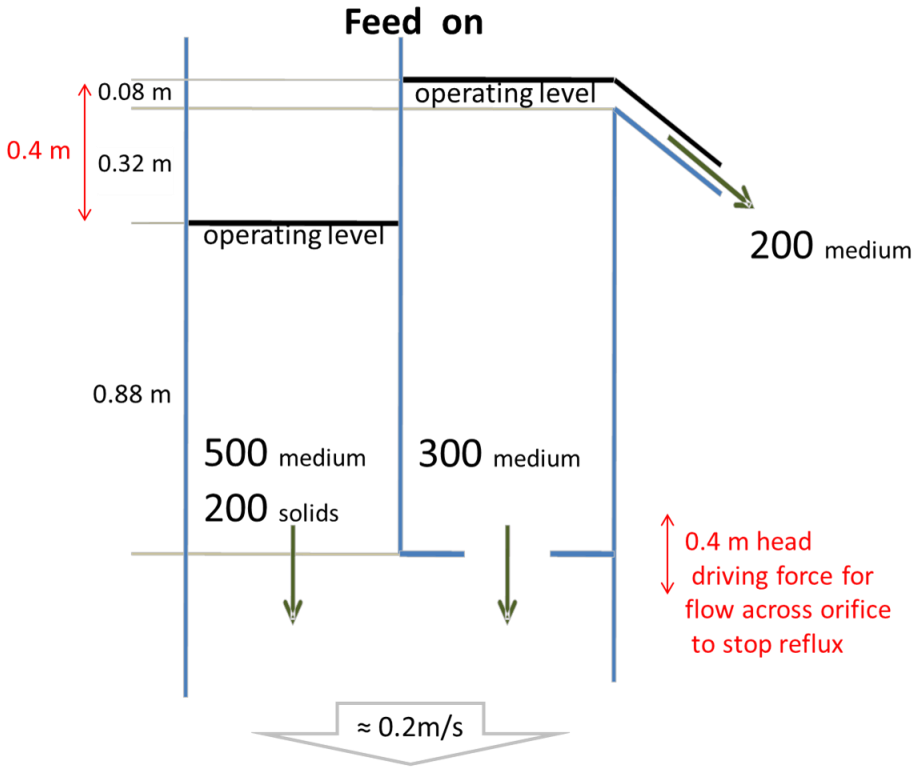

Figure 4.10: Schematic of wing tank cross-section for coal feed on (800 m³/h medium + 200 m³/h solids) (Crowden et.al. 2013)

The wing tank must meet two key objectives. Firstly, it must be capable of operating at a constant level while receiving incoming feed solids and medium. Achieving a constant level allows the DMC to be fed at a constant flowrate and pressure. In some plants this is achieved by the use of a splitter box before the wing tank to separate excess medium off into the correct medium sump (Crowden et.al. 2013). In other plants such as New Acland, the excess medium is allowed to enter the seal side of the wing tank and then overflow at the seal leg of the wing tank with the overflow feeding into the correct medium sump. Variable speed pumps are also common in plants to balance out minor variances in wing tank level to provide a more consistent feed to the DMC.

The key objective is to have a uniform downward flow rate to the DMC feed pump of approximately 0.2 m/s. This reduces the tendency of more buoyant particles to raft inside the wing tank, while being sufficiently low in velocity to avoid entraining air. (Crowden et.al. 2013) Maintaining a consistent downward flowrate means that coarse feed entering the wing tank follows a direct path to the pump inlet. The profile of a wing tank is typically tall and narrow to ensure a direct path to the pump and promote plug flow. Although flows inside the wing tank are turbulent, it was noted by Askew (1983) that wing tank flows resemble that of variable volume plug flow devices. This notion is supported by the RFID residence time data collected in the New Acland plant. (as detailed in Chapters 3.3 and 3.4) Very little variation in travel times existed between the de-sliming screen and the drain and rinse screens for particles following the same route as a piece of coal through the wing tank and DMC.

The wing tank was modelled in a function outside of the main script called wing_tankVec.m. The Wing tank function was a relationship between the feed to the wing tank, the volumetric feed to the DMC and the volumes in the wing tank on the coal and seal leg sides. Initially a boundary was assumed around the entire wing tank. Inputs to the wing tank included initial volumes of the coal and seal sides of the tank, the coal and medium flowrate into the wing tank from the desliming screen (to_wing) and the drained medium returning from the drain side of the drain and rinse screens (from_DR_drain). The drain was also multiplied by a splitter factor (y) which accounted for any proportion of drained medium that was split to the coal side of the wing tank. In the New Acland case study, y=1. The volumetric flow rate of the DMC feed pump at the base of the wing tank was also considered (DMCfeedvol). Outputs of the wing_tankVec.m function included the

wing tank overflow (W_overflow) which flows from the seal leg to the correct medium sump, the tank level and the seal level. (Figure 4.11)

Figure 4.11 Inputs and outputs to the Wing Tank function

The wing tank function calculated the levels in the wing tank and in the seal leg using a spline equation which was based on the tank geometry (height to volume relationship) and then used this to calculate the orifice flowrate and head in the wing tank. An orifice plate which separated the coal side of the wing tank from the seal leg was considered in these calculations due to its influence on relative head in the two sides of the tank. Under normal operation, medium flows from the seal leg into the coalside of the wing tank to deter rafting of coal into the overflow. The differential head between the coal-side and the seal-side of the wing tank is significant in driving the flows through the orifice plate and therefore determining the orifice velocity. The flow rate through an orifice is calculated as follows (Crowden et.al. 2013):

Q = C x a x SQRT(2 x g x H)

$$Q = C \times a \times \sqrt{2 \times g * H}$$

Q	Flow rate m^3/s
H	Head m
a	Area of orifice opening in m^2
g	gravity constant 9.8 m/s^2

C= 0.9	smooth, rounded, tube running full
C= 0.8	tube running full
C= 0.6	submerged square profile circular hole orifice
C= 0.6	sharp lipped circular orifice

For the New Acland CHPP dynamic model, the orifice calculation was modified to account for flow direction through the orifice. To do this, a flow direction factor, k, was added and this was influenced by whether the differential head (DeltaP) was positive or negative:

Qorifice = k* C * a * sqrt(2*g*abs(DeltaP)) **22**

Where:

Qorifice – the flowrate through the orifice (m^3/s)

dorifice = 0.310 metres (orifice hole diameter)

a = area of the orifice plate hole and is calculated as the area of a circle of diameter, dorifice.

C = 0.6 for a submerged square profile circular hole (New Acland case)

g = 9.81 m/s^2

DeltaP = is the differential head between the seal level and the coal-side tank level

DeltaP = (seal_level) – (Wtank_level)

k = is the flow direction through the orifice plate. If the coal-side tank level is higher than the seal seal-side level, Delta P is less than zero and therefore, k will be -1. If flow is positive, ie. in the normal direction, k is +1.

As the square root of a negative number will result in an error, the absolute value of Delta P was used in the orifice flow equation and the k value moved outside of the square root part of the equation.

From the orifice flowrate, the velocity through the orifice can also be calculated as follows:

Vel_orifice (m/s) = Qorifice / a **23**

Ideally the velocity through the orifice should exceed 0.2 m/s to prevent rafting. Under normal operation, the seal level will typically be higher than the coal-side tank level. During feed off conditions, that is, when no raw coal feed is present, the circulating medium in the wing tank should be sufficient to maintain a seal level where medium is just touching the overflow, ie. virtually zero overflow. (Crowden et.al. 2013) The coal-side tank level is typically higher than the height of the orifice plate when running. The orifice plate sizing is normally adjusted during commissioning to ensure that wing tank levels are maintained during operation which in turn ensures a continuous head delivered to the DMC pump. (Crowden, et.al. 2013)

Although the DMC feed pump is capable of variable speed operation, the pump speed at New Acland is set as constant by the control room operator during normal running. Minor adjustments may be made as the pump wears, and when grade changes require higher or lower DMC pressures. The operator alters the pump speed until the desired pressure is reached, and then leaves it unchanged until a new coal type comes through the plant. When feed is added to the wing tank, there is sufficient free space designed into the coal-side to accommodate the coal and medium. This additional coal increases the level of the coal-side and therefore decreases the differential head between the seal side and coal side. (Crowden, et.al. 2013) The correct medium and dilute pumps are also typically fixed at constant speed. This means that the flowrate into and out of the wing tank changes by the amount of returning medium and the amount of coarse feed entering the tank.

Once the orifice flowrate has been determined, the new seal volume (Sealvol) and wing tank volume (Tankvol) could be determined by doing a mass balance around both sides of the tank, considering the orifice to be one of the streams:

Sealvol= Sealvol_old + from_DR_drain .* y – Qorifice

This is the calculation of seal volume with zero overflow.

Tankvol = Tankvol_old + to_wing + (1-y)*from_DR_drain - DMCfeedvol + Qorifice

A provision was made here for a plant where a splitter box exists above the wing tank to divide the drain flows between the coal and seal sides of the wing tank, however, in the New Acland case, one hundred percent of the flow was to the seal side (y=1).

The overflow from the seal side of the wing tank to the correct medium sump was then determined using tank geometry to set limits. If the seal volume was below the volume of the overflow, the W_overflow was set to zero cubic metres per second. If the seal volume was greater or equal to the overflow volume, the following formula determined the overflow rate:

W_overflow = (y .* from_DR_drain - Qorifice)

Once the overflow flowrate was determined, the new seal volume was able to be calculated by considering the drainage flowrate from the drain and rinse screens, the flow through the orifice and the wing tank overflow.

Sealvol= Sealvol_old + y*from_DR_drain - Qorifice - W_overflow

The wing tank function outputs return the values of seal level, wing tank level and overflow volumetric flowrate back to the main script. The medium to coal ratio is then calculated in the main script and also the DMC pressure based on the head from the wing tank.

A clean_coal function is used to partition the raw coal based on its washability for an initially pre-determined value for d50c (cutpoint) and Ep. Here, the Whiten Partition model has been used. The washability data uploads from a .csv file. This format was chosen to enable multiple washability data sets to be used. The Ep and d50c values will change and update as the model iterates through the set number of iterations. It should be noted that Ep values determined by plant experiment or tracer test may differ from the Ep values in the empirical model. This is a common issue when relating the JKMRC Wood model back to plant data and is often the reason for an adjusted Ep. The clean coal function outputs the mass of partitioned clean coal, volume of clean coal and clean coal density back into the main script. The volume pumped from the wing tank (DMCfeedvol) then considers the clean coal density to calculate mass flowrates from the partition model.

As the coal circulates through the dense medium circuit, some breakdown of clays and small coal occurs. This is accounted for using a slimes factor. The size consistency of the slimes is predetermined using a slimes factor multiplied by the size distribution of the raw coal feed. An assumption has been made in the model that 2% of the raw coal breaks down and becomes an integral component of the medium. The new size distribution is adjusted according to the slimes factor in each iteration. This is important for the model as in practice, a build-up of contamination, or non-magnetics will occur, particularly if the bleed to the dilute is closed. This level of non-magnetics changes and affects the stability of the medium. As the vectors in the model are component vectors split by coal, water, magnetics and non-magnetics, it is possible to change the components using the slimes factor calculation.

Drain and Rinse Screens

The drain and rinse screens are modelled based on Firth and O'Brien's medium recovery models Crowden et.al (2013). These models calculate the medium drain rates and fines recovery for the screens using the flowrates calculated and product by size data adjusted for slimes breakdown. Information about screen apertures, open area and screen

dimensions are required for this part of the model. The calculation of the amount of water reporting to the oversize flow stream, Rf and the number of presentations of the particles to the screen deck surface is determined. The effect of the N value is to influence the curvature of the partition curve. As a screen wears, the amount of undersize reporting to the drain will increase. The percentage of material reporting to the drain (drain_percent) is then used in the main script. This is calculated for all drain screens, product and reject, and enables determination of the drained medium returning to the wing tank.

Drain = Pdrain +Rdrain

from_DR = Comb_Drain_delay (Drain,Drain_delta)

The latter relationship is a function that uses the delays calculated from residence time testing to determine the stream from the drain and rinse back to the wing tank seal leg.

The remaining medium not reporting to the drain side is accounted for by difference and is sent to the rinse side of the drain and rinse screens. A similar calculation is used for the rinse screen model, however the amount of rinse water added is also taken into account. The function “Rinsepd2” performs the calculation of partition of the rinse section of the drain and rinse screen and then returns the values for the product rinse volume, the amount of water and rinse water to the dilute back to the main script. The size distribution is then used to partition solids on the rinse screen. The proportion of rinsed medium to the dilute is then calculated for each screen. The clean coal and reject leaving the end of the rinse screens is then determined, accounting for some adhesion losses of magnetite on the coarse material entering the launders.

The final calculation sums the rinse medium flowing to the dilute as follows:

Rinse_to_dil = PRDilute + RRDilute

where PRDilute is calculated using the RinsePD2 function and RRDilute is calculated using the RRinse function and both represent the rinsed medium flows from the drain and rinse screens to the dilute sump. Once again, a delay is added (Comb_Rinse_delay) to account for time taken for flows to reach the dilute sump. The reject coarse entering the coarse launder is also accounted for by difference with adhesion losses taken into account.

Correct Medium Sump Balance

Once drain and rinse flows have been calculated, the correct medium sump balance can be done. The geometry of the correct medium sump is a conical bottomed vessel with a total volume of 35 cubic metres. The incremental changes in volume with respect to height have been calculated based on the tank geometry and with the use of the Matlab spline function on the conical section, the tank level can be determined from tank volume. For the cylindrical section, a regression equation was determined to accurately predict the height per unit volume. Once the slurry level in the sump reaches the bottom of the overflow, the program calculates the volume of excess slurry as the overflow amount after accounting for inputs and outputs to the tank.

To account for dynamic changes with time, the old volume (Sump_vol = CMvol_old) is recorded from the previous value and this is then added to by applying the volume balance around the sump for the next increment. The function for this calculation is CorrectSumpVec. In order to complete this calculation an initial value of flow from the magnetic separator is assumed. Similarly, the pumping rate from the Magnetite Pit (from_Mpit) is also assumed. The calculated volume is then recorded as the new value for Sumpvol and the next iteration commences. The level in the correct medium sump from the spline equation is then used to calculate the pump head for the correct medium pump. The Correct sump volume is then updated as follows:

Sump = CMVol_old + from_MagSeps + W_overflow + from_Mpit
CM_Vol = CMVol_old + from_MagSeps + W_overflow + from_Mpit – from_CM

where from_CM is the proportion of the sump pumped out in m3/s
and W_overflow is the overflow from the wing tank

The overflow of the correct medium sump is calculated only if the level exceeds the height of the overflow pipe. This is calculated as the difference in the volume (CM_vol) and the pumpout volume (from_CM).

The pipework exiting the correct medium sump has an automatic water addition valve before the pump and then the line splits after the pump into a bleed stream into the dilute sump, and a feed stream to the desliming screen. The function of this auto water valve

(control_water) has been described earlier and the water stream (control_water) combines with the water pumped from the correct medium sump (from_CM) to create a larger stream This variable is still called “from_CM” but as it is later in the code, the variable updates with the new figure.

Due to the location of the 100mm diameter bleed line on the top of the horizontal 600mm diameter correct medium pipe (Figure 4.12), it is theoretically possible that some settling in the pipe may result in lower density material preferentially entering the bleed line, however this cannot be determined without further sampling.

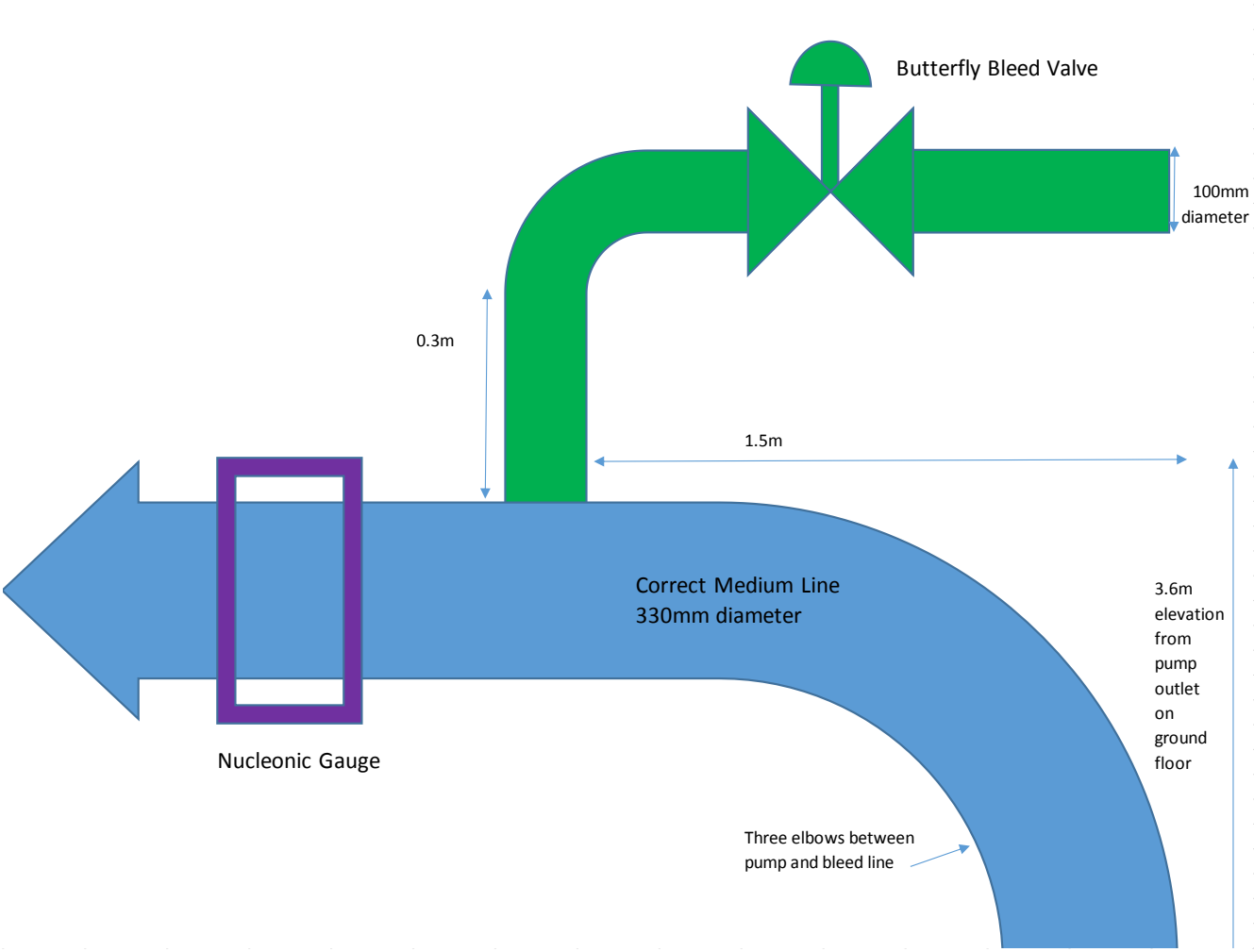

Figure 4.12 Elevation sketch of the 100mm bleed line tee off the main correct medium line.

Occasional blockages due to rafting coal suggest that the flowrate through the wing tank orifice is not always sufficient. For the purposes of the model, the same composition is assumed for the correct medium line and the bleed tee off point. This is important to note because the nucleonic gauge is situated downstream and is also in a horizontal section of pipe. Calculation of the bleed stream to the dilute sump is achieved using a manual input

variable which splits the correct medium stream by a set proportion. The bleed to dilute line (Bleed_to_Dil) is calculated to include a delay for transport time. The dilute sump balance is then able to be determined.

The Dilute Sump

The dilute sump is a cylindrical vessel with a conical bottom and a total volume of nine cubic metres. The geometry of the sump was determined from the construction drawings and was used to calculate the volume in a similar manner to the correct medium sump calculation. A spline equation was then used to determine sump level for a specific calculated volume. This spline calculation is part of the DiluteSumpVec function which uses inputs of return rinse medium (Rinse_to_dil), make-up water (Clarif_water), and floor sump contents (Floor_drain). An initial volume (DilVol_old) is set and this value is replaced with each new iteration. Since the floor sump pumps its material onto the end of the rejects screen and into the underpan, which flows back to the dilute sump, it was assumed that the floor sump pumps directly into the dilute sump for the purpose of the model. Further, it was noted that in an overflow situation, both the dilute and the correct medium sumps would flow into the floor sump and then back into the dilute sump and therefore, the floor sump could be considered as part of the dilute sump system for the purpose of modelling the dilute sump balance.

The dilute sump function outputs are tank level (Diltank_level), dilute sump overflow volume (Dil_overflow), new sump volume (Dil_Vol), and the pumpout rate to the magnetic separators taking into account any transport delays (from_Dil). Since magnetic separators typically do not cope well with surges in flow or inconsistent levels, the pump would normally be run at a fixed speed to ensure consistent flow.

Magnetic Separators

The magnetic separator section of the model is calculated in a separate function, MagSepVec2 which is based on Firth and O'Brien's work in Crowden et al. (2013). A magnetic separator concentrate and tailings stream have been determined from this function. These streams return to the correct medium sump and to the desliming water make-up sump respectively. The proportion of magnetite losses and removal of non-magnetics can be calculated also using this function. Some difficulties were experienced

getting this function to work effectively and eventually the use of the function was abandoned in favour of a constant recovery rate of 99.9% and an entrainment rate of 25%.

4.4 Outcomes from Model Development

A dynamic multi-component model of a coal DMC circuit was successfully built using MatlabTM as a software platform. The model incorporated non-magnetics thereby enabling monitoring of non-magnetics in the circuit with plant fluctuations. Model design utilised existing empirical models for each unit operation in the circuit. The following chapter outlines the validation of the dynamic model of the DMC circuit at new Acland against data collected from Plant 2. The dynamic model script is detailed in the appendices.

4.5 Model Analysis and Validation

A step-wise process was used to test and validate the dynamic model. Once the framework of the model was in place a process of iteration began. Each change to the code script was checked by running the model and analysing results. As iterations were run of the model, issues were identified and compared with plant data. The simulations were then repeated and checked. Due to the iterative looping nature of the dynamic model, and also due to the delays built into the model, this process took a considerable amount of time. Often one issue would lead to a series of other issues, resulting in a lengthy search to find the root cause of the problems. Eventually, the problems were resolved and the validation results described below are a comparison with both plant results, normal operating conditions and laboratory results.

Predictions of circuit behaviour - Comparison of Density

Figure 4.13 and 4.14 show the density response in the dynamic model compared with the density response in the plant. The figure 4.14 case was really a worst case scenario with a feed off event occurring just prior to an extreme density change.

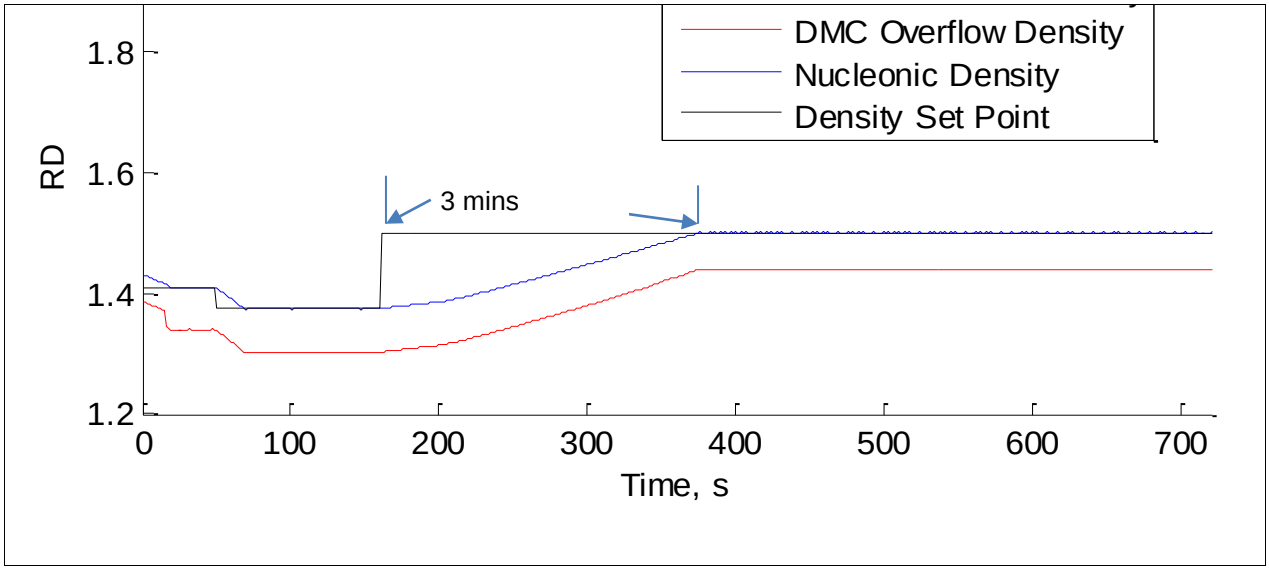

Figure 4.13 Matlab density (minutes 1=60s, 2=120s, 3=180s, 4=240s, 5=300s, 6=360s, 7=420s). Plant feed variation was switched off in this particular instance.

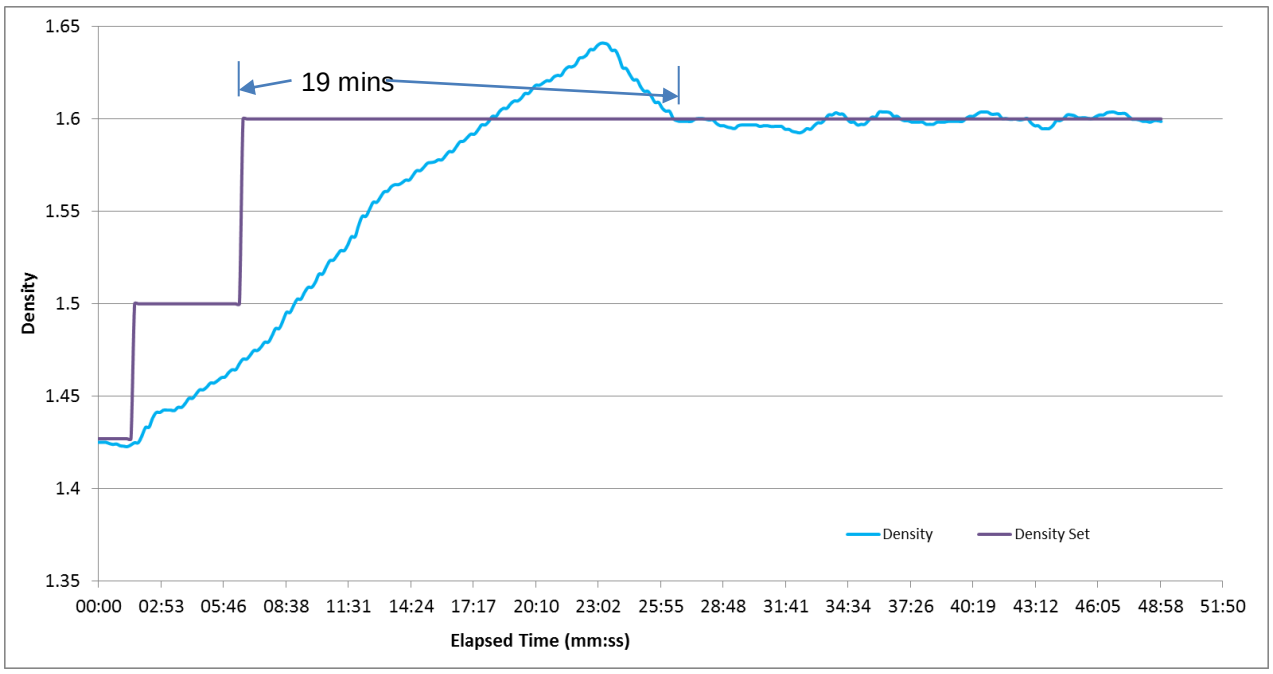

Figure 4.14: Plant data from 25/3/2014 showing plant response to an upwards stepwise density set point change.

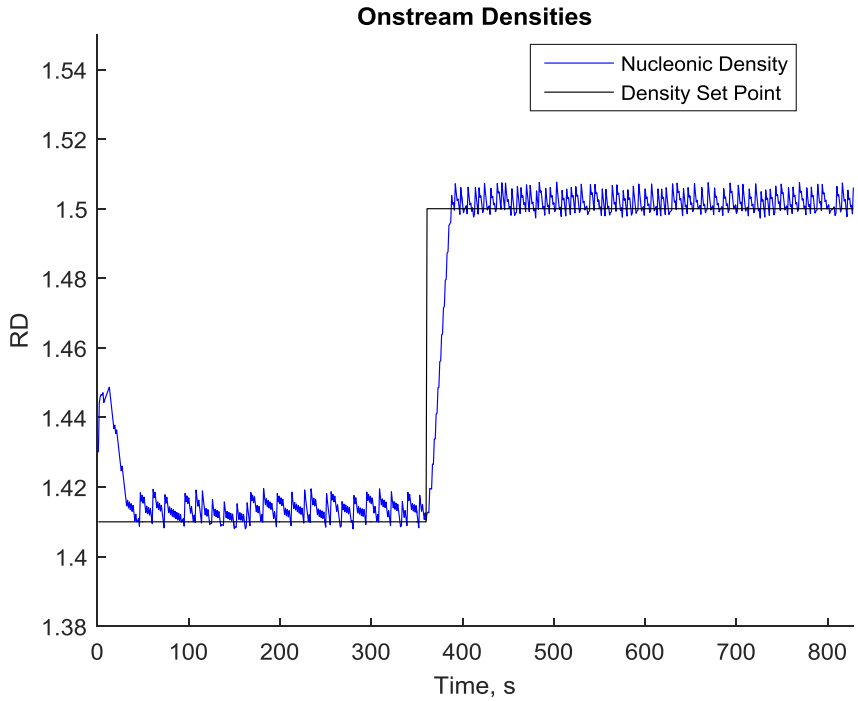

Figure 4.15: Dynamic model density response was too fast.

The density controller gain was adjusted until it resembled the plant in figure 4.14

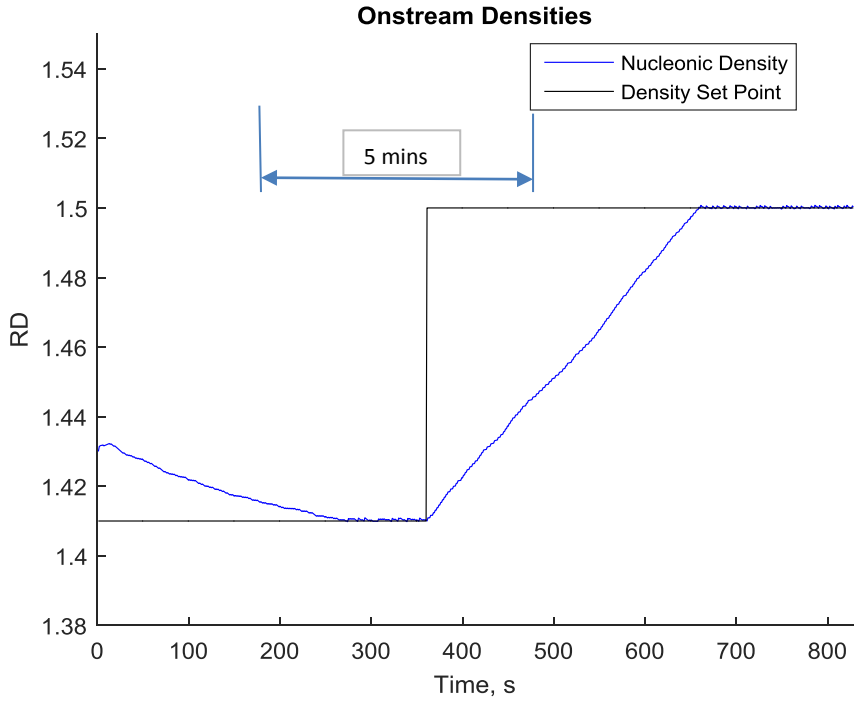

Figure 4.16 Dynamic Model Density response was adjusted to give a more realistic time for density change.

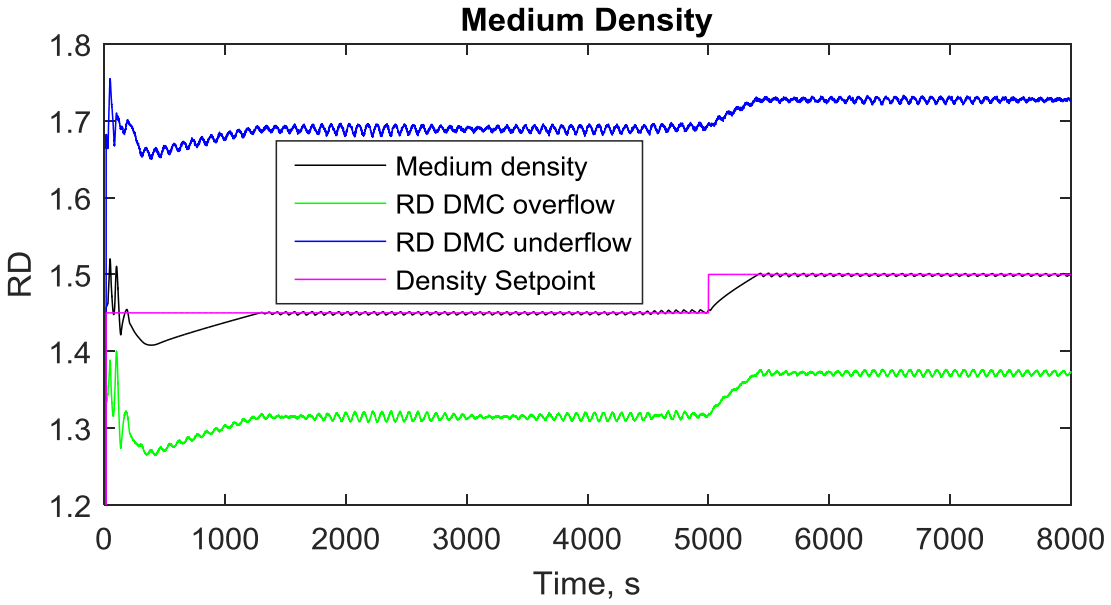

Figure 4.17: Plant start up condition at time zero with a density set point rise at 5000s and dynamic model response compared against set point.

Figure 4.17 above shows the densities of the medium and set points from an initial start up condition. At start-up, delays are significant in influencing flows to various parts of the circuit. This also influences the action of the automatic water valve density adjustment. Modelling of faster methods to achieve stable density operation after start-up (eg. an overdense sump) would be a useful future application of the dynamic model.

Figure 4.18 shows another density response to a drop in density. In this situation the density response is faster, dropping from 19 minutes to 5 minutes. By comparison, the dynamic model appears to respond relatively well, albeit a little slower than the plant situation (Figure 4.19a) however this is somewhat dependent on the gap that the density needs to move. Opening the bleed while changing density resulted in a longer time than when the bleed was closed. This is discussed further in the discussion around Fig 4.24 The speed of density movement can be adjusted to match plant outputs using the autowater controller. Fig 4.19b shows a different density change and the response was faster at the higher density range.

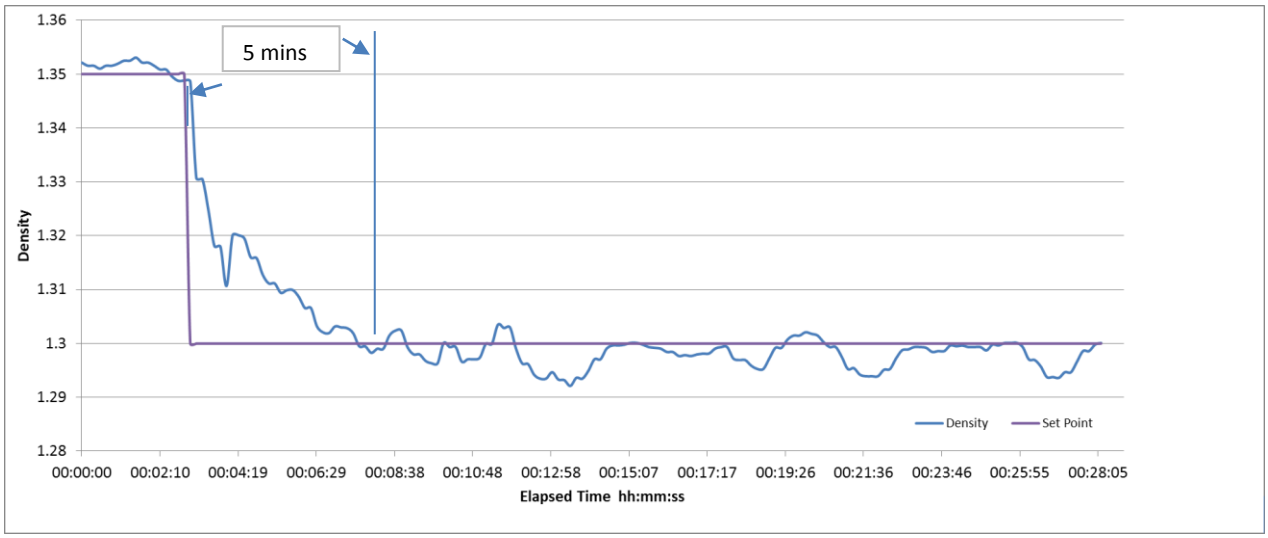

Figure 4.18: Plant data from 26/03/2014 showing plant response to a downwards density set point change

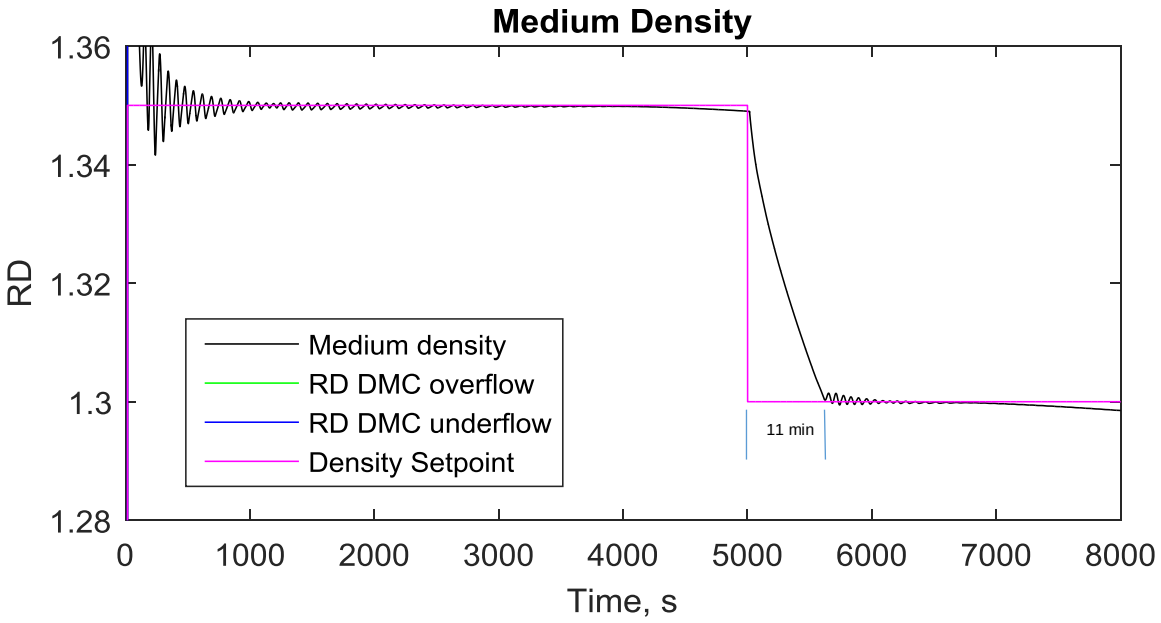

Figure 4.19a Dynamic model was adjusted to drop the density in the plant from 1.35 to 1.30

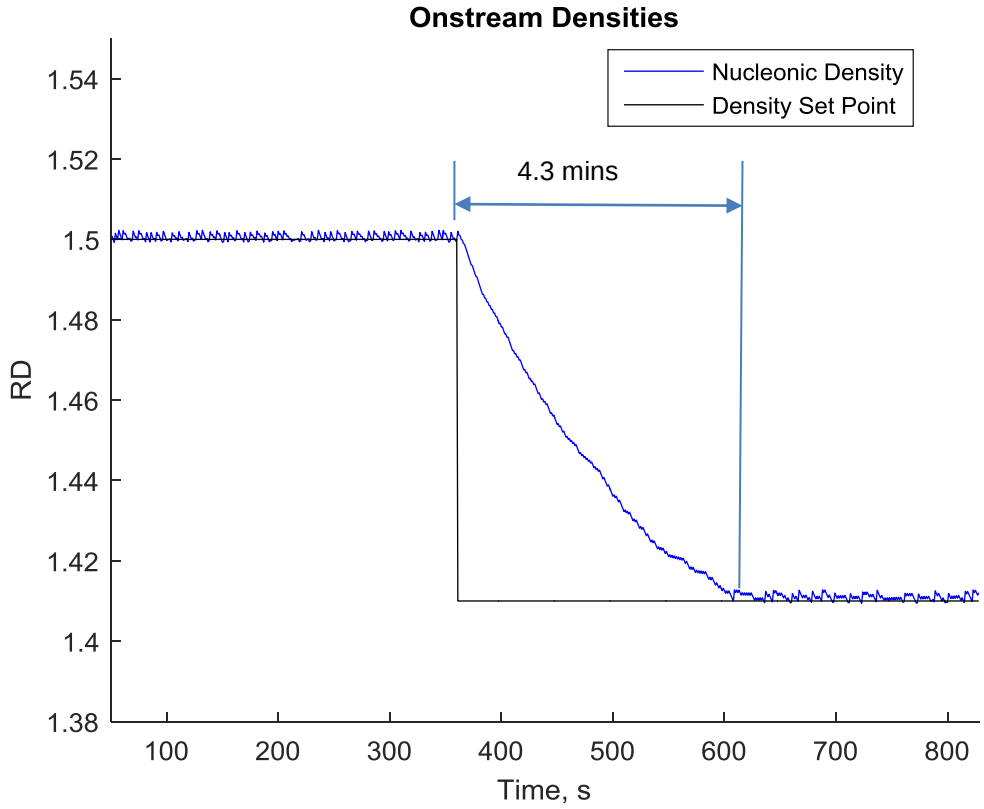

Figure 4.19b Dynamic model was adjusted for a different density drop in the plant. Here, the response of the controller is faster, partly due to the higher operating density range.

Predictions of circuit behaviour - Comparison of DMC Pressure

In addition to the density parameter, the model also considered the DMC pressure. This is usually in the form of a gauge located in the feed line to the DMC, and often within one metre of the DMC unit. The figures 4.20 to 4.22 below show the plant results compared with the dynamic model result for pressure. On the 25th March the plant feed was turned off on two occasions, the latter occasion being for a prolonged period of time. The causes of the feed off periods in this case were unrelated to the dense medium circuit. One of the conveyors had to be shut down due to a tracking issue which took some time to rectify. As a result of the lengthy outage, density (Fig 3.8) and non-magnetics concentration (Fig 3.9) initially dropped considerably. Upon re-starting from the feed off condition, it took time for the density to build up and for non-magnetics to re-establish in the system. Had the control room operator reduced the amount of water flowing off the desliming screen into the wing tank, the density could have been maintained at a higher level, thereby reducing the amount of time for density to recover. Similarly, the bleed could have been closed to reduce loss of non-magnetics while the plant feed was offline. Note the pressure response to the short plant feed outage (t = 20minutes, Fig 4.20) was considerably more rapid than the response for the longer feed outage (t = 180 minutes, Fig 4.20).

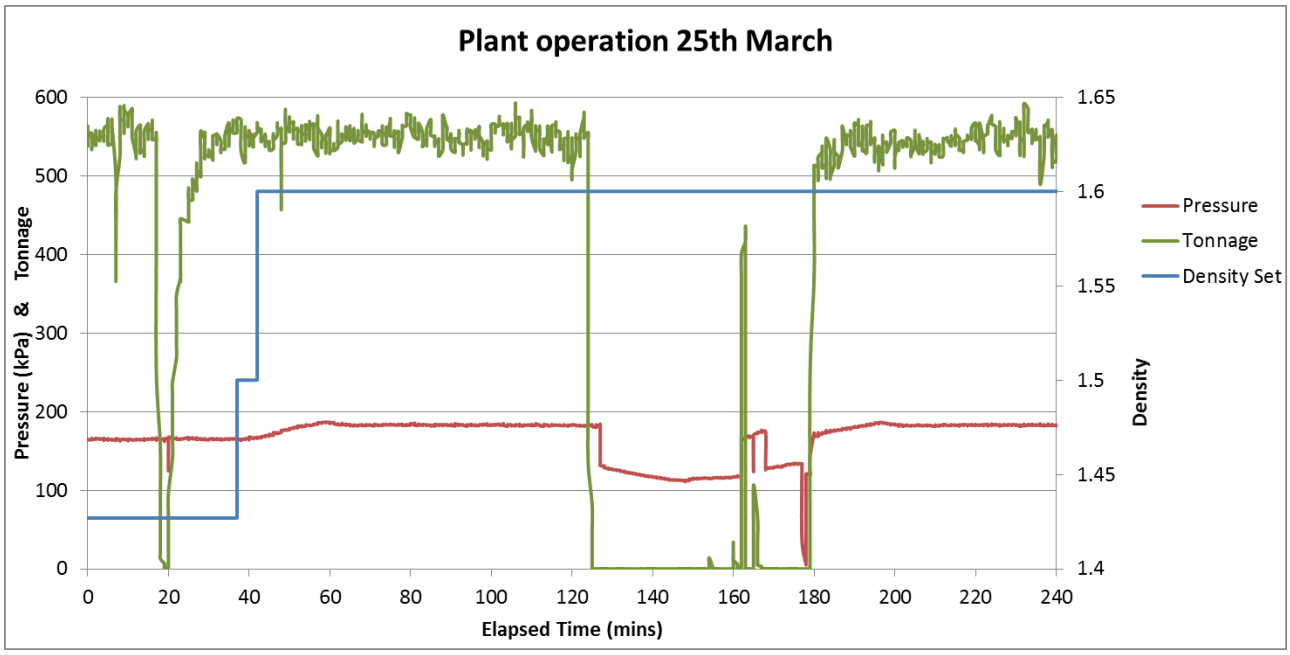

Figure 4.20: Typical pressure response (red) during plant events. Two feed off periods occurred during this particular test work. (25/3/2014) The causes of the feed off periods in this case were unrelated to the dense medium circuit. One of the conveyors had to be shut down due to a tracking issue which took some time to rectify.

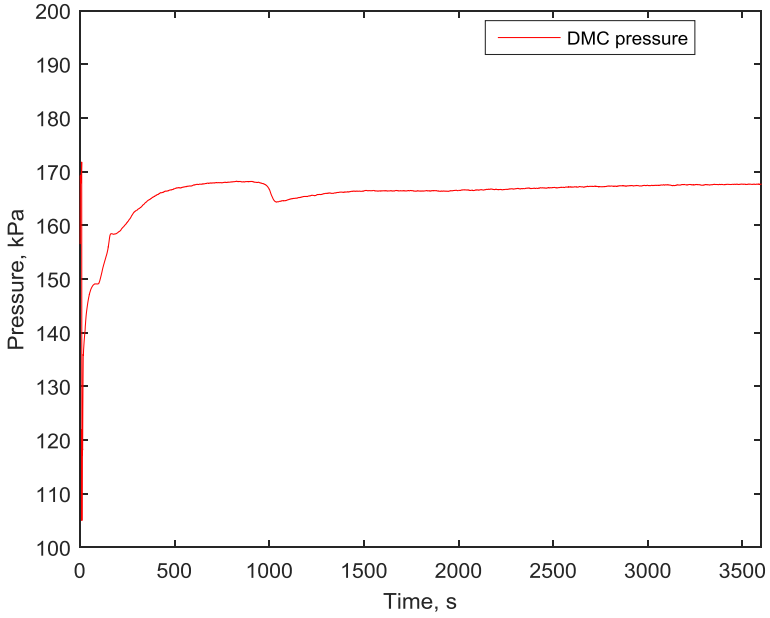

Figure 4.21: Pressure curve from the dynamic model. The curve is similar to the plant start up after the feed off events in the previous graph (at 180 mins Fig 4.20).

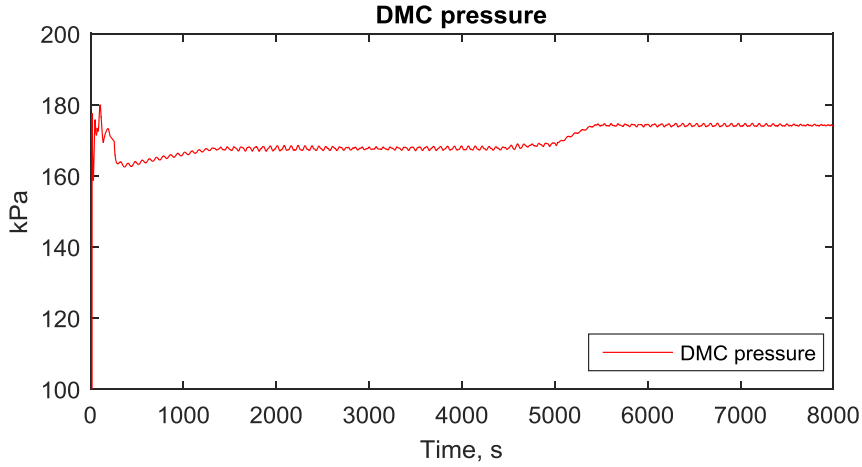

Figure 4.22: Another example of DMC pressure modelled from plant start-up. In this case, the time scale is longer. Note: pressure change at 5000s (83mins) was due to a density set point change upward in the model.

Predictions of circuit behaviour - Comparison of Non-magnetics

The level of non-magnetics in the correct medium was expected to change over time, both with removal of non-magnetics by bleeding out of the correct medium into the dilute, and also through breakdown of clays in the raw coal feed. This was simulated using a slime factor (essentially an allowance for breakage) in the dynamic model. Plant data collected and analysed for percent non-magnetics aligns with the dynamic model responses. Figure

4.23 below shows a comparison of % non-magnetic material in the correct medium after a plant start up over time (4.23a) with the plant model dynamic response (4.23b). (Firth et.al. 2014).

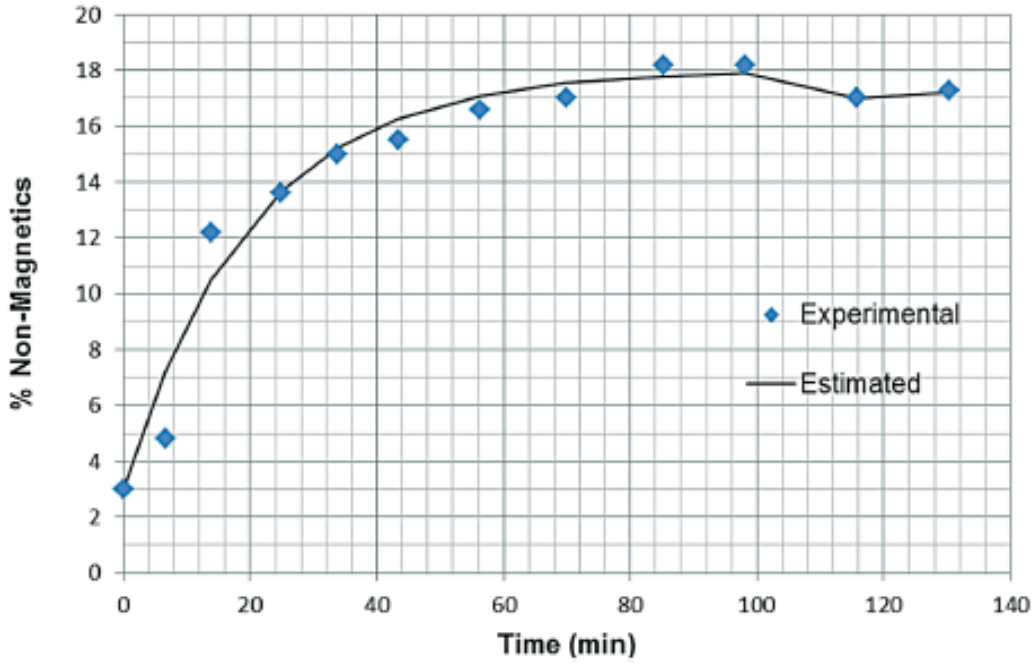

Figure 4.23a: Build-up of % non-magnetics from plant start up condition (Firth et.al 2014). (Timescale conversions: 20 mins = 1200 seconds, 4500s = 75minutes)

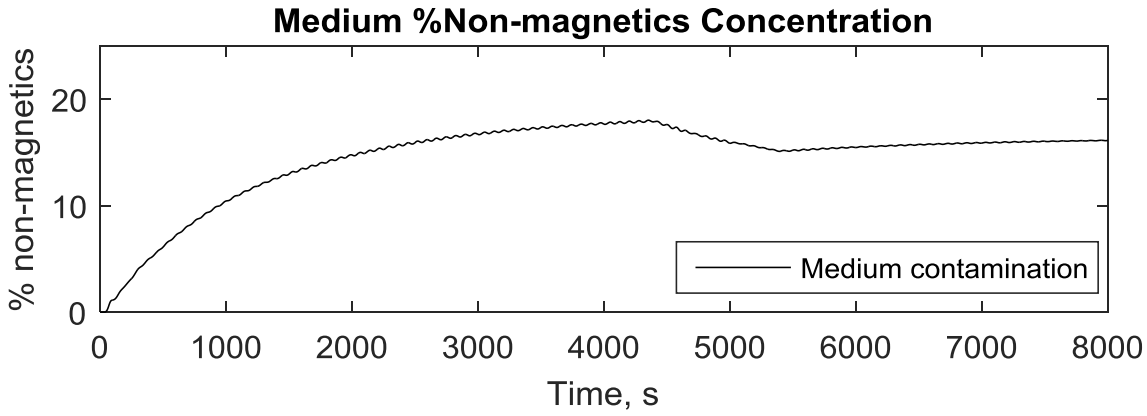

Figure 4.23b: Build-up of non-magnetics in the dynamic model from start-up. (Density change at 5000s, bleed opened at 4400s)

While the dynamic model response is slightly faster, this can vary with the amount of bleed and the relative amounts of non-magnetics at the start. The model reaction to opening the bleed is shown in Figure 4.24 a and b. If an operator opens the bleed, non-magnetics can be lost as rapidly as it is generated through breakage, or, as was demonstrated in the plant experiments, non-magnetics

could be lost at a faster rate than it was generated. Figure 4.24c shows the effect on the dynamic model of also adding magnetite with the bleed open. (with the same conditions as in 4.24a and b.)

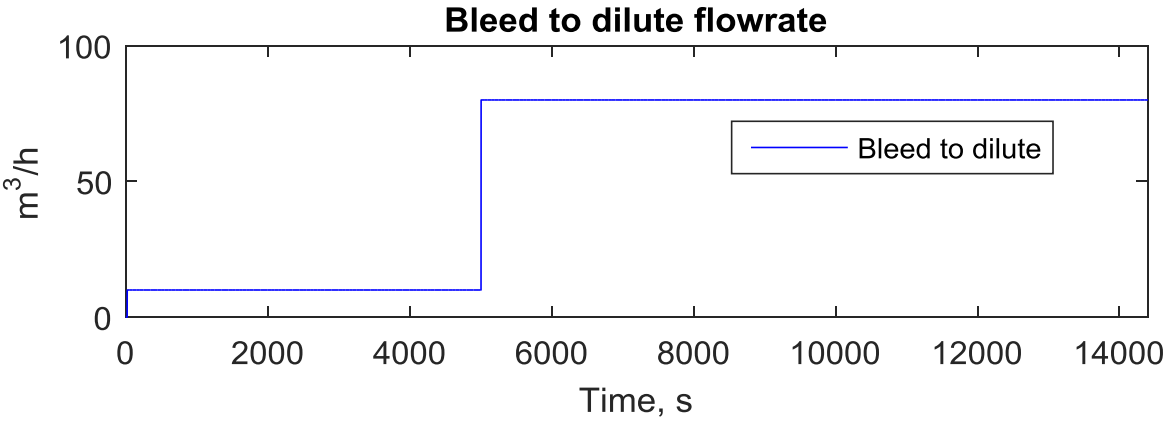

Figure 4.24a: Bleed opened fully at 5000 seconds. 4.24c is the response from the model.

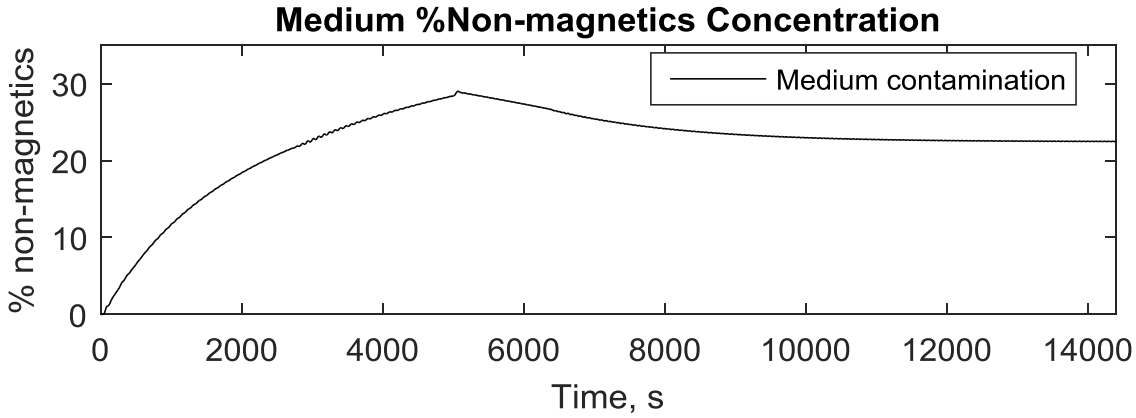

Figure 4.24b: Model response to bleed being opened fully at 5000 seconds. Note the drop off in the amount of non-magnetics in the circuit.

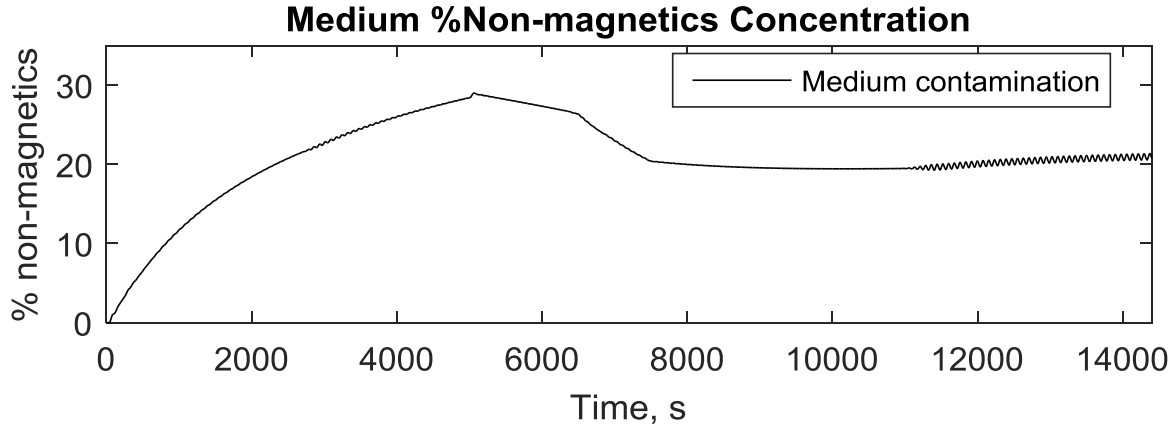

Figure 4.24c: Model response to bleed being opened fully at 5000 seconds with magnetite addition at 6500 seconds. Note the additional drop off in the amount of non-magnetics in the circuit once magnetite is added. This is in line with expectations.

Predictions of circuit behaviour - Comparison of Plant Results

In order to compare typical plant operating parameters, the plant process flow drawings (PFD's) were analysed. It was noted that the plant typically operates at 500 to 550 tonnes per hour of raw coal feed unless there is a problem which requires the plant to operate at a lower rate, for example, a constrained thickener. Much of the experimental data collected was at the 550 tph operating rates, however, the PFDs indicated that the plant name-plate capacity was lower. Despite this difference in tonnage, it was felt that the PFDs gave a reasonable estimate of flowrate ratios through the plant for the purpose of designing the dynamic model.

The wing tank level and seal level can be seen in the first graph of Figure 4.25. It would normally be expected that the seal level would exceed the height of the wing (coal) side in the wing tank and this is demonstrated in the graph. It is also clear that the seal in the tank has reached its normal overflow condition (Figure 4.26).

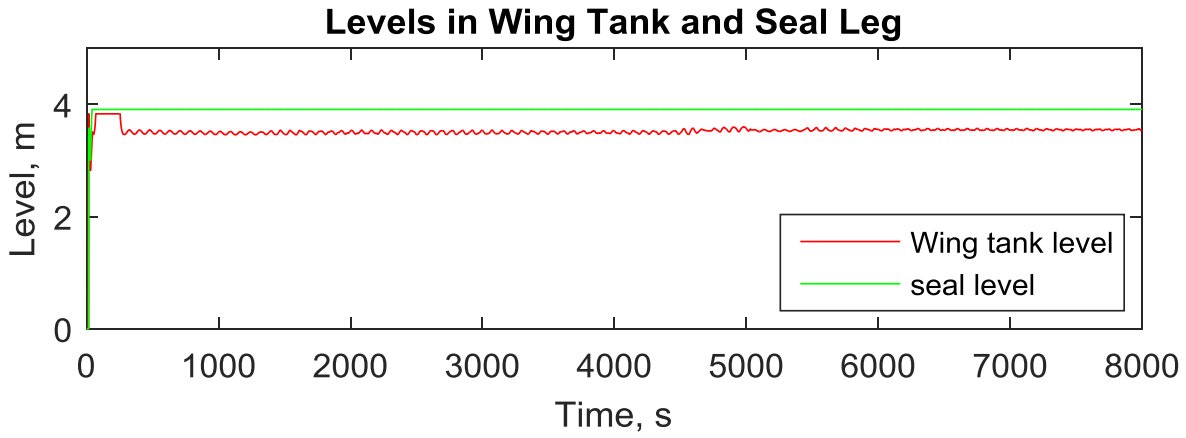

Figure 4.25: Wing Tank and seal leg levels. Seal level is in overflow condition.

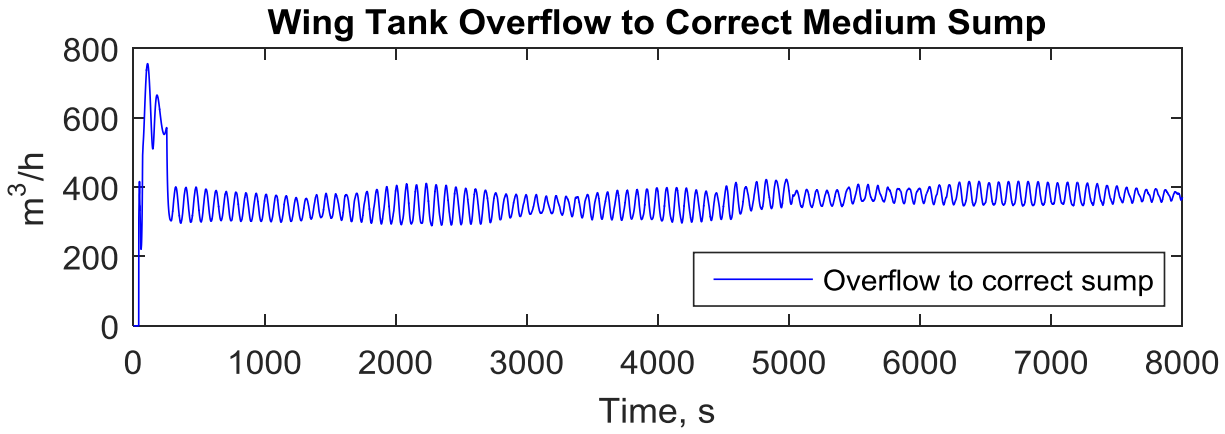

Figure 4.26: Wing tank overflow from the seal leg into the correct medium sump. After the initial flows at start-up, flow steadies.

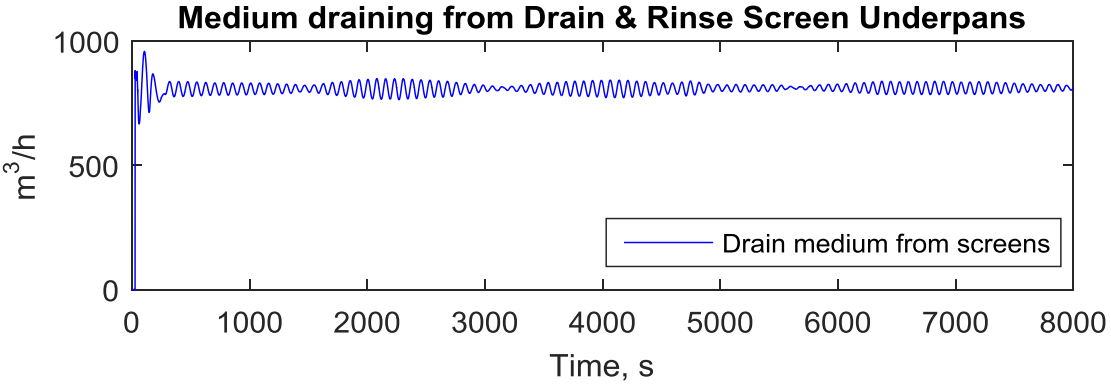

Figure 4.27: The drain and rinse underpans drain back to the correct medium sump. There is an initial delay until feed comes on. Flow then steadies.

The flows of drain-side medium returning from the drain and rinse screen to the seal leg of the wing tank are visible in figure 4.27 above. There is some initial instability, but flows quickly smooth out.

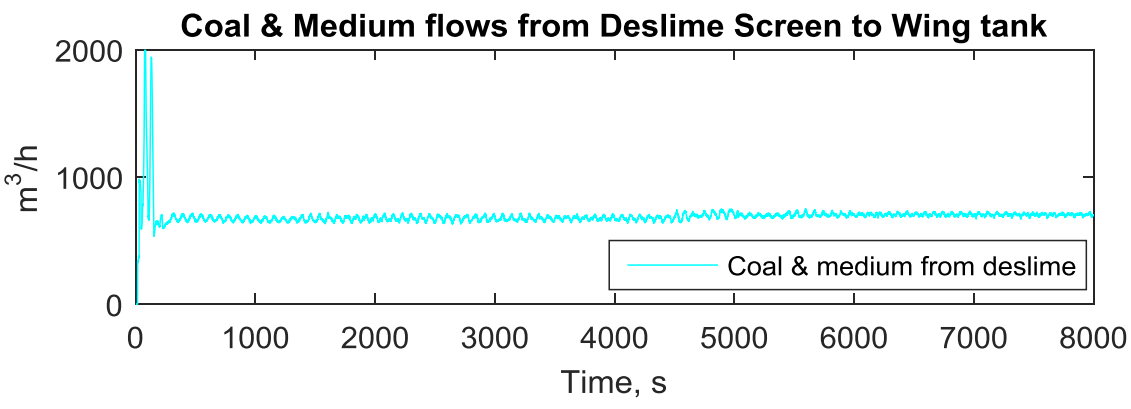

Figure 4.28: Coal and medium flows from the desliming screen to the wing tank. At startup there is an initial surge. It is thought that this surge relates to a slight mis-match in delay times in the model.

Figure 4.28 shows the coal and medium flows from the desliming screen to the wing tank. Although on normal plant startup there may be an initial surge, it is not expected to be of this magnitude. It is thought that fluctuations in the automatic water addition and a mis-match in delays are responsible for the apparent surge of medium on the graph. Delays were measured between the desliming screen and the drain and rinse screens and between the correct medium sump entry point and the drain and rinse screens, however some interpolation of the results was necessary to determine the delay times for smaller sections of the circuit. The accuracy of the delays could therefore be considered to be less precise for the sections around the wing tank. The coal and medium from the deslime graph in Fig 4.28 can be seen to reflect the wing tank overflow in figure 4.26. It can be seen that the majority of the surge carries over into the seal leg and overflows the wing tank. The seal leg essentially has a smoothing effect on the circuit and by the time the coal and medium arrives at the DMC, the flows have smoothed out considerably. Figure 4.29 and Figure 4.30.

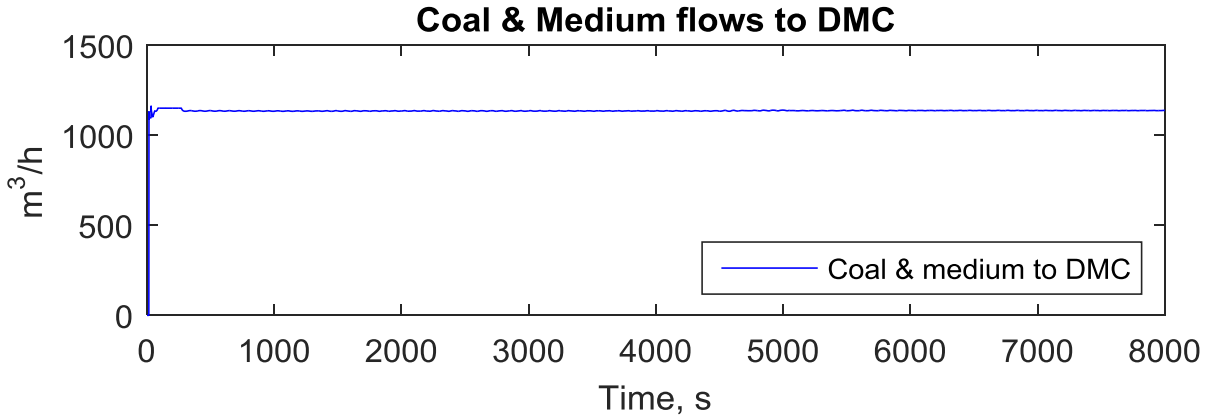

Figure 4.29: Coal and medium flows to the DMC

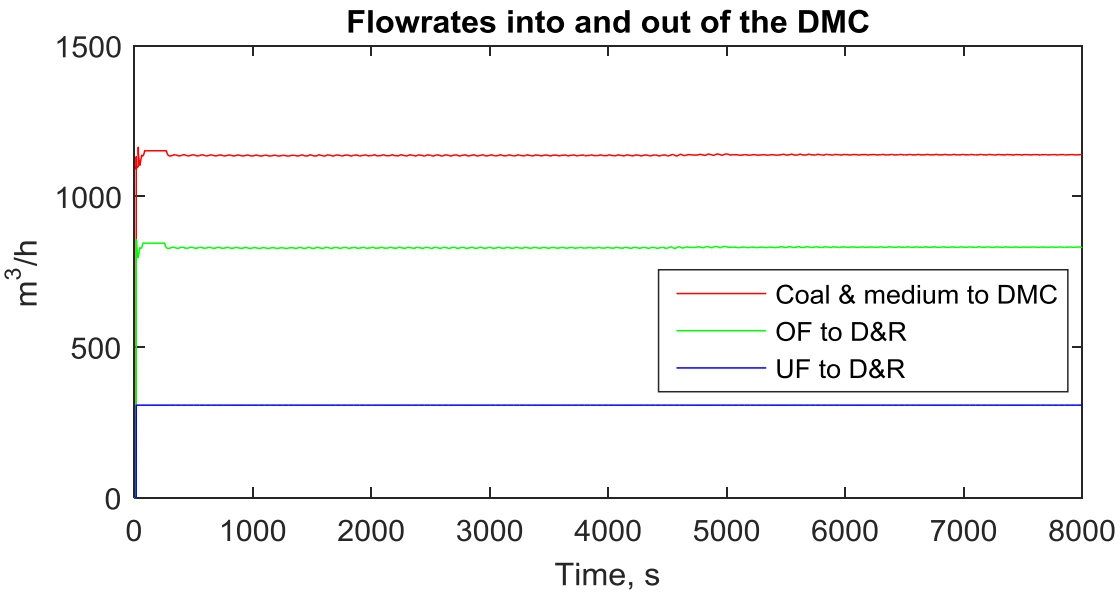

Figure 4.30 Flowrates into and out of the DMC

Flowrates into the DMC were smooth despite a surge in medium coming from the desliming screen into the wing tank. This graph also shows the DMC underflow and DMC overflow flowrates of medium and coal travelling to the drain and rinse screens. The surge is smoothed out using the seal leg overflow on the wing tank.

The level in the correct medium sump is also fairly steady (Figure 4.31) and the surge assists in filling the correct medium sump.

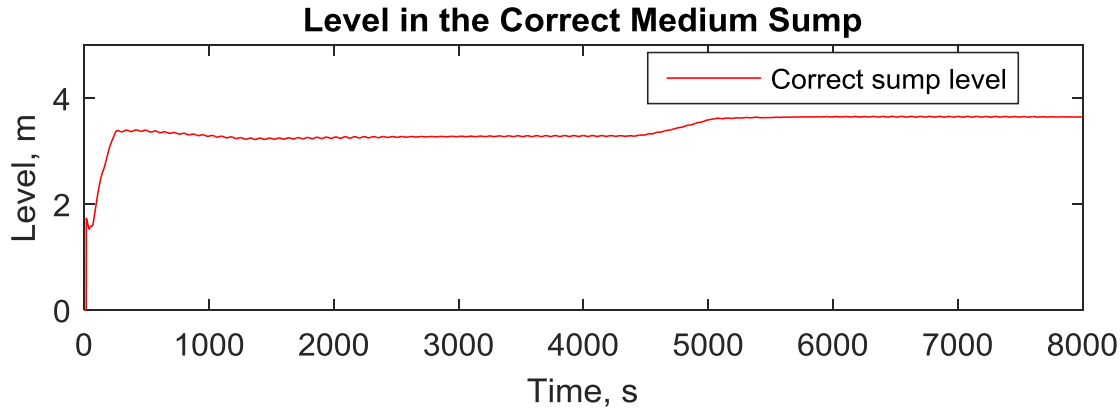

Figure 4.31 – The level in the correct medium sump helps to absorb the surge coming from the wing tank seal leg.

During start up, the medium to coal ratio is initially unstable but steadies to hover around 4:1 which is within the normal range for good operation. (Figure 4.32)

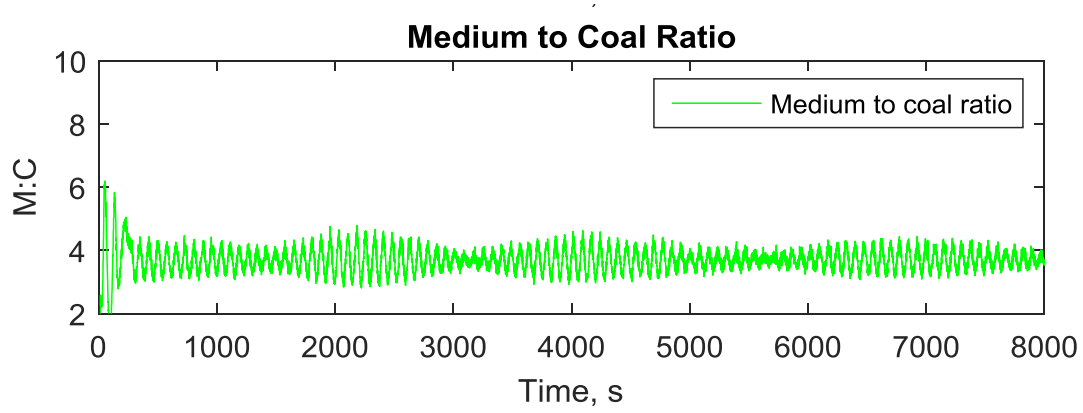

Figure 4.32: The medium to coal ratio is approximately 4:1 which is within expected range.

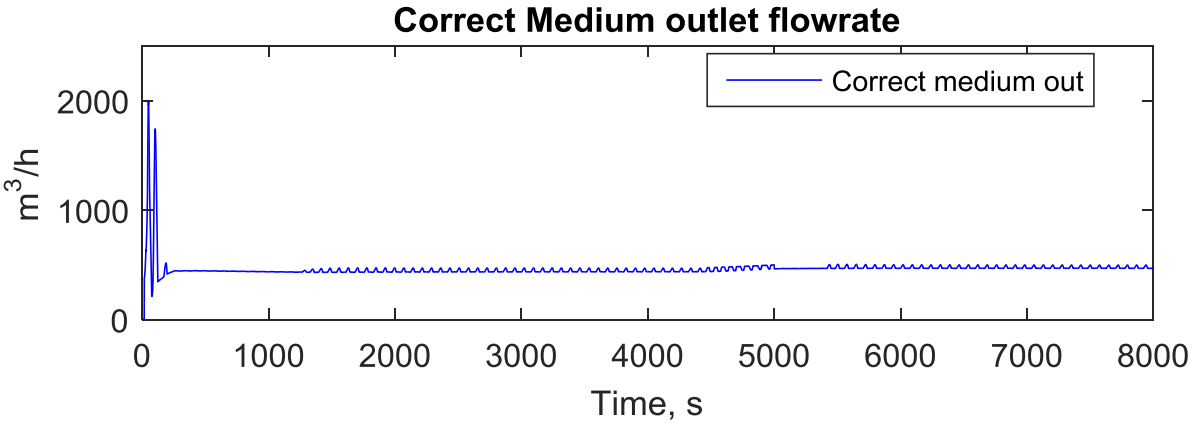

Figure 4.33: Plant flowrates for Correct medium and magnetite.

The initial surge in correct medium pumped from the correct medium sump (Fig 4.33) is related to the automatic water addition valve on the base of the sump.

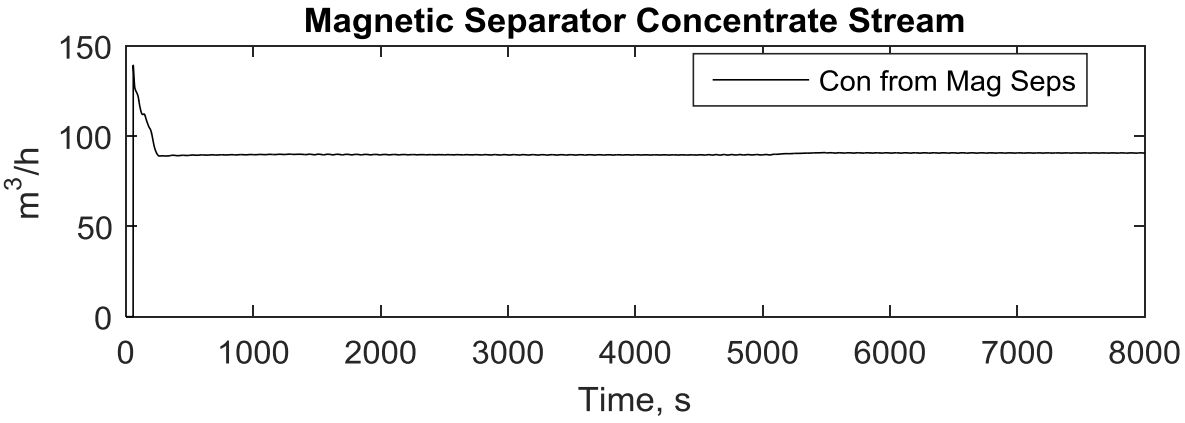

Figure 4.34: Flows from magnetic separator concentrate stream back to the correct medium sump.

The graphs in Figure 4.33 and 4.34 above can be seen to reflect the correct medium flowrate and additions of concentrated magnetite from the magnetic separators. During the test run, magnetite from the magnetite pit was also added to the circuit in Figure 4.35 below. This was used to stabilise upward density adjustments.

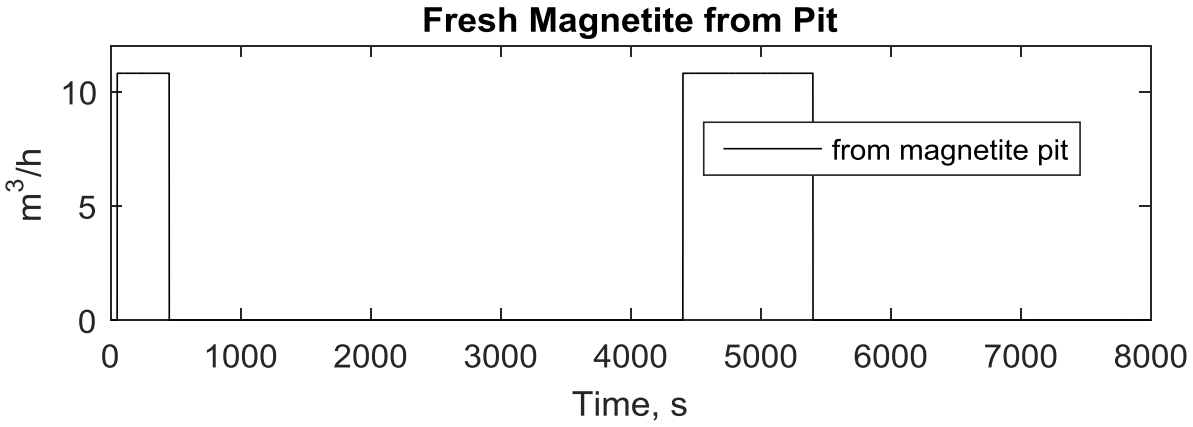

Figure 4.35: Fresh magnetite addition from the magnetite pit

This magnetite addition occurred at start up and just prior to the upward density change at 5000 seconds. This was found to assist with shortening the time of the density adjustment. In practice, this is done regularly by operators prior to upward density set point changes.

To assist with density control, a water addition control valve exists at the base of the correct medium sump and is controlled using a feedback control system based on the density set point. When the density is detected as too high, the water valve is opened to compensate by adding water to the system. The function of the auto water valve is shown in the figure 4.36 below. It is clear that in the initial start-up, this water valve causes the surge in the medium flows (Figure 4.33). Introduction of an increased delay or better tuning of the proportional integral controller may help to alleviate this initial plant surge.

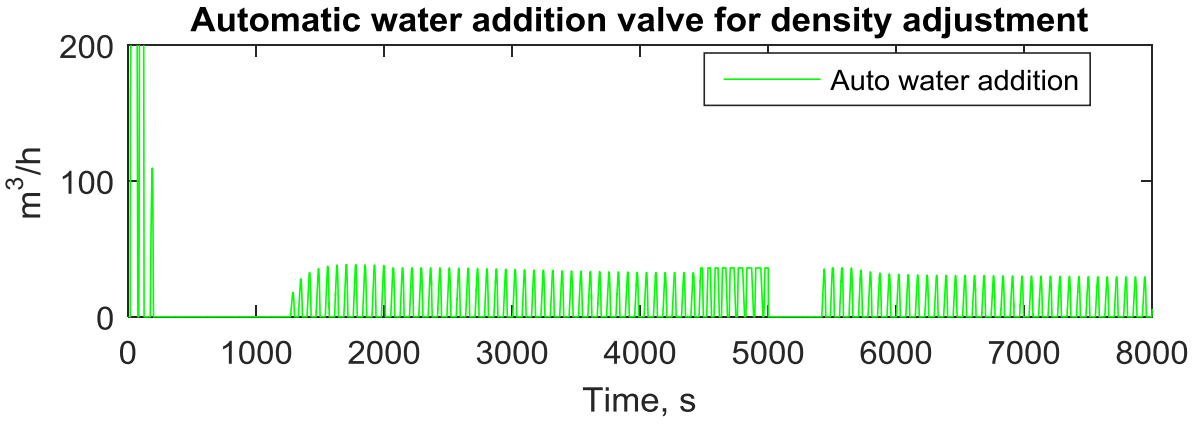

Figure 4.36 Automatic water addition valve for density adjustment

The automatic water valve on the base of the correct medium sump is controlled using a feedback loop to the nucleonic gauge. There is considerable instability initially which leads to a surge in medium at start-up.

Predictions of circuit behaviour - Dilute circuit operation

Dilute sump operation is demonstrated by the figures 4.37 to 4.41 below. Rinse water from the drain and rinse screens flows back to the dilute sump and flows are generally steady. The bleed to the dilute was set as a constant value after a short delay. The operators in the plant normally operate this valve to moderate volume.

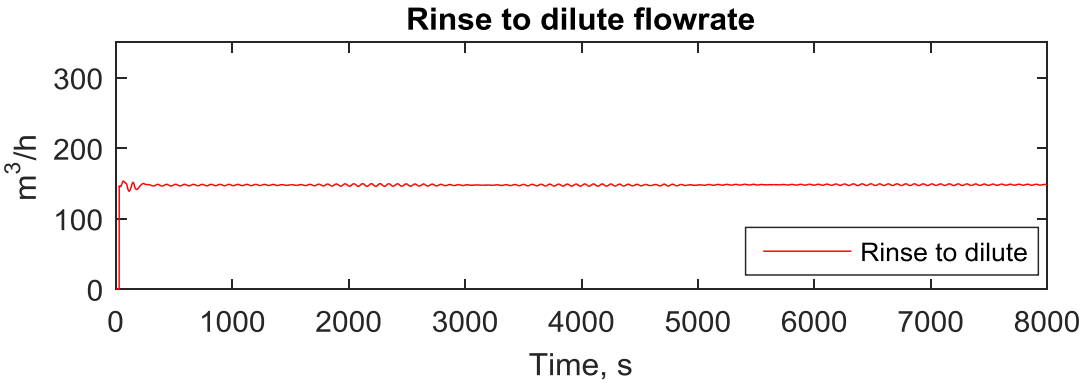

Figure 4.37 Flow from the rinse underpan of the drain and rinse screen to the dilute sump.

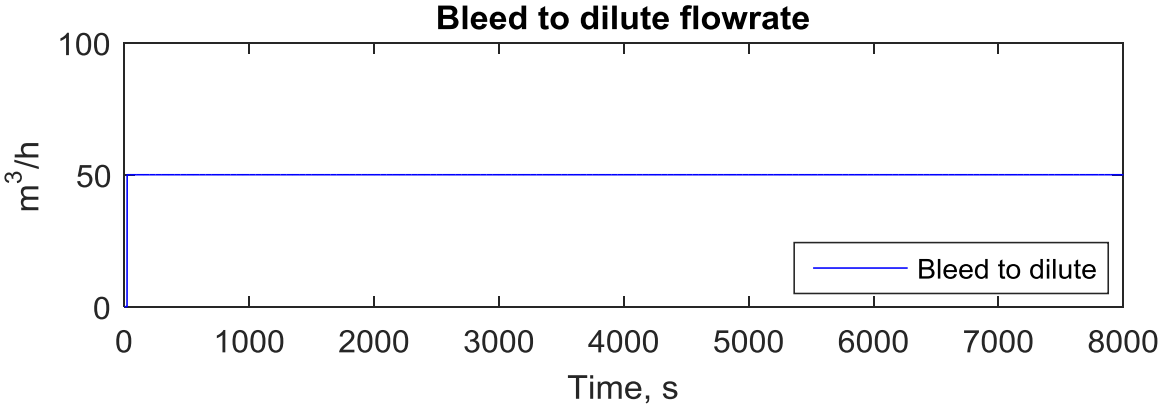

Figure 4.38 Bleed to the dilute has been set as a fixed value with a small delay.

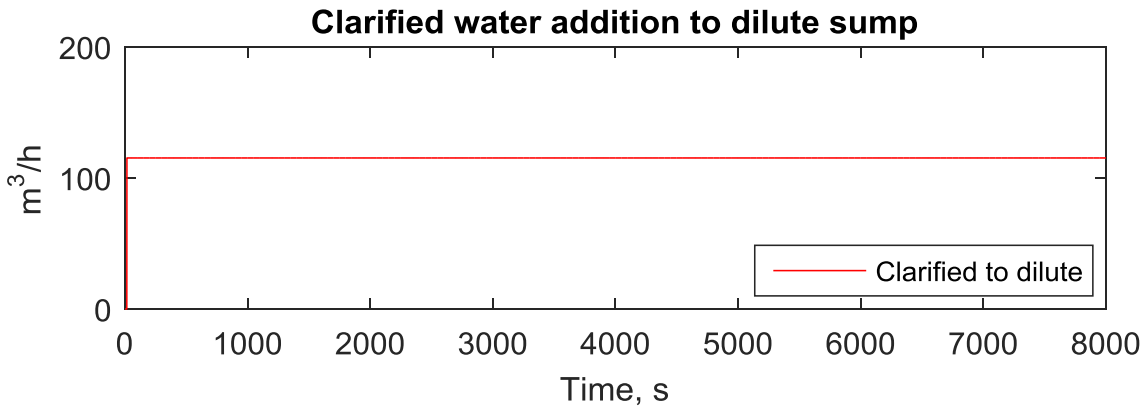

Figure 4.39 Flow rate of clarified water make-up into the dilute sump to maintain level. In practice some centrifuge effluent would also be present.

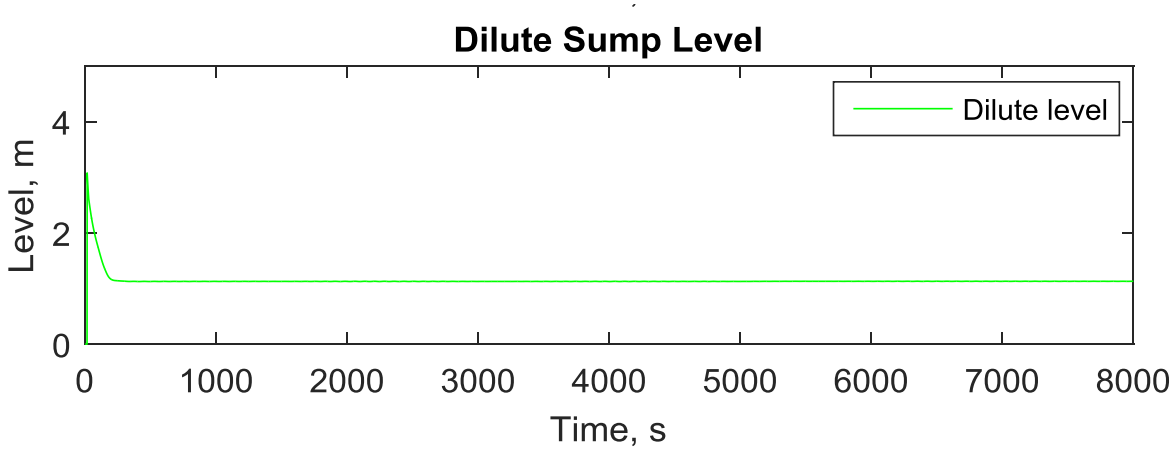

Figure 4.40: The level in the dilute sump from start – up condition.

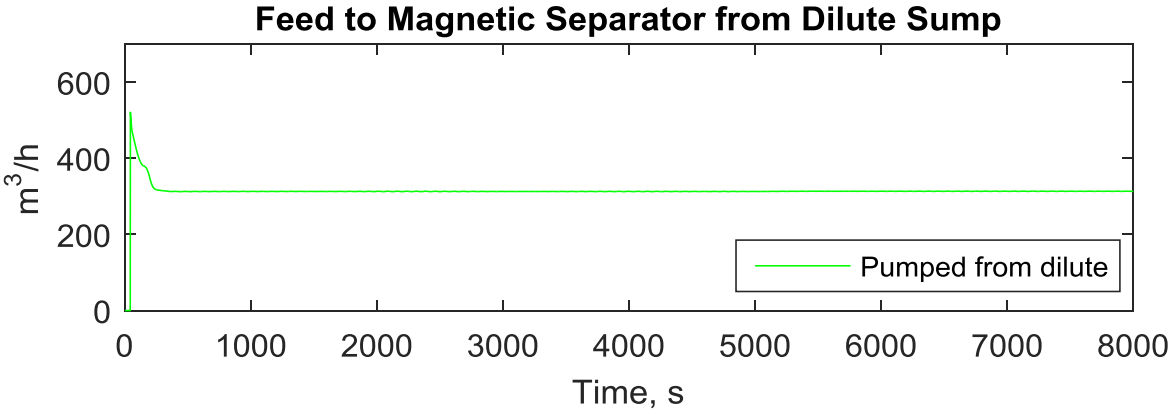

Figure 4.41: The magnetic separator is fed from the dilute sump. This pump is set to deliver based on the head in the dilute sump.

Predictions of circuit behaviour - Comparison of the Component Balance

The component balance for each unit operation was checked to ensure that all streams in and out and all components were consistent. This was done on a unit by unit basis as the model was developed. Any discrepancies in the balances were corrected as the model was built. The differential was a measure of circuit stability and can be seen in figure 4.42 below. It relates directly to the proportion of non-magnetics in the medium. Initially the differential is higher but as the level of non-magnetics climbs, the differential drops. Figure 4.43 and 4.44 have been added to indicate the corresponding differential changes with changing density set point. As is evident from the graphs below, the differential remained within in the stable region below 0.5, though was relatively high.

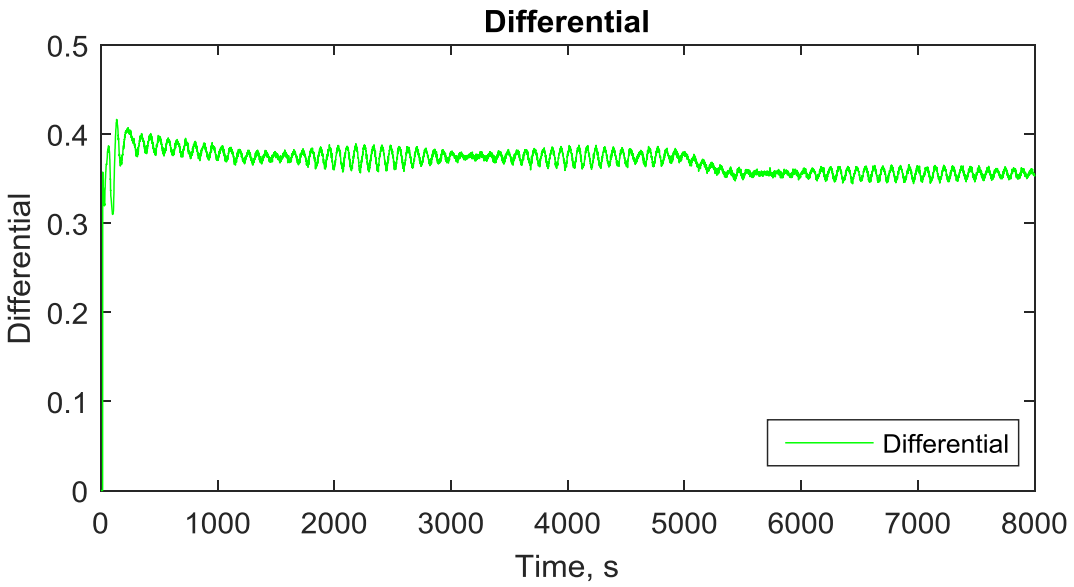

Figure 4.42 The differential is a measure of the difference between overflow and underflow density. The drop in differential can be seen also in the non-magnetics graph below and corresponds to the density change at 5000s.

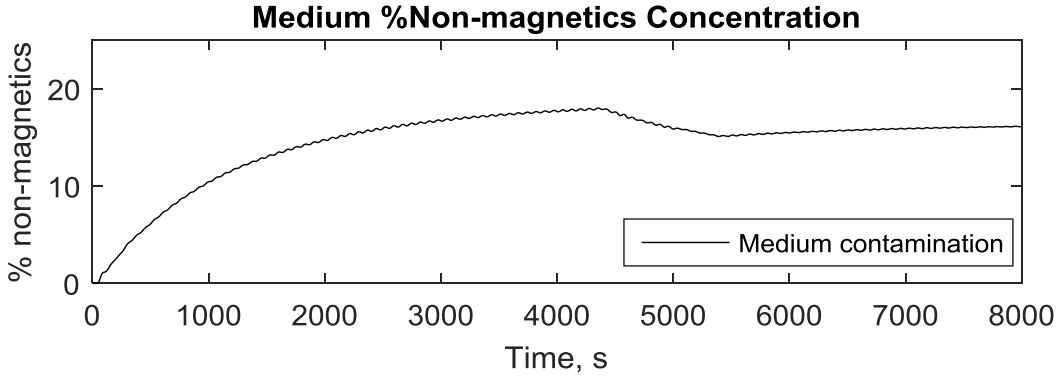

Figure 4.43 Corresponding non-magnetics concentration

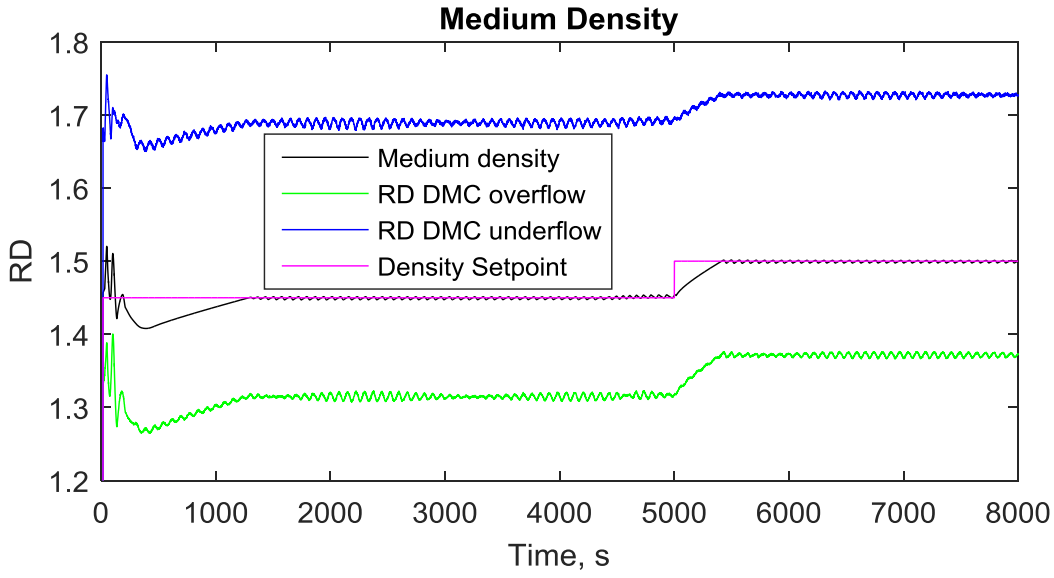

Figure 4.44: Corresponding change in density setpoint. Figs 4.42 and 4.43 show the change in non-magnetics and differential for comparison.

4.6 Model Validation Conclusions

The dynamic model developed has demonstrated the ability to realistically predict typical plant behaviour. Sump levels, DMC pump pressures, density changes and flowrates have been successfully replicated, as has the build-up of non-magnetics in the medium. Sump levels were shown to fluctuate and the medium to coal ratio controlled within a reasonable range. The verification of the dynamic model has shown that the model generally describes circuit behaviour and that the model will be able to be used for prediction of behaviour as well as for operator training. Residence times for particles from the RFID tracer work were used to predict delays in the model.

As the structure of the dynamic model is still in its rudimentary form, the opportunity exists to take this modelling work further. The addition of more user friendly features such as a graphical user interface would be helpful as would the opportunity to incorporate or substitute in different unit operations. Future refinements would benefit from using this model to analyse a range of different coal washabilities. As most coal producers are familiar with Excel but not with Matlab, the option of an excel spreadsheet seems reasonable as a future addition.

5 Conclusions, Applications and Further Work

5.1 Conclusions

For convenience, the conclusions have been drawn in the order of appearance in this thesis.

It was identified through an extensive literature review that:

- Past research into dynamic models has been limited by a lack of available plant data, computer memory and processing capability. Empirical models for DMC circuits such as those detailed in Crowden et al. (2013) have been significantly improved since early modelling work was done and a wider range of plant information is now able to be collected.
- Dynamic modelling of changes in the coal medium composition has not been sufficiently studied. Recent studies of changes in DMC medium composition (O'Brien, et al. 2013) have shown that the level of non-magnetics influences medium stability when targeting a low density cut-point and therefore has an influence on plant behaviour.
- Novel instruments in use at the New Acland CHPP provided information that was previously unavailable.
- Advancements in RFID density tracer technology created an opportunity for additional plant data such as residence times for individual density tracer particles to be collected using a novel method.

To address the research deficiencies identified, a programme of experimental work was devised and a dynamic model was developed. Plant observations and physical measurements were conducted as part of the experimental work phase of the research and were later used to verify the model. Findings as a result of this experimental work are detailed below:

Plant work involved the testing of a number of cases. The findings of each case are listed below:

- Case A: Good density change
    - After a density increase during stable operation, the level of non-magnetics was found to reduce with an increase in correct medium bled to the dilute circuit.
    - A feed off event which occurred during the trial demonstrated a rapid loss of non-magnetics from the medium, suggesting that the amount of non-magnetics in the coarse coal circuit is strongly affected by the feed.
    - Despite a low differential (stable medium) and a carefully orchestrated good density change, the medium took over an hour to recover back to the level of non-magnetics before the density change.
- Case B: Unstable Volume
    - When operating at a high level in the correct medium sump, and at a low density set point, the plant demonstrated difficulty in maintaining a sufficiently low density due to excess magnetite. This suggested that an alternative means of removing concentrated magnetite such as an over-dense or magnetite pit return line was needed as an alternative to returning magnetite to the correct medium sump.
    - When the correct medium sump and the dilute sump were in an overflow situation, the level of non-magnetics also became difficult to control. An initial drop in non-magnetics was noticed upon opening of the bleed to 100%, and a slight recovery of non-magnetics was noted when the bleed was closed down to 20%.
    - In a situation of unstable volume, it is difficult for the plant operator to achieve stable density operation. Volume control becomes a predominant issue at the expense of non-magnetics and density control.
- Case C: Stepwise density change
    - A step-wise density change resulted in a slower density response when compared with a single change in density.

- The level of non-magnetics dropped markedly when the feed was left off for an extended period of time. Density also dropped.
- The level of non-magnetics dropped when the bleed was opened, and began rising when the bleed was closed.
- After start up, the level of non-magnetics took over 60 minutes to return to prior levels despite operating on a high relative density.
- Time taken to reach density was slower when the amount of non-magnetics was low and the plant feed had been off for a considerable time. Yield losses were estimated at 17% over 11 minutes.

- Case D: Low density stability
  - Non-magnetics levels did not respond as well when sumps were in an overflow situation, however a drop in non-magnetics was noticeable when the bleed was opened.
  - Stability at low density was impacted by volume control due to excess magnetite.
  - Due to the fact that the plant had run at very high density just prior to the low density change, the medium was very stable on the test date and no surging events occurred.
- Case E: Desliming sprays response test
  - Closing the desliming sprays had the effect of rapidly increasing the level of non-magnetics in the medium.
  - The rate of build-up of non-magnetics was 2% over 2 minutes.
  - The use of desliming sprays to control non-magnetics was not feasible for this particular plant design due to the sensitivity of the water balance, however the concept may work for other designs.
  - Ultimately another means of adding non-magnetics to the medium such as thickener underflow may need to be investigated.
- Case F: Tracer Testing

- Recently developed RFID density tracers were used to measure the residence times of individual particles travelling through the DMC circuit. This novel method of measuring residence time had not been previously done.

- RFID residence time testing of coal particles travelling through the dense medium yielded valuable information on time delays within the circuit and assisted with model development.

- Times measured for tracers to travel through the DMC circuit were surprisingly short, with the times from the desliming screen through the DMC to the drain and rinse screens ranging from thirty-six seconds to just over two minutes. This route was representative of large coal particles travelling through the circuit. There was no significant difference based on the density of the coal particle for this pathway.

- The time for a coal particle to travel from the weightometer to the drain and rinse screens ranged between two minutes and three and a half minutes. This highlighted the rapid response of the circuit to changes in feed.

- The time taken for particles to travel through the medium differed for denser tracers of the same size when compared with low-density particles and with particles of near gravity. This was concluded to be the result of settling out of heavier particles from the medium, and floating of lighter particles out of the medium. Particles that were close to the cut point had a strong tendency to flow as part of the medium and not segregate out. This resulted in shorter time travel for near gravity particles. Particles of very high and very low density took up to 39 minutes to travel through the circuit.

- The prediction of cut point for different sized tracer particles showed an unusual cut point reversal between the 13mm RFID and 32mm standard tracers. This was observed on three separate occasions and it was concluded that the effect was real. The observations were also confirmed when a literature review of a thesis by Wood (1990) demonstrated similar effects. It was also determined that the original cause postulated by Wood was incorrect as no float sink chemicals were present in the case of the

tracer tests at New Acland, therefore eliminating chemical absorption as a possible cause.

The outcomes of the experimental work were used to develop and verify a dynamic model of the New Acland dense medium circuit. The model used existing empirical relationships that are accepted by industry as providing reasonable predictions of plant behaviour. Non-magnetics concentration in the medium was predicted using a breakage model and results were verified against past plant event data collected during the experimental work stage. The development of a dynamic model of a coal dense medium circuit was facilitated by the use of novel plant instrumentation at New Acland, advances in RFID technology, the collection of a broad range of data from plant events, and an in-depth investigation by CSIRO into medium behaviour. The findings from the modelling work are detailed below:

- The construction of a multi-component dynamic model of a coal DMC circuit was successfully achieved and a breakage model was incorporated into the dynamic model enabling monitoring of non-magnetics in the circuit.
- The dynamic model was able to achieve realistic predictions of plant behaviour. This was demonstrated using the examples of density, non-magnetics and DMC pressure. Sump levels were shown to fluctuate and the medium to coal ratio controlled within a reasonable range.
- The model was tested on a limited range of washability data, however could be expanded to other washability data sets in future.
- The verification of the dynamic model has shown that the model generally describes circuit behaviour and that the model will be able to be used for prediction of circuit behaviour as well as for operator training.

This research differs from past research efforts in that novel instrumentation and techniques have been used to collect experimental data, and the inclusion of medium components to predict the proportion of non-magnetics in the medium has not previously been attempted. Changes that result from fluctuations in magnetite additions, density adjustments and the bleed valve which diverts non-magnetics to the magnetic separators can also be incorporated into the dynamic model. Benefits derived from this project

include improvements to plant operation through better use of dense medium circuits and improved understanding of dense medium circuit fluctuations. Potential applications of this model and future research areas are identified in the following chapters.

5.2 Applications of the Dynamic Model

The research undertaken as part of this PhD was done with a goal of generating a net improvement for coal CHPPs. Improvements in yield and combustible recovery are always sought after and this has been kept in mind in the design of experiments. Fast density changes can reduce yield loss from misplaced coal, however as the time period of yield loss is small during a density change, losses may not be noticeable unless data on coarse product and reject mass flowrates is recovered in real time from instruments. Non-magnetics is unseen in the dense medium, and operators cannot easily control it without knowing what drives it. A plant operator can observe DMC surging event by visually monitoring the rejects screen loadings and product weightometers, but may not realise that the cause of the surging may relate to unstable medium or a lack of non-magnetics. If a surge is observed in real time, changes can be made to the level of non-magnetics to better stabilize the medium. Clearly, there are opportunities to recover coal that are being lost due to either a lack of instrumentation, or a lack of knowledge of what is happening in real time.

The dynamic model can help to identify opportunities to recover coal by simulating real plant events and allowing the operator or plant metallurgist to see what happens to various outputs in response. The applications of this model as a tool are for education purposes, but also for control system and plant improvement. Designers can use a dynamic model to try different design improvements or plant layouts. In Australia, we are fortunate that many dense medium plants across the country are fairly similar in design. Some may have slightly different circulation routes of the medium, but essentially there are similarities that can lead to a more routine application of the research across the industry. The plant at New Acland was a single stage DMC and spirals circuit, with the absence of flotation. Some plants that process hard coking coals, such as those in the Bowen Basin, have multiple stages, and flotation. In future, it would be beneficial to apply the model to a more complex plant and include the finer circuits.

Dense medium circuits have evolved over the years from falling density systems with over-dense sumps and magnetite thickening circuits, to the present day rising density systems with faster response and considerably fewer items of larger capacity equipment. Certainly there has been a saving in terms of capital with these newer designs, but the metallurgical

cost of this change has not been entirely clear. The observations made at New Acland CHPP suggest that at very low operating density set points, the plant experienced difficulties in removing magnetite from the circuit. This led to an overflow situation in the correct medium and dilute circuits where excess water was added by the automatic water valve to compensate for the concentrated magnetite being added back into the correct medium by the magnetic separators. This was a case of a rising density system working against itself. The operators' normal solution to the problem was to plan in advance for a density drop by removing any build-up of excess magnetite from floor sumps and to lower sump levels in the hours prior to the downward density change. In the case observed, an extreme density change from 1.6 to 1.35 was noted. This change proved too much for the system to cope with, and the resulting overflowing of sumps to the CHPP floor demonstrated the relative merits of over-dense storage for returning concentrated magnetite. Trialling the return of over-dense magnetite to the magnetite pit or into an additional over-dense sump could be done using the dynamic model before any capital is spent on equipment.

Given that magnetic separators are now far more efficient leading to the virtual elimination of auxiliary magnetic separators from circuits, the amount of equipment required to support an overdense system in a modern rising density plant is likely to be far less than for a falling density plant. Magnetite thickeners have been largely eradicated in favour of cyclone thickeners, or direct feed of magnetic separator concentrate into the correct medium stream. Diverting the magnetic separator concentrate stream to the magnetite pit may be the simplest solution, allowing the operator to hold back some magnetite when orchestrating a density change downwards, or to quickly add concentrated magnetite to rapidly bring the density up. In some cases, the solution may lie in a splitter arrangement where plants can divert excess magnetite back into the magnetite pit when targeting a low density. The most economical method of trialling the change would be to assess performance using the dynamic model. If the dynamic model was able to demonstrate that the change would be of benefit, then plant design for either a pilot or full scale trial could commence.

A key benefit that should be seen from dynamically modelling an over-dense system would be the relative reduction in the time required to achieve the target density. It has been established from the experimental data, that a single density change rather than an incremental change reduces the time taken to reach a target density. Where a density

change up occurs, capacity to add extra concentrated magnetite via an over-dense system would suggest that the density response could be achieved faster, thereby losing minimal yield during the adjustment period.

A cheap interim solution to achieving rapid density change might include installation of an air-sparge in the base of the correct medium sump to assist with better mixing of the medium in the sump. This again could be tested using RFID tracers and modelling the change in delay times.

The control of non-magnetics during a density change was found to be achieved by turning off the de-sliming sprays. Before implementing an engineering change to add dense medium non-magnetics in metered amounts, the build-up of non-magnetics could be simulated in the dynamic model. Research work by CSIRO is currently underway to add non-magnetics back into a dense medium circuit and the outcomes of this work could feed into dynamic modelling.

The use of RFID tracers to measure partition performance of the coal was a great advancement on existing tracer technology. Whereas a small army of seven or more volunteers were required to run a standard tracer test, the RFID tracers were able to be achieved using one to two experienced people. Recent work at other sites has led to development of permanent antennae designs which enable the plant metallurgist to run regular checks on their coal types. This is a remarkable change from the industry status quo. Novel application of the RFID tracers for residence time measurement could also be applied to a much broader context. The RFID technology could be used to track coal quality by following batches from specific strip, block and seam locations in the mine deposit through to the port. This would enable ports to keep track of coal types and their origins by means of mounting antennas over conveyors. Similar uses could be applied to the rail lines where batches or individual rail wagons could be tracked and then modelled in a dynamic model.

Dynamic modelling and RFID technology could be further used to link with geological modelling to provide the CHPP with instant feed washability information. Identification of bottlenecks and lead times in the supply chain could be accurately determined using RFID technology to assist with observations.

5.3 Recommendations for Further Work

The development of a dynamic model of a dense medium cyclone circuit has led to many opportunities for further work. This research modelled a single DMC circuit for a thermal coal operation. Scope exists to expand the modelling work into other plants with secondary DMC's and also plants that operate within other density ranges. The dynamic model could be refined with the inclusion of other unit operations and a graphical user interface. Further testing at other sites would assist in tuning the model.

Other enhancements could include the addition of an over-dense system and use of the model integrate bore core washability data for a particular mine. Long term use of Matlab may be difficult due to its high cost to industry participants, and it may be better to adapt the model into other software options such as a macro operated Microsoft Excel product, or a C++ program in future.

The level of non-magnetics measured during plant experiments as part of this and other ACARP projects suggests that it would be very useful to have an online non-magnetics gauge in place. Similarly, the under-pan density gauges have proven sufficiently robust to be installed in other plants and to be used for measurement of differential and therefore medium stability. The installation of a computer console in the plant control room which reads tags from the plant instruments could allow the operator to look at online washability using the dynamic model and to identify early warnings when the dense medium cyclone is becoming unstable.

The Walloon coal measures are well known for their problematic clay types (Crisafulli, 1985) and more detailed studies characterising clay types in the medium would yield useful knowledge on rheology which could be used in the model. Scope exists to further experiment with non-magnetics and their use as a stability modifier by comparison with using a finer grade of magnetite. This change could have significant operational cost savings.

RFID tracer experiments undertaken as part of this PhD identified a discrepancy in cut points close to the top-size of the DMC. It was found that this effect was repeated in a

number of cases. Further investigation and interrogation of the Pivot Phenomenon developed in earlier work by I.A.Scott (1988) on the relationship between particle size and cut-point, particularly when close to the designed top-size of the larger DMCs would be worthwhile, particularly since the diameters of current DMC's could be up to fifteen times the DMC diameters used in Scott's experimental work.

Dynamic modelling coupled with RFID technology also has significant potential for use in the coal chain logistics and mine planning. It could be used for tracking batches from the pit or tracking rail wagons.

6 References

Addison, C.B. (2010) Development of a Multi-Stream Monitoring and Control System for Dense Medium Cyclones. Masters Thesis, Feb 3, 2010, Virginia Polytechnic Institute and State University, Blacksburg, Virginia,

Askew, H. Dynamic Simulation and Automatic Control of Dense Medium Circuits. H.Askew. Thesis (1983) The University of Queensland

Cavanough, G.L., Holtham,P.N., and Powell, T.M. (2008) *Medium Density Measurement without the need for a Gamma Ray Source*. Australian Coal Preparation Society, Conference 2008.

Clarkson, C., Edward, D., Davidson, J., Lahey, A., (2002) *Analysis of Large Diameter Cyclone Plant Performance*, 9th Australian Coal Preparation Conference, Yeppoon, Oct 2002

Clarkson, C., and Holtham, P. (1988) *Efficiency of Large Diameter Dense Medium Cyclones,* Australian Coal Review, April 1988.

Clarkson, C.J. and Wood, C.J., (1991) *A model of dense medium cyclone performance.* In Proc. 5th Australian Coal Preparation Conf., Ed. P.J Lean, 1991, pp. 65-79

Collins,B., Turnbull, T., Wright,R., and Ngan,W., Separation Efficiency in Dense Medium Cyclones, Trans. Inst. Min. Met. Sec. C, 92, C38-C51 (1983) - Secondary citation from (He and Laskowski 1993)

Crisafulli,P., Le Page, A., Stockton, N., *The Effects of Clay Contamination on the Handling and Preparation of Walloon Coals*, 1985, Third Australian Coal Preparation Conference, Wollongong, NSW.

Crowden, H. 2011. Private correspondence

Crowden,H. et. al. (2013) ACARP Report C19047 Dense Medium Cyclone Handbook, Authors, Crowden, H., Atkinson, B., Clarkson, C., Firth, B., O'Brien, M., Wiseman, D., Wood, C., pp ii, 98, p171

Cresswell, M. (2005) DMS Powders 9th Technical Dense Medium Symposium, "A selected review of DMS Application and Engineering Design Practice", Bateman Minerals Ltd.)

Davidson, J. (2000) *Large Heavy Medium Cyclones The Theiss Experience – When should they be used?* Thiess internal correspondence.

Davis.J.J (1981) A study of magnetic recovery using wet drum magnetic separators at West Cliff washery, B.Sc.(Hons) Thesis, The University of Queensland

Davis,J. and Lyman,G., (1983) *Magnetite recovery using a Wet Drum Separator*, Proc. AusIMM, V287, pp51-60

Davis, J.J., (1987) A Study of Coal Washing Dense Medium Cyclones PhD thesis, The University of Queensland

Davis,J.J., Napier-Munn, T.J., *The Influence of medium Viscosity on the Performance of Dense Medium Cyclones in Coal Preparation,* Proc. 3rd International Conference on Hydrocyclones, Oxford, England, 1987

de Korte, G.J., and Engelbrecht, J. (2007) *Dense Medium Cyclones* in Designing the Coal Preparation Plant of the Future, Edited by Arnold, B.J., Klima, M.S. and Bethell, P.J., Society for Mining , Metallurgy and Exploration, Inc. (SME), Colorado, USA.,(pp 62,64,69,)

Dunglison, M.E and Napier-Munn, T.J "A New General Model of the Dense Medium Cyclone" The Australian Coal Preparation Society Queensland Branch Symposium, Emerald (1999), Julius Kruttschnitt Mineral Research Centre, The University of Queensland.

Dunglison, M.E. (1999) A General Model of the Dense Medium Cyclone, PhD Thesis, Julius Kruttschnitt Mineral Research Centre, The University of Queensland.

Engelbrecht, J.A. (1990) The effect of changes in cyclone design variables on dense medium separation, Proc. Samancor Dense Medium Conference, Cairns, 1990.

Engelbrecht and Bosman (1994) *Design Criteria for an Improved Large Diameter Dense Medium Cyclone*, Fifth Samancor Symposium on Dense Medium Separation, 1st - 2nd September, 1994, Bongani Sun Lodge, Eastern Transvaal, Sth Africa.

Firth, B., Holtham,P., O'Brien,M., Hu,S., Dixon, R., Burger, A., Sheridan, G., Joint Evaluation of Monitoring Instruments for Dense medium Cyclones – ACARP Project C17037, November, 2010.

Firth, B., O'Brien,M., McNally, C., *Influencing Factors for Dense Medium Cyclones*, ACARP Project C18040, Australian Coal Association Research Programme, February 2011.

Firth, B., Holtham,P., O'Brien, M., Hu,S., Dixon,R., Burger, A., Scott,N., *Linkage of Dynamic Changes in DMC Circuits to Plant Conditions*, ACARP Report C50152, Australian Coal Association Research Program, February 2013.

Firth,B., O'Brien,M., Holtham,P., Scott,N., Hu,S., Dixon,R., Burger,A., (2014) *Dynamic Impacts of Plant Feed and Operating practices on a Dense Medium Cyclone (DMC) Circuit*, 15th Australian Coal Preparation Conference Proceedings 14-18th Sept 2014, Gold Coast, Australia

He, Y.B., Laskowski, J.S. (1993) Effect of Dense Medium Properties on the Separation Performance of a Dense Medium Cyclone, Minerals Engineering, Vol7, no.2/3, PP 209-221, 1994.

Himmelblau, D.M. (1989) Basic Principles and Calculations in Chemical Engineering, Prentice-Hall International, USA. (pp 628)

Honaker, R.Q., Luttrell, G.H., and Bethell, P. (2007) *Status of Current Coal Preparation Research*, Designing the Coal Preparation Plant of the Future, 2007, Society for Mining , Metallurgy, and Exploration, Inc. (SME), Colorado, USA, pp 182

Hu,S and Firth,B (2010) *Prediction of Operating Performance of Dense Medium Cyclones from Medium Densities*, 13th Australian Coal Preparation Conference, Mackay, Qld, 12th to 17th September, 2010

Kempnich, R. (2000) "Coal Preparation – a World View, Proceedings, 17th International Coal Preparation Exhibition and Conference, Lexington, Kentucky, USA, Keynote Address.

Leach,K.R., and Meyers,A.D. Impact of Drain Rate on Density and Level Control in Dense Medium Cyclone Circuits, SME, 2010.

Lyman, G.J. Askew,H. Wood,C,J. Davis J.J. "Dynamic Modelling of Dense Medium Cyclone Washing Circuits", North West Queensland Branch Mill Operators' Conference, September 1982, Australian Institute of Mining and Metallurgy.

Masinja, J. H., Mathematical Models of Dense Medium Adhesion (1992) The University of Queensland, JKMRC PhD Thesis.

Mengelers, J. *The influence of Cyclone Diameter on Separating Performance and Economy*, (1982) IX International Coal Preparation Congress, New Delhi

Meyer, E.J. The Development of Dynamic Models for a Dense Medium Separation Circuit in Coal Beneficiation. (2010) University of Pretoria

Meyer, E.J. and Craig, I.K. Coal dense medium speartion dynamic and steady-state modelling for process control, (2014), Minerals Engineering, 65, 2014, 98-108.

Meyer, E.J. and Craig, I.K. (2010) The development of dynamic models for a dense medium separation circuit in coal beneficiation, Minerals Engineering, 23, 2010, pp791-805

Meyer, E.J. and Craig, I.K. (2011) Development of a Steady-State Partition Curve from a Dense Medium Cyclone Dynamic Model in Coal Beneficiation, 18th IFAC World Congress, Milano, Italy, Aug 28-Sept 2nd, 2011

Napier-Munn, T.J., Morrell,S., Morrison,R.D., Kojovic,T. (2005), Mineral Comminution Circuits – Their Operation and Optimisation, Julius Kruttschnitt Mineral Research Centre, Queensland, Australia

Napier-Munn, T.J. and Scott, I.A. (1990) The effect of Demagnetisation and ore contamination on the viscosity of the Medium in a Dense Medium Cyclone Plant, 1990, Minerals Engineering, Vol 3, No. 6, PP. 607-613, Great Britain.

Napier-Munn, T., Bosman, J., and Holtham, P., "Innovations in Dense Medium Separation Technology" SME Conference, 2013, Denver, Colorado – (not published as part of the proceedings)

Norrgran, D. *Wet Drum Magnetic Separators for Heavy Media Application*, Society for Mining, Metallurgy & Exploration, Inc. (SME) 2010.

O'Brien, M., Firth, B., *Quality of Dense Medium*, ACARP Project C15053, Australian Coal Association Research Program, February 2008.

O'Brien, M., Firth, B., McNally, C., Taylor, A., ACARP Project C20051 – The Effect of Dynamic Changes in Medium Quality in Coal Processing, February 2013.

O'Brien,M., and Taylor, A., (2013) - private correspondence regarding magnetite sizing.

O'Brien, M. (2016) Private correspondence regarding test results for non-magnetics.

Osborne, D.G., (1988) Coal Preparation Technology, Vol 1. pp199-206, Graham & Trotman Ltd., London

Phillips, D.I., *An evaluation of Heavy Media Control Circuits* Society for Mining, Metallurgy, and Exploration Inc. (SME), 2010.

Rayner, J.G., The Development of Process Models of the Wet Drum Magnetic Separator, 1999, Julius Kruttschnitt Mineral Research Centre, The University of Queensland, PhD Thesis, Brisbane.

Scott, I.A. (1988) *A Dense Medium Cyclone Model based on the Pivot Phenomenon*, The University of Queensland, PhD Thesis.

Scott,N., Holtham,P., Firth,B., O'Brien,M., (2013) *On-line Simulation & Dynamic Analysis of Dense Medium Cyclone Circuits.*, International Coal Preparation Congress, 2013, Istanbul, Turkey.

Scott,N., Wood,C., Holtham,P., O'Brien,M., Firth,B., (2015) *Integration of Plant Residence Time Measurement Into a Dynamic Model of a Coal Dense Medium Circuit*, Coal Prep 2015, April 27-29th2015, Lexington, Kentucky, USA.

Sheridan, G. Magnetic field based non-contact measurement of the concentration of magnetite in slurry, 2011, The University of Queensland, Masters Thesis

Stamicarbon (Anon), Guide to the calculation of H.M. Cyclone and W.O. Cyclone Plants, (December 1985), Stamicarbon bv, The Netherlands

Stamicarbon (Anon), The Heavy Medium Cyclone Washery for Minerals and Coal (1969), Stamicarbon nv, The Netherlands

Williamson, M.M., and Davis, J.J., (2002), *Cleaning Coarse and Small Coal Dense Medium Processes,* in Swanson, A.R., (Ed.), Australian Coal Preparation Monograph Series, Vol 111, Part 8, pp. 3-4,

Wiseman, D.M., McKee, D.J., Lyman, G.J. (1987) *Dynamic Simulation of Coal Preparation Circuits and Control Systems*, NERD&D Project No. 839, JKMRC, University of Qld, Sept 1987.

Wood, C.J (1990) *A Performance Model for Coal-Washing Dense Medium Cyclones*, PhD Thesis, Julius Kruttschnitt Mineral Research Centre, University of Queensland, p202,

Wood,C.J. (1990), Coal-Washing Dense Medium Cyclones. A JKMRC Handbook for Operators and Plant Designers. Julius Kruttschnitt Mineral Research Centre, Brisbane, Australia

Wood, C.J., Davis,J.J., and Lyman,G.J., 1989, *Towards a Medium Behaviour Based Performance Model for Coal-Washing Dense Medium Cyclones*, Coal Preparation, Vol 7, pp183-197, Gordon and Breach Science Publishers, United Kingdom.

Wood, C.J. (2012) Personal conversation

Wood, C.J., Wood, R.F., and Hicks,M.W. (2014) *Radio-Detectable Density Tracers: Experience to Date*, Fifteenth Australian Coal Preparation Conference, 14th – 18th September 2014, Gold Coast, Queensland, Australia.

Zhang, W. Development and Application of HM Suspension Density-Viscosity Detection Device., Society for Mining, Metallurgy & Exploration Inc. (SME), 2010.

7 Appendices

7.1 Appendix 1: Main Script from Matlab Dynamic Model

```
%SIMVEC DYNAMIC MODEL OF A DENSE MEDIUM CYCLONE CIRCUIT
MAIN SCRIPT

close all;
clear;
clc;

global DMC_delay
global Drain_delay
global Rinse_delay
global from_Dil_delay
global MSCon_delay
global Bleedsplit_delay
global Deslime_delay
global Bleed_delay
global to_Wing_delay

global WashData;

%-------------------------------------------------------------------
%
%                  INITIAL SET UP FOR FIRST ITERATION
%
%-------------------------------------------------------------------
        % DMC & MEDIUM DENSITY & CONTROL

head = 9.0;                    % DMC head m

RD = 1.45;                     % start up medium density
RD_old = RD;
RD_SP = RD;
```

```
RDX_old = 1.45;                    % this is a test density measurement

Kp = 6000;                      % RD control proportional gain 3000
Ki = 6000;                     % RD controller integral gain  5000
Isum = zeros(1,10);               % integral sum
auto_water_base = [0 0.001 0 0 0.001]; % always added water 3.6 m3/hr
auto_water = [0 0.001 0 0 0.001];    %

M2C = 4.0;                      % medium to coal ratio by volume

        %-------------------------------------
        % WING TANK

y=1;                          % fraction from DR screen to seal side
from_DR = [0 0 0 0 0];                          % m3/s
DMCfeedvol = [0 0 0 0 0];                        % m3/s
to_wing = [0 0 0 0 0];                         % m3/s
W_overflow = [0 0 0 0 0];                        % no overflow
tankvol_old = [1 5.3050 0.7670 0 7.072];             % 7 m3, 1.48 RD
sealvol_old = [0 0.8737 0.1263 0 1.0];              % 1 m3, 1.48 RD
Wtank_level = 2.704;             % coal side level at orifice level m

        %-------------------------------------
        % CORRECT MEDIUM SUMP

CMvol_old = [0 3.5 2.5 0 6.0];          % correct sump vol 6.65 m3
Mag_sep_CV = [0 0 0 0 0];                % overdense Mag Sep conc
from_Mpit = [0 0 0 0 0];                % magnetite addition
CM_overflow = [0 0 0 0 0];               % no overflow (to floor) m3/s
bleed_frac = 50;                       %50/35 % CM bleed, 0 - 60 m3/hr
from_CM =[0 0.1548 0.0236 0 0.1791];    %% medium from CM sump
%
        %-------------------------------------
        % DILUTE MEDIUM SUMP
```

```
DilVol_old = [0 6.5644 0.1167 0 6.5711];        % dil sump vol, 1.20 RD
Rinse_to_dil = [0 0 0 0 0];                     % dilute from mag seps m3/s
Floor_drain = [0 0 0 0 0];                      % no floor drain on startup
Clarif_water = [0 0.032 0 0 0.032];         %.032    % inc all other water in 79m3/hr
.022

        %-------------------------------------
        % DRAIN & RINSE SCREENS

drain_area_prod = 8.88;     % drain area of each product screen m2
drain_area_rej = 7.4;       % drain area reject screen m2
drain_ap = 1.4;             % screen aperture in mm
PRinse_water = 90;          % product rinse water m3/h (for 2 screens)115
RRinse_water = 40;          % reject rinse water m3/hr 55
Rinse_areaP = 6.0;          % area of product rinse screen
Rinse_areaR = 4.0;          % area of reject rinse screen
adh_loss = 0.0025;          % magnetite adhesion loss

        %-------------------------------------
        % TRANSPORT DELAYS

Bleedsplit_delay = zeros(5,60)';% from CM to bleed valve
to_Wing_delay = zeros(5,60)';   % from deslime screen to wing tank delay
DMC_delay = zeros(5,60)';       % feed to DMC
Drain_delay = zeros(5,60)';     % combined drain to wing tank
Rinse_delay = zeros(5,60)';     % combined rinse to dilute sump
from_Dil_delay = zeros(5,60)';  % from the dilute to the mag seps
MSCon_delay = zeros(5,60)';     % from mag sep con to correct sump
Deslime_delay = zeros(5,60)';   % from bleed valve to deslime
Bleed_delay =  zeros(5,60)';    % from bleed valve to dilute sump


Bleedsplit_delta = 15;          % dead time from correct to bleed valve
```

```
Deslime_delta = 7;            % dead time from bleed valve to deslime
Wing_delta = 6;               % dead time from deslime to wing tank
DMC_delta = 15;               % dead time feed to DMC
Drain_delta = 12;             % dead time combined drain to wing tank
Rinse_delta = 12;             % dead time combined rinse to dilute sump
from_Dil_delta = 28;          % dead time dilute sump to mag seps
MSCon_delta = 12;             % dead time from mag sep con to correct
Bleed_delta = 6;              % dead time from bleed valve to dilute sump

% Values measured from RFID Tracer Residence Time Tests:
%Delay            Description                          Delay time(s)
%-------------------------------------------------------------------
%Bleedsplit_delta   Dead time from correct sump to bleed valve      15
%Deslime_delta     Dead time from bleed valve to deslime          7
%Wing_delta        Dead time from deslime to wing tank            6
%DMC_delta         Dead time from feed to DMC                     15
%Drain_delta       Dead time from combined drain to wing tank     12
%Rinse_delta       Dead time from combined rinse to wing tank     12
%from_Dil_delta    Dead time from dilute sump to mag seps         28
%MSCon_delta       Dead time from mag sep cons to correct sump    12
%Bleed_delta       Dead time from bleed valve to dilute sump      6
%-------------------------------------------------------------------

%-----------------------------------
        % RAW COAL

        % row 1 is mean size (mm), row 2 is mass % retained

size_consist=[37, 18, 10, 6, 3, 1.4, .7, .46;
          23.4, 43.1, 18.0, 8.6, 3.3 2.0, 0.8, 0.8];
mean_feed =450;          %305 mean feed rate tph
feed_dev = 10;           % feed variation +/- 10 tph
mean_coal_density = 1.45;   % mean raw coal density t/m3
slimes_factor = 0.02;       % proportion of coarse that breaks to slimes
```

```
slimes_frac = 0.008;        % proportion of slimes in raw coal

WashData = csvread('NACWashData.csv');

        %-----------------------------------
        % DESLIME SCREEN

        % Whiten deslime screen model, pre-compute partition numbers
        % screen cut size 1.4 mm w/w

d50c_size = 1.4;
alpha = 5.0;
dd50c=size_consist(1,:)/d50c_size;
PN=(exp(alpha*dd50c)-1)./(exp(alpha*dd50c)+exp(alpha)-2);
vol_screen_water=0.01;          % m3/s wash water with O/S = 36 m3/hr

%-------------------------------------------------------------------
sim_time =8000;           % 14400seconds of simulation
%-------------------------------------------------------------------
%
%                       MAIN LOOP
%
%###################################################################
########

for i =  1:sim_time

   if i > 5000
     % bleed_frac = 45;
      RD_SP = 1.5;
   end

   if i > 50
     from_Mpit = [0 0.002 0.001 0 0.003];
```

```
end

if i > 450
from_Mpit = [0 0 0 0 0];
end

if i > 4400
   from_Mpit = [0 0.002 0.001 0 0.003];
end
if i > 5400
   from_Mpit = [0 0 0 0 0];
end


% get feed tonnes, screen, convert to tonnes/s & m3/s

feed = mean_feed + feed_dev*randn(1);
OStonnes=sum(feed*PN.*(size_consist(2,:)/100));        % tonnes/hr
coal_vol = OStonnes/mean_coal_density;                 % m3/hr
vol_coal_ps = coal_vol/3600;                           % m3/s
vol_slimes = vol_coal_ps * slimes_frac;

% assemble raw coal vector

total_vol = vol_coal_ps + vol_screen_water;      % add slimes
raw_coal = [vol_coal_ps vol_screen_water 0 vol_slimes total_vol];

% medium from correct sump up to bleed valve after dead time

to_Bleedvalve = BleedValve_delay(from_CM, Bleedsplit_delta);% dead time

if to_Bleedvalve(5) > 0
   B = (bleed_frac/3600) .* to_Bleedvalve(1:4) ./ to_Bleedvalve(5);
   Bleed= [B bleed_frac/3600];
```

```
    to_Deslime = to_Bleedvalve - Bleed;
else
    to_Deslime = [0 0 0 0 0];
    Bleed = [0 0 0 0 0];
end

% Measure density after bleed valve

[RD] = Nucleonic(to_Deslime, RD_old);
RD_old = RD;

% then up to deslime screen, with dead time

Medium = DeslimeStream_delay(to_Deslime, Deslime_delta);

% raw coal added to medium

to_wing = raw_coal + Medium;

% coal & medium to wing tank, with dead time

to_wing = Wing_delay(to_wing, Wing_delta);

%-------------------------------------------------------------------
%
%                    WING TANK & DMC
%
%-------------------------------------------------------------------

     % use the Wood DMC model to calculate DMC feed vol given current head

[Qf, ufsplit, Qu, Qo, ufRD, ofRD, d50c]= DMC(head, RD, M2C);

% given that Qf determine the total head from the pump curve
```

```
H_in = -0.0039 *  Qf + 24.2;          % pump curve fit, for water

% given these components of the head (tank level varies), calculate
% a new DMC head

static_head = 13.0;                % m from Metso data
friction_head = 1.2;               % m from Metso data
head = H_in - static_head - friction_head + Wtank_level;

DMCfeedvol(5) = Qf/3600;
DMCfeedvol(1:4) = (tankvol_old(1:4) ./ tankvol_old(5))...
                .* DMCfeedvol(5);
DMCFeed = DMCfeedvol;

[DMCfeedvol]= DMC_feed_delay (DMCFeed, DMC_delta);       % dead time

if DMCfeedvol(5) > 0;              % feed reached DMC yet?

   [Wtank_level,seal_level,W_overflow,tankvol_old,sealvol_old]=...
   wing_tankVec(to_wing,from_DR,DMCfeedvol,tankvol_old,sealvol_old,y);

   % check wing tank balance BW

   BW = to_wing + from_DR - W_overflow - DMCfeedvol;
   BW(BW<0.000001)=0;

   M2C = (Qf-coal_vol) / coal_vol;       % update M2C with known vols
   pressure = 1000 * head * 1.3 * RD /101.94;       % pressure in kPa

   % partition the raw coal

   [yield,cc_vol,cc_density] = clean_coal(d50c, 0.001); % est Ep 0.001
```

```
    product_vol = DMCfeedvol(1) * yield / 100;          % m3/s
    reject_vol = DMCfeedvol(1) * (1 - yield / 100);     % m3/s
    product_mass = product_vol * cc_density;            % t/s
    reject_mass = DMCfeedvol(1) * mean_coal_density - product_mass;
    reject_density = reject_mass / reject_vol;          % t/m3
    ufRD;                                   %DMC underflow RD
    ofRD;                                   %DMC overflow RD

%-------------------------------------------------------------------
%
%                   SLIMES BREAKDOWN
%
%-------------------------------------------------------------------

    slimes1 = size_consist(2,1:6) * slimes_factor;
    slimes2 = size_consist(2,1:6) - slimes1;
    newslimes = 100 - sum(slimes2);
    new_size_consist = [slimes2 , 0.2*newslimes, 0.8*newslimes];

%-------------------------------------------------------------------
%
%                   PRODUCT & REJECT DRAIN SCREENS
%
%-------------------------------------------------------------------

% 1. PRODUCT DRAIN SCREEN
% DMC overflow vector & total medium: water, mags, slimes

    Qo_comps(1) = product_vol;
    Qo_comps(2:4) = DMCfeedvol(2:4) .* (1 - ufsplit);
    Qo_comps(5) = sum(Qo_comps(1:4));
    Qo_med = sum(Qo_comps(2:4));        % medium is water, mags, slimes
    if Qo_med == 0                  % check for zero on startup
      Qo_med = 0.001;               % keep just positive
```

```
end

% product by size so we can screen it

product_by_sizeM = (product_mass .* new_size_consist/100); %  mass
product_by_sizeV = product_by_sizeM ./ cc_density;       % coal vol

[PDrain_percent, PRf, PN] = ...
    Drainpd2(Qo_med, drain_area_prod, drain_ap, 0.15, product_mass);

% partition coal, oversize to rinse, undersize to drain medium

PNPD = PRf + (1-PRf) .* (size_consist(1,:)./ drain_ap) .^ PN;
PNPD(PNPD > 1) = 1 ;                    % limit PN to 1
Pdrain_OS = product_by_sizeV .* PNPD;
Pdrain_US = product_by_sizeV - Pdrain_OS;

% drain the product medium

Pdrain(1) = sum(Pdrain_US);
Pdrain(2) = Qo_comps(2) * (PDrain_percent/100);
Pdrain(3) = Qo_comps(3) * (PDrain_percent/100);
Pdrain(4) = Pdrain_US(8) + Qo_comps(4)*(PDrain_percent/100);
Pdrain(5) = sum(Pdrain(1:4));

% leaving what does not drain to go to the product rinse screen

QoRinse(1) = sum(Pdrain_OS);
QoRinse(2) = Qo_comps(2) - Pdrain(2);
QoRinse(3) = Qo_comps(3) - Pdrain(3);
QoRinse(4) = Qo_comps(4) - Pdrain(4);
QoRinse(5) = sum(QoRinse(1:4));

%-----------------------------------------------------------------
```

```
% 2. REJECT DRAIN SCREEN
% DMC overflow vector & total medium: water, mags, slimes

Qu_comps = DMCfeedvol - Qo_comps;
Qu_med = Qu_comps(5);
if Qu_med == 0                    % check for zero on startup
    Qu_med = 0.001;                % keep just positive
end

% reject by size so we can screen it

reject_by_sizeM = (reject_mass .* new_size_consist/100); % mass
reject_by_sizeV = reject_by_sizeM ./ reject_density;

[RDrain_percent, RRf, RN] = ...
  Drainrej2(Qu_med, drain_area_rej, drain_ap, 0.15, reject_mass);

% partition reject on reject drain screen

PNRD = RRf + (1-RRf) .* (size_consist(1,:)./ drain_ap) .^ RN;
PNRD(PNRD > 1) = 1;                % limit PN to 1
Rdrain_OS = reject_by_sizeV .* PNRD;
Rdrain_US = reject_by_sizeV - Rdrain_OS;

% drain the reject medium

Rdrain(1) = sum(Rdrain_US);
Rdrain(2) = Qu_comps(2) * (RDrain_percent/100);
Rdrain(3) = Qu_comps(3) * (RDrain_percent/100);
Rdrain(4) = Rdrain_US(8) + Qu_comps(4) * (RDrain_percent/100);
Rdrain(5) = sum(Rdrain(1:4));

% leaving what does not drain to go to the reject rinse screen
```

```
    QuRinse(1) = sum(Rdrain_OS);
    QuRinse(2) = Qu_comps(2) - Rdrain(2);
    QuRinse(3) = Qu_comps(3) - Rdrain(3);
    QuRinse(4) = Qu_comps(4) - Rdrain(4);
    QuRinse(5) = sum(QuRinse(1:4));

%-----------------------------------------------------------------------

% asssemble combined drain medium vector & delay it

    Drain = Pdrain + Rdrain;

    from_DR = Comb_Drain_delay (Drain, Drain_delta);

%-----------------------------------------------------------------------

    % 3. PRODUCT RINSE

    Qo_medR = sum(QoRinse(2:4)) * 3600;                    % m3/hr

    [Prod_rinse_vol,PRinse_W_2dil, water_OS, NPR] = Rinsepd2(Qo_medR, ...
                PRinse_water, product_mass, Rinse_areaP);    % m3/hr

    % partition solids on product rinse screen

    PNPR = (size_consist(1,:) ./ drain_ap) .^ NPR;
    PNPR(PNPR > 1) = 1;
    PRinse_OS = Pdrain_OS .* PNPR;
    PRinse_US = Pdrain_OS - PRinse_OS;

    % drain the product rinse medium

    PRDilute(1) = sum(PRinse_US); %sum(PRinse_US(1:7));
```

```
PRDilute(2) = PRinse_W_2dil / 3600;
PRDilute(3) = QoRinse(3) * (1-adh_loss);        % 0.5% adhesion loss
PRDilute(4) = PRinse_US(8); %QoRinse(4);
PRDilute(5) = sum(PRDilute(1:4));

% final clean coal product off the screen

RProduct(1) = sum(PRinse_OS);
RProduct(2) = water_OS;
RProduct(3) = QoRinse(3) * adh_loss;       % there's the adhesion loss
RProduct(4) = 0;
RProduct(5) = sum(RProduct(1:4));

% BP is a check the coal volume balances in all size fractions
% from the cyclone across the drain then rinse
% BPC is a check the 4 components by volume balance

BP = product_by_sizeV-Pdrain_US-PRinse_OS-PRinse_US; % coal bal check
BP(BP<0.000001)=0;

BPC = Qo_comps-Pdrain-PRDilute-RProduct;
BPC(BPC<0.000001)=0;
%-------------------------------------------------------------------------

% 4. REJECT RINSE

Qu_medR = sum(QuRinse(2:4)) * 3600;                    % m3/hr

[Rej_rinse_vol, RRinse_W_2dil, water_US, NRR] = RRinse(Qu_medR, ...
            RRinse_water, reject_mass, Rinse_areaR);    % m3/hr


PNRR = (size_consist(1,:) ./ drain_ap) .^ NRR;
PNRR(PNRR > 1) = 1;
```

```
RRinse_OS = Rdrain_OS .* PNRR;
RRinse_US = Rdrain_OS - RRinse_OS;

% drain the reject rinse medium

RRDilute(1) = sum(RRinse_US);
RRDilute(2) = RRinse_W_2dil / 3600;
RRDilute(3) = QuRinse(3) * (1-adh_loss);       % 0.5% adhesion loss
RRDilute(4) = RRinse_US(8);
RRDilute(5) = sum(RRDilute(1:4));

% final reject off the end of the screen

RReject(1) = sum(RRinse_OS);
RReject(2) = water_US;
RReject(3) = QuRinse(3) * adh_loss;
RReject(4) = 0;
RReject(5) = sum(RReject(1:4));

% BR is a check the reject volume balances in all size fractions
% from the cyclone across the drain then rinse
% BRC is a check the 4 components by volume balance

BR = reject_by_sizeV-Rdrain_US-RRinse_OS-RRinse_US;
BR(BR<0.000001)=0;

BRC = Qu_comps-Rdrain-RRDilute-RReject;
BRC(BRC<0.000001)=0;

% now the total vector of rinse to dilute sump and delay it

Rinse_to_dil = PRDilute + RRDilute;
[Rinse_to_dil] = Comb_Rinse_delay (Rinse_to_dil, Rinse_delta);
```

```
%-------------------------------------------------------------------
%
%                    CORRECT MEDIUM SUMP
%
%-------------------------------------------------------------------

    [CMtank_level, CM_overflow, CMVol, from_CM] =...
        CorrectSumpVec(CMvol_old, Mag_sep_CV, W_overflow, from_Mpit);
    CMvol_old = CMVol;                    % update sump volume


% [RDX] = Nucleonic(from_CM, RDX_old)
% RDX_old = RDX;

    % check correct sump balance

    BCC = W_overflow + Mag_sep_CV + from_Mpit - from_CM;
    BCC(BCC<0.000001)=0;

    [PV, Int] = PI2(RD, RD_SP, Kp, Ki, Isum);        % density control
 if i<5
   control_water=0;    %% medium from CM sump
 end
    control_water = auto_water_base + auto_water .* PV;
    control_water(control_water < 0) = 0;            % limit to 0
    if i > 2000                          % don't limit during start
        control_water(control_water > 0.01) = 0.01; % limit water
    end

    if i<15
    from_CM =[0 0.1548 0.0236 0 0.1791];    %% medium from CM sump
    end

    from_CM= from_CM + control_water;         % auto water addition
```

```
%-------------------------------------------------------------------
%
%                    DILUTE MEDIUM SUMP
%
%-------------------------------------------------------------------

   % divert the bleed stream

   Bleed_to_Dil = Bleed;

   % bleed to dilute sump after dead time

   [Bleed] = BleedStream_delay(Bleed_to_Dil, Bleed_delta);

   [Diltank_level, Dil_overflow, Dil_Vol, from_Dil]=...
      DiluteSumpVec(DilVol_old, Rinse_to_dil, Bleed,...
      Floor_drain, Clarif_water);
   DilVol_old = Dil_Vol;

   % pump dilute to mag seps after dead time

   Dil_to_MagSeps = from_Dil;
   [from_Dil] = MagSeps_feed_delay(Dil_to_MagSeps, from_Dil_delta);

   % check the dilute balance

   BDC = Rinse_to_dil + Bleed + Clarif_water - from_Dil;
   BDC(BDC<0.000001)=0;

%-------------------------------------------------------------------
%
%                    MAGNETIC SEPARATORS
%
```

```
%-----------------------------------------------------------------------

    [Mag_sep_CV, Mag_sep_TV] = MagSepVec2(from_Dil);% con & tails m3/hr
    Mags_to_correct = Mag_sep_CV;

    % mag sep con to correct sump after dead time

    [Mag_sep_CV] = MagSepC_delay(Mags_to_correct, MSCon_delta);

%-----------------------------------------------------------------------

    aa(i) = Wtank_level;
    bb(i) = seal_level;
    cc(i) = CMtank_level;
    dd(i) = Diltank_level;
    ee(i) = M2C;
    ff(i) = from_CM(5)*3600  ;
    gg(i) = (1-bleed_frac)* from_CM(5) * 3600;
    hh(i) = Bleed(5) * 3600;
    jj(i) = to_wing(5) * 3600 ;
    kk(i) = DMCfeedvol(5) * 3600;
    ll(i) = from_DR(5) * 3600;
    mm(i) = from_Dil(5) * 3600;
    nn(i) = RD;
    oo(i) = Rinse_to_dil(5) * 3600;
    pp(i) = pressure;
    qq(i) = W_overflow(5)*3600;
    ss(i) = from_Mpit(5) * 3600;
    tt(i) = control_water(5)*3600;
    uu(i) = Qo;
    vv(i) = Qu;
    ww(i) = Mag_sep_CV(5) * 3600;
    xx(i) = 100 * (from_CM(4)*1.5)/((from_CM(3)*4.8) + (from_CM(4)*1.5)); %
medium contamination
```

```
        zz(i) = Clarif_water(5)*3600;
        magsloss = (RReject(3) + RProduct(3) + Mag_sep_TV(3)) * 4800 / ...
              (OStonnes / 3600);            % instantaneous kg/tonne
        za(i) = ofRD;                    %DMC Overflow Density
        zb(i) = ufRD;                    %DMC Underflow Density
        zc(i) = RD;                     %Medium Density
        zd(i) = RD_SP;                    %Setpoint for density
        ze(i) = ufRD-ofRD;               %ufRD-ofRD = differential
    end
end

RESULT = [from_CM; Bleed; to_Deslime; to_wing; DMCfeedvol; W_overflow;...
          from_Mpit; from_DR; Rinse_to_dil; Clarif_water; from_Dil; ...
          Mag_sep_CV; Mag_sep_TV];

RESULT2 = [PRinse_US; PRinse_OS; RRinse_US; RRinse_OS;...
           Pdrain_US; Pdrain_OS; Rdrain_US; Rdrain_OS];

csvwrite('SimResult.dat', RESULT);
csvwrite('SimResult2.dat', RESULT2);
%_____________________________________________________________________
_______
%Set Positions for figure1
fig1 = figure;
set(0,'Units','pixels') ;
scnsize = get(0,'ScreenSize');
position = get(fig1,'Position');
outerpos = get(fig1,'OuterPosition');
borders = outerpos - position;
    edge = -borders(1)/2;
    pos1 = [edge,...
      (scnsize(4)* (2/3)-500),...
       scnsize(3) - edge,...
     scnsize(4)-40];
```

```
set(fig1,'OuterPosition',pos1)


% DMC PLOTS

%figure;
subplot(2,2,1)
plot(kk, 'r')
axis([0 sim_time 0 1500])
hold
plot(uu, 'g')
plot(vv, 'b')
h = legend ('Coal & medium to DMC','OF to D&R', 'UF to D&R','Location','best');
set(h,'Interpreter','none')
xlabel('Time, s')
ylabel ('m^3/h')
title('Flowrates into and out of the DMC')


subplot(2,2,2)
plot(nn, 'k')
axis([0 sim_time 1.2 1.8])
hold
plot(za, 'g')
plot(zb, 'b')
plot (zd,'m')
h = legend ('Medium density','RD DMC overflow', 'RD DMC underflow','Density
Setpoint','Location','best');
set(h,'Interpreter','none')
xlabel('Time, s')
ylabel ('RD')
title('Medium Density')
```

```
subplot(2,2,3)
plot(pp, 'r')
h = legend ('DMC pressure','Location','best');
set(h,'Interpreter','none')
axis([0 sim_time 100 200])
xlabel('Time, s')
ylabel ('kPa')
title('DMC pressure')

subplot(2,2,4)
plot(ze, 'g')
h = legend ('Differential','Location','best');
set(h,'Interpreter','none')
axis([0 sim_time 0 0.5])
xlabel('Time, s')
ylabel ('Differential')
title('Differential')


% WING TANK PLOTS
fig2 = figure;
set(0,'Units','pixels') ;
scnsize = get(0,'ScreenSize');
position = get(fig2,'Position');
outerpos = get(fig2,'OuterPosition');
borders = outerpos - position;
    edge = -borders(1)/2;
    pos1 = [edge,...
      (scnsize(4)* (2/3)-500),...
       scnsize(3) - edge,...
     scnsize(4)-40];

set(fig2,'OuterPosition',pos1)
```

```
%figure;
subplot(3,2,1)
plot(aa, 'r')
axis([0 sim_time 0 5])
hold
plot(bb,'g')
h = legend ('Wing tank level', 'seal level',2,'Location','best');
set(h,'Interpreter','none')
xlabel('Time, s')
ylabel ('Level, m')
title('Levels in Wing Tank and Seal Leg')

subplot(3,2,2)
plot(ll, 'b')
h = legend ('Drain medium from screens','Location','best');
set(h,'Interpreter','none')
axis([0 sim_time 0 1000])
xlabel('Time, s')
ylabel ('m^3/h')
title('Medium draining from Drain & Rinse Screen Underpans')

subplot(3,2,3)
plot(jj, 'c')
h = legend ('Coal & medium from deslime','Location','best');
set(h,'Interpreter','none')
axis([0 sim_time 0 2000])
xlabel('Time, s')
ylabel ('m^3/h')
title('Coal & Medium flows from Deslime Screen to Wing tank')

subplot(3,2,4)
plot(qq, 'b')
h = legend ('Overflow to correct sump','Location','best');
set(h,'Interpreter','none')
```

```
axis([0 sim_time 0 800])
xlabel('Time, s')
ylabel ('m^3/h')
title('Wing Tank Overflow to Correct Medium Sump')

subplot(3,2,5)
plot(kk, 'b')
h = legend ('Coal & medium to DMC','Location','best');
set(h,'Interpreter','none')
axis([0 sim_time 0 1500])
xlabel('Time, s')
ylabel ('m^3/h')
title('Coal & Medium flows to DMC')

subplot(3,2,6)
plot(ee, 'g')
h = legend ('Medium to coal ratio','Location','best');
set(h,'Interpreter','none')
axis([0 sim_time 2 10])
xlabel('Time, s')
ylabel ('M:C')
title('Medium to Coal Ratio')

%-------------------------------------------------------------------------
% CORRECT SUMP PLOTS

%figure
fig3 = figure;
set(0,'Units','pixels') ;
scnsize = get(0,'ScreenSize');
position = get(fig3,'Position');
outerpos = get(fig3,'OuterPosition');
borders = outerpos - position;
    edge = -borders(1)/2;
```

```
    pos1 = [edge,...
      (scnsize(4)* (2/3)-500),...
       scnsize(3) - edge,...
      scnsize(4)-40];

set(fig3,'OuterPosition',pos1)



subplot(3,2,1)
plot(cc, 'r')
h = legend ('Correct sump level','Location','best');
set(h,'Interpreter','none')
axis([0 sim_time 0 5])
xlabel('Time, s')
ylabel ('Level, m')
title('Level in the Correct Medium Sump')

subplot(3,2,2)
plot(ww, 'k')
h = legend ('Con from Mag Seps','Location','best');
set(h,'Interpreter','none')
axis([0 sim_time 0 150])
xlabel('Time, s')
ylabel ('m^3/h')
title('Magnetic Separator Concentrate Stream')

subplot(3,2,3)
plot(qq, 'g')
h = legend ('Overflow from wing tank','Location','best');
set(h,'Interpreter','none')
axis([0 sim_time 0 800])
xlabel('Time, s')
ylabel ('m^3/h')
title('Wing Tank Overflow')
```

```
subplot(3,2,4)
plot(ss, 'k')
h = legend ('from magnetite pit','Location','best');
set(h,'Interpreter','none')
axis([0 sim_time 0 12])
xlabel('Time, s')
ylabel ('m^3/h')
title('Fresh Magnetite from Pit')
hold

subplot(3,2,5)
plot(ff, 'b')
h = legend ('Correct medium out','Location','best');
set(h,'Interpreter','none')
axis([0 sim_time 0 2500])
xlabel('Time, s')
ylabel ('m^3/h')
title('Correct Medium outlet flowrate')

subplot(3,2,6)
plot(tt, 'g')
h = legend ('Auto water addition','Location','best');
set(h,'Interpreter','none')
axis([0 sim_time 0 200])
xlabel('Time, s')
ylabel ('m^3/h')
title('Automatic water addition valve for density adjustment')

%-----------------------------------------------------------------------
% DILUTE SUMP PLOTS

%figure
fig4 = figure;
```

```
set(0,'Units','pixels') ;
scnsize = get(0,'ScreenSize');
position = get(fig4,'Position');
outerpos = get(fig4,'OuterPosition');
borders = outerpos - position;
    edge = -borders(1)/2;
    pos1 = [edge,...
      (scnsize(4)* (2/3)-500),...
       scnsize(3) - edge,...
      scnsize(4)-40];

set(fig4,'OuterPosition',pos1)

subplot(3,2,1)
plot(oo, 'r');
h = legend ('Rinse to dilute','Location','best');
set(h,'Interpreter','none')
axis([0 sim_time 0 350])
xlabel('Time, s')
ylabel ('m^3/h')
title('Rinse to dilute flowrate')

subplot(3,2,2)
plot(hh, 'b')
h = legend('Bleed to dilute','Location','best');
set(h,'Interpreter','none')
axis([0 sim_time 0 100])
xlabel('Time, s')
ylabel ('m^3/h')
title('Bleed to dilute flowrate')

subplot(3,2,3)
plot(mm, 'g')
h = legend('Pumped from dilute','Location','best');
```

```
set(h,'Interpreter','none')
axis([0 sim_time 0 700])
xlabel('Time, s')
ylabel ('m^3/h')
title('Feed to Magnetic Separator from Dilute Sump')

subplot(3,2,4)
plot(zz, 'r');
h = legend('Clarified to dilute','Location','best');
set(h,'Interpreter','none')
axis([0 sim_time 0 200])
xlabel('Time, s')
ylabel ('m^3/h')
title('Clarified water addition to dilute sump')

subplot(3,2,5)
plot(dd, 'g');
h = legend('Dilute level','Location','best');
set(h,'Interpreter','none')
axis([0 sim_time 0 5])
xlabel('Time, s')
ylabel ('Level, m')
title('Dilute Sump Level')

subplot(3,2,6)
plot(xx, 'k');
h = legend('Medium contamination','Location','best');
set(h,'Interpreter','none')
axis([0 sim_time 0 25])
xlabel('Time, s');
ylabel ('% non-magnetics')
title('Medium %Non-magnetics Concentration')
% END OF MAIN SCRIPT
%-----------------------------------------------------------------
```

7.2 Appendix 2: Graph outputs from Dynamic Model

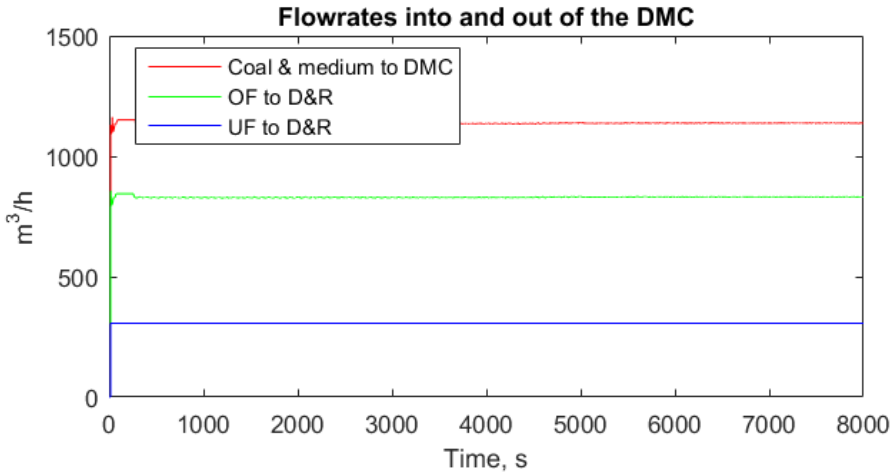

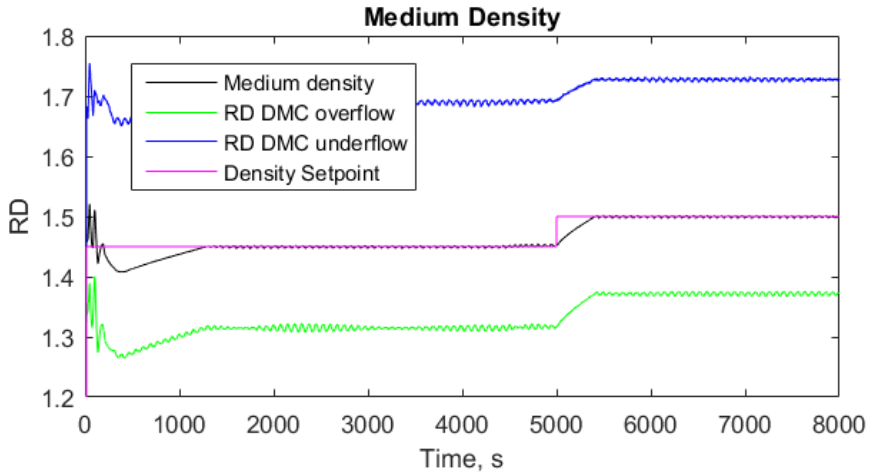

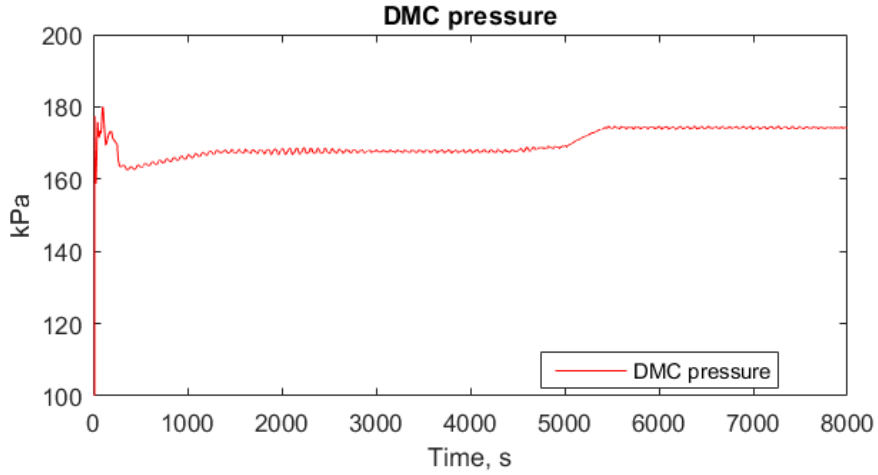

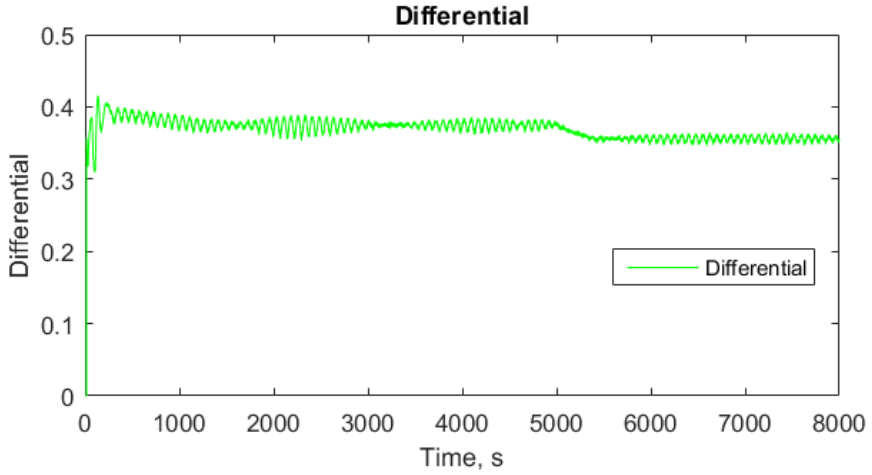

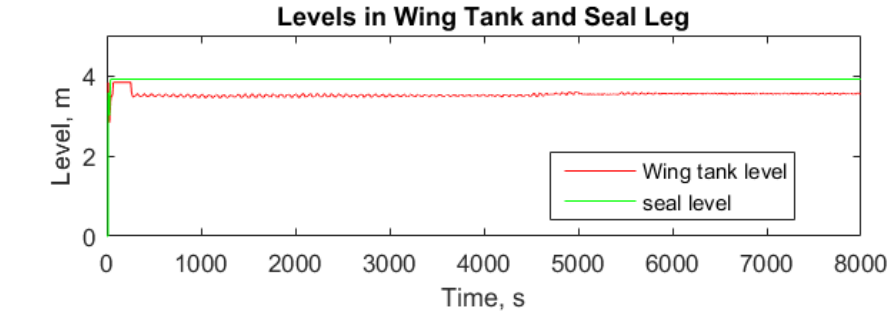
Levels in Wing Tank and Seal Leg
Level, m
Time, s
Wing tank level
seal level

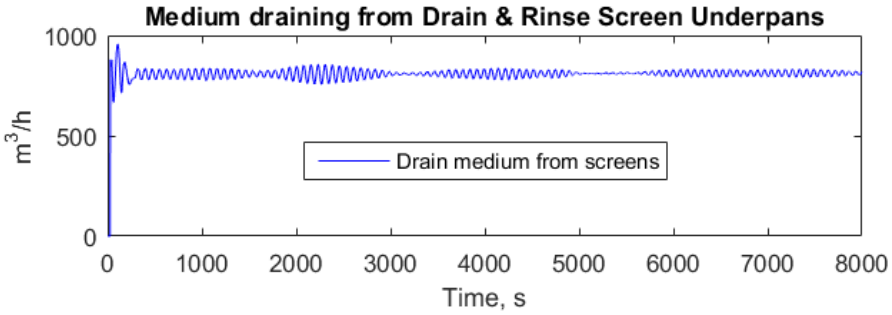
Medium draining from Drain & Rinse Screen Underpans
m3/h
Time, s
Drain medium from screens

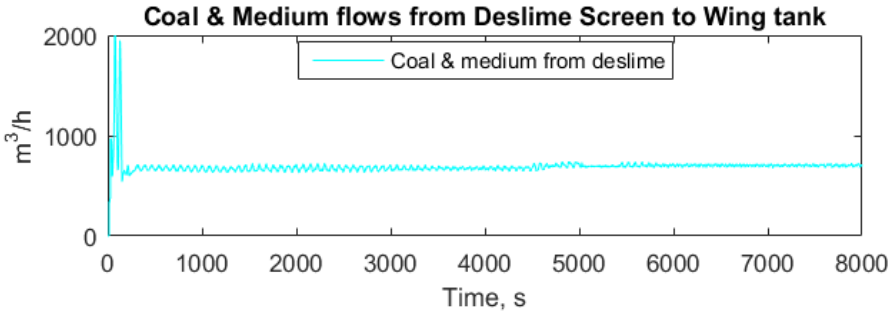
Coal & Medium flows from Deslime Screen to Wing tank
m3/h
Time, s
Coal & medium from deslime

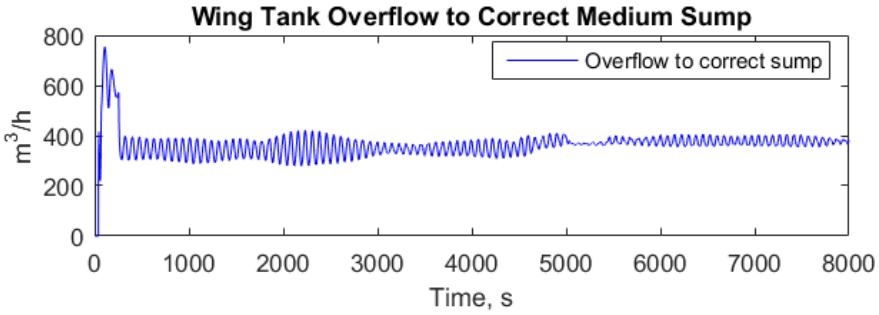
Wing Tank Overflow to Correct Medium Sump
m3/h
Time, s
Overflow to correct sump

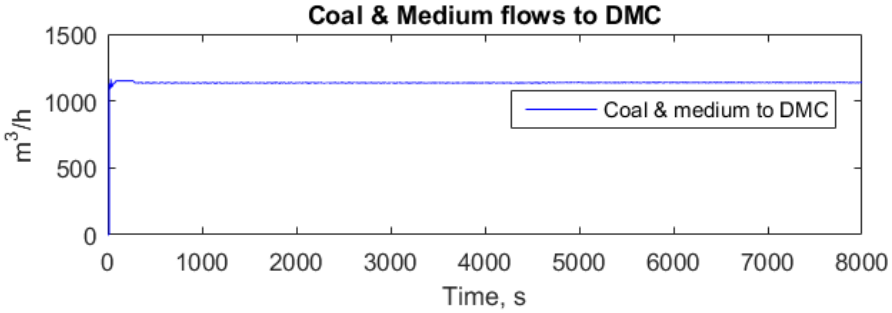
Coal & Medium flows to DMC
m3/h
Time, s
Coal & medium to DMC

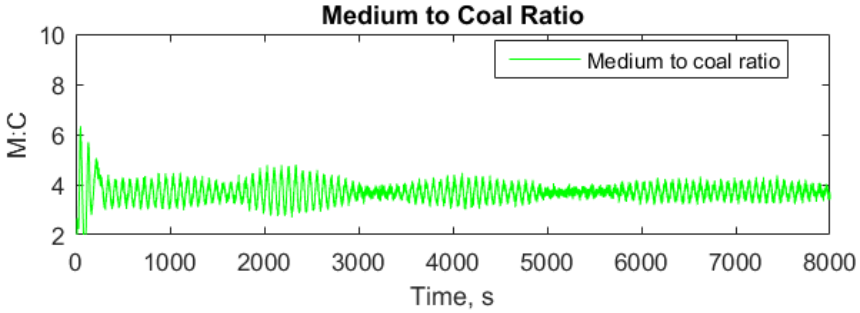
Medium to Coal Ratio
M:C
Time, s
Medium to coal ratio

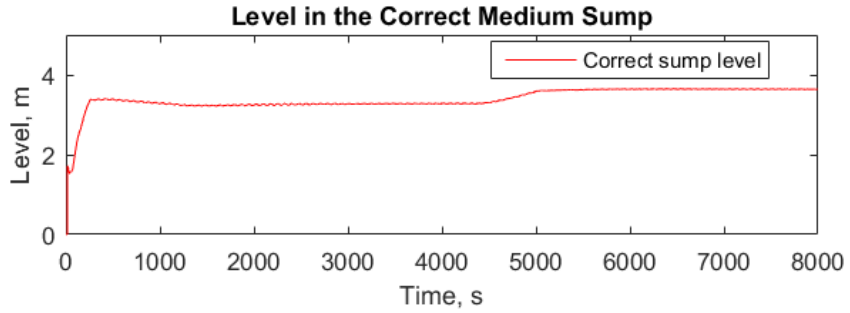
Level in the Correct Medium Sump
Correct sump level
Level, m
Time, s

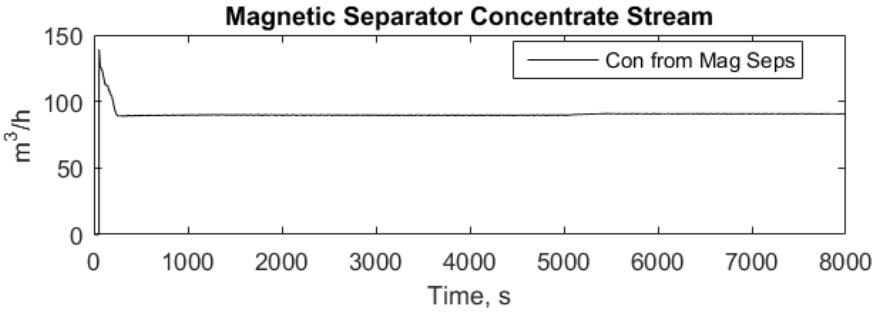
Magnetic Separator Concentrate Stream
Con from Mag Seps
m3/h
Time, s

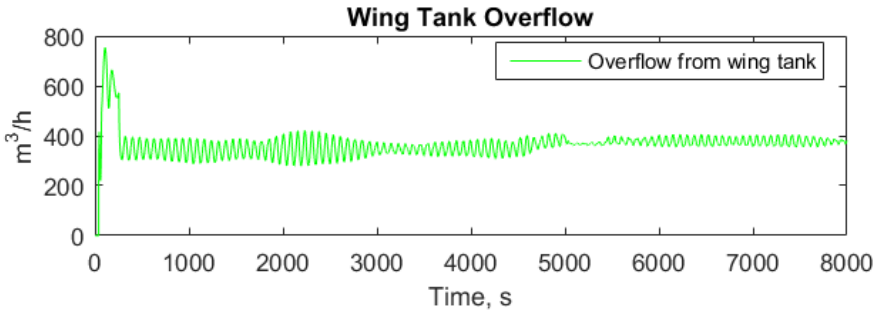
Wing Tank Overflow
Overflow from wing tank
m3/h
Time, s

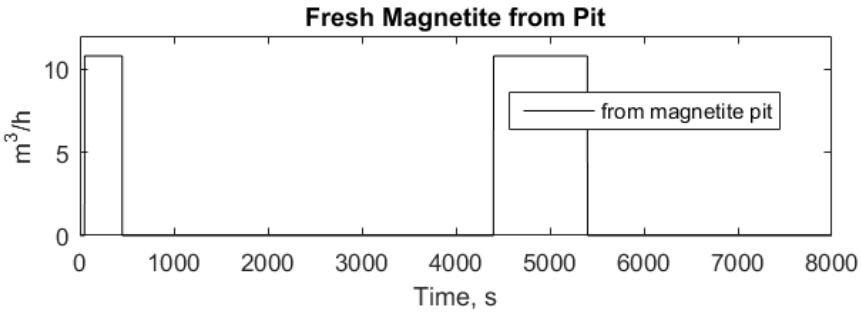
Fresh Magnetite from Pit
from magnetite pit
m3/h
Time, s

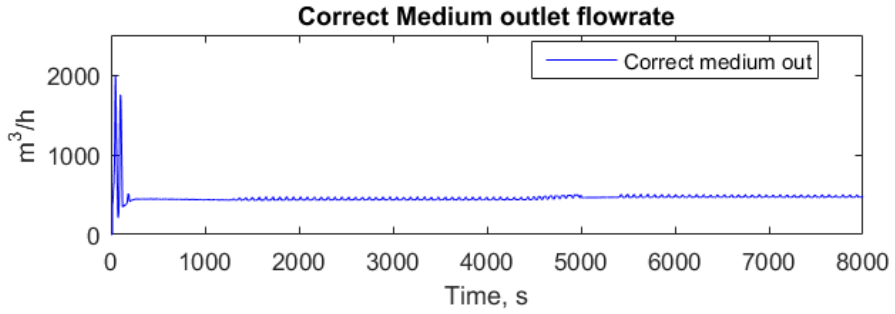
Correct Medium outlet flowrate
Correct medium out
m3/h
Time, s

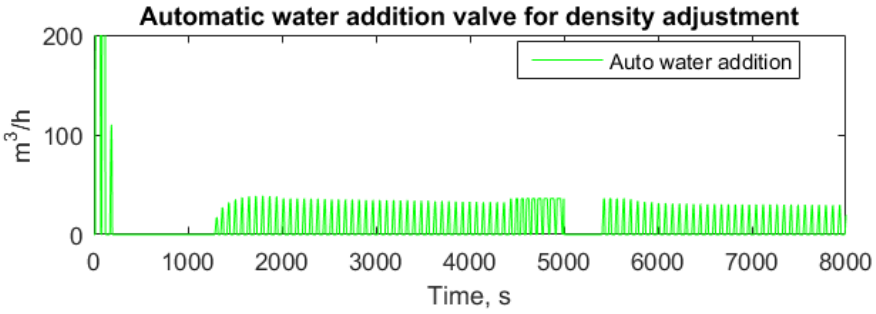
Automatic water addition valve for density adjustment
Auto water addition
m3/h
Time, s

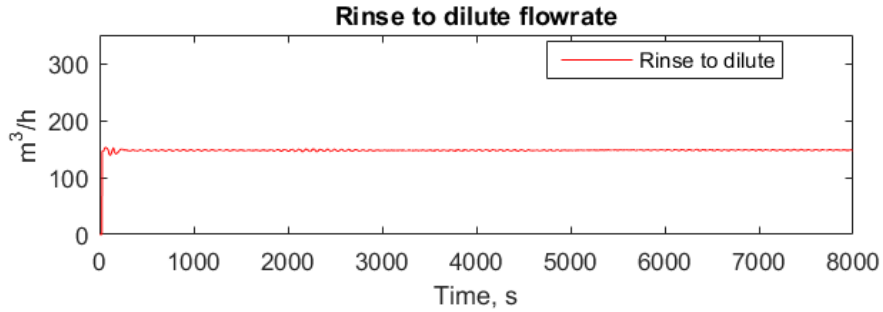
Rinse to dilute flowrate
Rinse to dilute
m3/h
Time, s

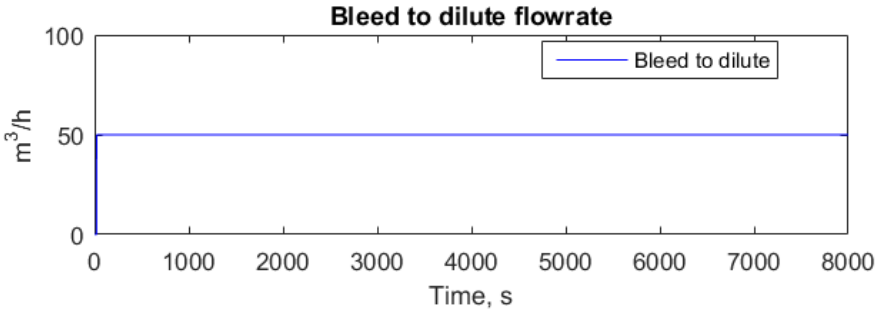
Bleed to dilute flowrate
Bleed to dilute
m3/h
Time, s

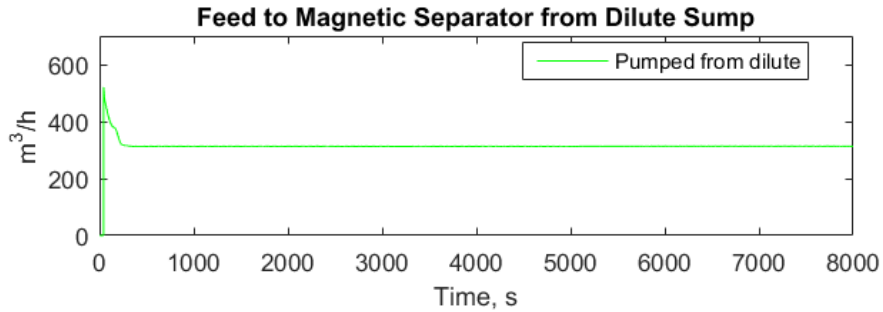
Feed to Magnetic Separator from Dilute Sump
Pumped from dilute
m3/h
Time, s

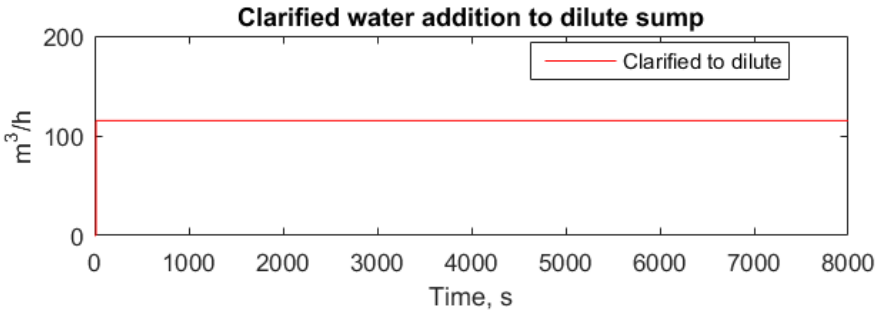
Clarified water addition to dilute sump
Clarified to dilute
m3/h
Time, s

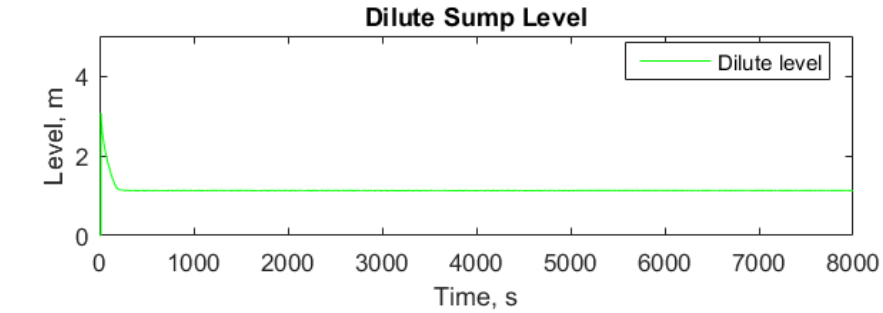
Dilute Sump Level
Dilute level
Level, m
Time, s

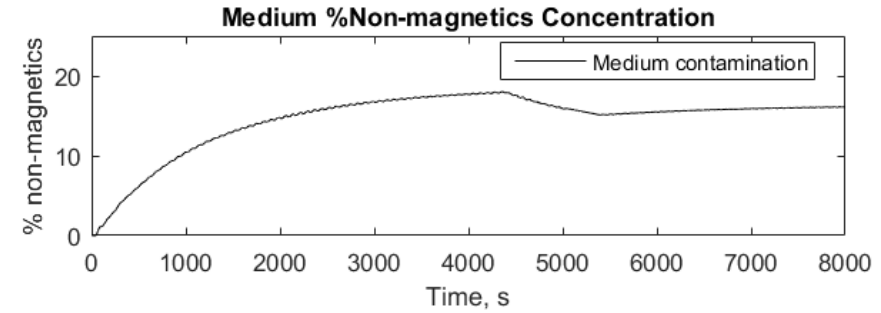
Medium %Non-magnetics Concentration
Medium contamination
% non-magnetics
Time, s

7.3 Appendix 3: Functions from Matlab Dynamic Model

function [delayed_output]= BleedStream_delay(in1, in2)

```
% this is the delay between the bleed valve and the dilute sump

global Bleed_delay

Bleed = in1;                % input vector
delta = in2;                % delay seconds

if delta == 0
   delayed_output = Bleed;
else
   delayed_output = Bleed_delay(delta,:);
   Bleed_delay(2:delta,:) = Bleed_delay(1:delta-1,:) ;
   Bleed_delay(1,:) = Bleed;
end
%-------------------------------------------------------------------------
```

Published with MATLAB® R2015b

function [delayed_output]= BleedValve_delay(in1, in2)

```
% this is the delay between the correct medium & bleed valve

global Bleedsplit_delay

Bleed = in1;                % input vector
delta = in2;                % delay seconds

if delta == 0
   delayed_output = Bleed;
else
   delayed_output=Bleedsplit_delay(delta,:);
   Bleedsplit_delay(2:delta,:) = Bleedsplit_delay(1:delta-1,:) ;
   Bleedsplit_delay(1,:)= Bleed;
end
%-------------------------------------------------------------------------
```

Published with MATLAB® R2015b

function[cc_mass,cc_vol,cc_density] = clean_coal(d50, Ep)

```
global WashData

PN_coal=100./(1+exp(1.0986*(WashData(:,1)-d50)/Ep));

cc_mass_vec = PN_coal.*WashData(:,2)/100;        % clean coal by density
cc_mass = sum(cc_mass_vec);                      % yield mass %
cc_vol = sum(cc_mass_vec./WashData(:,1));        % yield vol %
cc_density = cc_mass/cc_vol;                     % clean coal mean RD
```

Published with MATLAB® R2015b

function [delayed_output]= Comb_Drain_delay (in1, in2)

```
% this is the delay between the combined drains and the wing tank

global Drain_delay

Drain = in1;                % input vector
delta = in2;                % delay seconds

if delta == 0
    delayed_output = Drain;
else
    delayed_output=Drain_delay(delta,:);
    Drain_delay(2:delta,:) = Drain_delay(1:delta-1,:);
    Drain_delay(1,:)=Drain;
end

%-----------------------------------------------------------------------
```

Published with MATLAB® R2015b

function [delayed_output]= Comb_Rinse_delay (in1, in2)

```
% this is the delay between the combined rinse and the dilute sump

global Rinse_delay

Rinse = in1;                % input vector
delta = in2;                % delay seconds

if delta == 0
    delayed_output = Rinse;
else
    delayed_output = Rinse_delay(delta,:);
    Rinse_delay(2:delta,:) = Rinse_delay(1:delta-1,:);
    Rinse_delay(1,:) = Rinse;
end
%-----------------------------------------------------------------------
```

Published with MATLAB® R2015b

```
function [CMtank_level, overflow, CM_Vol, from_CM]=...
                CorrectSumpVec(in1, in2, in3, in4)
%-------------------------------------------------------------------------
%
%                       CORRECT SUMP
%
% The correct medium sump is cyclindrical in shape. It has a lower cone
% with a volume of 10.351 m3 and a height of 2.182 m. The cylindrical
% portion of the sump has a height of 2.438 m. The total height is 4.62 m
% with an overflow weir 0.25m below the top edge ie at a height of 4.37 m.
% The internal diameter is 3.8 m.
% See Sedgman drawing M97-6-3-1115

% input:        in1: vector of CMVol_old in m3              [C W M NM T]
%           in2: vector from mag seps m3/s              [C W M NM T]
%           in3: vector of wing tank overflow m3/s      [C W M NM T]
%           in4: vector from magnetite pit m3/s         [C W M NM T]
%
% output:       sump level (CMTank_level) m
%           vector overflow onto the floor m3/s         [C W M NM T]
%           updated tank volume CMVol_old m3            [C W M NM T]
%           pumped out of tank (from_CM) m3             [C W M NM T]
%

%-------------------------------------------------------------------------

% get the inputs, constrain positive

CMVol_old = in1;            % current volume in the CM tank m3
CMVol_old(CMVol_old < 0) = 0;
from_MagSeps = in2;         % input to tank m3
from_MagSeps(from_MagSeps <0) = 0;
W_overflow = in3;           % overflow from wing tank seal side m3/s
W_overflow(W_overflow < 0) = 0;
from_Mpit = in4;            % makeup magnetite volume m3/s
```

```
from_Mpit(from_Mpit < 0) = 0;

% sump lower cone, height versus volume from TankVols.xls

ht= [0.073 0.145 0.218 0.291...
    0.364 0.436 0.509 0.582...
    0.655 0.727 0.800 0.873...
    0.946 1.018 1.091 1.164...
    1.236 1.309 1.382 1.455...
    1.527 1.600 1.673 1.746...
    1.818 1.891 1.964 2.037...
    2.109 2.182];

 vol=[0.041 0.093 0.156 0.232...
     0.321 0.425 0.545 0.682...
     0.838 1.013 1.209 1.426...
     1.666 1.930 2.219 2.535...
     2.878 3.249 3.650 4.083...
     4.547 5.044 5.575 6.142...
     6.745 7.387 8.067 8.787...
     9.548 10.351];

% correct pump Q vs H from CorPump.xls

Q_CM = [1.38 58.71 104.60 144.94 176.60 203.37 232.43 260.35 285.31...
        315.24 340.28 366.46 392.08 430.32 472.31 496.86 528.01 560.21...
        592.01 623.72];

H_CM = [5.51 5.58 5.59 5.60 5.53 5.45 5.32 5.20 5.05 4.87 4.66 4.42...
        4.21 3.79 3.31 3.05 2.75 2.30 1.89 1.50];

Sump_vol = CMVol_old(5);

if Sump_vol < 10.351          % still in the lower cone
```

```
    % interpolate height from volume, data pre-computed in TankVols.xls

    CMtank_level = spline(vol,ht,Sump_vol);

elseif Sump_vol  > 10.351;

    % upper cylinder, so calculation now easy

                CMtank_level = 2.182 + (Sump_vol - 10.351)/(pi*3.8^2/4);
end

% use level & pump curve to calculate volume pumped out (from_CM)
% pump curve Q in m3/hr, H in m

CMfixed_head = 7;
CM_head = CMfixed_head - CMtank_level;
Q = spline(H_CM, Q_CM, CM_head);
if Q <= 0
    Q = 0;
end

from_CMT = Q / 3600;                    % change to m3/s

% update correct sump volume with inputs

Sump = CMVol_old + from_MagSeps + W_overflow + from_Mpit;

if Sump(5) <= 0
    from_CM =[0 0 0 0 0];
else
    from_CM = (Sump ./ Sump(5)) .* from_CMT;    % proportion to pumped out
end

CM_Vol = CMVol_old + from_MagSeps + W_overflow + from_Mpit - from_CM;
```

```
CM_Vol(CM_Vol< 0) = 0;                  % don't let sump vol go neg

if CMtank_level >= 4.370
    overflow = CM_Vol - from_CM;        % overflow to floor
    CMtank_level = 4.370;
else
    overflow = [0 0 0 0 0];
end
```

Published with MATLAB® R2015b

function [delayed_output]= DeslimeStream_delay(in1, in2)

```
% this is the delay between the bleed valve and the dilute sump

global Deslime_delay

Deslime = in1;                  % input vector
delta = in2;                  % delay seconds

if delta == 0
       delayed_output = Deslime;
else
   delayed_output=Deslime_delay(delta,:);
   Deslime_delay(2:delta,:) = Deslime_delay(1:delta-1,:) ;
   Deslime_delay(1,:)= Deslime;
end
%--------------------------------------------------------------------------
```

Published with MATLAB® R2015b

```
function [Diltank_level, overflow, Dil_Vol, from_Dil]=...
                DiluteSumpVec(in1, in2, in3, in4, in5)
%-------------------------------------------------------------------------
%
%                       DILUTE SUMP
%
% The dilute medium sump is cyclindrical in shape. It has a lower cone
% with a volume of 1.521 m3 and a height of 1.092 m. The cylindrical
% portion of the sump has a height of 3.358 m. The total height is 4.450 m
% with an overflow weir 0.25 m below the top edge ie at a height of 4.20 m.
% The internal diameter is 1.8 m.
% See Sedgman drawing M97-6-3-1116

% input:        in1: vector of DilVol_old in m3
%           in2: vector of dilute from rinse screens m3/s C W M NM
%           in3: vector of bleed from CM sump m3/s C W M NM
%           in4: vector of floor drain water m3/s C WM NM m3/s
%           in5: vector of makeup clarified water for level control m3/s
%
% output:       sump level (DilTank_level) m
%           vector of overflow onto the floor m3/s
%           updated tank volume DilVol m3
%           vector of dil pumped out to mag seps m3/s
%



%-------------------------------------------------------------------------

% get the inputs all vectors of components [C W M NM T]

DilVol_old = in1;           % current volume in the CM tank m3
DilVol_old(DilVol_old < 0) = 0;
Dil_from_DR = in2;          % from rinse tank m3/s
Dil_from_DR(Dil_from_DR < 0) = 0;
bleed = in3;                % bleed from CM sump m3/s
```

```
bleed(bleed < 0) = 0;
floor_drain = in4;          % floor drain m3/s
clarif_water = in5;         % clarified water for level control m3/s

Dil_diam = 1.8;             % sump diameter m

% sump lower cone, height versus volume from TankVols.xlx

ht = [0.109 0.218 0.328 0.437...
      0.546 0.655 0.764 0.874...
      0.983 1.092 ];

vol = [0.062 0.140 0.234 0.348...
       0.482 0.638 0.818 1.025...
       1.258 1.521];

% dilute pump Q vs H from DilPump.xls

Q_Dil = [0.21 49.28 78.89 116.05 166.28 199.59 235.10 266.38 311.88...
         351.42 381.08  413.02 444.87 476.32 510.38 546.09 577.95...
         607.10 647.82 690.57 750.77 800.73];

H_Dil = [13.24 13.37 13.46 13.40 13.41 13.23 13.18 12.94 12.71 12.44...
         12.09 11.70 11.41 11.06 10.73 10.32 9.88 9.58 8.99 8.40...
         7.58 6.93];

Sump_vol = DilVol_old(5);

if Sump_vol < 1.521       % still in the lower cone

    % interpolate height from volume, data pre-computed in TankVols.xls

    Diltank_level = spline(vol,ht,Sump_vol);

elseif Sump_vol > 1.521
```

```
    % upper cylinder, so calculation now easy

    Diltank_level = 1.092 + (Sump_vol - 1.521)/(pi*Dil_diam^2/4);
 end

if Diltank_level >= 4.20        % sump overflow level m
                    Diltank_level = 4.20;          % max height of sump m
elseif Diltank_level < 0;
        Diltank_level = 0.0;
end

% use level & pump curve to calculate volume pumped out (from_Dil)
% pump curve Q in m3/hr, H in m
% pump efficiency versus clear water 0.963

Dfixed_head = 13.7;                    % based on Metso data
Dil_head = Dfixed_head - Diltank_level;
Q = spline(H_Dil, Q_Dil, Dil_head);
if Q < 0
    Q = 0;
end
from_Dil(5) = Q / 3600;             % change to m3/s

% update dilute sump volume totals

Sump = DilVol_old + Dil_from_DR + bleed + floor_drain...
          + clarif_water;          % sump contents in components

if Sump(5) <= 0
    from_Dil = [0 0 0 0 0];
else
    from_Dil = (Sump ./ Sump(5)) .* from_Dil(5); % proportion to pumped out
end
```

```
Dil_Vol = DilVol_old + Dil_from_DR + bleed + floor_drain...
          + clarif_water - from_Dil;

Dil_Vol(Dil_Vol< 0) = 0;

% check for overflow to floor

if Diltank_level >= 4.20
    overflow = Dil_Vol - from_Dil;     % overflow to floor
else
    overflow = 0.0;
end
```

Published with MATLAB® R2015b

```
function[Qf, ufsplit, Qu, Qo, ufRD, ofRD, d50c]= DMC(head, RD, M2C)

% fixed DMC data

diam=1300;                  % cyclone diameter (mm)
do=559;                     % vortex finder diameter
du=520;                     % spigot diameter

p=37;                       % magnetite grind

%-------------------------------------------------------------------
%check head, RD & M2C

if head < 0 || head > 15
        head = 9;
end
if RD < 1.2
        RD = 1.2;
elseif RD > 1.8
   RD = 1.8;
end
if M2C < 2
        M2C = 2;
end

%-------------------------------------------------------------------
%
%                       WOOD DMC MODEL
%
%-------------------------------------------------------------------

Qf =(2.87*10^-5*diam^2.3*head^0.46*(du/do)^0.17);          % Qf m3/hr

ufsplit =9.29*diam^-0.31*head^-0.46*(du/do)^4.16;          % Qu/Qf
```

```
Qu =Qf*ufsplit;                                                    %
Qu m3/hr

Qo =Qf - Qu;                                                       %
Qo m3/hr

ufRD = RD+0.00728*(RD*ufsplit^(0.194*(RD-2.07))....
      -RD)*p^1.34*head^0.562*diam^-0.145*(1-0.5/M2C);          % UF RD

ofRD = RD-1.52*(RD-(RD-ufsplit*ufRD)/(1-ufsplit));          % OF RD

d50c = RD + 0.125 + 0.154*ufRD - 0.215*ofRD;                % d50c

%------------------------------------------------------------------------
```

Published with MATLAB® R2015b

function [delayed_output]= DMC_feed_delay (in1, in2)

```
% this is the delay between the wing tank & DMC

global DMC_delay

DMC_feed = in1;                 % input vector
delta = in2;                    % delay seconds

if delta == 0
    delayed_output = DMC_feed;
else
    delayed_output=DMC_delay(delta,:);
    DMC_delay(2:delta,:) = DMC_delay(1:delta-1,:);
    DMC_delay(1,:)=DMC_feed;
end


%------------------------------------------------------------------------
```

Published with MATLAB® R2015b

```
function[Drain_percent, Rf, N] = Drainpd2(in1, in2, in3, in4, in5)

%------------------------------------------------------------------------
%
%                    PRODUCT DRAIN SCREEN MODEL
%
%------------------------------------------------------------------------

% This model uses Firth and O'Brien's empirical model detailed in Chapter
% 12 of the Dense Medium Cyclone Handbook, Crowden et.al. 2013
% Note calcs in empirical formula are in m3/hr
%
% constants:        C1 = 87 altered from DMC handbook
%                   C2 = 0.12
%                   ThiC = 0.15
%
% inputs:           in1 the DMC medium overflow (ie for 2 screens)
%                   in2 drain area of each screen m2
%                   in3 aperture of screen in mm
%                   in4 open area fraction
%                   in5 coarse in feed to drain screen tph
%
% outputs:          per cent of medium draining through
%                   Rf fines recovery
%                   N number of presentations to screen deck
%------------------------------------------------------------------------

Q_OF = in1;
drain_area_pd = in2;
aperture = in3;
OA = in4;
Coarse = in5;

% constants
```

```
C1 = 87.0 ;        % 105 in the Firth model;
C2 = 0.12;
ThiC = 15;

% calculation for 1 of 2 screens

Q_OF = Q_OF / 2;  %flowrate to overflow
Qprime = Q_OF/drain_area_pd; %Q'= flow to drain per m^2 screen
if Qprime == 0                          % check not zero during startup
    Qprime = 0.001;
end

SDR_pd = (C1 *Qprime^0.5 * aperture^0.5 * OA^0.5)/ exp(C2 * ThiC);
Drain_percent = 100 * (SDR_pd * drain_area_pd) / Qprime;
%product drain specific drain rate and drain %
if Drain_percent > 90.0
    Drain_percent = 90.0;
end

Rf = 1 - Drain_percent / 100; %fines recovery
N = 0.67 * Qprime ^0.66 / (Coarse / drain_area_pd) ^0.62; %number of presentations to
screen
```

Published with MATLAB® R2015b

```
function[Drain_percent, Rf, N] = Drainrej2(in1, in2, in3, in4, in5)

%------------------------------------------------------------------------
%
%                       REJECT DRAIN SCREEN MODEL
%
%------------------------------------------------------------------------

% This model uses Firth and O'Brien's empirical model detailed in Chapter
% 12 of the Dense Medium Cyclone Handbook, Crowden et.al. 2013
% Note calcs in empirical formula are in m3/hr
%
% constants:        C1 = 105
%                   C2 = 0.12
%                   ThiC = 0.15
%
% inputs:           in1 the DMC medium overflow (ie for 2 screens)
%                   in2 drain area of each screen m2
%                   in3 aperture of screen in mm
%                   in4 open area fraction
%
% outputs:          per cent of medium draining through
%                   Rf fines recovery
%                   N number of presentations to screen deck
%------------------------------------------------------------------------

Q_UF = in1;
drain_area_rej = in2;
aperture = in3;
OA = in4;
Coarse = in5;

% constants

C1 = 60.0 ;                         %105;
```

```
C2 = 0.12;
ThiC = 15;

Qprime = Q_UF/drain_area_rej;
if Qprime == 0                          % check not zero during startup
    Qprime = 0.001;
end

SDR_rej = (C1 *Qprime^0.5 * aperture^0.5 * OA^0.5)/ exp(C2 * ThiC);
Drain_percent = 100 * (SDR_rej * drain_area_rej) / Qprime;

if Drain_percent > 90.0
    Drain_percent = 90.0;
end

Rf = 1 - Drain_percent / 100;
N = 0.67 * Qprime ^0.66 / (Coarse / drain_area_rej) ^0.62;
```

Published with MATLAB® R2015b

```
function [delayed_output]= MagSepC_delay(in1, in2)
% this is the delay between Mag sep con & correct sump

global MSCon_delay

MSCon = in1;                % input vector
delta = in2;                % delay seconds

if delta == 0
   delayed_output = MSCon;
else
   delayed_output = MSCon_delay(delta,:);
   MSCon_delay(2:delta,:) = MSCon_delay(1:delta-1,:) ;
   MSCon_delay(1,:) = MSCon;
end
%--------------------------------------------------------------------------
```

Published with MATLAB® R2015b

function [delayed_output]= MagSeps_feed_delay(in1, in2)

```
% this is the delay between the combined rinse and the dilute sump

global from_Dil_delay

from_Dil = in1;                 % input vector
delta = in2;                    % delay seconds

if delta == 0
    delayed_output = from_Dil;
else
    delayed_output = from_Dil_delay(delta,:);
    from_Dil_delay(2:delta,:) = from_Dil_delay(1:delta-1,:);
    from_Dil_delay(1,:) = from_Dil;
end
%-------------------------------------------------------------------------
```

Published with MATLAB® R2015b

```
function[Mag_sep_CV, Mag_sep_TV] = MagSepVec2(Mag_sep_FV)
%------------------------------------------------------------------------
%
%                    MAGNETIC SEPARATOR MODEL
%
%------------------------------------------------------------------------
%
% Inputs:   feed component vector [C W M NM T]
% Outputs:  component vectors for concentrate & tails [C W M NM T]

Density_vector = [1.5 1.0 4.80 1.5];              % component densities

Mag_sep_feedV = Mag_sep_FV(5); % total m3/s

if Mag_sep_feedV <= 0
   Mag_sep_feedV = 0.001;
end

Mag_sep_compsM =Mag_sep_FV(1:4) .* Density_vector(1:4); % CWMN mass t/s
Mag_sep_feedT = sum(Mag_sep_compsM);                  % total tps

if Mag_sep_compsM (4) <= 0
   Mag_sep_compsM (4) = 0.001;
end

if Mag_sep_feedT <= 0
   Mag_sep_feedT = 0.001;
end

M2NM = Mag_sep_compsM(3) / Mag_sep_compsM(4);          % mags to non-mags

if M2NM <= 0
   M2NM = 0.001;
end
```

```
Mass_pcS = 100*(Mag_sep_compsM(3) + Mag_sep_compsM(4))...
          / Mag_sep_feedT;  % m% solids in feed

if Mass_pcS > 20
   Mass_pcS = 20;
end

%Mag_losspc = (1 + 2.7 * M2NM ^-0.7) * (Mag_sep_feedV*3600)^-0.13...
%           * Mass_pcS^0.12;

Mags_recpc = 99.9; %100 - Mag_losspc;

%NM_entrain = (4.5 * (100 * Mag_sep_compsM(4)/ Mag_sep_feedT)^-0.23) * ...
%           (100 * Mag_sep_compsM(3) / Mag_sep_feedT)^0.96;   % entrain %
NM_entrain = 25.0;
% assemble mag product vector & total m3/hr

Mag_sep_CV(1) = Mag_sep_FV(1) * 0.25;
Mag_sep_CV(2) = Mag_sep_FV(2) * 0.25;
Mag_sep_CV(3) = Mag_sep_FV(3) * Mags_recpc/100;
Mag_sep_CV(4) = Mag_sep_FV(4) * NM_entrain/100;
Mag_sep_CV(5) = sum(Mag_sep_CV(1:4));


% assemble mag tails vector & total m3/hr

Mag_sep_TV = Mag_sep_FV - Mag_sep_CV;
```

Published with MATLAB® R2015b

function [delayed_output]= MSCon_delay(in1, in2)

```
% this is the delay between Mag sep con & correct sump

global MSCon_delay
yo
MSCon = in1;                % input vector
delta = in2;                % delay seconds

delayed_output=MSCon_delay(delta,:)
MSCon_delay(2:delta,:) = MSCon_delay(1:delta-1,:)
MSCon_delay(1,:)=MSCon


%------------------------------------------------------------------------
```

Published with MATLAB® R2015b

function[RD]=Nucleonic(in1, in2)

```
% inputs:   in1 vector of components of correct medium output C W M NM T
%           in2 RD from last measurement
%
% outputs:  new RD
%
%-------------------------------------------------------------------------

time_c =0.01;                           % filter time constant
density_vec = [1.5 1 4.8 1.5];              % component densities
to_Deslime = in1;
RD_old = in2;

if to_Deslime(3) <= 0                    % check there is magnetite
    to_Deslime(2) = 2;                   % in start up delay
    to_Deslime(3) = 0.3;                 % so force an RD of 1.5ish
    to_Deslime(5) = 2.3;
end

Massvec = to_Deslime(1:4) .* density_vec ;      % component masses
RD_calc = sum(Massvec) / to_Deslime(5);         % sum the masses / volume
RD = time_c * RD_calc + (1 - time_c) * RD_old;  % filter
```

Published with MATLAB® R2015b

function[PV, Isum] = PI2(in1, in2, in3, in4, in5)

```
MV = in1;                       % measured RD
MV(MV <= 0)= 1.52;              % default startup measured RD
SP = in2;                       % RD setpoint
Kp = in3;                       % proportional gain
Ki = in4;                       % integral time
Isum = in5;                     % integral

Error = MV - SP;                % error

shift_Isum = Isum(1:9);         % push the Isum vector down one
Isum(1) = Error;
Isum(2:10) = shift_Isum;

Int = sum(Isum)/10;             % integral sum

PV = Kp * Error + Ki * Int;     % control output
```

Published with MATLAB® R2015b

function[Rinse_vol, Rinse_W_2dil, water_OS, N] = Rinsepd2(in1, in2, in3, in4)

```
%--------------------------------------------------------------------
%
%                    RINSE SCREEN MODEL
%
%--------------------------------------------------------------------

% This model uses Firth and O'Brien's empirical model detailed in Chapter
% 12 of the Dense Medium Cyclone Handbook, Crowden et.al. 2013
%
% inputs:          in1 the medium vol to rinse m3/hr
%                  in2 total volume of rinse water m3/hr
%                  in3 coarse particles to rinse screen tph
%                  in4 area of rinse screen m2
%
% output:          rinse volume m3/hr
%
%--------------------------------------------------------------------

Q_to_rinse = in1;   % vol of medium to rinse screen
Rinse_water = in2;  % volume of rinse water used m3/hr
Coarse = in3;       % tonnage of coarse particles to rinse tph
Rinse_area = in4;   % area of rinse screen m2

% per cent mass (of the overflow stream) of the rinse water remaining
% with coarse particles

rem_water = 20;     % can be adjusted but typical of end screen moisture %

% calculation, this is for two screens

water_OS = (Coarse * rem_water/100)/(1 - rem_water/100);
Rinse_W_2dil = Rinse_water - water_OS;
```

```
Rinse_vol = Q_to_rinse + Rinse_water - water_OS;    % m3/hr through screen
N= (0.67 *((Q_to_rinse + Rinse_water)/Rinse_area)^0.66)/...
    (Coarse / Rinse_area)^0.62;
```

Published with MATLAB® R2015b

function[Rinse_vol, Rinse_W_2dil, water_US, N] = RRinse(in1, in2, in3, in4)

```
%------------------------------------------------------------------------
%
%                       RINSE SCREEN MODEL
%
%------------------------------------------------------------------------

% This model uses Firth and O'Brien's empirical model detailed in Chapter
% 12 of the Dense Medium Cyclone Handbook, Crowden et.al. 2013
%
% inputs:          in1 the medium vol to rinse m3/hr
%                  in2 total volume of rinse water m3/hr
%                  in3 coarse particles to rinse screen tph
%                  in4 area of rinse screen m2
%
% output:          rinse volume m3/hr
%
%------------------------------------------------------------------------

Q_to_rinse = in1;   % vol of medium to rinse screen
Rinse_water = in2;  % volume of rinse water used m3/hr
Coarse = in3;       % tonnage of coarse particles to rinse tph
Rinse_area = in4;   % area of rinse screen m2

% per cent mass (of the overflow stream) of the rinse water remaining
% with coarse particles

rem_water = 20;     % can be adjusted but typical of end screen moisture %

water_US = (Coarse * rem_water/100)/(1 - rem_water/100);
Rinse_W_2dil = Rinse_water - water_US;
Rinse_vol = Q_to_rinse + Rinse_water - water_US;    % m3/hr through screen
N= (0.67 *((Q_to_rinse + Rinse_water)/Rinse_area)^0.66)/...
    (Coarse / Rinse_area)^0.62;
```

Published with MATLAB® R2015b

function [delayed_output]= to_MagSeps (in1, in2)

```
% this is the delay between the combined rinse and the dilute sump

global from_Dil_delay

from_Dil = in1;                 % input vector
delta = in2;                % delay seconds

delayed_output=from_Dil_delay(delta,:);
from_Dil_delay(2:delta,:) = from_Dil_delay(1:delta-1,:);
from_Dil_delay(1,:)=from_Dil;

%-------------------------------------------------------------------------
```

Published with MATLAB® R2015b

function [delayed_output]= to_Wing_delay(in1, in2)

```
% this is the delay between the bleed valve and the dilute sump

global to_Wing_delay

to_Wing = in1;                % input vector
delta = in2;                  % delay seconds

delayed_output=to_Wing_delay(delta,:);
to_Wing_delay(2:delta,:) = to_Wing_delay(1:delta-1,:) ;
to_Wing_delay(1,:)= to_Wing;

%------------------------------------------------------------------------
```

Published with MATLAB® R2015b

function [delayed_output]= Wing_delay(in1, in2)

```
% this is the delay between the bleed valve and the dilute sump

global to_Wing_delay

to_Wing = in1;                  % input vector
delta = in2;                  % delay seconds

if delta == 0
    delayed_output = to_Wing;
else
    delayed_output=to_Wing_delay(delta,:);
    to_Wing_delay(2:delta,:) = to_Wing_delay(1:delta-1,:) ;
    to_Wing_delay(1,:) = to_Wing;
end
%-----------------------------------------------------------------------
```

Published with MATLAB® R2015b

```
function[Wtank_level,seal_level,W_overflow,Tankvol,Sealvol]=...
   wing_tankVec(in1,in2,in3,in4,in5,in6)

% inputs 1 - 5 are vectors [C W M NM T]
% inputs:   in1 (to_wing) coal & medium from deslime m3/s
%           in2 (from_DR_drain) drain medium from DR screens m3/s
%           in3 (DMCfeedvol) the volume pumped out based on the head m3/s
%           in4 (tankvol_old) the existing volume in the coal side m3
%           in5 (sealvol_old) the existing volume in the seal side m3
%           in6 fraction of drain medium to seal side
%
% outputs:  tank_level level on coal side m
%           seal_level level on seal side m
%           W_overflow overflow to CM sump m3/s vector [C W M NM T]
%           updated tankvol_old m3/s vector [C W M NM T]
%           update sealvol_old m3/s vector [C W M NM T]
%
%-------------------------------------------------------------------------

dorifice=0.31;              % orifice diameter in metres
a = (pi * dorifice^2)/4;    % a = orifice opening area in m^2
C=0.6;                      % constant for round orifice
g=9.81;                     % acceleration due to gravity

to_wing = in1;
to_wing(to_wing < 0) = 0;
from_DR_drain = in2;
from_DR_drain(from_DR_drain < 0) = 0;
DMCfeedvol = in3;
DMCfeedvol(DMCfeedvol < 0) = 0;
Tankvol_old = in4;
Tankvol_old(Tankvol_old < 0) = 0;
Sealvol_old = in5;
Sealvol_old(Sealvol_old < 0) = 0;
y = in6;
```

```
    % get height in coal side from volume (relative to tank bottom)

V = [0.000 0.100 0.200 0.300 0.400 0.500 0.600 0.700 0.800 0.900 1.000...
     1.022 1.042 1.101 1.164 1.228 1.295 1.364 1.434 1.507 1.582 1.659...
     1.737 1.817 1.899 1.983 2.069 2.156 2.245 2.335 2.427 2.521 2.616...
     2.654 2.660 2.757 2.854 2.951 3.049 3.146 3.243 3.340 3.437 3.535...
     3.632 3.729 3.826 3.923 4.021 4.118 4.215 4.312 4.409 4.507 4.604...
     4.701 4.798 4.895 4.993 5.090 5.187 5.284 5.381 5.479 5.576 5.673...
     5.770 5.867 5.965 6.062 6.159 6.256 6.353 6.451 6.548 6.645 6.742...
     6.839 6.898];

H = [0.000 0.086 0.171 0.257 0.343 0.429 0.514 0.600 0.686 0.772 0.857...
     0.876 0.893 0.941 0.987 1.031 1.074 1.116 1.156 1.196 1.234 1.271...
     1.308 1.344 1.379 1.413 1.446 1.479 1.512 1.543 1.574 1.605 1.635...
     1.647 1.650 1.700 1.750 1.800 1.850 1.900 1.950 2.000 2.050 2.100...
     2.150 2.200 2.250 2.300 2.350 2.400 2.450 2.500 2.550 2.600 2.650...
     2.700 2.750 2.800 2.850 2.900 2.950 3.000 3.050 3.100 3.150 3.200...
     3.250 3.300 3.350 3.400 3.450 3.500 3.550 3.600 3.650 3.700 3.750...
     3.800 3.830];

    Sump_vol = Tankvol_old(5);
    Sump_vol(Sump_vol > 6.898) = 6.898;

    Wtank_level = spline(V, H, Sump_vol);

    % get height in seal side from seal volume (relative to tank bottom)

    Seal_vol = Sealvol_old(5);

    if  Seal_vol<=0
       seal_level=2.701;                    % height to base of seal leg
    elseif Seal_vol>0 && Seal_vol<=3.043;       % partially full
       seal_level = (Seal_vol + 3.8909)/1.44;
    elseif Seal_vol > 3.043
```

```
    seal_level = 4.815;                 % max height of seal leg
end

%-----------------------------------------------------------------------
% ORIFICE CALCULATION
% Delta P equals the height of seal leg minus tank level
% if DeltaP is negative then flow reverses UP the seal leg

DeltaP = seal_level - Wtank_level;  % pressure drop across the orifice
if DeltaP < 0
    k=-1;
else
    k=1;
end

% vol flow rate through the orifice plate in the seal leg, m3/s

Qorifice(5) = k * C * a * sqrt(2*g*abs(DeltaP));

%-----------------------------------------------------------------------
% WING TANK LOGIC
% fill the wing tank, Tankvol is the coalside volume, Sealvol is the
% seal leg side volume

Seal = Sealvol_old + from_DR_drain .* y;        % seal side components
Qorifice = (Seal ./ Seal(5)) .* Qorifice(5);    % components

Sealvol= Sealvol_old + from_DR_drain .* y - Qorifice;

Tankvol = Tankvol_old + to_wing + (1-y)*from_DR_drain ...
    - DMCfeedvol + Qorifice ;

% seal side overflowing?

if Sealvol(5) < 1.742
```

```
    W_overflow = [0 0 0 0 0];                % not overflowing
elseif Sealvol(5) >= 1.742                   % overflowing
    W_overflow = (y .* from_DR_drain - Qorifice);
end

Sealvol= Sealvol_old + y*from_DR_drain - Qorifice - W_overflow;
```

%--

Published with MATLAB® R2015b

7.4 Appendix 4: Published Papers

Scott,N., Holtham,P., Firth,B., O'Brien,M., (2013) On-line Simulation & Dynamic Analysis of Dense Medium Cyclone Circuits., International Coal Preparation Congress, 2013, Istanbul, Turkey.

Firth,B., O'Brien,M., Holtham,P., Scott,N., Hu,S., Dixon,R., Burger,A., (2014) Dynamic Impacts of Plant Feed and Operating practices on a Dense Medium Cyclone (DMC) Circuit, 15th Australian Coal Preparation Conference Proceedings 14-18th Sept 2014, Gold Coast, Australia

Firth, B., Holtham,P., O'Brien, M., Hu,S., Dixon,R., Burger, A., Scott,N., Linkage of Dynamic Changes in DMC Circuits to Plant Conditions, ACARP Report C50152, Australian Coal Association Research Program, February 2013.

Scott,N., Wood,C., Holtham,P., O'Brien,M., Firth,B., (2015) Integration of Plant Residence Time Measurement Into a Dynamic Model of a Coal Dense Medium Circuit, Coal Prep 2015, April 27-29th2015, Lexington, Kentucky, USA.

O'Brien,M., Firth,B., Holtham,P., Hu,S., Scott,N., Burger,A., Optimisation and Control of Dense Medium Cyclone Circuits, International Coal Preparation Congress, July 2016, St Petersburg, Russia

7.5 Appendix 5: Standard Deviations from Tracer Residence Times

Additional results below were included for the tracer residence times. The standard deviations are included here, however it is important to note that in some cases, the value of this measurement is low. In situations where more than one pathway could be taken by a particle, the standard deviation was high. This makes logical sense because the data in those cases is multi-modal and it is reasonable to expect high variation given that the routes taken aren't necessarily the same.

Test	Residence time From	Residence time to	Average	Min	Max	SD
A	Desliming Screen	Drain & Rinse Product 1	00:57	00:37	01:41	0.0001
	Desliming Screen	Drain & Rinse Product 2	01:00	00:36	01:56	0.0002
	Desliming Screen	Drain & Rinse Rejects	01:02	00:43	02:11	0.0002
	Desliming Screen	Drain & Rinse Overall	01:01	00:36	02:11	0.0002

For the desliming screen the standard deviation was as follows and suggested that there is low variation in travel times of the data.

For the other areas tested, standard deviations ranged as follows:

Test	Residence time From	Residence time to	Average	Min	Max	SD
B	DMC Overflow/Underflow	Drain & Rinse Screen	00:20	00:15	00:26	0.00003

This standard deviation suggested that there is low variation in travel times of the data. In reality, the particles travelled a total of approximately 10 metres with no chance of deviation.

Test	Residence time From	Residence time to	Average	Min	Max	SD
C&D	Drain underpan	Drain and Rinse Screen	02:36	00:43	29:06	0.0029

Tracers were placed in drain under-pans and collected at the coarse overflow launder on the drain and rinse screens. These particles followed the medium and substantial variation was evident in the data.

Test	Residence time From	Residence time to	Average	Min	Max	SD
E	Feed Weigher	Drain and Rinse Screen	02:25	02:00	03:27	0.0002

These tracer particles entered at the feed weightometer and followed the coal through the process. There was little opportunity for particles to be delayed and all appear to have gone straight through the DMC without deviating into the medium stream.

Test	Residence time From	Residence time to	Average	Min	Max	SD
F	Magnetic Separator	Drain and Rinse Screen	09:50	01:10	39:36	0.0070

These particles entered at the concentrate launder of the magnetic separator and then routed through the correct medium sump. Some particles took considerable time to flush through the system suggesting that they may have stayed with the medium for quite a long time before joining the coarse coal. The standard deviations reflect this variation.

Test	Residence time From	Residence time to	Average	Min	Max	SD
G	Deslime Water Sump	Drain and Rinse Screen	08:37	02:09	35:51	0.0072

Particles placed into the Deslime water make-up sump appeared to have taken varied routes or held up in the system before entering the coarse coal pathway. The likelihood that particles just settled out and sat in the bottom of this tank for a while cannot be discounted as the relative density of the fluid (water) to the particles is considerably different. As a consequence, standard deviation was poor and the minimum and maximum times also suggest wide variation from one particle to the next.

Test	Residence time From	Residence time to	Average	Min	Max	SD
H	Crusher Feed	Drain and Rinse Screen	01:55	01:36	02:25	0.0002

Predictably, these particles followed the coarse coal route, having been introduced to the coal stream at the feed to the crusher. Standard deviation is relatively low as there is very little chance of particles not following the coal stream unless they were to raft up into the seal leg of the wing tank and overflow to the correct medium sump. On the day of the testwork, it is suggested that rafting in the wing tank was highly unlikely and no evidence of rafting was found.

Test	Residence time From	Residence time to	Average	Min	Max	SD
I	Wing Tank Overflow	Drain and Rinse Screen	06:53	01:23	31:48	0.0046

Particles entering at the wing tank overflow mimicked the action of a rafting particle. They were placed in the overflow which reported to the correct medium sump and these particles had multiple routes which they could follow. Judging by the minimum time, some particles went straight through the correct medium pump and directly back to the wing tank, however others to a far longer route, either settling out in the correct medium sump, or following the bleed line across to the dilute sump before returning in a water stream back to the start of the process. (The magnetic separator effluent line returns to the deslime water make-up sump.) Standard deviations were poor in this case which is not surprising.